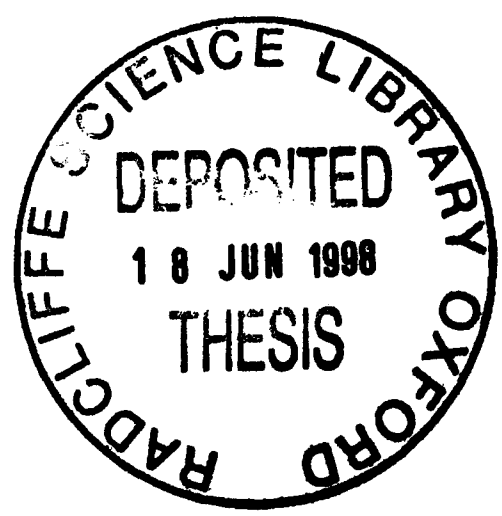
STRUCTURE AND FUNCTION OF CD31

A thesis submitted for the degree of Doctor of Philosophy in the University of Oxford

Justin Philip Newton

St. John's College



ABSTRACT

STRUCTURE AND FUNCTION OF CD31

Justin P. Newton, St. John's College
Submitted for the degree of D.Phil., at the University of Oxford, Trinity term 1997

The regulated interaction of leukocyte with endothelium is of key importance during normal immune surveillance and leukocyte infiltration to sites of infection in the inflammatory response. This thesis is concerned with the structure and function of CD31 (platelet-endothelial cell adhesion molecule-1), one of the adhesion molecules implicated in these processes. Previous work has shown both *in vivo* and *in vitro* that CD31 is involved in the final step of leukocyte recruitment, transmigration across the endothelial monolayer.

CD31 mediated adhesion is complex, since it is capable of mediating multiple adhesive interactions, both to itself (homophilic adhesion) and to other ligands (heterophilic adhesion). In order to study homophilic adhesion, an heterologous cell-protein assay was used in combination with recombinant chimeric CD31Fc fusion proteins, ICAM-3/CD31 chimeras and chimeras between human and murine CD31. These reagents located the homophilic binding site to the NH_2-terminal domains 1 and 2, but also define a non-binding accessory role for the membrane proximal domains. Using site-directed mutagenesis to target all of the exposed charged residues in domain 1 and a subset of charged residues in domain 2, five residues were identified, mutations in which resulted in inhibition of homophilic adhesion. These residues map to both faces of the domain 1 immunoglobulin-like fold, suggesting that each molecule of CD31 interacts with two others. A novel zipper model of homophilic adhesion involving CD31 lateral association analogous to that seen amongst cadherins is proposed on the basis of these results.

Evidence for lateral association of CD31 to form dimers was obtained from biophysical, biochemical and molecular biology techniques. These show that Cd31 exists in an equilibrium between monomeric and dimeric forms both in solution as soluble recombinant protein, and at the cell surface. In solution the affinity of the interaction was calculated to lie in the range 12-14μM.

A large panel of anti-CD31 monoclonal antibodies were generated and tested for their ability to effect homophilic adhesion. Inhibitory antibodies were identified, mapping throughout the extracellular domain, away from the ligand binding site. In addition possible stimulating antibodies mapping to the membrane proximal domains were also identified. This indicates that CD31 may be induced to undergo conformational changes which effect homophilic adhesion, and it is proposed that these conformational changes may be linked to the ability of CD31 to form laterally associated dimers.

Using the reagents described above, a screen of haematopoietic cell lines identified a novel heterophilic interaction, which was shown to be mediated by the integrin αvβ3. Protein-protein assays were used to confirm a direct physical association between CD31 and αvβ3, and to map the integrin binding site to the third immunoglobulin-like fold of CD31. The functional significance of this interaction was assessed in neutrophil transmigration assays, in which both anti-CD31 and anti-αvβ3 antibodies were found to partially inhibit neutrophil transmigration.

For my parents

ACKNOWLEDGEMENTS

First and foremost, I would like to thank my supervisor Dr. David Simmons for his continuing advice, encouragement and support over the past three years, in particular for teaching me that there are only three things that can go wrong with an experiment. I would also like to thank my colleagues, past and present, in the Cell Adhesion and Molecular Haemopoiesis Laboratories for their invariably excellent advice and good humour, and for providing such a supportive work environment.

I owe much to various colleagues and collaborators in Oxford and beyond and I would like to thank them for their technical expertise so freely given and for their intellectual insights. In particular I would like to thank Andrew May and Drs Amit Sharma, Yvonne Jones and Karl Harlos at the Laboratory of Molecular Biophysics; Dr. Russell Wallis at the Glycobiology Institute; Drs Robin Aplin and David Harvey at the Oxford Centre for Molecular Sciences; Ian Collins at R&D Systems, Abingdon; Matthew Wakelin and Dr. Sussan Nourshargh at the National Heart and Lung Institute, Imperial College, London; Dr. Neil Barclay at the Sir William Dunn School of Pathology; and Professor Iain Campbell at the Biochemistry Department.

I also thank the Yamanouchi Research Institute for generously funding my Studentship, and providing the facilities to write this thesis. In particular, I would like to thank Drs. Julia Spragg and Ian Bird for providing advice, reagents and bench space. I also thank the Imperial Cancer Research Fund Laboratories at the Institute of Molecular Medicine, Oxford for providing the facilities and resources used to complete this thesis. In particular I would like to thank the support staff without whom laboratory work would have been impossible (especially Carol Bowden).

Finally, I would like to thank my friends for making my time in Oxford so pleasurable. In particular I would like to thank Charles Morgan, Judy Hirst and Sarah Fawcett - house mates from heaven; Elaine Ferguson, Sylvie Freeman, Adele Hartnell, James Munday, Helen Floyd, Ann Cornish, Mary Vinson, Rangana Choudhur, Deepa Nath, Alison Cody and Lisa Williams for making lab life entertaining.

ABBREVIATIONS

BCECF,AM	2',7'-bis-(2-carboxyethyl)-5-(and-6)-carboxyfluorescein, acetoxymethyl ester.
BSA	Bovine Serum Albumin
CAM	Cell Adhesion Molecule
CD	Cluster of Differentiation
cDNA	complementary Deoxyribonucleic Acid
DEAE-dextran	Diethylaminoethyl-dextran
DMSO	Dimethyl sulphoxide
DNAse	Deoxyribonuclease
ECD	Extracellular domain
ECL	Enhanced Chemiluminescence
EDTA	Ethylenediaminetetraacetic acid
ELISA	Enzyme-Linked Immunsorbant Assay
FCS	Foetal Calf Serum
FITC	Fluorescein isothiocyanate
GPI	Glycosylphosphatidyl-inositol
HRP	Horseradish Peroxidase
HUVEC	Human Umbilical Vein Endothelial Cells
ICAM	Intercellular Adhesion Molecule
Ig	Immunoglobulin
IgSF	Immunoglobulin superfamily
IL	Interleukin
INF	Interferon
kDa	Kilodalton
mAb	Monoclonal antibody
OAc	acetate
OD	Optical Density
PAGE	Polyacrylamide Gel Electrophoresis
PBS	Phosphate Buffered Saline
PCR	Polymerase Chain Reaction
PECAM	Platelet Endothelial Cell Adhesion Molecule
PEG	Polyethylene glycol

PIPLC	Phosphatidylinositol phospholipase C
PMSF	Phenylmethylsulphonyl Fluoride
RNAse	Ribonuclease
rpm	revolutions per minute
s.d	Standard deviation
SDS	Sodium Dodecyl Sulphate
TBS	Tris Buffered Saline
TM	Transmembrane
TNF	Tumour Necrosis Factor
Tris	Tri(hydroxymethyl)aminomethane
TRITC	Tetramethylrhodamine isothiocyanate
VLA	Very Late Antigen

CONTENTS

CHAPTER ONE: INTRODUCTION

A. Historical Perspectives 1
B. Leukocyte-endothelial adhesive interactions 3
C. Adhesion receptors between leukocytes and endothelium 4
1. Selectins and their ligands 4
1.1 Selectins 4
1.1.1L-selectin 5
1.1.2 P-selectin 6
1.1.3 E-selectin 6
1.2 Selectin ligands: Sialomucins 7
1.2.1 L-selectin ligands 7
1.2.2 P-selectin ligands 8
1.2.3 E-selectin ligands 8
2. Integrins 9

2.1 Integrin structures 10
2.2 "Outside-in" signalling 12
2.3 "Inside-out" signalling 13
3. Immunoglobulin superfamily 14
3.1The immunoglobulin fold 14
3.2 ICAM family 16
3.3 VCAM-1 18
3.4 CD31/PECAM-1 19
3.5 MAdCAM-1 21
3.6 L1 21
3.7 JAM-1 22
4. Other adhesion molecules
4.1 CD44 23
4.2 VAP-1 and VAP-2 24
D. Regulation of adhesion and leukocyte extravasation
1. Adhesion cascades and the multi-step paradigm 24
1.1 Rolling 25
1.2 Triggering and firm adhesion 26
1.3 Transmigration 26
E. Organisation of endothelial cell-cell junctions and implication for transmigration 28
F. Outline of the thesis 29

CHAPTER TWO: MATERIALS AND METHODS

2.1 Media, solutions, and other reagents 31
2.1.1 Bacterial culture medium 31
2.1.2 Solutions for molecular biology 31
2.1.3 DNA sequencing solutions 32
2.1.4 Transfection solutions 33
2.1.5 Protein solutions 33

2.2 Cell culture and transfection **34**
2.2.1 Cell culture 34
2.2.2 Isolation and purification of human neutrophils 35
2.2.3 Transient transfection of COS cells 35
2.3 Antibodies **36**
2.3.1 Generation of antibodies against the extracellular domain of CD31 36
2.3.2 Generation of antibodies against the cytoplasmic tail of CD31 37
2.3.3 Commercial antibodies 38
2.4 Molecular Biology and DNA manipulation **38**
2.4.1 Plasmid preparation
a. Large scale preparation (Maxiprep) 38
b. Small scale preparation (Miniprep) 39
2.4.2 Preparation of chemically competent bacteria 40
a. MC1061/p3 40
b. XL1-Blue 41
2.4.3 Bacterial transformation 41
2.4.4 Oligonucleotide synthesis 41
2.4.5 PCR amplification 42
2.4.6 TA-cloning of PCR products 43
2.5 Generation of constructs to dissect CD31 mediated adhesion **43**
a. CD31 extracellular domain deletion series 43
b. GPI-anchored CD31 45
c. Cell expressed ICAM-3 (CD50)/CD31 chimeras 45
d. Soluble ICAM-3 (CD50)/CD31 chimeras 46
e. Human/murine CD31 chimeras 47
f. CD31 ECD/EGFr TM-TK 47
g. Site-directed mutagenesis by recombinant PCR 48
h. CD31 (D1-D2)/(D4-D6)Fc 49
2.6 Sequencing **50**
2.7 Protein analysis and manipulation **50**
2.7.1 Production and purification of recombinant soluble chimeric CAM-Fc proteins 50
2.7.2 ELISA of Fc and other proteins 51
2.7.3 Purification of integrin αvβ3 52
2.7.4 Solid phase integrin αvβ3-ligand interaction 53
2.7.5 Biotinylation of cell surface proteins, western blotting and immunoprecipitation 54
2.7.6 Chemical cross-linking 56
2.7.7 Analytical ultracentrifugation 56
2.7.8 Silver staining of protein gels 56
2.7.9 Dual colour immunoflourescence 56
2.8 Cell Adhesion Assays **57**
2.8.1 Adhesion of transfectants and cell lines to recombinant protein 57
2.8.2 Neutrophil adhesion/transmigration assays 57
2.8.3 Time lapse video microscopy 58

CHAPTER THREE: DISSECTING THE HOMOPHILIC BINDING SITE OF CD31
3.1 Introduction **59**
3.2 Results **63**

3.2.1 CD31 homophilic adhesion is mediated by the extracellular domain 63
3.3 Mapping the CD31 homophilic binding site in the extracellular domain 68
3.3.1 Generation and characterisation of ant-CD31 monoclonal antibodies which effect CD31 homophilic adhesion 68
3.3.2 Use of ICAM-3 (CD50)/CD31 chimeras to investigate the role of the NH_2-teminal extracellular immunoglobulin-like domains 72
3.3.3 Use of mouse/human CD31 chimeras to identify the homophilic binding site 78
3.3.4 Site-directed mutagenesis of CD31 immunoglobulin-like domains 1 and 2 80
3.3 Discussion **87**

CHAPTER FOUR: CD31 EXISTS IN BOTH MONOMERIC AND DIMERIC FORMS
4.1 Introduction **100**
4.2 Results **101**
4.2.1 Generation of soluble recombinant monomeric CD31 (D1-D6)STOP protein 101
4.2.2 CD31 (D1-D6)STOP protein forms dimers in solution 103
4.2.2.1 Analytical ultracentrifugation 103
4.2.2.2 Quasi-dynamic light scattering 114
4.2.2.3 Native non-denaturing gel electrophoresis 117
4.2.3 Chemical cross-linking studies with wild type and mutant CD31 (D1-D6)STOP protein 118
4.2.4 CD31 cross-linking at the cell surface identifies CD31 dimers 122
4.2.5 A CD31 extracellular domain/epidermal growth factor receptor cytoplasmic tyrosine kinase domain chimera is constitutively autophosphorylated. 123
4.3 Discussion **127**

CHAPTER FIVE: STRUCTURAL STUDIES ON CD31
5.1 Introduction **133**
5.2 Results **133**
5.2.1 Crystallisation trials with CD31 (D1-D6)STOP protein 133
5.2.2 Bacterial expression of CD31 fragments 136
5.3 Discussion **143**

CHAPTER SIX: IDENTIFICATION AND CHARACTERISATION OF HETEROPHILIC LIGANDS FOR CD31
6.1 Introduction **145**
6.2 Results **145**
6.2.1 Adhesion of a panel of cell lines representing stages of haematopoiesis 145
6.2.2 Mutational analysis of CD31 binding to pro-monocytic cell line U937 150
6.2.3 Comparison of U937 binding to CD31, MUC18, and NCAM deletion series 152
6.2.4 Development of a solid phase CD31-αvβ3 protein-protein interaction assay 154
6.2.5 Localisation of the heterophilic αvβ3 binding site on CD31 to domain 3 158
6.2.6 Binding to the integrin αvβ3 is not mediated by acidic residues in the CD-loop 162
6.3 CD38 does not support adhesion via CD31 164
6.4 Discussion **167**

CHAPTER SEVEN: FUNCTIONAL CONSEQUENCES OF CD31 ENGAGEMENT

7.1 Introduction **174**

7.2 Results **175**

7.2.1 Engagement of CD31 on monocytes and endothelium enhances cell motility and induces changes in cell morphology 175

7.2.2 Exposure of HUVEC to CD31 and fibronectin causes changes to cellular tyrosine phosphorylation status 177

7.3 Role of CD31 and integrin avb3 in transmigration of monocytes across endothelial monolayers. 179

7.4 Discussion **181**

CHAPTER EIGHT: GENERAL CONCLUSIONS AND SUGGESTIONS FOR FURTHER WORK

A. Conclusions and Discussion 185

B. Suggestions for further work/areas of investigation 188

REFERENCES **192**

APPENDIX A: List of mutagenic primers

APPENDIX B: Copies of publications

Chapter One: Introduction

A. Historical Perspectives

The ability of cells to sense and integrate information from their immediate environment relies upon interactions with each other and with the surroundings. Co-ordination of this information is essential for the growth and development of multicellular organisms (Gumbiner, 1996). Such interactions range from stable cell-cell contacts involved in the maintenance of tissue architecture, mediated, for example by cadherins (forming the zonula adhaerens junctions) or occludin (in tight junctions) in epithelia and endothelia (Furuse *et al.*, 1994), to the transient, dynamic interactions observed in leukocyte biology (Springer, 1990).

Adhesive interactions between cells have been studied for more than a century in a variety of different models, initially on a phenomenological basis. Amongst the earliest observations that cell adhesion is an intrinsic property of the cells of multicellular organisms were classic experiments performed on marine sponges by H.V. Wilson (1907). Wilson observed that marine sponges could be broken up into individual cell suspensions, which if left in saline spontaneously aggregated and eventually regenerated sponges. If the dissociated cells from different species were mixed together, chimeric sponges were not generated, and the aggregates that formed were comprised exclusively of cells from a single species. Similarly the process of leukocyte adhesion to, and extravasation through, endothelial monolayers was first observed over a century ago using intravital microscopy.

For many decades however, the molecular basis of cell adhesion remained unclear. The most important breakthrough in resolving the molecular players came from the application of immunological approaches combined with biochemical purification and molecular biology. The principle of this approach was to raise monoclonal antibodies against cell surface antigens and then to identify those which inhibited cell adhesion. This methodology was first applied to the study of slime moulds (Beug *et al.*, 1973), and later in vertebrates to affinity purify NCAM leading to its molecular cloning (Brackenbury, *et al.*, 1977; Thiery *et al.*, 1977). It was still, however, a relatively slow and tedious process requiring large quantities of antibody to affinity purify the antigen for subsequent peptide sequencing and

cloning. The field was greatly accelerated by the development of expression cloning techniques (reviewed by Seed, 1995), which allowed for the rapid identification of full length cDNAs for many cell adhesion molecules. As a result, in the past decade there has been an explosive increase in the number of cell adhesion molecules cloned and characterised. For example, following the most recent Leukocyte Typing Workshop (1996), monoclonal antibodies recognising over 160 cell surface molecules expressed specifically on leukocytes have been identified, of which around 50% have been shown to function as adhesion molecules. Similarly the number of adhesion molecules identified on other cell types, such as endothelial, epithelial and neuronal, continues to grow rapidly.

Fortunately, adhesion molecules largely fall into families based upon structural/sequence homologies: selectins, mucins, cadherins, integrins, and members of the immunoglobulin superfamily. The cloning of many of the molecules involved in adhesive processes, such as leukocyte migration from the vascular compartment, has allowed the physiological observations of leukocyte rolling, adhesion and transmigration to be explained at a molecular level by models involving multistep, sequential engagement of adhesion and signalling receptors (Butcher, 1991; Springer, 1995; Imhof and Dunon, 1995). This thesis is concerned with the molecular analysis and function of a single cell adhesion molecule, CD31 (also known as Platelet-Endothelial Cell Adhesion Molecule-1, PECAM-1). CD31 is a member of the immunoglobulin superfamily (IgSF) which is involved in both stable homotypic interactions between endothelial cells, and in transient heterotypic leukocyte-endothelial interactions during the process of transmigration. In order to place CD31 in its correct biological context, the introduction to this thesis will review three aspects of leukocte-endothelial and inter-endothelial interactions. First, the process of leukocyte recirculation and recruitment. Second, the structure/function relationships of the principle families of adhesion molecules involved in leukocyte adhesion to and transmigration across endothelium. Third, how these molecules co-operate in multi-molecular adhesion cascades to regulate and integrate leukocyte adhesion and extravasation during normal immune surveillance and during acute inflammatory responses.

B. Leukocyte-endothelial adhesive interactions

Leukocytes represent the principle cell types in mediating the body's defence against infection by a range of micro-organisms. Leukocytes can be divided into two groups, 1) granulocytes (neutrophils, eosinophils, and basophils) and macrophages, which are involved in non-specific cytotoxicity/phagocytosis of invading micro-organisms, and 2) lymphocytes (B- and T-cells) which are involved in the generation of antigen-specific immune responses. All of these cell types are derived from haematopoietic precursors in the bone marrow, but circulate as mature cells in the blood. This represents a fundamental topological problem for the effective surveillance of the tissues, since with the exception of the spleen, where small penicillar arterioles terminate open ended in the parenchyma (Fawcett, 1994), the blood vessels form a closed system. In order to protect the body from infectious organisms, the cells of the immune system must circulate as nonadherent cells in the blood, but when required adhere to, and migrate across the endothelium and move as adherent cells into the tissue. Leukocytes undergo this switch from non-adherent to adherent phenotype in response to a variety of different cues.

Naive lymphocytes generally survive for around 25 days in the absence of antigenic stimulation and undergo continuous recirculation. These cells show no tissue specific homing and are thought to recirculate randomly via histologically distinct postcapillary venules, known as high endothelial venules (HEV) (Stamper and Woodruff, 1976; Ager, 1987), through tissues, before draining into the secondary lymphatic system (lymph nodes, Peyer's patches, tonsils and spleen) and via the thoracic duct back into the blood (Gowans and Knight, 1964). Most recirculating lymphocytes selectively bind to the endothelium of HEV, whilst ignoring normal vascular endothelium. The lymphoid organs collect antigen from epithelial surfaces, somatic tissues, and blood and present it to naive lymphocytes in the context of specialised microenvironments such as germinal centres that drive antigen-induced differentiation while at the same time culling autoreactive cells.

Antigenic stimulation along with appropriate secondary signals, results in the activation of an immune response, and the generation of memory lymphocytes (characterised by conversion from $CD45RA^+$ to $CD45RO^+$ marker status). Memory lymphocytes also traffic via lymphoid organs, but unlike naive cells, they can also access and recirculate through extralymphoid immune effector sites such as intestinal lamina propria, inflamed skin, and

joints. Moreover, whilst the homing behaviour of naive cells is relatively non-specific, memory lymphocytes show a strong tendency to migrate preferentially to the site of initial antigen exposure. For example in sheep, $CD45RO^+$ lymphocytes draining from the gut labelled with FITC were found to preferentially migrate back to the gut via Peyer's patches (Mackay *et al.*, 1992). Similarly plasmablasts expressing IgA are targeted to mucosal surfaces of the body (Butcher and Picker, 1996). The existence of HEV as specific sites of exit during recirculation, and of tissue specific recirculation by memory lymphocytes, implies that there must be specific ligand-receptor interactions at these sites. It has been shown for example that naive lymphocytes utilise L-selectin to bind peripheral node addressin (PNad, which includes CD34, GlyCAM and other protein cores) and to the mucosal addressin, MAdCAM. Similarly, Cutaneous Lymphocyte Associated-antigen (CLA) on lymphocytes has been shown to promote homing to the skin, binding via E-selectin expressed on the endothelial venules.

In contrast to lymphocytes, mature granulocytes circulate in the blood for very short periods (perhaps as little as a few hours), and do not recirculate via HEV to the lymph. Instead, granulocytes (primarily neutrophils) adhere to normal vascular endothelium in the post capillary venules following inflammatory stimulation or tissue injury. This adhesive interaction also recruits lymphocytes which modulate the immune response. The magnitude and the temporal characteristics of the response vary with the nature of the inflammatory stimulus, and can be rapidly induced and decreased, or can be maintained long term. This indicates that the molecules involved in mediating leukocyte adhesion to non-HEV vascular tissues are highly regulated and this is discussed further below.

C. Adhesion receptors between leukocytes and endothelium

1. Selectins and their ligands

1.1 Selectins

The selectin family of oligosaccharide binding adhesion molecules is comprised of three members: L-selectin which is expressed on leukocytes (Lasky *et al.*, 1989; Siegelman *et al.*, 1989; Tedder *et al.*, 1989; Camerini *et al.*, 1989), P-selectin, which is expressed on platelets and endothelial cells (Johnston *et al.*, 1989), and E-selectin which is expressed on endothelial cells alone (Bevilacqua *et al.*, 1989). The selectins share a common modular structural organisation in their extracellular domains, which are comprised of an amino

terminal calcium-dependent (C-type) lectin domain, an epidermal growth factor (EGF)-like domain, and between two and nine short consensus repeats (SCR) first identified in complement binding proteins (Figure 1.1). All of the selectins mediate adhesion to carbohydrate bearing ligands via the C-type lectin domains. The C-type lectin domain is the most conserved portion of the molecule, with around 60-70% sequence homology (Tedder, 1995), and together with the EGF domain forms the ligand binding site. The three-dimensional structure of the ligand-binding region of human E-selectin has been determined to 2.0Å resolution (Graves *et al.*, 1994), and shows that the overall fold is similar to the lectin domain from rat mannose binding protein (MBP), and that residues involved in mediating adhesion identified by site-directed mutagenesis are either clustered around the Ca^{2+} co-ordination site, or form a discrete patch thought to contact the oligosaccharide ligands directly. The SCP domains are less well conserved (around 40% homology), and do not play a role in ligand binding. They have however, been shown to be important in the physiological functioning of selectins, since truncated forms of P-selectin lacking the SCP domains do not support adhesion under flow conditions (Patel *et al.*, 1995).

1.1.1 L-selectin

L-selectin is expressed by all leukocytes and although originally described as a lymphocyte homing receptor for HEV (Gallatin *et al.*, 1983) its widespread distribution suggests a much broader role. L-selectin has been shown to contribute to both lymphocyte and neutrophil entry into sites of inflammation; antibodies to L-selectin block homing of lymphocytes into lymph nodes, and soluble recombinant L-selectin IgG Fc fusion proteins are inhibitory in inflammatory mouse models (Watson *et al.*, 1990; Watson *et al.*, 1991). L-selectin deficient mice generated by gene disruption show defects in lymphocyte rolling on HEV, localisation of lymphocytes into lymph nodes, and in neutrophil recruitment in a model of acute peritoneal inflammation (Arbones *et al.*, 1994). L-selectin expression is modulated. Cell activation by chemokines downregulates L-selectin expression by inducing cleavage from the cell surface, which is dependent upon a novel zinc metalloprotease identified by inhibition with hydroxamic acid compounds (Kahn *et al.*, 1994, Walcheck *et al.*, 1996). Ligation by monoclonal antibody or by ligand can also induce activation-dependent L-selectin cleavage. Shedding is suggested to be important for maintaining

normal selectin mediated rolling (Walcheck *et al.*, 1996), although this remains controversial (Allport *et al.*, 1997).

1.1.2 P-selectin

P-selectin is constitutively expressed by both platelets and endothelial cells, but is stored in cytoplasmic bodies, known as Weibel-Palade bodies. P-selectin can be translocated to the plasma membrane within minutes upon activation by a variety of inflammatory mediators, including histamine, thrombin, C5a complement factor, and various neuropeptides (Geng *et al.*, 1990; Smith *et al.*, 1992; Sugama *et al.*, 1992). The increase in cell surface P-selectin is transient. Initial translocation to the cell surface is followed by rapid internalisation and degradation in the lysosomes, which is thought to be important in avoiding chronic inflammatory responses. Gene knockout studies in mice have shown that the loss of P-selectin impairs the normal recruitment of neutrophils in a number of inflammatory models (Mayadas *et al.*, 1993), but that P- and E-selectin are essentially functionally redundant (Frenette *et al.*, 1996). In addition to a role in binding lymphocytes, P-selectin is also involved in platelet adhesion to endothelium, and the formation of clots, since P-selectin deficient mice are prone to prolonged haemorrhage (Frenette *et al.*, 1995; Subramaniam *et al.*, 1996).

1.1.3 E-selectin

E-selectin has the most restricted distribution and is probably the most specific inducible molecule expressed on endothelial cells. It has been shown to be involved in the adhesion of neutrophils, monocytes, and T-cell subsets to inflamed but not normal tissues. Gene targeted disruptions of E-selectin show no specific defects (Labow *et al.*, 1994), however in contrast to wild-type mice, lymphocyte rolling was inhibited by antibodies against P-selectin, suggesting that E- and P-selectin are functionally redundant or at least functionally overlap. This has been confirmed using double knockout mice deficient in both E- and P-selectin (Frenette *et al.*, 1996). Expression of E-selectin on endothelial cells is transcriptionally upregulated by IL-1, TNF-α and bacterial lipopolysaccharides (LPS), leading to a peak of expression 3-6 hours post-stimulation, which declines to basal levels within 48 hours. E-selectin expression is inhibited by transforming growth factor β (TGFβ) and IL-4.

1.2 Selectin ligands:Sialomucins

Following the molecular cloning of the various selectins it became obvious, given the presence of a lectin-like domain, that the selectins were likely to bind to oligosaccharides. The seminal advance in selectin ligand research came with the discovery that carbohydrate structures, specifically α(1→3)fucosylated derivatives of a tetrasaccharide known as Lewis x and sialyl Lewis x (sLe^x), are ligands for the selectins (reviewed by Springer and Lasky, 1994). Later results demonstrated that sulphation and phosphorylation of the L- and P-selectin ligands at sites discrete from the sLe^x core, either on the protein itself or as modifications of the oligosaccharide, were required for high affinity interaction between selectins and their ligands (Imai *et al.*, 1993; Pouyani and Seed, 1995; Wilkins *et al.*, 1995). The binding specificities of the selectins for specific target cell types suggests that although the carbohydrate ligands share similarities, the cell surface molecules bearing these ligands also confer specificity. As summarised below (and in Figure 1.1), a number of ligands have been identified for the selectins. With the exception of the E-selectin ligand, ESL-1, these ligands belong to a recently defined family of mucin like cell adhesion molecules called sialomucins (Shimizu and Shaw, 1993). The sialomucins are serine/threonine rich proteins that are heavily O-glycosylated, and have an extended structure to allow the exposure of multiple terminal sugars.

1.2.1 L-selectin ligands

Three L-selectin ligands have been identified from peripheral lymph node addressin (PNAd) purified with antibody MECA-79: GlyCAM-1, CD34 and an uncloned 200kDa protein. GlyCAM-1 is expressed predominantly in HEV which is consistent with a role for lymphocyte homing to the lymph nodes. However since it is expressed as a soluble form it is not clear if its main role is as an adhesive ligand, as a soluble competitor of membrane bound ligands, or in upregulating adhesion through cross-talk to β2 integrins (Hwang *et al.*, 1996). CD34 is a widely expressed sialomucin, found on most blood vessels, as well as haematopoietic progenitors (Simmons *et al.*, 1992). The L-selectin ligand activity is dependent upon appropriate post-translational glycosylation and sulphation, so that L-selectin mediated adhesion is specific to subsets of CD34 appropriately modified. Interestingly CD34 expression by endothelial cells is regulated by cytokines in a reciprocal fashion to the selectins, so that inflammatory cytokines such as IL-1, INF-γ and TNF-α reduce CD34 expression whilst increasing selectin, VCAM-1 and ICAM-1 expression (see

below). Hence CD34 is thought to promote recirculation of lymphocytes under normal, but not inflammatory conditions.

The fourth ligand for L-selectin is the mucosal addressin MAdCAM-1 (Berg *et al.*, 1993). MAdCAM is a transmembrane protein which has domain structure which reflects its binding properties. Human MAdCAM (Shyjan *et al.*, 1996) has two NH_2-terminal immunoglobulin like domains of which the first is involved in binding to the integrin $\alpha4\beta7$ (Berlin *et al.*, 1993), followed by a mucin-like region which is thought to bind to L-selectin. In murine MAdCAM (Briskin *et al.*, 1993), the mucin-like domain is followed by a third immunoglobulin-like fold which is similar to IgA, although the functional significance of this domain is not clear. More recently, the P-selectin ligand, PSGL-1 (see below) has also been shown to bind to L-selectin (Guyer *et al.*, 1996).

1.2.2 P-Selectin ligands

The best characterised P-selectin ligand is PSGL-1, which has been shown to mediate P-selectin dependent adhesion under both static and flow conditions (Sako *et al.*, 1993). It was isolated by an expression cloning strategy using COS cells co-transfected with 3/4-fucosyl-transferase and the cDNA library to be screened, thus allowing the ligand to be expressed and correctly glycosylated for functional ligand activity. PSGL-1 is a transmembrane sialomucin of 110kDa which forms intermolecular disulphide-linked dimers on the surface of leukocytes.

1.2.3 E-Selectin ligands

Several different leukocyte cell surface structures have been reported as mediating E-selectin adhesion. To date the most well characterised and cloned ligands are the E-selectin ligand-1 (ESL-1), and PSGL-1. ESL-1 appears to be unique amongst selectin ligands since it is not a sialomucin but a variant of the cysteine-rich fibroblast growth factor receptor, except for a unique 70-amino acid NH_2-terminal domain of mature ESL-1 (Steegmaier *et al.*, 1995). Although E- and P-selectins bind to PSGL-1, this appears to involve different regions of the structure. The 10 amino terminal residues of PSGL-1 are required for P-selectin binding and contain a tyrosine residue which becomes sulphated, but these amino acids are not required for E-selectin adhesion. A number of other E-selectin ligands have been reported, including CLA, (Berg *et al.*, 1991), L-selectin (Picker *et al.*, 1991;

Kishimoto *et al.*, 1991), CD66 (Kuijpers *et al.*, 1992), and even β2 integrins (Kotovuori *et al.*, 1993). Recent reports however indicate that CLA is an isoform of PSGL-1 (Keiffer *et al.*, 1997), and the *in vivo* functional relevance of ligands other than PSGL-1 and ESL-1 remains to be established.

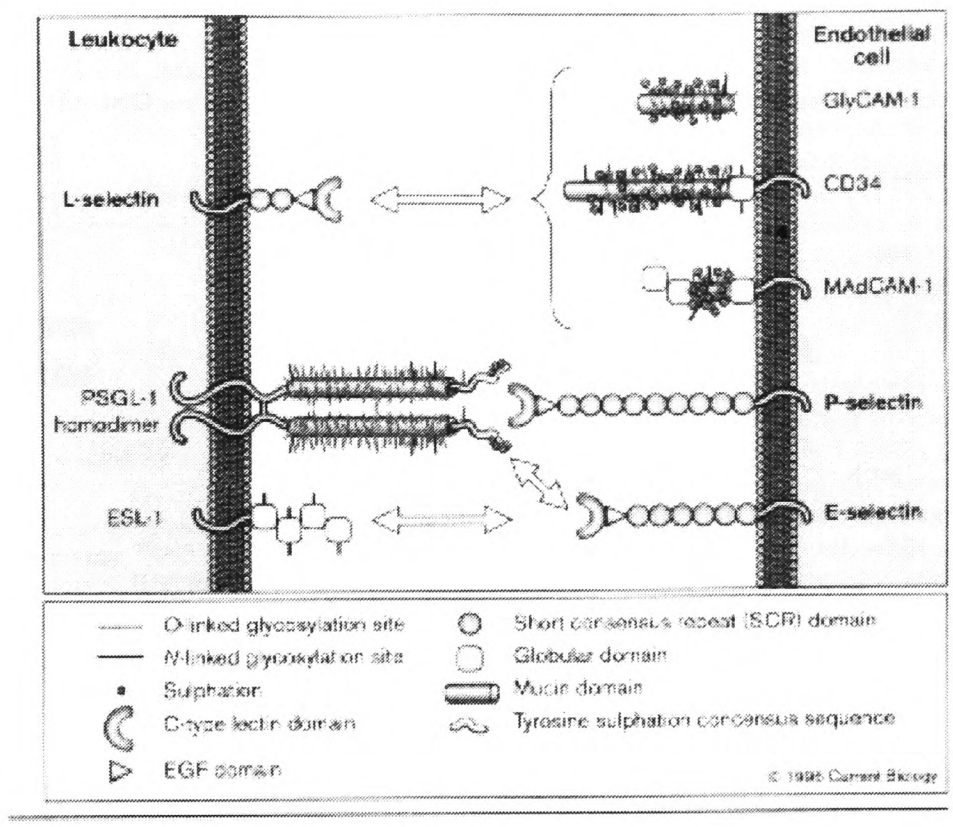


Figure 1.1 The domain organisation of the selectins and their cloned physiological ligands. Ligands which have only been identified by biochemical means, or for which there is limited evidence for a physiological role are not shown. Figure taken from Rosen and Bertozzi (1996).

2. Integrins

In contrast to the selectins discussed above which mediate adhesive interactions exclusively between leukocytes and endothelium, members of the integrin family are involved in a diverse range of biological processes. Integrins were originally identified as playing a major role in maintaining tissue integrity and binding extracellular matrix, however integrins are also involved in dynamic processes such as fertilisation (Wassarman, 1995), development, would healing and angiogenesis (reviewed by Hynes, 1992), in addition to leukocyte-endothelial interactions. Leukocytes are well endowed with integrins (Figure 1.2). Of the twenty two integrins identified to date, leukocytes express thirteen, of which seven have are involved in leukocyte-endothelial interactions (Stewart *et al.*, 1995). In addition to mediating leukocyte-endothelial interactions during inflammation, leukocyte integrins are also important in other aspects of immune function, such as antigen presentation, cell-mediated cytotoxicity and phagocytosis (Springer, 1990). The importance

of the broad range of immune functions mediated by integrins is demonstrated by clinical syndromes arising from mutations in the genes coding for these proteins (for example LAD, leukocyte adhesion deficiency) and by the dramatic, often lethal phenotypes that result in mice deficient in integrins (see Fassler *et al*, 1996 for review).

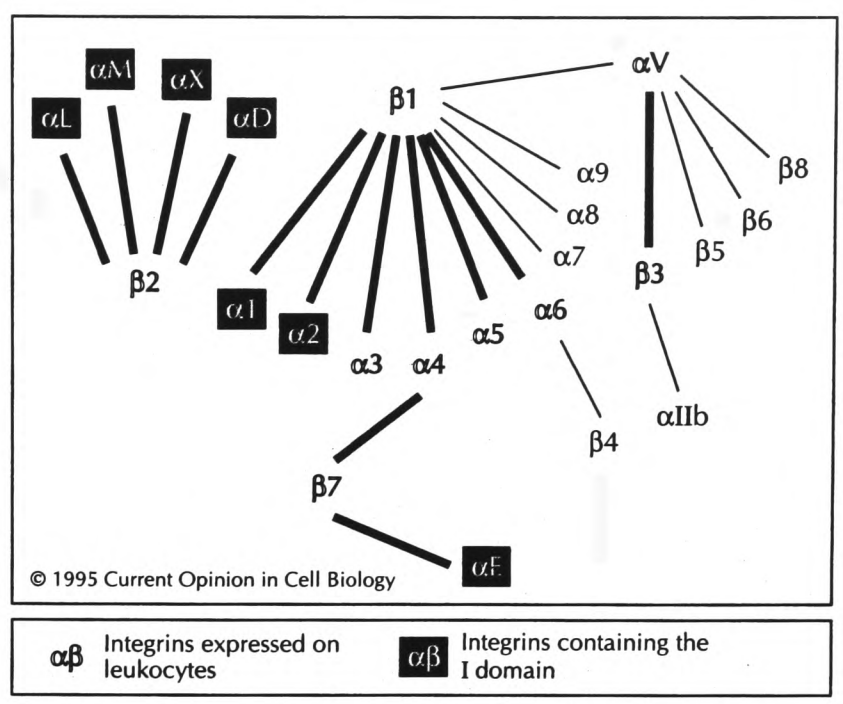


Figure 1.2. The integrin family of receptors. Lines show recognised αβ subunit pairings, with solid lines denoting integrins expressed on leukocytes. Integrins containing the inserted (I or A) domains are indicated. Taken from Stewart *et al.*, 1995.

2.1 Integrin structures

Integrins are heterodimers, comprised of non-covalently associated α and β chains. To date, 16 α chain subunits, and 8 β chain subunits have been identified. The formation of αβ heterodimers is not a stochastic process, and only certain combinations are "allowed" (see figure 1.2). Cellular adhesive properties are regulated by the selective expression of the integrin repertoire and by the modulation of their binding properties.

The extracellular regions of the α-subunits are comprised of seven homologous, tandemly repeated domains of around 50 amino acids. Repeats 4-7 (or in some integrins 5-7) contain cation-binding sequences, similar to the EF-hand fold in cytosolic Ca^{2+} binding proteins such as calmodulin. Seven integrin α subunits (α1,α2,αE,αL,αM,αX,and αD) contain a domain of 200 amino acids inserted between the second and third N-terminal repeats. This inserted or "I"-domain is homologous to the "A" domain of von Willebrand factor and to the heterotrimeric G-protein α-subunits, and has been shown to contain a single cation binding site. For α-subunits containing an I-domain there is now considerable evidence to implicate this region in ligand binding (for review see Mould, 1996). For many I-domain

containing integrins it is possible to recapitulate the adhesive properties of the integrin heterodimers with recombinant I-domain alone (Randi and Hogg, 1994; Zhou *et al.*, 1994; Calderwood *et al.*, 1997). The I-domain forms a relatively small part of the extracellular domain of seven integrin α-subunits, however recent modelling of the tandem repeats present in all α-subunits has predicted that these repeats fold into β-propeller domains (Springer, 1997), that are most closely related to the β-subunit of heterotrimeric G-proteins. This protein domain is comprised of seven four-stranded β-sheets arranged in a torus around a pseudosymetry axis. For integrins which lack an I-domain, the integrin ligand binding and Mg^{2+} divalent cation binding site are predicted to be formed by loops on the upper surface of the β-propeller, whilst the Ca^{2+} binding sites are predicted to lie on the lower face of the β-propeller. The use of a similar folds by integrins and heterotrimeric G-proteins, suggests that by analogy the integrin Ca^{2+} binding domains may be able to interact with the I-domains in a regulated fashion, indeed the fact that I domain is linked to the β-propeller domains by hinge-like loops indicates that the domains may move relative to one another, which is consistent with the idea of integrins as allosteric proteins proposed by Mould and others (see below).

Although not all of the α-subunits contain an I-domain, all of the β-subunits contain a conserved sequence in their NH_2-terminal region, which, based on hydropathy plots, appears to contain an I-domain Rossmann-like fold similar to that for the solved I-domains from a number of integrins (Lee *et al.*, 1995). This hypothesis is supported by the observation that for β3 integrins the primary binding site for ligand-mimetic RGD-peptides lies within this region (D'Souza *et al.*, 1988; Smith and Cheresh, 1988; Pasqualini *et al* 1995). In addition, mutations in this domain of several β subunits have been shown to lead to loss of ligand binding (Loftus *et al.*, 1990; Bajt *et al.*, 1995; Puzon-McLaughlin and Takada; 1997), and by swapping sequences from this region between subunits to change ligand binding specificities (Takagi *et al.*, 1997). Finally, it has also been shown that a recombinant fragment containing the putative I-domain like from the β3 subunit was competent to bind directly to fibrinogen (Alemany *et al.*, 1996). Taken together these studies suggest that multiple binding sites in the NH_2-terminal regions of both α and β subunits co-operate in ligand binding.

A distinctive feature of integrins is their ability to modulate the level of adhesiveness rapidly and reversibly. This is essential in the process of leukocyte recruitment into sites of inflammation, since leukocytes must switch from a non-adhesive phenotype when moving in the blood under flow conditions, to an adherent phenotype during adhesion to and transmigration across the endothelial lining, and subsequent emigration into inflamed tissues. There appear to be at least two different mechanisms by which integrins are capable of regulating their adhesive properties. Firstly by increasing their affinity for individual ligands (see for example Ortlepp *et al.*, 1995), and secondly by receptor clustering to increase avidity, rather than affinity (Vankooyk *et al.*, 1994; Stewart *et al.*, 1996). There is ample evidence that integrins can change their affinity for their ligands, and that for integrins with multiple ligands, choice of ligand is determined by the activation state of the integrin, so that for example LFA-1 binds ICAM-1 at a lower activation state than to ICAM-3 (Buckley *et al.*, 1997). Control of integrin adhesiveness appears to be a bi-directional process influenced both by the extracellular environment of the cell ("outside-in") and cellular activation ("inside-out").

2.2 "Outside-in" signalling

A number of extracellular factors have been shown to regulate integrin mediated adhesion, including divalent cations (Dransfield *et al.*, 1992), monoclonal antibodies and bound ligand. Several lines of evidence suggest that ligand binding sites on integrins are cryptic and only become exposed on integrin activation. Using the platelet integrin αIIbβ3 as an example, first the proteolytic digestion patterns of active and inactive conformers of αIIbβ3 suggest that the sequences implicated in ligand recognition lie at the subunit interface (Calvete *et al.*, 1992). Second, a β3 mAb which binds to residues 109-128, an area known to be involved in RGD binding is only recognised by active conformers of αIIbβ3. Third, fluorescent resonance energy transfer experiments have shown a changed spatial separation or orientation on activation of αIIbβ3 (Sims *et al.*, 1991). Collectively these data suggest that the ligand binding site is located at the interface between subunits and that slight changes in relative orientation occur controlling exposure of the ligand binding site (Calvete, 1994). This has led to the proposal that integrins function as allosteric cell adhesion molecules (Mould, 1995; Humphries, 1996) which exist in either active or inactive conformations, so that only the active form is competent to bind ligand. It is proposed that extracellular factors such as divalent cations, or in experimental situations

stimulating and blocking monoclonal antibodies, bind to the integrin leading to conformational changes which favour the active ligand binding conformation. The idea that conformational changes occur within integrins is supported by the recently solved crystal structures for I-domains from the αM subunit containing co-ordinated Mg^{2+} or Mn^{2+} divalent cations. Significant changes are observed in the orientation and pitch of the NH_2-terminal portion of the I-domain relative to the COOH-terminal regions, although the authors proposed that the Mn^{2+} conformation represented the inactive conformation (Lee *et al.*, 1995a; Lee *et al.*, 1995b), contrary to *in vitro* cell adhesion assays where Mn^{2+} is usually found to activate integrins. This hypothesis would explain the observation that many stimulatory and inhibitory antibodies have been mapped to sites distant from the ligand binding site.

Following ligand engagement by integrins, signals are transduced into the cell, resulting in reorganisation of the actin cytoskeleton, recruitment of integrin receptors into focal adhesions and the generation of cytoplasmic signals. These properties are dependent upon the integrin cytoplasmic domains. Several proteins have been identified which interact directly with the cytoplasmic tails of different integrins, including cytoskeletal proteins α-actinin, talin, and filamin (reviewed Dedhar and Hannigan, 1996) and regulatory and signal transducing proteins including β3-endonexin (Sattil *et al.* ,1995), the integrin-linked kinase (ILK) (Hannigan *et al.*, 1996), cytohesin-1 (Kolanus *et al.*, 1996) and possibly focal adhesion kinase (FAK). It is postulated that the conformational changes induced by ligand binding to the extracellular domain are transmitted to the cytoplasmic tail leading to exposure of binding sites for cytoplasmic proteins in a fashion analogous to the exposure of cryptic ligand binding sites in the extracellular domains. This is consistent with the observation that a salt bridge exists between α and β subunit cytoplasmic tails of αIIbβ3, disruption of which by site-directed mutation leads to constitutive integrin activation and intracellular signalling (Hughes *et al.*, 1996).

2.3 "Inside-out" signalling.

Cell activation by chemokines, phorbol esters, or other mitogens, frequently leads to a rapid transient increase in integrin mediated adhesion. Increased integrin adhesiveness is caused by the activation of intracellular signalling pathways. For example, ectopic overexpression of R-Ras causes cell attachment and spreading in nonadherent cells, whilst dominant-

negative forms of R-Ras inhibit cell attachment, implicating small GTPases in the regulation of integrin adhesiveness (Zhang *et al.*, 1996). The role of signalling proteins, and small GTPases in particular, in regulating integrin adhesive phenotypes is also suggested by the observation that the assembly of integrin adhesion complexes, and the resulting downstream signalling events, require Rho/Rac GTPases (Hotchin and Hall, 1995) One possibility is that activation of the cell initiates signal transduction cascades which drive the assembly of integrin associated signalling complexes, leading to transmission of conformational changes to the extracellular domain and exposure of ligand binding sites.

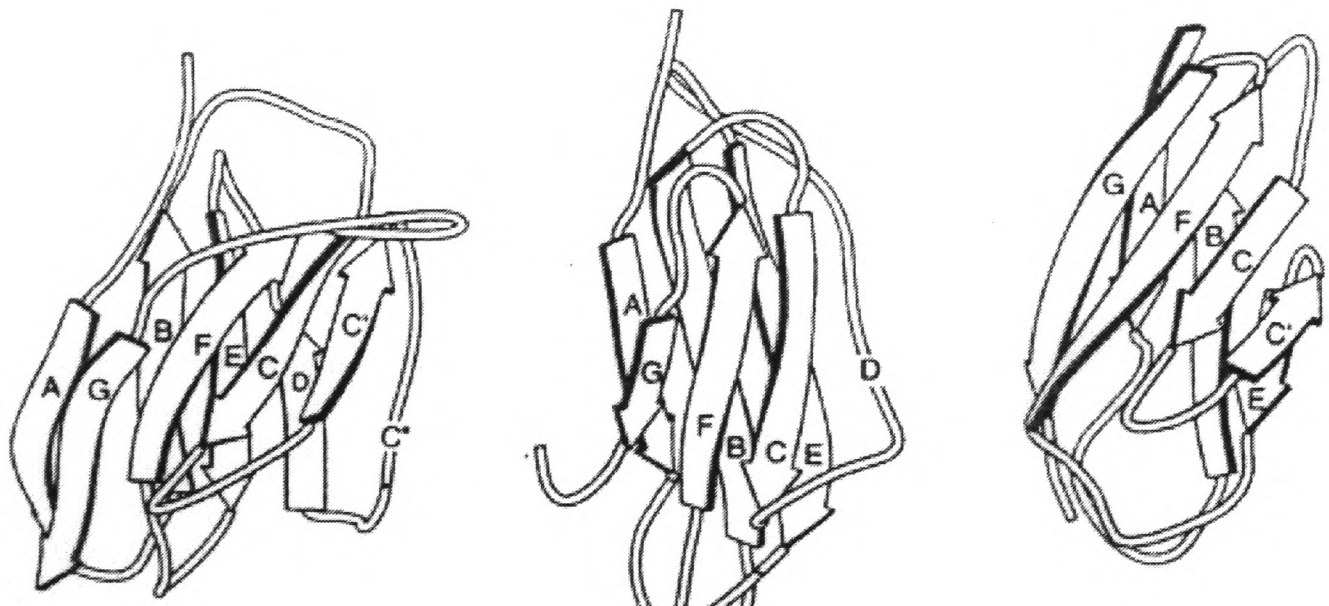
3. Immunoglobulin superfamily

3.1 The immunoglobulin fold

The immunoglobulin superfamily (IgSF) is a diverse family of proteins that perform a range of functions in cell-cell interactions, including cell adhesion, soluble ligand-receptor interactions and antigen recognition. The common feature within this family of proteins are that the extracellular domains are comprised of independently folding domains, or modules, (Campbell and Downing, 1994), usually encoded by a single exon, which share sequence homology (at low levels, typically in the range 10-30%) and topology with immunoglobulins (Williams and Barclay, 1988). Each immunoglobulin domain is comprised of 70-100 amino acids folded into two β-sheets comprised of anti-parallel β-strands each containing 5-10 amino acids. Between the β-sheets a hydrophobic core is formed from inward pointing hydrophobic amino acids that alternate with out-pointing hydrophilic residues in the β-strands. The interaction between the two sheets is further stabilised by the presence of a conserved disulphide bond.

Originally immunoglobulin superfamily members were further subdivided into three structurally defined "sets" on the basis of multiple sequence alignments; the V-set, C1-set and C2-set (Figure 1.3). V-set members show features in common with the variable antigen binding domains of immunoglobulins and contain more amino acids than the C1 and C2 subsets, which show strongest homology to the constant domains of immunoglobulins. Typically V-set domains have 65-75 residues between the conserved cysteines, and there are four β-strands in each β-sheet, plus a short β-strand segment across the top of the domain. In C-set domains the sequence between the disulphides is shorter at 55-60 residues. The distinction between C1 and C2 sets is based upon the fact that the C1 set

shows strong topological similarities to the constant portion of immunoglobulins, whereas the C2 subset has a number of sequence anomalies in the conserved sequences of C1 set domains. The structural determination of a number of canonical C2-set domains (telokin, VCAM-1, ICAM-2) showed that the sequence characteristics as originally defined are shared by two structurally distinct groups, a redefined C2 set and a new I set, which is structurally intermediate between V set and C1 sets (Harpaz and Chothia, 1994).



V-Set Domain C1-Set Domain C2-Set Domain

Figure 1.3 Ribbon diagrams for representative immunoglobulin domains. The V-Set domain is from the V_H of human NEW Fab fragment, the C1-set domain is from β_2-microglobulin, and the C2-set domain is from CD4 domain 2. Taken from Barclay et al., 1993

The immunoglobulin fold mediates a variety of interactions, for example antigen-antibody complexes (reviewed by Mariuzza *et al.*, 1993), heterophilic interactions with integrins such as ICAM-1,2,3/LFA-1, VCAM-1/VLA-4, MAdCAM-1/α4β7 and CD31/αvβ3 (reviewed by Newham and Humphries 1996), pseudo-homophilic interactions, e.g. CD2/CD48 (Van der Merwe *et al.*, 1995), and fully homophilic interactions such as NCAM-NCAM and CD31-CD31. A comparison of structures solved at atomic resolution shows that the regions peripheral to the hydrophobic core, such as the edge strands of the β-sheets and the loops that link the strands, can have quite different conformations. Mirroring this structural diversity different immunoglobulin-folds utilise different regions to interact with their ligands.

In antigen-antibody complexes, antigen recognition and binding is mediated by loops at the NH_2-terminal end of the fold. A recurring theme amongst integrin-IgSF interactions is the utilisation of acidic residues presented either in the NH_2-terminal portion of the loop joining the CD β-strands on the CFG face of the Ig fold, for example the QIDS motif in VCAM-1 (Renz *et al.*, 1994, Clements *et al.*, 1994, Chiu *et al.*, 1995), or in the C strand itself, as in the GIETS/LETS motif identified in ICAMs (Staunton *et al.*, 1990, Holness *et al.*, 1995, Klickstein *et al.*, 1996, Cassanovas *et al.*, 1997). In the case of CD2/CD48, a pseudo-homophilic interaction, mutagenesis data implicates an adhesive surface comprised of the equivalent GFCC'C'' faces of the immunoglobulin fold in both CD2 and CD48 (Van der Merwe *et al.*, 1995).

Of the 200 or so known members of the immunoglobulin superfamily, six are thought to participate in leukocyte-endothelial cell interactions, ICAM-1 (CD54), ICAM-2 (CD102), VCAM-1 (CD106), CD31 (PECAM-1), L1, and most recently identified JAM-1 (Figure 1.4)

3.2 ICAM family

The ICAM family (ICAM-1,2,3) were originally identified as ligands for the leukocyte β2 integrin LFA-1 (CD11a/CD18), and are products of distinct but homologous genes (for review see Simmons, 1995) whose extracellular domains are comprised of 5, 2, and 5 immunoglobulin-like folds respectively. ICAM-1 and ICAM-3 are more closely related to each other than to ICAM-2 and are found to map closely to each other on chromosome 19, whilst ICAM-2 maps to chromosome 17q23-25 (Sansom *et al.*, 1991, Ropers and Mohrenweier, 1993, Bossy *et al.*, 1994). By raising functional blocking antibodies to ICAM-1, ICAM-2, and ICAM-3 it has been shown that all of the LFA-1 dependent antigen-specific T cell responses are accounted for by the interaction of LFA-1 with these three adhesion molecules (de Fougerolles *et al.*, 1994). Although this finding suggests that there are no further ICAM ligands for LFA-1 two ICAM related molecules, telencephalin and the LW blood group protein have recently been cloned. Telencephalin is a brain segment specific neuronal adhesion molecule whose extracellular domain is comprised of nine immunoglobulin-like domains (Yoshihara *et al.*, 1994). The five NH_2-terminal domains are closely related to ICAM-1 and ICAM-3, and telencephalin also maps to chromosome 19. Importantly it has also been shown that telencephalin binds constitutively

to LFA-1, although the role of telencephalin is probably to bind LFA-1 expressing microglia rather than leukocytes (Mizuno *et al.*, 1997, Tian *et al.*, 1997). The LW blood group antigen expressed on red blood cells is comprised of two immunoglobulin like domains (Bailly *et al.*, 1994) with homology to the ICAMs which also binds to LFA-1 (Bailly *et al.*, 1995). The LW antigen is thought to play a role in haematopoiesis since it is expressed on early erythroid progenitors in addition to red blood cells.

The most closely related regions in all of the ICAM family are in the NH_2-terminal domains. The LFA-1 binding site for all three classical ICAMs have been localised to domain 1 (Staunton *et al.*, 1990, Li *et al.*, 1993, Holness *et al.*, 1995). Site-directed mutagenesis in combination with the crystal structure of ICAM-2 shows that critical glutamate residues involved in mediating adhesion to LFA-1 reside on a flat surface on the CFG face, where the glutamate residue is located at the COOH-terminal end of the C-strand (Holness *et al.*, 1995, Klickstein *et al.*, 1996, Cassanovas *et al.*, 1997). This residue is believed to interact with the I-domain of CD11a via a co-ordinating divalent cation (Qu *et al.*, 1995; Qu *et al.*, 1996). In addition to the conserved acidic residues on the CFG face, additional residues, especially in the E-F-loop of domain 1, are also thought to be involved in ligand binding and may provide "specificity" determining residues.

Despite the high degree of homology between the ICAMs, their distribution patterns and functions are very different. ICAM-1 is expressed at low levels on resting leukocytes and at very low levels on endothelium and fibroblasts, however, it is rapidly upregulated by inflammatory cytokines such as IL-1β, TNF-α and INF-γ. In contrast, ICAM-2 is expressed constitutively but at relatively low levels on lymphocytes, endothelial cells and platelets, whereas ICAM-3 is constitutively and abundantly expressed on leukocytes. Unlike ICAM-1, expression of ICAM-2 and ICAM-3 is not induced by cytokines. Induction of ICAM-1 on endothelium and other cell types by inflammatory cytokines is therefore likely to increase adhesion between the endothelium and leukocytes, whilst the role of ICAM-2 may be in basal leukocyte trafficking and recirculation. This hypothesis is supported by the results from mice deficient in ICAM-1 (Sligh *et al.*, 1993) which have shown that ICAM-1 is the main inflammatory ligand for LFA-1. Since ICAM-3 is expressed at very high levels on all leukocytes, including resting leukocytes, it has been suggested that it is involved in the initiation of immune responses rather than in leukocyte transmigration. This is

consistent with the observation that ICAM-3 is the predominant ligand for LFA-1 on professional antigen presenting cells such as human blood dendritic cells (Starling *et al.*, 1995). In this respect it is interesting to note that LFA-1 appears to require a higher activation state to bind ICAM-3 than ICAM-1 (Buckley *et al.*, 1997), which may present an activation "threshold" to prevent inappropriate stimulation of leukocytes by dendritic cells in the absence of appropriate specific signals such as antigen recognition.

In addition to LFA-1, various ICAMs also bind to other ligands. ICAM-1 binds to the leukocyte integrin Mac-1 (CD11b/CD18) via domain 3 (Diamond *et al.*, 1991), as well as to *Plasmodium falciparum* infected erythrocytes (Berendt *et al.*, 1992), Rhinovirus (Staunton *et al.*, 1990) and fibrinogen (Languino *et al.*, 1993; Duperray *et al.*, 1997). In addition CD43 (Rosenstein *et al.*, 1991), and hyaluronan (McCourt *et al.*, 1994) have also been reported to bind to ICAM-1, although the status of these ligands has not been confirmed on subsequent analysis. Recently it has also been shown that ICAM-3 binds to the novel leukocyte integrin αdβ2 (CD11d/CD18), but the biological significance of this interaction has not been established (Van der Vieren et al., 1995).

3.3 VCAM-1 (CD106)

VCAM-1 was first identified as a cytokine inducible cell adhesion molecule expressed on endothelial cells and involved in the adhesion of leukocytes to endothelium. It was cloned in a remarkable tour de force with expression cloning by screening a subtracted library of cytokine inducible endothelial molecules for the binding of lymphoid cell lines to COS cells expressing pools of clones from the library. Individual COS cells binding labelled leukocytes were picked and plasmid DNA recovered for subsequent rounds of screening (Osborn *et al.*, 1989). A single VCAM-1 gene gives rise to three isoforms through alternative splicing. The prevalent form of VCAM-1 in humans has an extracellular domain of seven IgSF domains, in which domains 1-3 are homologous to domains 4-6 (Polte *et al.*, 1990). A minor 6 IgSF domain variant lacking domain 4 (and the form originally cloned by Osborn and co-workers) is also present in human and mouse. A third variant, thus far observed only in the mouse, comprised of domains 1-3 expressed on a GPI membrane anchor has also been detected. Interestingly, in the mouse this appears to be the form most readily induced by inflammatory cytokines (Terry *et al.*, 1993).

The primary ligand for VCAM-1 is VLA-4/α4β1 (Elicess *et al.*, 1990), although the integrin α4β7 is also capable of binding to VCAM-1 *in vitro*, but this may not be a physiologically significant interaction *in vivo*. The interaction between VCAM-1 and VLA-4 can be mediated either by domain 1 or 4, although adhesion to domain 1 appears to be the preferred site and 1 occurs at 4°C without cell activation, whilst adhesion to domain 4 requires cell activation (Needham *et al.*, 1994; Kilger *et al.*, 1995). The integrin α4β7 however exhibits the converse pattern, and binds preferentially via domain 4 (Kilger *et al.*, 1995). Intriguingly, binding between VLA-4 and VCAM-1 is also affected by CD24 expression, so that in CD24 deficient mice lymphocytes bind preferentially to domain 4 of VCAM-1 (Kilger *et al.*, 1995). The residues required for adhesion of VCAM-1 domain 1 to both VLA-4 and α4β7 have been extensively investigated (Renz *et al.*, 1994, Clements *et al.*, 1994, Chiu *et al.*, 1995 and Jones *et al.*, 1995) and consist of a common acidic motif in the CD-loop (QIDS), in addition to specific residues involved in conferring specificity of adhesion to the two integrins.

Unlike the ICAMs, VCAM-1 can support the rolling and firm adhesion of cultured T-lymphocytes out of flow, independently from selectin mediated rolling (see section D below). This may be due to the apparently unique ability of VCAM-1 compared to other IgSF/integrin interactions, to bind to VLA-4 via domain 1 without any previous cell activation and priming. It is possible that tethering and rolling on VCAM-1 might occur via domain 1, with domain 4 engaged at the firm adhesion step (Stewart *et al.*, 1995).

3.4 CD31/PECAM-1

This thesis is concerned with the structure and function of CD31, also known as Platelet Endothelial Cell Adhesion Molecule-1 (PECAM-1). CD31 is widely expressed on cells of the vascular compartment, including endothelial cells, platelets, myeloid cells, subsets of T-lymphocytes, and on $CD34^+$ haematopoietic progenitor cells. Consequently, CD31 is in a unique position to mediate a range of homotypic and heterotypic cell-cell interactions. CD31 is a member of the immunoglobulin superfamily whose extracellular region of 574 amino acids is composed of six immunoglobulin-like domains, followed by a single transmembrane passing domain and a cytoplasmic domain of 118 amino acids (for review see Newman, 1997). The CD31 gene covers around 60kb on chromosome 17 (Kirschbaum *et al.*, 1994), most strikingly the cytoplasmic tail is encoded by six exons from which it is

possible to derive a number of splice variants, the expression of which has been shown to be controlled in a developmentally specific manner (Baldwin *et al.*, 1994) and to influence the adhesive properties of CD31 expressing cells in heterologous systems (DeLisser *et al.*, 1994).

CD31 is involved in a wide range of adhesive interactions. The distribution of CD31 at the junctions between cells in endothelial monolayers was suggestive of a homophilic interaction, and this has subsequently been confirmed in a number of heterologous models (Albelda *et al.*, 1991; Fawcett *et al.*, 1995, Sun *et al.*, 1996a). In addition to a homophilic mode of adhesion a number of heterophilic ligands have been identified, including cell surface glycosaminoglycans (DeLisser *et al.*, 1992), the integrin αvβ3 (Piali *et al.*, 1995, Buckley *et al.*, 1996, see Chapter 6), a 120kDa ligand expressed on T-cells (Prager *et al.*, 1996), and CD38 (Professor F. Malavasi, personal communication, see also Chapter 6)

A large body of evidence, both *in vitro* and *in vivo* has shown that CD31 is involved in the transendothelial migration of monocytes and neutrophils (Vaporciyan *et al.*, 1993; Muller *et al.*, 1993; Bogen *et al.*, 1994; Liao *et al.*, 1995; Wakelin *et al.*, 1996). In *in vitro* assays, treatment of either endothelial monolayers or leukocytes with anti-CD31 monoclonal antibodies inhibit the transmigration of leukocytes across the endothelial monolayer. Microscopic examination showed that the inhibition did not affect leukocyte adhesion to endothelium, but blocked subsequent transmigration across the monolayer. That anti-CD31 monoclonal antibodies were effective in blocking transmigration when either endothelial cells or leukocytes were treated suggested that a homophilic interaction are involved. However, the presence of multiple ligands for CD31 expressed on both endothelium and leukocytes makes interpretation of these results problematic.

The residues and domains involved in both homophilic and heterophilic adhesion have proved difficult to define, and there has been considerable debate as to the precise details even for homophilic adhesion, with a number of contradictory models proposed (Fawcett *et al.*, 1995; Sun *et al.*, 1996a). In addition to directly mediating adhesive interactions, CD31 also indirectly influences the adhesive phenotype of CD31-bearing cells. CD31 homophilic engagement has been shown to enhance β1, β2 and β3 integrin mediated adhesion (Tanaka *et al.*, 1992, Piali *et al.*, 1992, Leavesley *et al.*, 1994, Fawcett *et al.*, 1995, Berman *et al.*,

1995, Jackson *et al.*, 1997), a process which seems to reflect the ability of CD31 to transduce signals. Much recent work has shown that CD31 becomes tyrosine phosphorylated on Y_{686} in response to a number of physiological signals such as osmotic shock, shear flow, engagement of IgE receptors, or platelet aggregation (Osawa *et al.*, 1997, Lu *et al.*, 1997, Sagawa *et al.*, 1997, Jackson *et al.*, 1997) leading to the recruitment of the SH2 bearing cytoplasmic tyrosine phosphatase SHP-2.

3.5 MAdCAM-1

The structure and expression patterns of MAdCAM-1 have been described previously in the context of its role as a ligand for L-selectin. MAdCAM-1 also binds the integrin α4β7, which is expressed preferentially by lymphocyte subsets that home to mucosal tissues in the gut, and increased expression of MAdCAM-1 in mucosal endothelium is associated with inflammatory bowel disease (Crohn's disease. Ulterative colitis). The integrin binding site is located within the NH_2-terminal immunoglobulin-like domain, and has been demonstrated to consist of an acidic LDT motif in the putative CD-loop (Viney *et al.*, 1996), analogous to the QIDS motif in VCAM-1, although unlike VCAM-1, MAdCAM-1 does not bind to VLA-4 (Berlin *et al.*, 1993).

3.6 L1

L1 (also known as Ng-CAM/NILE) is a 200kDa adhesion molecule, whose extracellular region is composed of six immunoglobulin-like domains followed by five fibronectin type III repeats. These are linked by a transmembrane helix to a small intracellular domain (Moos *et al.*, 1988). L1 was originally defined as a neural cell adhesion molecule that plays an important role in neurogenesis, nerve growth and fasciculation (Rathjen and Schachner, 1984). Consistent with this role mutations in the gene for L1 result in the related genetic diseases X-linked hydrocephalus, MASA syndrome (mental-retardation, aphasia, shuffling gait and adducted thumbs) and spastic paraplegia type I (Rosenthal *et al.*, 1992; Vits *et al.*, 1994; Jouet *et al.*, 1994). In neuronal cells, L1 regulates adhesion by a number of mechanisms; by direct homophilic adhesion (Holm *et al.*, 1995), heterophilic interaction with the axon associated cell adhesion molecule axonin-1/TAG-1 (Buchstaller *et al.*, 1996) and assisted homophilic interactions between L1 and L1/NCAM complexes (Kadmon *et al.*, 1990, reviewed by Feizi, 1994). In addition to a role in neurite development, more recent studies have also shown that L1 is expressed on lymphoid cells (Kowitz *et al.*,

1992), and that lymphoid cells expressing L1 can bind in an L1-specific, divalent cation and temperature dependent manner to non-induced endothelioma cells (Hubbe *et al.*, 1993). Recently, both α5β1 (Ruppert *et al.*, 1995) and αvβ3 (Montgomery *et al.*, 1996) have been shown to be ligands for L1, binding via RGD-sequences in immunoglobulin-like domain 6. Interestingly, Ruppert and co-workers also showed that cellular activation by phorbol esters, concanavalin-A or anti-CD3 cross-linking mAbs caused a downregulation in L1 expression, with a time course that mirrored L-selectin shedding, and have suggested that this may represent a mechanism of negative feedback following inflammatory stimuli.

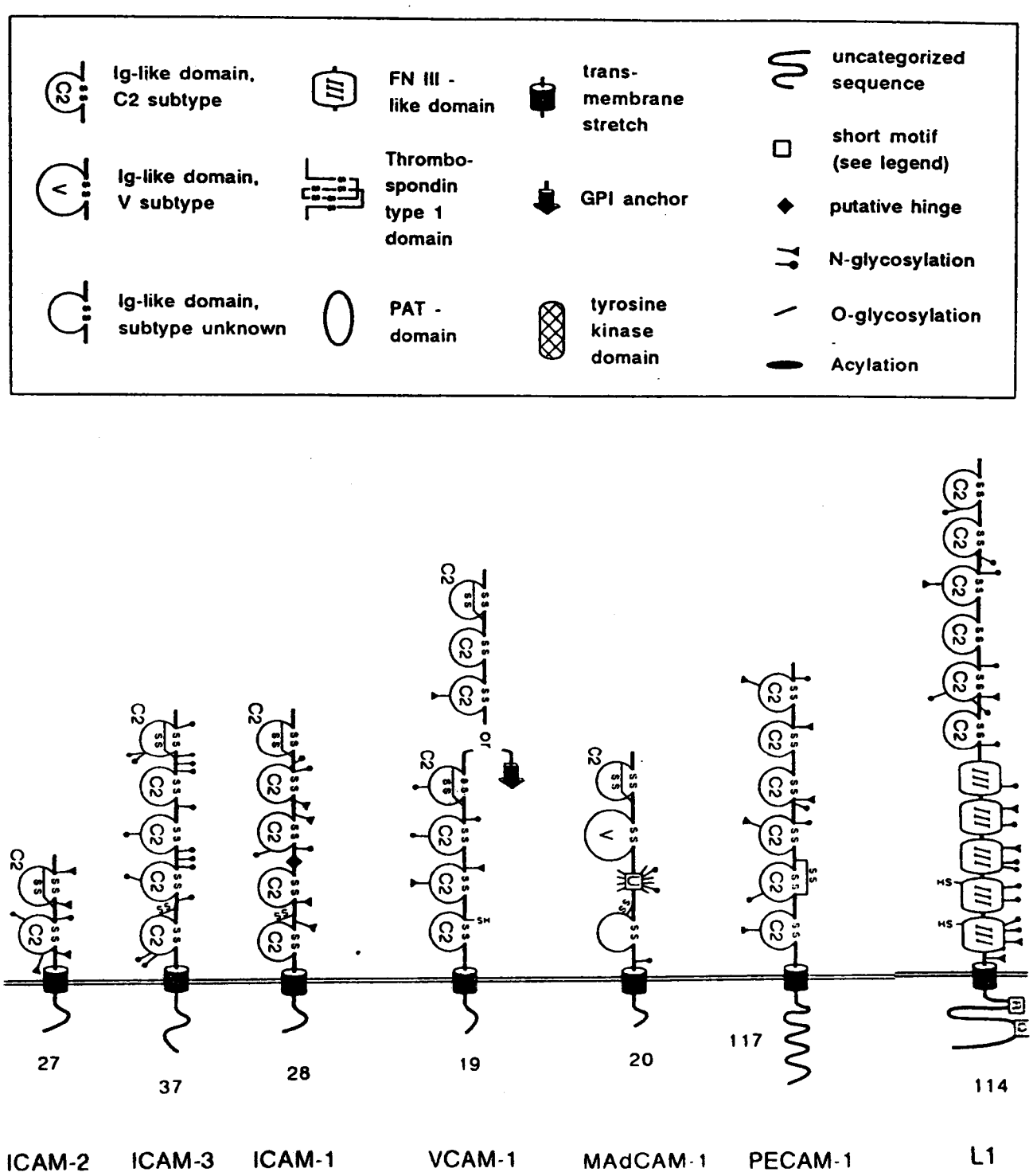


Figure 1.4 Schematic representation of immunoglobulin superfamily members involved in leukocyte-endothelial interactions adapted from Brummendorf and Rathjen, 1994. JAM-1, which has recently been cloned, is not shown, but has an extracellular region comprised of two V-set domains, a single transmembrane pass, and a short cytoplasmic tail of 75 residues.

3.7 JAM-1

JAM-1 (Junctional Adhesion Molecule-1) is a recently cloned member of the immunoglobulin superfamily whose extracellular domain is comprised of two V-set domains (Martin-Padura *et al.*, submitted). JAM-1 co-distributes with tight junction components in both endothelial and epithelial cells suggesting a role in homotypic cell adhesion. In addition antibodies against JAM-1 have been shown to block monocyte transmigration *in vivo* in an air-pouch model, and *in vitro* in both spontaneous and chemokine induced (monocyte chemotactic protein-1 and -3, MCP-1 and MCP-3) monocyte transmigration experiments. In a similar result to that obtained with anti-CD31 monoclonal antibodies, the anti-JAM-1 mAb BV11 was found to inhibit transmigration, but not adhesion of monocytes to endothelium.

4. Other adhesion molecules

4.1 CD44

CD44 is an abundantly expressed cell surface glycoprotein which is expressed on haematopoietic and non-haematopoietic cells (epithelial, endothelial, mesothelial, mesenchymal and cells in the nervous system), which binds hyaluronan (Arrufo *et al.*, 1990). The ability of CD44 to bind hyaluronan is highly regulated, so that for example leukocytes expressing CD44 do not bind hyaluronan constitutively, but do so following activation (Lesley *et al.*, 1994). The mechanisms implicated in regulating binding include clustering, altered glycosylation (Bartolazzi *et al.*, 1996), differential splicing (Bennett *et al.*, 1995b) and interactions with the cytoskeleton (Lesley *et al.*, 1993). CD44 is present in multiple isoforms varying in apparent molecular weight from 80-250 kDa. This large variation in molecular weight is due to extensive alternative splicing. In the standard form of CD44 without variable exons (CD44H), the extracellular domain is comprised of a 250 amino acid NH_2-terminal domain which contains the hyaluronic acid binding site and is homologous to the link domains from cartilage proteins. This is followed by a membrane proximal mucin-like domain which is heavily glycosylated and is also modified with chondrotin sulphate (Jackson *et al.*, 1995), a transmembrane segment, and a cytoplasmic tail of 70 amino acids. Other CD44 isoforms are generated by the insertion of various combinations of at least nine exons (v2-v10) into the mucin-like sequences (Screaton *et al.*, 1993). These variable exons also encode mucin-like sequences containing approximately

30% serine/threonine residues which carry both O- and N-linked oligosaccharides. In addition the v3 exon is covalently modified by heparin sulphate, which may provide binding sites for chemokines and be involved in the immobilisation and presentation of inflammatory mediators on endothelium (Bennett *et al.*, 1995a). CD44 contributes to the adhesion of leukocytes to endothelial cells via hyaluronan (DeGrendele *et al.*, 1996). The presence of certain variant exons, particularly v6 and v3, are associated with increased metastatic potential of tumours (Bartolazzi *et al.*, 1995, Lesley *et al.*, 1993)

4.2 VAP-1 and VAP-2

Vascular associated proteins -1 and -2 were identified as being involved in leukocyte adhesion to synovium and endothelium (Salmi and Jalkanen, 1992). Neither VAP-1 or VAP-2 have been identified at a molecular level. VAP-1 is a sialoglycoprotein of 90kDa expressed on endothelial cells in venules of most human lymphoid tissue, except that associated with mucosa, and recent work has shown it to be involved in non-L-selectin dependent adhesion of lymphocytes to HEV under conditions of flow (Salmi and Jalkanen, 1996), and in lymphocyte homing to inflamed skin (Arvilommi *et al.*, 1996). VAP-2 is a 70kDa protein constitutively expressed on endothelium, B-cells, and $CD8^+$ T-cells which is believed to play a role in lymphocyte adhesion to endothelium (Airas *et al.*, 1993)

D: Regulation of adhesion and leukocyte extravasation

1. Adhesion cascades and the multi-step paradigm

Intravital microscopy identified three distinct steps involved in leukocyte-endothelial transmigration. Following initial contact between leukocytes and endothelial cells some leukocytes slow by rolling along the vessel wall, then slow further and spread on the endothelium adhering firmly, before transmigrating between endothelial cells. Based upon these physiological observations and the cloned adhesion molecules described previously, Butcher (1991) proposed a multistep, sequential cascade of leukocyte binding to endothelium. In the same year direct evidence for this model was produced by Lawrence and Springer (1991) by reconstituting the observed pattern of rolling and firm adhesion using purified adhesion molecules in an *in vitro* chamber to show that P-selectin mediated rolling and ICAM-1 was required for firm adhesion. This permitted time-lapse microscopic examination of adhesion under defined, physiologically relevant flow conditions. Initial

studies concentrated on neutrophils, although subsequent work has also confirmed the generality of this model to other leukocyte subsets, including T-lymphocytes, monocytes, eosinophils and lymphocytes homing to HEV. Essentially the model can be divided into four distinct but overlapping steps: First, primary adhesion leading to rolling/tethering. Second, leukocyte activation by membrane bound cytokines and other inflammatory mediators. Third, cell spreading and strong adhesion, and fourth, transmigration/diapedesis (Figure 1.5).

1.1 Rolling.

Data from selectin deficient mice, antibody blockade and soluble recombinant selectin-IgG Fc chimeras have shown that selectins are involved in the initial adhesion of leukocytes to endothelium, and subsequent slowing of leukocyte velocity by rolling. The large number selectin ligands suggests that cells may utilise different combinations of selectins/ligands to mediate rolling, allowing synergy in selectin function (reviewed by Ley and Tedder, 1995). The ability to roll is thought to be conferred by the high tensile strength of the selectin-carbohydrate ligand interaction and the rapid on/off rate (Alon *et al.*, 1995). Recent work has shown that selectin mediated rolling is dependent upon the correct sub-cellular localisation of the selectins to the tips of microvilli present on the surface of leukocytes, since mutations in the L-selectin cytoplasmic tail which prevent this localisation appear to block rolling mediated by L-selectin (von Andrian *et al.*, 1995). More recently it has also been shown that the integrins $\alpha4\beta1$ and $\alpha4\beta7$ can also mediate rolling under physiological flow conditions, by binding to VCAM-1 and MAdCAM-1 respectively (Berlin *et al.*, 1995; Alon *et al.*, 1995b). This later mechanism is likely to be important in mediating adhesion from flow in activated T-cells, which lack L-selectin.

It has also been shown that rolling can occur between cells other than leukocyte-endothelial cell interactions, for example neutrophils can undergo selectin mediated rolling on immobilised platelets (Buttrum *et al.*, 1993), and activated, adherent platelets can support all of the steps required for accumulation and emigration of neutrophils at sites of vascular injury (Diacovo *et al.*, 1996a). Similarly neutrophils have been shown to roll on neutrophils which are already adherent to endothelium in an L-selectin dependent interaction (Bargatze *et al.*, 1994), so that adherent neutrophils form nucleation sites initiating adhesion of neutrophils to endothelium. In an analogous fashion platelets have been shown to aid the

binding of lymphocytes to HEV by acting as inter-cellular bridges by binding to PNAd on HEV via P-selectin, and then binding P-selectin ligands such as PSGL-1 on leukocytes (Diacovo *et al.*, 1996b).

Ultimately, rolling allows the leukocyte to slow and adhere to the endothelial cell lining of the vasculature under hydrodynamic shear, permitting the second stage of leukocyte triggering to occur.

1.2 Triggering and Firm Adhesion

In order to undergo transmigration, leukocytes must adhere firmly to the endothelium and migrate to the endothelial cell-cell junctions, prior to undergoing transmigration. The switch from primary rolling contacts mostly mediated by selectins, as outlined above, requires the activation of β1 and β2 integrins to bind to their endothelial ligands (predominantly ICAM-1, ICAM-2, VCAM-1 and MAdCAM-1). Activation of integrins occurs extremely rapidly, possibly as soon as 1-3 seconds following initial cell-cell contacts and appears to involve G-coupled proteins (Bargatze *et al.*, 1993). Triggering appears to be induced by one of two different classes of molecules, the classical soluble chemoattractants, and cell surface molecules. Classical chemoattractants such as fMLP, C5a, PAF, or chemokines are small molecules and proteins which signal via seven transmembrane proteins coupled to heterotrimeric G-proteins (reviewed by Murphy 1994) resulting in inside-out regulation of integrin adhesion. Many of these chemoattractant molecules also aid subsequent transmigration by enhancing cell motility, chemotaxis and inducing changes in cell polarity. In addition to the classical chemoattractants, a variety of cell surface molecules may also activate integrins. For example the recently discovered CX_3C family of chemokines (Bazan *et al.*, 1997). In addition cell adhesion molecules may act as triggers, such as CD31 which is well established as an enhancer of β1, β2 and β3 integrin mediated adhesion following homophilic engagement. Similarly L-selectin engagement has been shown to trigger upregulation of β2 integrin activity (Simon *et al.*, 1995, Sikorski *et al.*, 1996).

1.3 Transmigration

The final step of leukocyte recruitment is transmigration, and this is perhaps the least well understood of the processes involved. Experiments have shown that transmigration does

not arise through increased permeability of the endothelial junctions, since the electrical resistance of the endothelial monolayer is maintained during the transmigration of leukocytes. This indicates that as inter-endothelial cell-cell junctions open to allow the leukocyte to pass through, a process which requires that endothelial cadherins and catenins undergo concerted disassembly and rearrangement (Delmaschio *et al.*, 1996), other transient interactions are made to maintain the overall integrity (for review see Brown, 1997). Transmigration has been shown to be inhibited either *in vivo* or *in vitro* by antibodies raised against the integrins α4β1 and α5β1, LFA-1 (CD11a/CD18), CD44, CD47 and CD31 (see Imhof and Duncan, 1995 and references herein), however, the precise role of these molecules has not been determined. It seems likely that the β1 integrins are involved in adhesion to and migration upon the perivascular extracellular matrix, however, the most interesting pair are CD31 and CD47 (also known as integrin associated protein, IAP). CD31 can form homophilic (CD31-CD31) contacts, and is expressed on both leukocytes and endothelium. Hence one attractive possibility is that CD31 homophilic contacts between leukocytes and endothelium are involved in maintaining vascular integrity. CD31 can also form heterophilic contacts with the integrin αvβ3, again both of which are widely expressed on leukocytes and endothelial cells, and αvβ3 is known to be associated with CD47, so one possibility that has been proposed is that these complexes interact during transmigration to control leukocyte progress and endothelial remodelling (Dunon *et al.*, 1996; Brown, 1997).

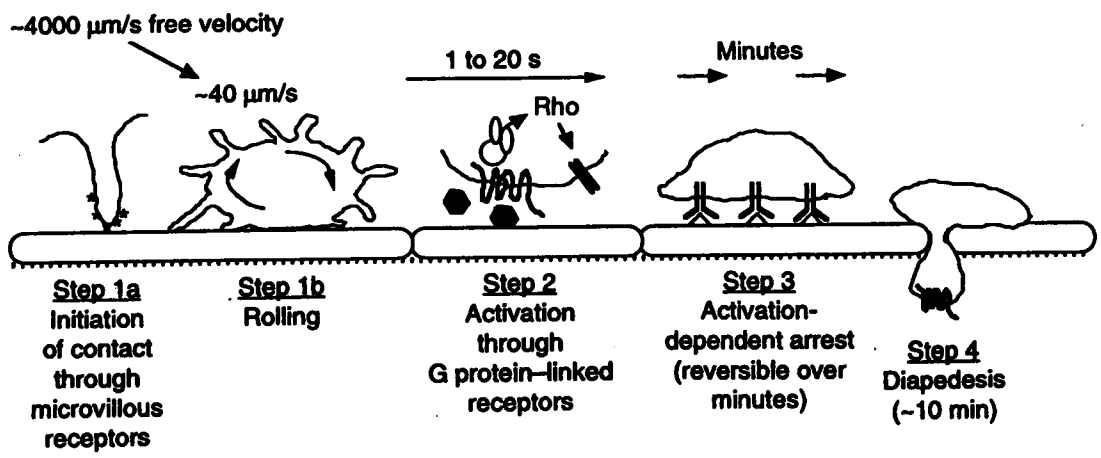


Figure 1.5 Multistep model of leukocyte-endothelial interactions during recruitment of leukocytes during recirculation and inflammation. The mean velocities of non-interacting and rolling lymphocytes from *in situ* microscopic studies in Peyer's patch HEV are shown. Taken from Butcher and Picker, 1996.

E: Organisation of endothelial cell-cell junctions and implication for transmigration

The endothelium is a continuous monolayer formed by cells linked to each other by different types of adhesive structures. Endothelial adherens junctions help to maintain polarity of the endothelial monolayer by restricting diffusion of proteins in the membrane, and are involved in the control of vascular permeability. In addition they are known to be involved in a large number of processes that affect the morphogenesis and physiology of the vessel wall, in addition to leukocyte transmigration described above, and pathological processes such as metastasis. Endothelial adherens junctions are comprised of transmembrane adhesion molecules, known as cadherins, that are organised in clusters at cell-cell contacts and connect via their cytoplasmic domains with a complex network of cytoskeletal proteins (reviewed by Huber *et al.*, 1996). Cadherins are single transmembrane pass glycoproteins, which usually consist of five homologous repeats of 110 amino acids in the extracellular domain. Despite virtually no sequence similarity, these repeats have a similar topology to the immunoglobulin superfamily fold, although they lack the characteristic disulphide bridge (Shapiro *et al.*, 1995). Cadherins are predominantly homophilic adhesion molecules and bind as dimers of dimers in a calcium dependent fashion to form supermolecular ribbons (Shapiro *et al.*, 1995). The cadherin cytoplasmic tail interacts with three proteins which belong to the so-called armadillo family, β-catenin, plakoglobin and p120, which themselves bind to α-catenin and vinculin (reviewed Peifer, 1995) and mediate linkage to the actin cytoskeleton. The cadherin-catenin complexes also recruit signalling molecules such as src-related kinases, small GTP binding proteins, and APC and are linked to cell cycle progression and endothelial morphogenesis. Intriguingly, CD31 forms a diffuse belt in a more basal position to the cadherins in the adherens junctions in unstimulated endothelial monolayers (Ayalon *et al.*, 1994). Inflammatory cytokines such as TNF-α and INF-γ induce a redistribution of CD31 from this basal position to the apical surface of the endothelium (Romer *et al.*, 1995), indicating that in the absence of appropriate stimulation inappropriate CD31 mediated leukocyte-endothelial interactions are blocked spatially. In addition to the adherens junctions and CD31, endothelial cells may form tight junctions and gap junctions (reviewed Dejana *et al.*, 1994), however these are prevalent in the major arteries and vascular branches, where little

transmigration occurs, and are virtually absent in post-capillary venules were most transmigration occurs, and are assumed not to play are role in mediating transmigration.

F: Outline of the thesis

CD31 is a cell adhesion molecule which is capable of mediating a wide range of adhesive interactions, both homophilic and heterophilic, in addition to functioning as an adhesion amplification signal for integrin mediated adhesion. It is widely expressed on cells of the vascular compartment, including vascular endothelium, platelets, monocytes, neutrophils, and subsets of T-cells. As such it is uniquely positioned to regulate the interaction of leukocytes with endothelium, and to participate in inter-endothelial interactions. Evidence from a large number of *in vivo* and *in vitro* studies have implicated CD31 as playing a key role in leukocyte transmigration, however it is not clear if transmigration involves homophilic, heterophilic or a combination of both modes of adhesion. Furthermore the mechanism of each mode of adhesion has been subject to contradictory findings from different research groups, for example the domains involved in mediating homophilic adhesion have been subject to vigorous debate for several years.

The major aim of this thesis has been to rigorously dissect CD31 mediated adhesion in order to clarify earlier contradictory findings. In Chapter three, the mechanism of homophilic adhesion is investigated using an extensive range of chimeric CD31 constructs, monoclonal antibodies, and site directed mutants to show that the homophilic binding site is located in the NH_2-terminus of the molecule, but that the membrane proximal domains play a key accessory role in the formation of stable adhesive contacts. This allowed a consensus model of CD31 homophilic adhesion to be proposed which is consistent with the results of all the major groups. One possibility suggested from this initial work was that CD31 may function as a dimer at the cell surface. In Chapter four, biophysical, molecular biology and biochemical techniques are used to show that CD31, either as soluble recombinant protein or cell surface expressed protein exists as an equilibrium between monomeric and dimeric forms. Chapter five, reports upon attempts to produce atomic resolution structures for either full length CD31 protein produced in mammalian cells, or fragments of CD31 produced in bacteria.

In addition to homophilic adhesion, CD31 has been proposed to bind to a number of non-CD31 heterophilic ligands. Chapter 6 describes the discovery that CD31 is a ligand for the integrin αvβ3, and the mapping of the integrin binding site to domain 3 of CD31. Finally, Chapter 7 investigates the functional role of CD31 homophilic and CD31-αvβ3 interactions in *in vitro* models of cell motility and transmigration.

Chapter Two: Materials and Methods

2.1 Media, solutions and other reagents

2.1.1 Bacterial culture medium

L Broth	Supplied by ICRF services 1% w/v Bacto-tryptone (Difco), 0.5% w/v yeast extract (Oxoid), 170 mM NaCl	
TYM broth	per Litre	20g bacto-tryptone 5g Yeast extract 100 ml 1M sodium chloride 10 ml 1M magnesium sulphate
	Autoclaved prior to use.	
SOB medium	per Litre	20g bacto-tryptone 5g yeast extract 100ml 1M sodium chloride 2.5ml 1M potassium chloride 10ml 1M magnesium chloride 10ml 1M magnesium sulphate
	Autoclaved prior to use.	
Frozen Storage Buffer (FSB)	per Litre	2.94g potassium acetate 7.46g potassium chloride 9.90g magnesium chloride 1.46g calcium chloride 0.02g hexamine cobalt chloride 100ml glycerol
Transformation buffer I (TFBI)	per 500 ml of solution	1.47g potassium acetate 4.95g manganese chloride 3.73g potassium chloride 0.73g calcium chloride 75 ml glycerol
	0.45µm filtered (not autoclaved) and stored at 4°C	
Transformation buffer II (TFBII)	per 500 ml of solution	1.05g MOPS (Sodium salt) 5.51g calcium chloride 0.37g potassium chloride 75 ml glycerol
	pH 7.0, 0.45µm filtered and stored at 4°C in 50 ml aliquots	
Antibiotics	Ampicillin was made up to 100 mg/ml in distilled water and stored at -20°C. Tetracycline made up as a stock solution of 30 mg/ml in 70% ethanol and stored at -20°C.	

2.1.2 Solutions for Molecular Biology

TE	10 mM Tris (pH 8.0), 1 mM EDTA	
10x TBE	Per litre of solution:	108g Tris base 55g sodium borate 9.3g EDTA (sodium salt) Final pH 8.2-8.4
50x TAE	Per litre of solution	242g Tris base 57.1 ml glacial acetic acid 100 ml 0.5M EDTA (pH 8.0)
	Ethidium Bromide stock solution (10 mg/ml) added to a final concentration of 20mg/ml	
Plasmid Extraction Solutions used in Alkaline Lysis:		
Solution I	per litre of solution	20 ml of 0.5m EDTA pH 8.0
	Working solution is 10mM EDTA pH8.0	
Solution II	per litre of Solution	40 ml of 5M sodium hydroxide 50 ml of 20% SDS
	Working solution is 0.2M NaOH, 1% SDS	
Solution III	per litre of solution	200g potassium acetate 80 ml glacial acetic acid
	Working solution is 5M potassium acetate (pH 4.7)	
DNA loading buffer	25% (w/v) Ficoll, 0.25% (w/v) Orange-G	
10X Ligation buffer	200mM Tris-HCl pH 7.6, 50mM magnesium chloride, 50mM DTT, 10mM ATP	
10x PCR buffer (for *Taq* polymerase)	600 mM Tris pH 8.5, 150 mM ammonium sulphate, 20 mM magnesium chloride	
10x PCR buffer (for *Pwo* polymerase)	200mM Tris.HCl, pH8.8, 100mM sodium chloride, 20mM magnesium sulphate, 100µM ammonium sulphate	

2.1.3 DNA sequencing solutions

5x Annealing Buffer	200 mM Tris pH 7.5 100 mM magnesium chloride 250 mM sodium chloride

Labelling mix	To 10µl of annealed template-primer the following cocktail was added on ice: 1µl of 0.1M DTT 2µl of a mixture of 7.5 µM dGTP, dCTP, dTTP 1µl of α-^{35}S dATP (10mCi/ml) 0.25µl Sequenase Version 2.0 (USB) 0.125µl NP-40 (0.5%).
Termination nucleotide mixtures	One for each dideoxy-nucleotide: all contain 80 µM each of dATP, dGTP, dCTP and dTTP and 50 mM NaCl and one containing 8 µM dideoxy-ATP, one containing 8 µM dideoxy-GTP and so on.
Stop solution	95% Formamide, 20 mM EDTA, 0.05% each of bromophenol blue and Xylene Cyanol

2.1.4 Transfection Solutions

DEAE-Dextran Solution	10 mg/ml of DEAE-Dextran (Sigma) 0.45µm filtered or autoclaved and stored at 4°C
Chloroquine Solution (1000x)	100 mM stock 1 ml aliquots stored at -20°C (deteriorates after thawing)
PBS-DMSO	PBS containing 10% (v/v) DMSO

2.1.4 Protein Solutions

SDS Electrophoresis Running Buffer (5x stock) per Litre	15g Tris base 72g Glycine 5g SDS
Resolving Gel 10% gel	10 ml of 30% Acrylamide/bis (29:1) 7.5 ml 1.5M Tris buffer pH 8.8 containing 0.4% SDS 12.5 ml distilled water 100 µl of 10% ammonium persulphate 10 µl of TEMED
Stacking Gel Preparation 5.5% Gel	0.83 ml of acrylamide stock 0.83 ml 0.5M Tris pH 6.8 containing 0.4% SDS 2.8 ml distilled water 20µl of 10% ammonium persulphate 5 µl TEMED

2X SDS Sample buffer	per 100ml	25 ml 0.5M Tris pH 6.8 20 ml glycerol 4g SDS 1 mg bromophenol blue
(for reducing buffer only)		2ml 2-mercaptoethanol
Protein Gel Fixative		25 ml isopropanol (propan-2-ol) 10 ml glacial acetic acid 65ml distilled water
One-step Coomassie stain		848 ml distilled water 100ml Ethanol 50ml acetic acid 2ml (0.5%) Coomassie blue (Sigma)
Transfer buffer for Western Blots made up to 1L with distilled water		3.03g Tris base (final pH 8.1-8.4) 14.4g Glycine 200ml methanol
Standard Lysis buffer		1-2 % NP40 or Triton X-100 20mM Tris pH 7.5-8.0 150mM NaCl (10 mM $MgCl_2$) sometimes omitted 5mM EDTA 1.0mg/ml leupeptin (Boehringer Mannheim) 1.0mg/ml aprotinin (Boehringer Mannheim) 1mM PMSF (Sigma)

2.2 Cell culture and transfection

2.2.1 Cell culture

Cell lines were obtained from the Imperial Cancer Research Fund Cell Production Service (Clare Hall, South Mimms, Hertfordshire, UK). Cell cultures were maintained at 37°C in an atmosphere of 95% air/5% CO_2 in humidified tissue culture incubators (Hereus). Suspension cell cultures were maintained in RPMI/10% FCS, anchorage dependent cells were maintained in DMEM/10% FCS. Basic culture media were supplied from the ICRF Central Service Facility (Clare Hall, South Mimms, Hertfordshire, UK) . Primary cultures of HUVEC (Human Umbilical Vein Endothelial Cells) were obtained from Clonetics Corp. (San Diego, California, USA), and maintained in Clonetics Endothelial Growth Medium (EGM) according to suppliers instructions. HUVEC were used at passage 2 to 5 for transmigration assays. All tissue culture plasticware was poly-L-Lysine coated and

supplied by the Falcon subsidiary of the Becton Dickinson group (Oxnard, California, USA) as were all centrifuge tubes and similar plastic items.

2.2.2 Isolation and purification of human neutrophils.

Peripheral venous blood was collected from health volunteers into EDTA tubes. 1ml of 6% dextran solution in PBS was added to 10ml blood, and the tubes inverted gently to mix. The majority of erythrocytes were allowed to sediment over 30 minutes at room temperature, and the upper leukocyte-rich portion was collected and layered over 15ml of Lymphoprep (Sigma). Samples were centrifuged at 1,500rpm for 30 minutes at room temperature, and the pellet (containing neutrophils and residual red blood cells) resuspended in 2ml 0.2% NaCl solution for 30 seconds, followed by 10ml of 1.6% NaCl solution. This procedure subjects the cells to a brief osmotic shock, before restoring isotonicity, resulting in the lysis of residual erythrocytes. The neutrophils were washed twice in PBS containing 1% glucose (1,500prm, 7 minutes at room temperature), before being resuspended in 10ml PBS containing 0.25% BSA and counted (using a Coulter Multisizer).

2.2.3 Transient transfection of COS cells

COS cells served as a "neutral" cellular background to express adhesion molecules of interest. They are an African Green Monkey derived fibroblast cell line, transformed with multiple copies of replication defective SV40 viral genome (Glutzman, 1981). These cells support replication to high copy numbers of episomal vectors containing the SV40 origin of replication, such as pCDM8 and its derivatives. COS-1 cells were routinely transfected with pCDM8 plasmids, with 40-80% efficiency as determined by FACScan analysis. For ease of handling, COS-1 cultures were maintained in 15cm tissue culture dishes. 12-24 hours prior to transfection, near confluent cultures were trypsinised and replated 1:2 and allowed to grow overnight. On the day of transfection, cells were trypsinised, replated 1:1 and allowed to adhere for 3-4 hours. Cultures were washed with PBS and transfected (3hr at 37°C) with cDNAs for different constructs (10-30μg/10^7 cells) using 400mg/ml DEAE-dextran as a facilitator with 100mM chloroquine in serum free DMEM followed by a 2 minute hypotonic shock with 10% DMSO in PBS (Simmons, 1993). Transfected cells were grown overnight in standard culture medium, and 24 hours post-transfection lifted with trypsin/EDTA and replated 1:1.

2.3 Antibodies

2.3.1 Generation of antibodies against the extracellular domain of CD31

Mouse monoclonals against CD31 were produced in collaboration with Mr. Del Watling (ICRF Biological Resources, Clare Hall, South Mimms, UK) and Mr. Ian Collins (R&D Systems Europe, Oxford, UK) according to standard protocols. Briefly, female Balb/c mice were immunised subcutaneously with recombinant CD31(D1-D6)Fc protein in complete Freunds adjuvant every two weeks over a ten week period. Mice were boosted by intravenous injection with either full length recombinant CD31(D1-D6)Fc or truncated recombinant forms in incomplete adjuvant to focus the immune response against specific domains, and spleens removed 5 days later. (All animal work was performed by Mr. Dell Wattling at ICRF Biological Resources, Clare Hall, UK). Splenic B-cells were fused to NS0 partners to generate hybridomas by PEG fusion, and cloned by limiting dilution in 96-well plates. (Hybridoma production and subsequent cloning was performed by Mr. Ian Collins at R&D Systems Europe). 9-10 days after the initial fusions, hybridomas were screen by ELISA against CD31(D1-D6)Fc and MUC-18 (D1-D5)Fc to select hybridomas which were CD31 specific, and did not cross-react with the Fc portion of the immunogen. CD31 specific hybridomas were expanded from 96-well to 24-well plates, and supernatants further screened by ELISA to determine which domain each supernatant recognised, and for functional effects in adhesion assays. Selected hybridomas were further subcloned by limiting dilution 2-3 times to ensure monoclonality of the antibody.

Rat anti-human CD31 antibodies were generated in collaboration with Dr. Julia Spragg (Yamanouchi Research Institute, Littlemore, Oxford, UK). It was hoped that this strategy might aid in the identification of novel blocking epitopes, since the majority of anti-human CD31 generated to date have been mouse monoclonals. Female AO rats were immunised with 25μg CD31 (D1-D6)Fc protein per injection, given subcutaneously with alum adjuvant. Each animal received a secondary immunisation after 6 to 8 weeks, and an intravenous boost after a further 4 months with 25μg immunogen and spleens taken 4 days later. Hybridomas were prepared as per standard protocols using SP2/0 cells as fusion partners. Individual hybridomas producing antibodies of interest were cloned by limiting dilution as described above.

2.3.2 Generation of antibodies against the cytoplasmic tail of CD31.

Polyclonal anti-sera specific for the cytoplasmic tail of CD31 were raised in rabbits against CD31 derived peptides specific for exon 11 (MRSPAVPLL), exon 12 (NHAMKPINDNKE), exon 13 (NSDVQYTEVQVSSA) and exon14/15 (ETVYSERKAVPDAVESR) selected on the basis of their predicted immunogenicity (using the method of Kolaskar (Kolaskar, 1990) using the GCG suite ANTIGENIC programme). Peptides were synthesised by standard fMOC chemistry (Peptide Synthesis Laboratory, ICRF, UK) and coupled to keyhole limpet haemocyanin (KLH) as a carrier protein, according to the method of Hancock and Evan, 1992. Briefly 6mg of each peptide were coupled to 6mg of KLH by dissolving in 3ml 0.1M $NaHCO_3$ and adding glutaraldehyde (Sigma ultrapure grade 1, 25% stock) to a final concentration of 0.05%. Coupling was allowed to proceed overnight with slow tumbling end-over-end in a glass tube. Coupling was quenched by addition of 1M glycine ethyl ester to a final concentration of 0.1M and incubating for 30 minutes at room temperature. The coupled carrier was precipitated with 15ml ice cold acetone (-70°C) and pelleted at 14,000 rpm for 30 minutes. The pellet was air dried and resuspended in 0.9% NaCl solution at a final concentration of 1mg carrier/ml (i.e. 6ml).

Rabbits were immunised sub-cutaneously with 200µg of coupled carrier protein in Freunds complete adjuvant, and sub-cutaneously boosted with 100µg of immunogen in incomplete adjuvant every two weeks for sixteen weeks. Rabbits were bled out ten days after the final boost. To test the response to immunogen, solid phase ELISAs were performed against recombinant GST-CD31 cytoplasmic tail (gift from Dr. Ian Bird, Yamanouchi Research Institute, Littlemore, Oxford, UK) coated onto 96-well Immunlon-3 plastic. Serial dilutions of immune and pre-immune sera in PBS were incubated for 1 hour at room temperature and bound rabbit antibody detected with peroxidase conjugated swine anti-rabbit diluted 1:10,000 in PBS (1 hour incubation at room temperature) and visualising with OPD substrate. Polyclonals against exons 12, 13, and 14/15 gave strong signals versus their respective pre-immune sera, and the IgG fraction purified by Protein-A sepharose chromatography.

2.3.3 Commercial Antibodies

The following monoclonal antibodies (mAbs) were obtained from commercial sources. Anti-human CD31 mAbs were: 9G11 [6], L133.1 (Becton Dickinson, Oxford, UK), CAL 31.1 [18], 10B5 (R&D Systems, Oxford, UK), additional anti-human CD31 mAbs were obtained from the VIth leukocyte typing workshop as follows: WM59, JC70A, 4G6, 158-2B3, 31-1B5, 31-7E4 and hec7. Anti-murine CD31 mAbs were as follows: Clone 390 (Serotech Ltd, Oxford, UK) and MEC 13.3 (PharMingen, San Diego, CA). Anti-ICAM-3 mAbs were CAL3.10 and KS128 [43]. Anti-integrin antibodies were: anti α_1-integrin clone 1 (Becton Dickinson, Oxford, UK), anti α_2-integrin clone HAS-4 (ICRF Hybridoma Unit, South Mimms, UK), anti α_3-integrin clone 11A3 (ICRF Hybridoma Unit, South Mimms, UK), anti α_4-integrin clone P2W7 (ICRF Hybridoma Unit, South Mimms, UK), anti a_V-integrin clone L230 (gift from Dr. John Marshall, Richard Diinbleby/ICRF Department of Cancer Research, Guy's and St. Thomas' Hospital, London, UK), anti $\alpha v\beta 3$-integrin clone LM609 (Chemicon International, Harrow, UK) and clone 23C6 (ICRF Hybridoma Unit, South Mimms, UK), anti $\alpha v\beta 5$-integrin clone P1F6 (Chemicon International, Harrow, UK), anti β_1-integrin clone 13 (Becton Dickinson, Oxford, UK), anti β_2-integrin clone WT.3 (R&D Systems, Oxford, UK), anti β_3-integrin clone RUU-PL7F12 (Becton Dickinson, Oxford, UK).

2.4 Molecular Biology and DNA manipulation.

Elementary protocols, such as restriction endonuclease digestion of DNA, agarose gel electrophoresis etc. are not described in detail and were performed as described in Sambrook, Fritsch and Maniatis (1989)

2.4.1 Plasmid preparation

(a) Large scale preparation (Maxiprep)

Bulk plasmid preparation for transfection was performed by caesium chloride gradient centrifugation following alkaline lysis. Initial 5ml saturated cultures of bacteria transformed with the plasmid of interest were used to inoculate 800ml of LB culture broth, supplemented with appropriate antibiotic(s) to ensure selection, and cultures grown overnight to saturation at 37°C with shaking at 250rpm. Bacterial cultures were pelleted by

centrifugation in a Beckman J6 centrifuge at 4,200 rpm for 5 minutes, and the supernatant discarded. Plasmids were extracted using alkaline lysis: Bacteria were resuspended in 40ml Solution I (10mM EDTA) and lysed by addition of 80ml Solution II (200mM NaOH, 0.1% SDS). Genomic DNA and protein were precipitated by the addition of 40ml Solution III (3M potassium acetate ,pH 5.0). The mixture was centrifuged at 4,200rpm for 5 minutes, and the supernatant filtered through a double thickness gauze into a 250ml centrifuge bottle. Plasmid DNA was precipitated from the supernatant by filling the bottle with propan-2-ol, and centrifuging again at 4,200prm for 15 minutes. Supernatant was discarded, and the pellet resuspended in 3.5ml of TE, pH8.0. 5.4g of caesium chloride was added and allowed to dissolve at 37°C. 250µl of 10mg/ml stock solution of ethidium bromide were added, and the mixture centrifuged in a vertical VTi80/90 rotor (Beckman ultracentrifuge T80-M) at either 80,000 rpm for 3h or 65,000 rpm overnight (>8h). Bands containing the DNA were isolated, and the ethidium bromide extracted with butan-1-ol saturated with 1M NaCl. Typical yields, as measured by OD_{260}, were 1-4ıng for pCDM8 derived plasmids.

(b) Small scale preparation (Miniprep)

Small scale plasmid preparation was performed using a modified alkaline lysis method, after Maniatis (Sambrook, Fritsch and Maniatis 1989). Bacterial colonies picked from culture plates were grown overnight in 2ml of LB with appropriate antibiotic selection. 1.5ml aliquots were transferred to minifuge tubes, and bacteria pelleted by a brief (30 second) centrifugation. Supernatants were aspirated, and bacteria resuspended in 100µl Solution I. 200µl of Solution II, followed immediately by 200µl of Solution III were added, and tubes mixed by inversion. Following centrifugation for 5 minutes, supernatants were transferred to a fresh minifuge tube, and 500µl of a phenol: chloroform mixture (1:1 v/v) added to each tube. Tubes were sealed and shaken for 1 minute, centrifuged for 5 minutes and the aqueous phase transferred to fresh tubes. The tubes were filled with propan-2-ol, sealed and shaken for 1 minute, before centrifuging for 5 minutes to pellet plasmid DNA. Pellets were washed with 70% ethanol and air-dried, before being resuspended in 40µl of TE containing pre-boiled RNase A at a final concentration of 0.5µg/ml. To aid resuspension and denature residual endonucleases, tubes were incubated for 5 minutes at 70°C. Typical yields were 5-30µg per 1.5ml culture.

For preparation of template plasmid DNA for fluorescent dye based PCR sequencing a modified version of the above protocol was employed. Cultures were grown overnight in LB and lysed by the sequential addition of solutions I, II and III as described above, centrifuged to remove cellular debris and transferred to a fresh tube. RNase A was added to a final concentration of 20µg/ml and incubated for 20 minutes at 37°C. The supernatant was extracted with phenol:chloroform and the aqueous phase precipitated with propan-2-ol as described above. Pellets were resuspended in 32µl of deionised water and plasmid DNA precipitated by the addition of 8µl of 4M NaCl and 40µl of autoclaved 13% PEG8000. Samples were mixed and incubated overnight at 4°C, and plasmid DNA pelleted by centrifugation for 15 minutes at 4°C. Supernatant was aspirated, and pellet washed with 70% ethanol, air dried and resuspended in 20µl deionised water.

2.4.2 Preparation of chemically competent bacteria.

Chemically competent *E.coli* bacteria were used for all transformations. Different *E.coli* strains were prepared by one of two methods described below, the choice between methods determined by historical precedent and empirical evidence that some strains give better results when prepared by a particular protocol. Rarely used strains, such as XL1-Red, ER2537 etc. were obtained as competent stocks from commercial sources.

(a) MC1061/p3

MC1061/p3 chemically competent bacteria were prepared according to the method of Simmons (Simmons, 1993) as follows. MC1061/p3 cells were streaked out on fresh plate and grown overnight. Single colonies were picked into 5ml of TYM, and grown for 3-4 hours with constant agitation to ensure good aeration. Cultures were diluted into 100ml of TYM in a 250ml flask, and grown to mid-log (OD_{600} = 0.5). Cultures were further diluted into 500ml of TYM in a 2L flask, and grown to mid-log phase. Bacteria were chilled on ice and pelleted in a Beckman J6 centrifuge at 4,000 rpm for 15 minutes. The pellet was resuspended very slowly and gently in 100ml TFBI solution on ice, and pelleted at 2,500 rpm for 10 minutes at 4°C. The bacteria were resuspended in 20ml TFBII solution and flash frozen in pre-chilled minifuge tubes with liquid nitrogen. Transformation efficiencies obtain with these cells were routinely in the range 5×10^7 to 5×10^8 transformants/µg plasmid DNA.

(b) XL1-Blue

XL1-Blue chemically competent bacteria were prepared according to the method of Hanahan (Hanahan, 1983) as follows. XL1-Blue cells were streaked onto fresh LB-agar plates and grown overnight. Single colonies were picked into 5ml SOB medium in a sterile universal container and grown overnight at 37°C. Cultures were diluted into 100ml SOB medium in a 250ml flask and grown to mid-log, before being chilled on ice and pelleted at 2,500 rpm for 10 minutes at 4°C. Bacteria were gently resuspended in 85ml FSB and pelleted again at 2,500 rpm for 10 minutes at 4°C. The pellet was resuspended in 20ml of FSB, fresh 700µl DMSO added to 3.5% (v/v), swirled and left on ice for 10 minutes. A further 700µl aliquot DMSO was added, swirled and left on ice for 5 minutes, and 100µl of competent bacteria were flash frozen on dry ice. Transformation efficiencies were typically 5×10^6 to 5×10^7 transformants/µg plasmid DNA.

2.4.3 Bacterial transformation.

All transformations were made using chemically competent *E.coli* strains. Frozen stocks were thawed on ice and aliquoted into individual 1.5ml Eppendorf tubes as required, allowing 50-100µl of bacteria/transformation. Plasmid DNA was added (typically 1µg of plasmid for plasmid propagation purposes, or 3µl of ligation mix), and the bacteria allowed to stand on ice for 30 minutes. Bacteria were heat shocked either for 5 minutes at 37°C (strain MC1061/p3) or 60 seconds at 42°C (all other strains e.g. XL1-Blue),and placed on ice for 2 minutes to recover. Bacterial transformations were then plated directly onto appropriate antibiotic selection plates, with drug free-zone as required. All transformations into MC1061/p3 were selected on ampicillin/tetracycline plates (both antibiotics at 12.5µg/ml) with drug free-zone. Transformations into XL1-Blue were generally with Amp^R containing plasmids, and selection was on ampicillin plates (antibiotic at 100µg/ml), without a drug-free zone.

2.4.4 Oligonucleotide synthesis

Oligonucleotides for PCR amplification and DNA sequencing were routinely synthesised in-house on an Applied Biosystems PCRMate 380B, using standard phosphoramatide coupling chemistry, according to manufacturers protocols. Exceptionally, some oligonucleotides were obtained from commercial sources or from the ICRF oligonucleotide synthesis lab (Clare Hall, South Mimms, UK). Primers synthesised in-house were cleaved

from solid matrix support with ammonium hydroxide solution on ice for 30-60 minutes, and deprotected by heating at 55°C for at least 4 hours. Crude oligonucleotides were either precipitated from solution by standard sodium acetate/ethanol treatment, or lyophilised. Oligonucleotides were resuspended in either 500µl of TE, pH8.0 for 200nmole scale synthesis, or in 75µl TE, pH8.0 for 30nmole scale synthesis, and used without further treatment. Primers used described in this thesis are summarised in Appendix A.

2.4.5 PCR Amplification

Amplification of DNA for constructs and site directed mutagenesis was performed using *Pwo* DNA polymerase (Boehringer Mannheim UK, Lewes, East Sussex). This possesses 3'-5' error correcting exonuclease activity, and gives rise to significantly fewer adventitious mutations than *Taq* polymerase, but also is highly processive in contrast to other error correcting thermostable DNA polymerases such *Pfu* (in trial experiments *Pwo* was found to give at least as high a product yield as obtained with *Taq*; data not shown)

Standard PCR amplification protocol was as follows:

1-2µg template plasmid DNA
10µl 10x *Pwo* PCR buffer
1µl 25mM dNTP mix
1µl of forward and reverse primer, used at 1mg/ml
0.5µl *Pwo* polymerase (2.5U)
dH_2O to 100µl.

Thermocycle (Techne Cyclogene with heated lid) parameters were as follows:

Denature 95°C for 30 seconds
Anneal 55°C for 45 seconds
Extend 72°C for 60 seconds

Repeat for a total of 10 cycles

Routine PCR (for screening of bacterial colonies, to check constructs etc.) was performed using *Taq* DNA polymerase as below:

1-2µg template DNA, or 1µl of bacterial culture
10µl 10x PCR buffer (2mM Mg^{2+}, pH8.5)
1µl 25mM dNTP mix
1µl of forward and reverse primer, used at 1mg/ml
1µl 10U*Taq* polymerase (ICRF Pic*Taq* DNA Polymerase, South Mimms, UK)
dH_2O to 100µl.

Thermocycle parameters were as above, using 10-30 cycles depending upon template concentration.

2.4.6 TA-Cloning of PCR products.

In many instances PCR products were digested with appropriate restriction endonucleases and cloned directly into the desired vector, however for some products this was not possible (for example, *Not*I restriction endonuclease does not cut efficiently near the ends of linear DNA molecules). In order to overcome this PCR products were cloned into an intermediate pGEM-T vector, before being excised with the desired restriction enzyme and ligated into the vector of choice. TA-cloning was developed to take advantage of the non-template dependent addition of single nucleotides to the 3' ends of PCR amplified products. *Taq* favours the addition of A residues, and can be cloned into vectors containing as suitable T overhang, more efficiently than they can be blunt cloned. *Taq* polymerase produced PCR products were phenol:chloroform extracted and precipitated by sodium acetate/ethanol and resuspended in 50µl of dH_2O. 1µl of PCR product was ligated into pGEM-T and transformed into *E.coli* XL1-Blue cells, and selected on ampicillin plates. *Pwo* polymerase does not add nucleotides in such a non-template dependent fashion. For *Pwo* polymerase produced PCR products, the PCR product was precipitated by sodium acetate/ethanol, and resuspended in 88µl dH2O. 10µl of 10x *Taq* PCR buffer, 1µl 25mM dNTP mix and 1µl of *Taq* DNA polymerase were added, and the mixture heated to 72°C for 10 minutes. This latter step is in effect a PCR extension cycle without primers and drives the addition of A nucleotides to the 3' ends of the PCR product. This was then cloned into pGEM-T vector as described above for *Taq* polymerase derived PCR products.

2.5 Generation of Constructs to Dissect CD31-mediated adhesion

a) CD31 Extracellular Domain Deletion Series. These constructs were produced by Dr. J. Fawcett (see DPhil thesis 1994, University of Oxford). A full length CD31 cDNA clone, isolated by transient expression screens of HUVEC cDNA libraries, was used as a template for all PCR constructs (Simmons *et al.*, 1990). The PCR strategy for construction of soluble forms was as follows: 4 cycles of 94°C, 60 seconds; 45°C, 120 seconds; 72°C, 120 seconds; followed by 30 cycles of 94°C, 30 seconds; 45°C, 30 seconds; 72°C, 90 seconds. Primers used were: forward amplification primer 5' GATC AAGCTT

GTCTTCACTCTCAGG ATG 3', and reverse amplification primers with common splice donor and *Bgl*II restriction site sequences 5' GATC AGATCT ACTTACCTGT plus domain specific reverse primers as follows: Domain 1, CAC CCT GGG ACT GGG CAC TCC 3'; Domain 2, AGA GAA GGA TTC CGT CAC GGT 3' ; Domain 3, GAA GGA AGA TTC CAG TTC GGG 3'; Domain 4, AAT CCT GGG CTG GGA GAG CAT 3'; Domain 5, CTG GAC CTC ATC CAC CGG GGC 3'; Domain 6, TTT CTT CCA TGG GGC AAG AAT 3'. PCR products were cut with *Hind*III and *Bgl*II and cloned into the pIG_1 vector (Fawcett *et al.*, 1992, Simmons 1993) cut with *Hind*III and *Bam*HI.

Two further extracellular domain deletion series were also produced to generate size specific controls for the CD31 domain deletion series described above, a MUC-18 series and an NCAM series. For the MUC-18 deletion series, a full length MUC-18 cDNA clone isolated by transient expression screens of HUVEC cDNA libraries (provided by Dr. D. Simmons) was used as a template. 10 cycles of PCR amplification were used to produce the desired fragments of the extracellular domain . The primers used were: common MUC-18 forward amplification primer (5' GATC AAGCTT ATG GGG CTT CCC AGG CTG 3') plus reverse amplification primers containing the common adapter sequence 5' GATC GGATCC ACTTACCTGT plus domain specific sequences as follows: domain 1, GTA GAC GCG GAG CTG GAT 3'; domain 2, GAA AAC AGG GAC GGT GAC 3'; domain 3, GTT CAC CAG TAG TTC CTG 3'; domain 4, AAA AAT GGC CAG CTT GAC 3'; domain 5, CCG GCT CTC CGG CTC CGG 3'.PCR products were cut with *Hind*III and *Bam*HI and cloned into the pIG_1 vector (Fawcett *et al.*, 1992, Simmons, 1993) cut with *Hind*III plus *Bam*HI. Constructs were verified by restriction digests and DNA sequencing.

Similarly, for the NCAM deletion series, a full length cDNA clone in pCDNA3 (provided by Dr. F. Walsh, United Medical and Dental School, London University) was used as a template for 10 cycles of PCR amplification to produce the desired fragments of the extracellular domain. Primers used were as follows: common NCAM forward amplification primer (5' GATC AAGCTT ATG CTG CAA ACT AAG GAT 3') plus reverse amplification primers containing the common adapter sequence 5' GATC GGATCC ACTTACCTGT plus domain specific sequences as follows: domain 1, GAT CTT CAC GTT GAC GGT 3'; domain 2 CAC ATT CAC AAT GAC CTG 3'; domain 3 TTT TGC

AAA GAC TTT GAG 3'; domain 4 GGC ATA TTG CAC TTC AAG 3'; domain 5 GGT GTC TGC TTG AAC AAG 3'.

b)GPI-anchored CD31. pGPI-CD31, a construct which gives rise to a glycosylphosphatidyl-inositol (GPI) linked form of CD31, lacking the transmembrane and cytoplasmic tail of CD31 was generated in stages by Dr. C.D. Buckley (see DPhil thesis 1996, University of Oxford). To generate pGPI the GPI-anchor signal peptide was amplified from an LFA-3 template in pCDM8 (provided by Dr. D. Simmons). Primers used were: LFA-3 forward amplification primer (5' ATAC GGATTCA AGC AGC GGT CAT TCA AGA 3') and LFA-3 reverse primer (5' ATCTAT GCGGCCGC AAA TGA GAA ATC AGA TGG CTT 3').The PCR product was digested with *Bam*HI and *Not*I and ligated into pCDNA3 to produce pGPI. The extracellular domain of CD31 was amplified using CD31 ATG forward amplification primer and CD31 GPI D6 reverse primer (5' TATA GATC TTT CTT CCA TGG GGC AAG AAT 3'), the PCR product digested with *Hind*III and *Bgl*II, and cloned into pGPI digested with *Hind*III and *Bam*HI.

c) Cell Expressed ICAM-3 (CD50)/CD31 Chimeras. Constructs in which specific immunoglobulin-like domains of CD31 were replaced by the equivalent domains from ICAM-3 (CD50) were generated as follows. ICAM-3 (D1)/CD31 (D2-D6)TM, in which the NH_2-terminal immunoglobulin domain of human full length CD31 is replaced by the equivalent domain from human ICAM-3, and ICAM-3 (D1-D2)/CD31 (D3-D6)TM, in which the two NH_2-terminal Ig domains of human full length CD31 are replaced by the equivalent domains from human ICAM-3, were generated by a two step recombinant PCR method (Higuchi *et al.*, 1988; Ho *et al.*, 1989). This approach offers the advantage over more traditional methods in that it does not require the use of either endogenous restriction sites, or the introduction of restriction sites by PCR, and can be performed extremely rapidly. CD31 in pCDM8 (Simmons *et al.*, 1990) or ICAM-3 in pCDM8 (Fawcett *et al.*, 1993) were used as templates for PCR amplification. For ICAM-3 (D1)/CD31 (D2-D6)TM, primers used were: ICAM-3 ATG forward amplification primer (5' ATAT AAGCTT ATG GTA CCA TCC GTG TTG TGG CCC 3'), ICAM-3 D1 reverse amplification primer with CD31 overhanging sequence (5' CAC CCT GGG ACT GGG CAC TCC ACG CTC CGG GAG CCC GTA CAC 3'), CD31 D2 forward amplification primer with ICAM-3 overhanging sequence (5' GTG TAC GGG CTC CCG GAG CGT GGA GTG CCC AGT

CCC AGG GTG 3') and CD31 STOP reverse amplification primer (5' TATCTGAT GCGGCCGC CTA AGT TCC ATC AAG GGA GCC 3'). For ICAM-3 (D1-D2)/CD31 (D3-D6)TM, primers were: ICAM-3 forward amplification primer, ICAM-3 D2 reverse primer with CD31 overhanging sequence (5'GTG GAA CTT GGG TGT AGA GAA GGG CAG GAC AAA GGT TCG GAG 3'), CD31 D3 forward amplification primer with ICAM-3 overhanging sequence (5'CTC CGA ACC TTT GTC CTG CCC TTC TCT ACA CCC AAG TTC CAC 3') and CD31 reverse amplification primer. PCR products were digested with *Hind*III and *Not*I, and cloned into pIG_1 vector digested *Hind*III/*Not*I. ICAM-3 (D1-D3)/CD31 (D4-D6)TM, ICAM-3 (D1-D4)/CD31 (D5-D6)TM and ICAM-3 (D1-D5)/CD31 (D6)TM were generated by PCR amplification of the required fragments of CD31 and ICAM-3. Primers used were as follows: ICAM-3 forward amplification primer, ICAM-3 D3 reverse amplification primer (5' ATAT GAATCC AAA GAC CGT CAA GTT CTC CCG 3'), ICAM-3 D4 reverse amplification primer (5' ATAT GAATTC TTT ATC TTT CCA TTT CAA GTG CTG 3'), ICAM-3 D5 reverse amplification primer (5' ATAT GAATTC ATT TCT ATC CTG TCA AGT AAG GTG 3'), CD31 D4 forward amplification primer (5' ATAT GAATTC GGG CTT GGA AAA TAG TTC TGT TAT 3'), CD31 D5 forward amplification primer (5' ATAT GGATTC CCC AGG ATT TCT TAT GAT GCC CAG 3'), CD31 D6 forward amplification primer (5' ATAT GAATTC AAT TCT ATC CTG TCA AGT AAG GTG 3') and CD31 reverse amplification primer. ICAM-3 PCR products digested with *Hind*III and *Eco*RI, and CD31 PCR products digested with *Eco*RI and *Not*I, were ligated into pCDM8 digested with *Hind*III and *Not*I.

d) Soluble ICAM-3 (CD50)/CD31 Chimeras. ICAM-3 (D1)/CD31 (D2-D6)Fc, ICAM-3 (D1-D2)/CD31 (D3-D6)Fc, CD31 (D1-D2)/ICAM-3 (D2-D5)Fc and CD31 (D1-D3)/ICAM-3 (D3-D5)Fc constructs were produced using the same two-step PCR strategy described above. ICAM-3 (D1)/CD31 (D2-D6)Fc and ICAM-3 (D1-D2)/CD31 (D3-D6)Fc were made using the same primers as their membrane bound equivalents, substituting CD31 D6 reverse amplification primer (5' GATC AGATCT ACTTACCTGT TTT CTT CCA TGG GGC AAG AAT 3') for the CD31 STOP reverse amplification primer. For CD31 (D1-D2)/ICAM-3 (D2-D5)Fc the following primers were used: CD31 ATG forward amplification primer (5'TCTG AAGCTT CCTGCAGTCTTCACTCTCAGG ATG 3'), CD31 D2 reverse amplification primer with ICAM-3 overhang (5' CGA CCC ACC CTC CAC TAC AGA GAA GGA TTC CGT CAC 3'), ICAM-3 D2 forward amplification

primer with CD31 overhang (5' GTG ACG GAA TCC TTC TCT GTA GTG GAG GGT GGG TCG 3') and ICAM-3 D5 reverse amplification primer (5' GATC AGATCT ACTTACCTGT CGA CGG GGG GGT CAC GGG 3'). For CD31 (D1-D3)/ICAM-3 (D3-D5)Fc the following primers were used: CD31 ATG forward amplification primer, CD31 D3 reverse amplification primer with ICAM-3 overhang (5' GGG GGT CAC GGG CAG GAC CTT GGA AAA TAG TTC TGT 3'), ICAM-3 D3 forward amplification primer with CD31 overhang (5' ACA GAA CTA TTT TCC AAG GTC CTG CCC GTG ACC CCC 3') and ICAM-3 D5 reverse primer. PCR products were digested *Hind*III/*Bgl*II and cloned into pIG_1 vector digested *Hind*III/*Bam*HI. Constructs were verified by restriction digests and sequencing.

e) Human/Murine CD31 chimeras. A full length cDNA encoding murine CD31 in pCDM8 was kindly provided by Professor William Müller (Rockefeller Univerity, New York, USA). Soluble recombinant murine CD31 (D1-D6)Fc was generated by PCR amplification from the murine CD31 template using a murine CD31 forward amplification primer at ATG (5' ATAT AAGCTT CAGTCGGCAGCAAAG ATG 3') and a murine reverse amplification primer incorporating a splice donor site (5' ATAT AGATCT ACTTACCTGT TTT CTT CCA TGG GGC AAG 3'). PCR product was digested with *Hind*III and *Bgl*II, and cloned into pIG_1 vector digested with *Hind*III and *Bam*HI. A soluble recombinant chimera, hCD31 (D1-D2)/mCD31 (D3-D6)Fc in which the first two domains of murine CD31 are replaced by the equivalent domains from human CD31 was generated as follows. Human CD31 in pCDM8 was cut with *Hind*III and *Bam*HI and the fragment corresponding to human CD31 D1-D2 isolated (*Hind*III cuts 5' to in the pCDM8 multiple cloning site, whilst *Bam*HI cuts at an endogenous restriction site at the boundary between domains 2 and 3 in both mouse and human CD31). Murine CD31 in pCDM8 was also cut with *Hind*III and *Bam*HI, and the fragment corresponding to murine CD31 D3-D6Fc in the pIG_1 vector isolated. The two fragments were ligated together, and the presence of the expected human and murine sequences confirmed by sequencing.

f) CD31 ECD/EGFr TM-TK. A chimeric CD31 extracellular domain/epidermal growth factor receptor cytoplasmic domain chimera was constructed by PCR. The extracellular domain of CD31 comprised of domains 1-6 was amplified with ten cycles of PCR using *Pwo* DNA polymerase from full length CD31 in pCDM8 (Simmons *et al.*, 1990) with the

standard forward amplification primer at the initiating methionine, incorporating an *Hind*III restriction site, and a reverse primer at the boundary between the extracellular domain and transmembrane portion incorporating a *Xba*I site (5' ATAT CTCAGA TTT CTT CCA TGG GGC AAG 3'). The epidermal growth factor receptor (EGFr) transmembrane and cytoplasmic domains were amplified from full length cDNA in SRα-Neo (gift, Dr. Ken Smith, ICRF Angiogenesis Laboratory, Institute of Molecular Medicine, Oxford University) with 15 cycles of PCR with *Pwo* DNA polymerase, using a forward amplification primer at the boundary between extracellular domain and the transmembrane, incorporating an *Xba*I site (5' ATAT TCTAGA ACT GGG ATG GTG GGG GCC 3'), and a reverse primer at the stop codon, incorporating a *Not*I restriction site (5' ATAT GCGGCCGC TCA TGC TCC AAT AAA TTC 3'). PCR products were precipitated, resolved on 1% agarose gels, bands excised and TA-cloned into pGEM-T vector, as described above. The CD31 fragment was excised with *Hind*III and *Xba*I from pGEM-T, and the EGFr fragment liberated by digestion with *Xba*I and *Not*I. Gel purified fragments were ligated together, into pCDM8 digested with *Hind*III and *Not*I to give CD31ECD/EGFr TM-TK in pCDM8.

g) **Site-Directed Mutagenesis by Recombinant PCR.** Single-point mutations in CD31 were made using a two step recombinant PCR methodology (Ho *et al.*, 1989) as outlined below. For each point mutation, two 39-mer complementary primers were synthesised, containing the desired point mutation and the flanking 5' and 3' regions, encompassing six codons each side of the point mutation. (A complete list of primers used to generate each of the point mutations is included in Appendix A). PCR amplification from CD31 in pCDM8, using each pair of mutagenic primers with outer flanking primers generated two PCR products, which were resolved by running 10μl of each PCR reaction on an agarose mini-gel and bands of interest excised. Crude PCR product was isolated by freezing the gel slices on dry ice for 5 minutes, and spinning through homemade glasswool spin columns. Columns were prepared by cutting the tip from a 1ml Eppendorf pipette and inserting a small plug of glasswool. Pipette tips were placed in 1.5ml Eppendorf tubes, frozen gel slices placed on the glass wool, and the column spun for 30 seconds at 14,000 rpm in the benchtop centrifuge. Typically 10-20μl of DNA containing solution was obtained, of which 10μl served as a template in a second PCR reaction using only the outer flanking primers. In this second reaction each template

serves initially as its own primer through the complementary overlapping sequence containing the mutation of interest, and is subsequently amplified by the outer flanking primers. For CD31 mutagenesis of domains 1 and 2, the outer flanking primers were a forward amplification primer at the initiating methionine (ATG) with an incorporated 5' *Hind*III restriction site (5' GATC AAGCTT GTCTTCACTCTCAGG ATG 3') and a reverse amplification primer at the boundary between immunoglobulin-like domains 2 and 3 (5' GATC AGATCT ACTTACCTGT AGA GAA GGA TTC CGT CAC GGT 3') containing a *Bgl*II restriction site. The resultant PCR product comprised of mutated extracellular domains 1 and 2 of CD31 was digested with restriction endonucleases *Hind*III and *Bgl*II and ligated into pIG_1 vector, previously digested with *Hind*III and *Bam*HI. Each mutant construct was completely sequenced to verify the presence of the desired mutation, and lack of adventitious PCR induced mutations. The use of *Pwo* polymerase significantly reduced the rate of spontaneous mutation as compared to *Taq* polymerase, such that for 27 point mutations only 30 individual clones were sequenced, compared with a spontaneous mutation rate in excess of 80% for *Taq* based mutagenesis (based on early trial experiments with *Taq*). Fully sequenced mutants were subcloned into CD31 background constructs (CD31 D1-D6Fc in pIG_1, CD31 D1-D3Fc in pIG_1, CD31 D1-D6STOP in pCDNA3 and CD31 D1-D6TM in pCDNA3) as required utilising the introduced 5' *Hind*III site and an endogenous *Bam*HI site at the boundary between domains 2 and 3. For mutations in domain 3 the flanking primers were the forward amplification primer at the initiating methionine (as described above), and a primer at the domain 3/4 boundary (5' GATC AGATCT ACTTACCTGT TTT TGC AAA GAC TTT GAG 3') containing the splice donor sequences and a *Bgl*II site, allowing the resulting point mutations to be directly cloned into pIG_1 vector and expressed as CD31 (D1-D3)Fc proteins

h) CD31 (D1-D2)/(D4-D6)Fc. CD31 lacking domain 3 was made by recombinant PCR using the CD31 forward amplification primer at ATG and CD31 reverse amplification primer at the D6/TM boundary (as used to generate full length CD31 (D1-D6)Fc). Recombinant primers were a domain 2 specific reverse primer with domain 4 over hangs (5' GTG ACG GAA TCC TTC TCT CCC GAA CTG GAA TCT TCC 3') and domain 4 specific forward primer with domain 2 overhangs (5' GGA AGA TTC CAG TTC GGG

AGA GAA GGA TTC CGT CAC 3'). Recombinant PCR product was digested *Hind*III/*Bgl*II and cloned into pIG_1 digested with *Hind*III/*Bam*HI.

2.6 Sequencing

For the majority of constructs, manual sequencing the dideoxy chain-termination method was used. For pCDM8 and pIG_1 based plasmids, CsCl purified maxiprep DNA was invariably used, since miniprep DNA did not to give sequence data of adequate quality. Double-stranded plasmid DNA (5µg) was denatured by incubating at 37°C for 15 minutes in the presence of 0.02M NaOH in a total volume of 100µl. The reaction was neutralised by the addition of 10µl of 3M ammonium acetate, pH5.0, and the DNA precipitated by filling the tube with ice cold 100% ethanol and centrifuging at 13,000g for 15 minutes at room temperature. The pellet was washed in 70% ethanol, and resuspended in 7µl of dH_20. For each sequencing reaction a tube was set up containing:

7 µl template DNA solution	(denatured)
1 µl sequencing primer	(used "neat" at a concentration of 1 mg/ml)
2 µl 5x annealing buffer	200mM Tris.HCl pH7.5, 100mM $MgCl_2$, 250mM NaCl

The tubes were heated to 70°C for 3 minutes, and sequencing primer allowed to anneal while cooling to room temperature over 15 minutes. This was then used as a template in the Sequenase Version 2 protocol (United States Biochemicals. Cleveland, Ohio, USA) according to the manufacturers protocol, and run out on a 8% acrylamide sequencing Gel (Sequi-Gen, BioRad, Hercules, California, USA) according to the manufacturers instructions. Fluorescent dye based linear cycle sequencing was occasionally used for non-pCDM8 derived templates (pGEM-T etc.) using miniprep DNA prepared as described previously as a template, and using the Applied Biosystems Taq FS sequence kit according to manufacturer's instructions.

2.7 Protein analysis and manipulation

2.7.1 Production and purification of recombinant soluble chimeric CAM-Fc fusion proteins.

The use of recombinant soluble adhesins comprised of the extracellular domain of the cell adhesion molecule (CAM) of interest fused to the constant portion of human IgG1 has been

reviewed (Simmons, 1993). Recombinant protein is produced from the pIG_1 vector in which a splice donor site is incorporated into the 3' end of the CAM cDNA (usually by PCR), which allows inframe translation by intracellular splicing to the splice acceptor sequences abutting the hinge region of the IgG1Fc. COS cells act as surrogate B-cells and produce the translated proteins as dimers. The Fc-tag allows for easy purification and subsequent immobilisation at normalised levels on plastic pre-coated with anti-human IgG(Fc specific) antibody.

COS cells were transiently transfected as described above, however following DMSO shock, the media was replaced with DMEM containing 0.5% FCS previously depleted of bovine IgG by prior incubation with Protein-A sepharose. After incubation for 4-7 days, culture supernatants were collected, cellular debris removed by centrifugation (10000 rpm for 20 minutes, Beckman JA10 rotor), and filtration through a 0.22μm bottle top filter. Sodium azide was added to 0.02%, and recombinant FC proteins purified by passing the supernatant over a Protein-A sepharose column, and eluting bound protein with 0.1M glycine, pH3.0. Eluted protein was collected into and neutralised with 1/10th volume of 2M Tris.HCl, pH8.0. Protein containing fractions were pooled and concentrated/buffer exchanged into 20mM Tris.HCl, pH8.0 or PBS using centricon-10 concentrators (Amicon).The purity and conformational integrity of proteins was verified by SDS-PAGE and by ELISA.

2.7.3 ELISA of Fc and other proteins.

Immulon-3 96-well plates (Dynatech Laboratories, Chantilly, VA) were coated with 1μg/well goat anti-human Fc immunoglobulin in bicarbonate buffer, pH9.6 (overnight incubation 4°C), blocked with 2% BSA in PBS for 2 hours at room temperature, and then coated with chimeric proteins (0.5μg/well) in PBS for 2 hours at room temperature. Non-Fc tagged proteins were added directly to the plate in appropriate buffer. Antibody was added in saturating amounts (neat hybridoma supernatants or appropriately diluted purified antibody), followed by peroxidase conjugated sheep anti-mouse immunoglobulin (1:2000 dilution, Amersham International). Each layer was incubated for 30 minutes at room temperature and followed by 4 washes. Bound antibody was visualised with O-phenylenediamine dihydrochloride (OPD) substrate (Sigma) made up in citrate-peroxide buffer (Sigma), and OD read at 450nm.

2.7.4 Purification of integrin αvβ3

Human integrin αvβ3 was purified from placenta or melanoma cell line DX3.

An anti-αvβ3 affinity column was prepared by coupling the monoclonal antibody 23C6 (a non-blocking anti-αvβ3 monoclonal antibody, obtained from Ian Hart, ICRF Hybridoma Unit, South Mimms, UK) to cyanogen bromide activated sepharose 4B beads (Pharmacia) according to manufacturers protocol. Briefly, the freeze dried gel was washed in 1mM HCl, pH2-3 to remove stabilising additives, and added to 40mg of 23C6 in Coupling Buffer (100mM NaHCO3, pH8.3, 500mM NaCl), to give around 5mg antibody per ml of gel. The coupling reaction was rotated overnight at 4°C, and excess ligand washed away with 5 gel volumes of Coupling Buffer. The gel was washed with four cycles of alternating pH, comprised of 100mM NaOAc, pH4.0, 500mM NaCl followed by 100mM Tris.HCl pH8.0, 500mM NaCl, prior to storage in PBS/0.2% sodium azide

Placentas were obtained by donation from the John Radcliffe Hospital, Maternity Unit, and stored frozen at -80°C until required. Frozen placentas were defrosted, the umbilical cord discarded, and homogenised in a blender with of 500ml Lysis Buffer (50mM Tris.HCl pH7.5, 150mM NaCl, 1mM $MnCl_2$, 1mM $MgCl_2$, 0.1mM $CaCl_2$, 0.5mM PMSF, aprotinin, leupeptin, and 1% Triton X-100 detergent). The homogenate was stirred overnight at 4°C and centrifuged at 1,500rpm in GPR benchtop centrifuge to pellet solid waste. The blood red supernatant was centrifuged in a Ti45 rotor at 30,000rpm for 1 hour at 4°C, precleared to remove excess human immunoglobulin by passing over a Protein A-sepharose column, and the supernatant applied by gravity feed to an affinity column based on the anti-αvβ3 antibody 23C6 coupled to cyanogen bromide activated sepharose (as described above). Supernatant was passed over the column 4-5 times and the column washed with 500ml of Lysis Buffer containing Triton X-100 followed by 500ml of Lysis Buffer without detergent. The column was equilibrated with 50ml of Column Wash Buffer (20mM NaOAc, pH4.5, 150mM NaCl, 1mM $CaCl_2$, 1mM $MgCl_2$ and 40mM β-octyl glucosid), and integrin eluted into 10 x 8ml fractions with Elution Buffer (20mM NaOAc, pH3.1, 150mM NaCl, 1mM $MnCl_2$, 1mM $MgCl_2$, 0.1mM $CaCl_2$, 40mM β-octyl glucosid), neutralising with 2ml 2M Tris.HCl, pH8.0. Fractions containing integrin were identified by SDS-PAGE, and fractions of interest concentrated and buffer exchanged by centrifugal dialysis using Centricon 100 columns (Amicon) into Integrin Buffer (20mM Tris.HCl, pH7.5,

150mM NaCl, 1mM $CaCl_2$, 1mM $MnCl_2$, 40mM β-octylglucosid). Typical yields were 2-3mg protein.

Integrin αvβ3 was also obtained from melanoma cell line DX3. Cultures were expanded to roller bottle scale, and typically 48-60 roller bottles were used per preparation. Cells were harvested in 1mM EDTA, pH8.0, centrifuged and resuspended in 1ml/roller bottle DMEM supplemented with 10mM HEPES, 0.25% BSA. Cells were lysed with 9ml/roller bottle of Lysis Buffer (as above for placenta preparations), pooled and allowed to stir for 2h at 4°C. The pale pink lysate was transferred to the Ti45 rotor and centrifuged at 30,000 rpm for 30 minutes at 4°C. The lysate was passed over the αvβ3 affinity column and subsequently eluted as described for the placenta preparation. Typical yields were 0.5 to 1 mg protein.

2.7.5 Solid-phase integrin αvβ3-ligand interaction

Direct interaction between purified αvβ3 integrin and purified recombinant Fc proteins was assessed using two methods, coating plastic with either the purified integrin or recombinant Fc proteins. Assays with integrin forming the solid phase were performed according to a modification of the method of Charo (Charo *et al.*, 1990). Briefly, purified integrin was diluted into Buffer A (1 x TBS containing 1mM $CaCl_2$, 0.02% sodium azide, 1mg/ml BSA) and coated at 400ng/well onto 96-well MAXISorb plates (Dynatech Research Laboratories, Virginia, USA) overnight at 4°C. Non-specific sites were blocked by 5% BSA in Buffer A for three hours at room temperature. Recombinant Fc proteins in Buffer B (1 x TBS, containing 1mM $CaCl_2$, 1mM $MnCl_2$, 1mg/ml BSA) were added to wells at 1μg/ml and allowed to bind for three hours at 30°C. Unbound protein was removed by washing with buffer B, and the Fc portion of bound protein detected using sheep anti-human (Fc-specific) antibody conjugated to horseradish peroxidase (HRP) diluted 1:2000 in Buffer B, incubating at room temperature for 30 minutes. HRP activity was detected colourmetrically with O-phenylenediamine dihydrochloride substrate (Sigma Chemical Company, Poole, UK), measuring absorption at 450nm.

For solution phase integrin binding assays, plates coated with Fc proteins or extracellular matrix ligands were prepared as per a standard ELISA. Purified integrin was diluted in buffer C (TBS containing 1mM $MnCl_2$, 0.1mM $MgCl_2$ and 0.1mM $CaCl_2$), at a final concentration of 20μg/ml and 2μg integrin added per well. Plates were incubated for 3

hours at 30°C, wells washed 3 times in buffer C, and bound integrin detected with anti-β3 integrin mAb F11 at 20μg/ml by incubating for 30 minutes at room temperature. Plates were washed 4 times in buffer C, and bound antibody detected with a 1:1000 dilution of sheep anti-mouse.HRP conjugated antibody in buffer C, and colour developed with OPD substrate.

2.7.6 Biotinylation of Cell Surface Proteins, Western blotting and Immuno-precipitation

Cell surface proteins were biotinylated by incubating $2x10^6$ cells in PBS containing 0.5mM sulpho-NHS-biotin for 10 minutes at 37°C, and quenched with TBS and washed with PBS. Cells were resuspended at $2x10^7$/ml in lysis buffer (10mM Tris.HCl pH7.5, 1% NP-40 (w/v), 150mM NaCl, 1mM EDTA, 0.5mM phenylmethylsulphonyl fluoride), and rolled for 1 hour at 4°C. Debris was removed by centrifuging at 13,000g for 20 minutes at 4°C, and the supernatants pre-cleared by incubating with an appropriate negative control antibody, in the presence of pre-washed Protein-G/Sepharose at 4°C for 2 hours. 5μg of antibody against surface molecule of interest were added to the cleared supernatants and incubated at 4°C overnight. Labelled proteins were isolated by affinity purification with protein A-Sepharose beads. After washing four times in lysis buffer, bound proteins were eluted by boiling in sample buffer under reducing conditions and resolved on 7.5% SDS-PAGE. Proteins were transferred onto a HighBond-N (Amersham) nitrocellulose blot, and blocked with 5% milk protein in PBS/0.1% Tween-20. Blots were washed twice in PBS/0.1% Tween-20, incubated with streptavadin-HRP (Horse Radish Peroxidase) diluted 1:1000 in PBS/0.1%Tween-20 for 1 hour at room temperature, and washed three times in PBS/0.1% Tween-20. Biotinylated proteins were detected using Enhanced Chemiluminescence (Amersham International, UK), according to the manufacturers instructions.

For Western blots, proteins were resolved by SDS-PAGE, transferred onto nitrocellulose and the membrane blocked as described above. Membranes were washed with TBS containing 0.1% Tween-20, and 20ml of TBS/Tween-20 containing 10μg of primary antibody added to the membrane for 1 hour at room temperature. Membranes were washed and 1:1000 dilution of HRP conjugated secondary antibody (predominantly anti-mouse HRP) added and bound antibody detected after 1 hour by ECL as described above.

2.7.7 Chemical Cross Linking

For soluble recombinant proteins, samples were buffer exchanged into PBS by dialysis/centrifugal dialysis, and diluted in PBS (pH7.4) to the desired concentration. The cross-linking agent bis(sulphosuccinimidyl)suberate (BS_3) was dissolved in PBS to generate a 10mM stock immediately prior to use, and added to protein samples at a final concentration of 1mM (at least 50-fold greater than the concentration of protein). BS_3 is a homobifunctional cross-linker with a reactive NHS-ester groups which react with primary amines (i.e. NH_2-terminal primary α-amine and the ε-amine groups of lysine residues).

Cross-linking was allowed to proceed for 30 minutes at room temperature, and quenched by the addition of Tris.HCl pH7.5 to a final concentration of 50mM for a further 15 minutes. The addition of Tris, which contains primary amines, serves to block any remaining cross-linker. 200ng of protein from each sample were run out on 4-20% Tris-glycine pre-cast gels (Novex, R&D Systems Europe, Abingdon) under non-reducing conditions, blotted onto nitrocellulose, blocked with 1% non-fat milk in TBS, and CD31 protein detected with a cocktail of anti-CD31 monoclonal antibodies (10μg of 9G11, CAL31.1 and 10B5 in 50ml TBS containing 0.05% Tween-20). Bound antibody was detected with a 1:1000 dilution of sheep anti-mouse.HRP conjugate in TBS containing 0.05% Tween-20, and visualised by ECL (Amersham International, Amersham), according to manufacturers instructions.

For cell expressed proteins, cross-linking was performed on 10^6 cells in PBS with BS_3 at a final concentration of 1-2 mM and at 4°C whilst rotating end-on-end. After 30 minutes, cross-linking was quenched by the addition of 50mM Tris.HCl, pH8.0, and 5mM iodoacetamide added to alkylate free sulphydryl groups and prevent the formation of intermolecular disulphides on lysis. After 10 minutes on ice, cells were pelleted and lysed in 0.5ml lysis buffer and sonicated. The sonicate was centrifuged at 14,000g for 10 minutes and soluble proteins precipitated from the supernatant with 500μl of ice-cold acetone. Samples were centrifuged at 14,000g for 30 minutes, the pellet washed in 70% ethanol, resuspended in non-reducing sample buffer containing 50mM iodoacetamide, heated to 100°C for 5 minutes, and subjected to SDS-PAGE on 4-20% Tris-glycine gels. CD31 containing protein complexes were identified by Western blotting as described above for recombinant protein.

2.7.8 Analytical Ultracentrifugation

Analytical ultracentrifugation was performed using a Beckman XL-A ultracentrifuge fitted with UV scanning optics. Equilibrium experiments were performed with a Yphantis 6-channel centrepiece in a AN-60Ti rotor to allow multiple concentrations of protein to be loaded simultaneously. Rotors and run schedules were as recommended by the manufacturer. Data was collected automatically, and analysed using the SEDPROG suite of programmes developed by Greg Ralston (Ralston and Morris, 1992).

2.7.9 Silver-staining of protein gels

Most protein gels were stained with Coomassie blue one-step stain overnight, however for protein gels with very little protein present, silver staining was used. Protein gels were fixed for 2 hours in 40% methanol/10% acetic acid, washed twice with 10% ethanol, three times with water (5 minutes/wash), and disulphides reduced by treating the gel with Farmer's Reducing agent (1% potassium ferricyanide, 1.6% sodium thiosulphate) for 5 minutes. Gels were extensively washed to remove the reducing agent, and soaked for 30 minutes in 0.1% silver nitrate solution. Following a brief rinse in water, gels were developed for 10-30 minutes with 3% sodium carbonate (Na_2CO_3)/0.01% formaldehyde, and colour development halted by the addition of 1% acetic acid. Gels were washed three times with water before being vacuum dried.

2.7.10 Dual colour immunoflourescence

Two colour immunoflourescence of COS cells expressing full length CD31 and GPI-CD31 was performed as follows. Transfected COS cells were plated at a density of $2.5x10^4$ cells per well in 8 well chamber slides (Nunc, Life Technologies), and grown overnight. Cells were washed twice in serum free DMEM medium, fixed for 10 minutes with ice cold (-20°C) methanol, and blocked with 20% goat serum in PBS for 20 minutes at room temperature. The extracellular domain of CD31 was detected using 9G11, a mouse anti-CD31 monoclonal, at 2μg/ml, incubating at room temperature for 30 minutes, and visualised with goat anti-mouse IgG TRITC conjugated secondary antibody (Sigma) for 20 minutes at room temperature. Cells were blocked for a second time with 20% goat serum incubating for 20 minutes at room temperature, the cytoplasmic tail of CD31 detected with the rabbit polyclonal serum described above, incubating for 30 minutes at room temperature, at 20μg/ml. Bound antibody was visualised with goat anti-rabbit IgG (whole

molecule) $(Fab)_2$ fragment FITC conjugated secondary antibody. Cells were washed three times with PBS between each step described above. The cells were observed under epiflourescence using a Zeiss Axiovert photomicroscope with 40x objective and photographed on Kodak Ektachrome 200. A combination of automatic and manual exposure times were used to ensure equal exposure times between different CD31 constructs.

2.8 Cell Adhesion Assays

2.8.1 Adhesion of transfectants and cell lines to recombinant protein

Immulon-3 96-well plates (Dynatech Laboratories Inc., Chantillay VA) were pre-coated overnight at 4°C with 1μg/well goat-anti-human-Fc Ig (Sigma, Poole, Dorset) in bicarbonate buffer, pH 9.6, blocked with PBS/0.25% bovine serum albumin (Fraction V) for 2 h at room temperature, and then coated with Fc chimeric proteins at 0.5μg/well in PBS for at least 2h at room temperature. This concentration of Fc protein was shown to be saturating both by ELISA and adhesion assay. Where antibodies were added to wells, these were added at 1μg/well or as neat culture supernatants and incubated for 15 minutes prior to the addition of cells. Cells were harvested in 2mM EDTA/PBS, labelled with the fluorescent dye BCECF-AM (Molecular Probes, Oregon, USA) for 30 minutes at 37°C, and washed twice in assay buffer (DMEM, 10mM HEPES buffer, 0.25% bovine serum albumin). Labelled cells were added to plates at either 5×10^4 cells/well (for COS cells and melanomas) or 1×10^5 cells/well (haematopoietic cells) in a volume of 50μl, to give a uniform monolayer of cells, and allowed to adhere (typically for 1h) at 37°C. Plates were washed with pre-warmed assay buffer until cells in the negative control wells were sufficiently removed as determined by visual inspection. Typically this was 2-3 times. Adhesion was quantitated using a Cytofluor II fluorescent plate reader (Millipore, Watford, UK), comparing the total input fluorescence and the bound fluorescence, to calculate the percentage of input cells bound. Where COS cells expressing different chimeric constructs were used in the same assay, the percentage input cells bound was corrected to take into account the transfection efficiency.

2.8.2 Neutrophil adhesion/transmigration assays

Transmigration and adhesion to endothelial monolayers was assessed according to the method of Bird *et al.*, 1993. HUVECs were grown to confluence on fibronectin coated

transwells in 24 well cluster plates (Becton Dickinson). Transwells were washed with HBSS containing 0.25% BSA, and endothelial cells stimulated by the addition of 600µl and 300µl of HBSS/BSA containing 1 ng/ml IL-1β to the lower well and transwell chamber respectively. HUVEC were maintained at 37°C for 4 hours to allow the induction proteins required for adhesion/transmigration to occur. After stimulation, endothelial monolayers were washed twice with HBSS/BSA, and 200µl of purified neutrophils (at 5 x 10^6 cells/ml) added to each transwell. The plates were incubated for 1 hour at 37°C to allow neutrophils to migrate across the endothelial monolayer into the lower chamber. Adhesion of neutrophils to the endothelial monolayer was assessed by removing the transwell chamber, washing the monolayer three times with HBSS/BSA to remove unbound neutrophils. Bound neutrophils were quantified by release of myeloperoxidases following cell lysis with 900µl 0.2% Triton X-100 solution 50µl of the resulting lysate was removed from each well and transferred to a 96-well plate. 200µl of TMB-substrate solution was added to each well, and colour allowed to develop for 10 minutes before stopping with 50µl of 1M sulphuric acid. Plates were read at 450nm. Migration was verified by visual inspection of the wells. Transwells were removed from the 24 well plate, and the plate spun (1,500rpm, 6 minutes, room temperature) to pellet migrated neutrophils. Neutrophil migration was quantitated by the release of myeloperoxidases on lysis as described above.

2.8.3 Time lapse video microscopy

Cells were added to 24-well cluster plates (4 x 10^5 cells/well) coated with the matrix of choice in growth medium supplemented with 20mM HEPES. Plates were viewed on a heated stage (maintained at 37°C), but without CO_2 or humidity control. Time lapse video microscopy was carried out using a Zeiss Axiovert 35 inverted microscope with phase contrast optics, fitted with a Panasonic WV-BL600 CCD camera. Time lapse iinages were recorded with a Panasonic AG-6720 VHS video recorder, and individual frames output with a Sony Video Graphics Printer UP-860-CE. Cells were followed for 10-60 minutes depending upon the experiment.

Chapter Three: Dissecting the Homophilic Binding Site of CD31

3.1 Introduction

The CD31 antigen was originally identified following the serological characterisation of antigens on endothelial cells in the mid-1980's as a heavily glycosylated glycoprotein of approximately 130kDa. It was subsequently shown to be widely expressed on cells of the vascular compartment, including circulating platelets, vascular endothelium, myeloid cells, around 50% of circulating lymphocytes (primarily $CD8^+$, CD45RA naive lymphocytes) and $CD34^+$ haemopoietic progenitor cells in human bone marrow. Molecular cloning of human CD31 identified CD31 as a member of the immunoglobulin superfamily (Simmons *et al.*, 1990, Stockinger *et al.*, 1990, Newman *et al.*, 1990) with homology to a number of cell adhesion molecules. The extracellular domain of CD31 consists of 574 amino acids forming six C2-type immunoglobulin domains (each encoded by a single exon (Kirshbaum *et al.*, 1994), a membrane-spanning hydrophobic region and a cytoplasmic tail of 118 amino acids. Subsequent cloning of murine CD31 (Xie and Muller, 1993), bovine CD31 (accession number: U35433) and ovine CD31(accession number: X98505) show that CD31 is well conserved amongst species orthologues (around 70% between mouse and man), with the highest degree of conservation in the cytoplasmic tail.

Early work demonstrated that CD31 (Albelda *et al.*, 1991) expressed in heterologous murine L-cells localised to cell-cell borders and was capable of supporting homophilic adhesion. However, studies by a number of groups have identified several potential heterophilic ligands for CD31, including cell surface glycosaminoglycans (DeLisser *et al.*, 1993, Watt *et al.*, 1993), the integrin $\alpha v\beta 3$ (Piali *et al.*, 1995, Buckley *et al.*, 1996, see also Chapter 6), and a 120kDa ligand expressed on T-cells following the downregulation of T-cell responses (Prager *et al.*, 1996). In addition it has also been shown that CD31 is capable of regulating adhesion by upregulating $\beta 1$, $\beta 2$, and $\beta 3$ integrin mediated adhesion following homophilic engagement (Tanaka *et al.*, 1992, Piali *et al.*, 1992, Leavesley *et al.*, 1994, Fawcett *et al.*, 1995, Berman *et al.*, 1995, Jackson *et al.*, 1997).

CD31 mediated adhesion is difficult to study *in vivo* and *in vitro* due to co-expression of potential heterophilic ligands and CD31 on both primary cell cultures and transformed cell lines. We have therefore used a reductionist methodology to characterise CD31 homophilic adhesion. The approach routinely used to study adhesion molecules in the laboratory, has been to express the adhesion molecule of interest in an heterologous "neutral" cell background and follow the ability of these cells to adhere to plastic coated with a ligand of interest. This strategy is further enhanced by the use of soluble recombinant chimeric forms of the ligand, comprised of the extracellular portion of the ligand fused at its carboxyl terminus to the Fc portion of human IgG1. This approach has a number of significant advantages over the earlier cell-cell based aggregation assays employed by other investigators. Firstly it allows the adhesive properties of a single adhesion molecule to be studied independently from other adhesion molecules, by allowing for appropriate controls such as mock transfectants and irrelevant chimeric proteins. Secondly, the use of soluble recombinant Fc tagged proteins allows the correct orientation and normalisation of coating density by presenting the Fc proteins using plastic pre-coated with an anti-human Fc antibody.

Previous work from this laboratory (Fawcett *et al.*, 1995) using an extracellular domain deletion series of CD31 consisting of the NH_2-terminal 1, 1-2, 1-3, 1-4, 1-5, and 1-6 immunoglobulin-like domains of CD31 fused to the Fc region of human IgG1 (CD31(D1)Fc through CD31(D1-D6)Fc respectively), has shown that when COS-1 cells expressing full length CD31(D1-D6)TM adhere to plastic coated with these domain deletion series proteins, only constructs containing membrane proximal domains 5 and 6 supported significant homophilic adhesion as compared to negative control protein MUC18(D1-D5)Fc (Figure 3.1a).

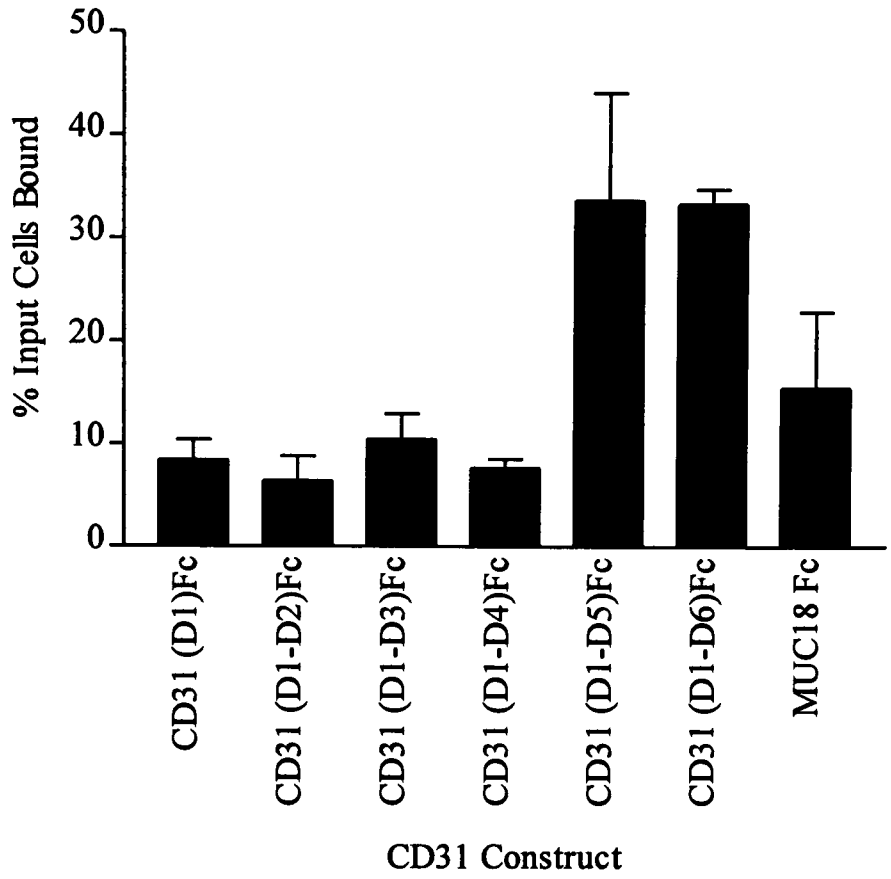


Figure 3.1a Homophilic adhesion to CD31 domain deletion series. Adhesion of COS-1 cells expressing full length CD31 to plastic coated with CD31 COOH-terminal domain deletion series proteins. Adhesion to control protein, MUC18 (D1-D5)Fc is included as a negative IgSF-Fc control. Results are expressed as the means of the percentage of input cells bound ± 1 SD. Only constructs containing membrane proximal domains 5 and 6 support significant homophilic adhesion above background adhesion to MUC18 (D1-D5)Fc, indicating that these domains are required for homophilic adhesion. Typically CD31 (D1-D5)Fc supports sub-maximal levels of adhesion, although in this assay the level is comparable with that seen for CD31 (D1-D6)Fc.

This result was surprising since similar deletion constructs of CD66 (Watt *et al* 1994), ICAM-3 (Fawcett *et al* 1993, Holness *et al* 1995) and sialoadhesin (Nath *et al* 1995) all demonstrate that the NH_2-terminal membrane distal immunoglobulin-like domains of these adhesion molecules are necessary and sufficient to support adhesion to both homophilic and heterophilic ligands. The finding that the membrane proximal domains of CD31 are involved in mediating homophilic adhesion was therefore unexpected. These findings do not however rule out a role for the NH_2-terminal domains in mediating homophilic adhesion. Evidence for the role of the NH_2-terminal domains in homophilic adhesion was obtained by antibody blockade and by use of truncated soluble recombinant forms of CD31 as inhibitors of adhesion (Fawcett *et al* 1995, Liao *et al.*, 1997). These showed that antibodies mapping to NH_2-terminal domains 1 and 2 inhibited homophilic adhesion, and that truncated forms of CD31 comprised of the NH_2-terminal domains 1-3 were capable of inhibiting CD31 homophilic adhesion, although they were not capable of directly supporting adhesion themselves. In order to explain the involvement of both membrane

proximal and membrane distal domains in CD31 homophilic adhesion, a model was proposed in which the NH_2-terminal domains 2 and 3 of CD31 on one cell bind to the membrane proximal domains 5 and 6 of CD31 expressed on an apposing cell, in an anti-parallel fully interdigitating mode of adhesion, with two binding sites on each molecules forming a double reciprocal interaction (figure 3.1b).

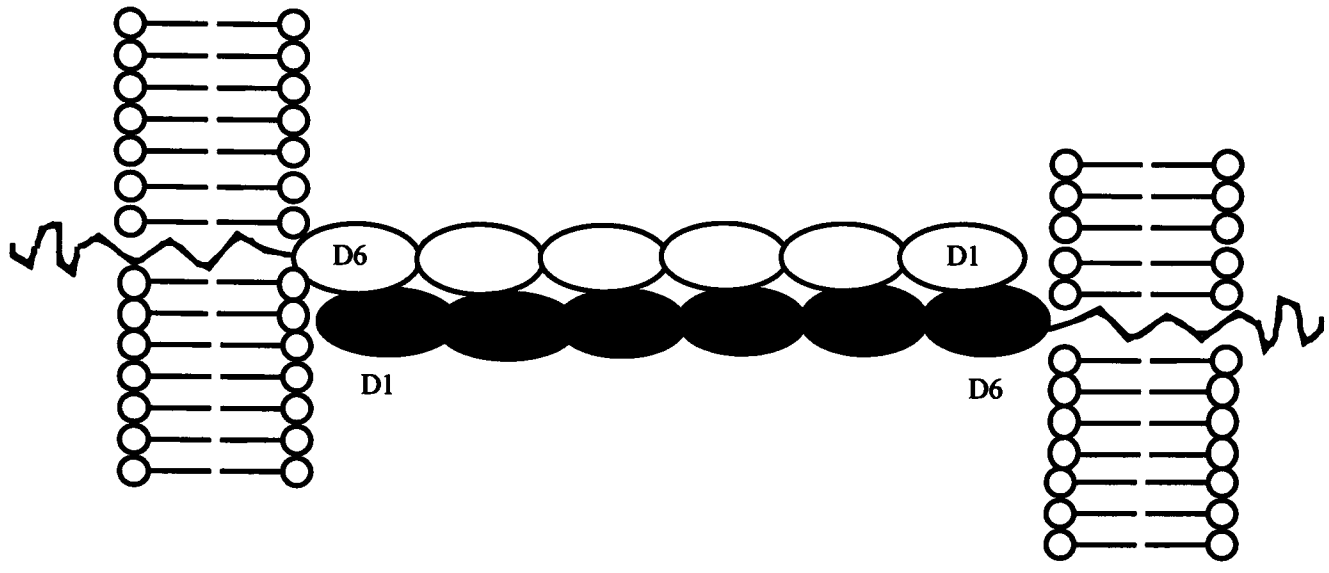


Figure 3.1b Anti-parallel fully interdigitating model of CD31 homophilic adhesion. Data from cell-protein adhesion assays, and adhesion blockade by antibodies and recombinant CD31 proteins implicate both NH2-terminal and membrane proximal domains in mediating homophilic adhesion. This was explained in an anti-parallel interdigitating model of adhesion in which the membrane proximal domains of CD31 on the surface of one cell bound to the membrane distal domains of CD31 expressed on an apposing cell surface, and *vice versa.*

The general applicability of the Fc-chimera/heterologous COS cell strategy has been questioned for CD31, since studies by Sun *et al.*, 1996a have suggested that exons 9 and 10 (the transmembrane domain and the first 15 amino acids of the cytoplasmic tail) are required for CD31 mediated homophilic adhesion. Clearly, if this were the case, the use of soluble chimeras comprised of the extracellular domain of CD31 fused to human Fc would not be an appropriate approach to dissecting CD31 homophilic adhesion.

The aims of this chapter were; (1) To show that the extracellular domain of CD31 is capable of supporting homophilic adhesion independently of the transmembrane and cytoplasmic tail, (2) to test the anti-parallel fully interdigitating model previously proposed using a range of chimeric constructs, and (3) to identify specific residues involved in mediating homophilic adhesion.

3.2 Results

3.2.1 CD31 homophilic adhesion is mediated by the extracellular domain

Studies by Sun *et al.*, 1996a have suggested that exons 9 and 10 (the transmembrane domain and the first 15 amino acids of the cytoplasmic tail) are required for CD31 mediated homophilic adhesion. To test this assertion, a glycosylphosphatidyl-inositol (GPI) anchored form of CD31 (CD31-GPI) was constructed (C.D. Buckley, DPhil Thesis, Oxford University, 1996) in which the transmembrane and cytoplasmic domains of CD31 are replaced by the 31 carboxyl terminal amino acids of LFA-3 to provide a GPI-anchor signal sequence (Seed, 1987). Previous studies have shown that these 31 amino acids of LFA-3 are necessary and sufficient for GPI-anchor formation (Harrison *et al.*, 1994). CD31-GPI was produced by a two step PCR protocol, firstly a 240bp fragment was amplified from LFA-3 cDNA (obtained by expression cloning, D. Simmons, unpublished data) containing the GPI-signal sequence using primers incorporating *Bam*HI and *Not*I restriction sites (see Methods and Materials) and cloned into pCDNA3 to generate pGPI. The extracellular domain of CD31 was similarly amplified using primers incorporating *Hind*III and *Bgl*II restriction sites and cloned into pGPI vector digested with *Hind*III and *Bam*HI to generate pCD31-GPI. In order to demonstrate the expression of a GPI-linked form of CD31 following transient expression in COS-1 cells, two independent methods were used. Firstly, the presence of a GPI-linkage was confirmed by treating COS transfectants with phosphatidyl-inositol phosholipase C (PIPLC) and following the loss of cell surface expression by FACScan (C. Buckley, personal communication). Full length CD31 expression was not significantly affected by PIPLC treatment (apparent increase of 5.5%), whereas CD31-GPI expression was reduced by 47.5%, comparable to a 37.8% reduction observed for CD14 on PIPLC treatment, which is known to be GPI-linked (Simmons *et al.*, 1989).

Secondly, it was demonstrated that the cytoplasmic tail of CD31 was not present by immunofluorescence with an antibody directed against the cytoplasmic tail of CD31. A rabbit polyclonal antibody was raised against a peptide derived from exons 14/15 of the cytoplasmic tail of CD31 (sequence ETVYSERKAVPDAVESR) coupled to keyhole limpet haemocyanin as immunogen. Crude sera were tested for cross-reactivity with a GST-CD31 cytoplasmic tail fusion provided by Dr. Ian Bird, Yamanouchi Research

Institute, Littlemore, UK (Figure 3.2a) and the IgG fraction from positive sera isolated by Protein-A Sepharose chromatography.

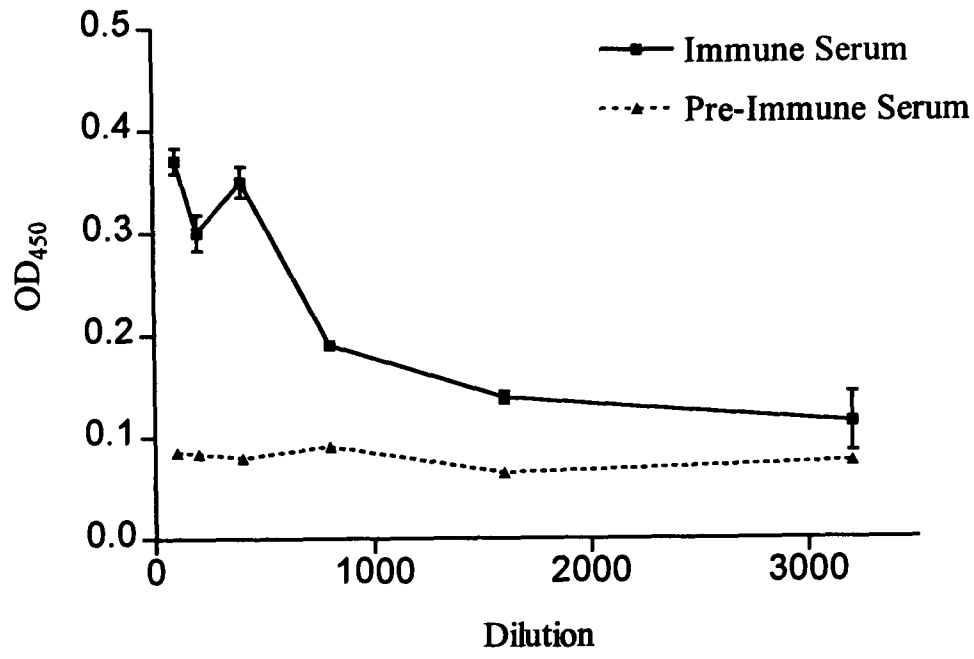


Figure 3.2a ELISA of immune and pre-immune sera against GST-CD31 cytoplasmic tail. Polyclonal antibodies were raised in rabbits against the peptide ETVYSERKAVPDAVESR coupled to keyhole limpet haemocyanin. Crude immune sera were tested by ELISA against CD31 cytoplasmic tail-GST fusion protein produced in *E.coli* (gift Dr. Ian Bird, Yamanouchi Research Institute, Oxford) coated on immunlon-3 96-well microtitre plates at 1μg/well, and blocked with 2% BSA. Rabbit serum was diluted in PBS and added 100μl/well, and incubated for 1 hour at room temperature. Wells were washed and bound antibody detected with horse-radish peroxidase conjugated swine anti-rabbit secondary reagent (1:10,000 dilution in PBS) for 1 hour at room temperature, washed, and visualised with OPD substrate.

Monospecificity of the sera against exon 14/15 was confirmed by peptide blockade with the immunising peptide but not a second peptide derived from the cytoplasmic tail (sequence NHAMKPINDNKE) in immunofluorescence staining of methanol fixed COS cells transiently expressing full length wild type CD31 (Figure 3.2b). Dual immunofluorescence staining of COS-1 cell transfectants expressing either full length wild type CD31 or CD31-GPI with 9G11 (a monoclonal antibody against the NH_2-terminal immunoglobulin-like fold of the extracellular domain of CD31) and the rabbit anti-CD31 cytoplasmic tail polyclonal antibody showed the expected co-localisation of staining in wild type CD31, but no detectable expression of the cytoplasmic tail in the GPI anchored form of CD31 (Figure 3.3). These results clearly demonstrate that the expected GPI-linkage is present, and that there is no detectable cytoplasmic tail.

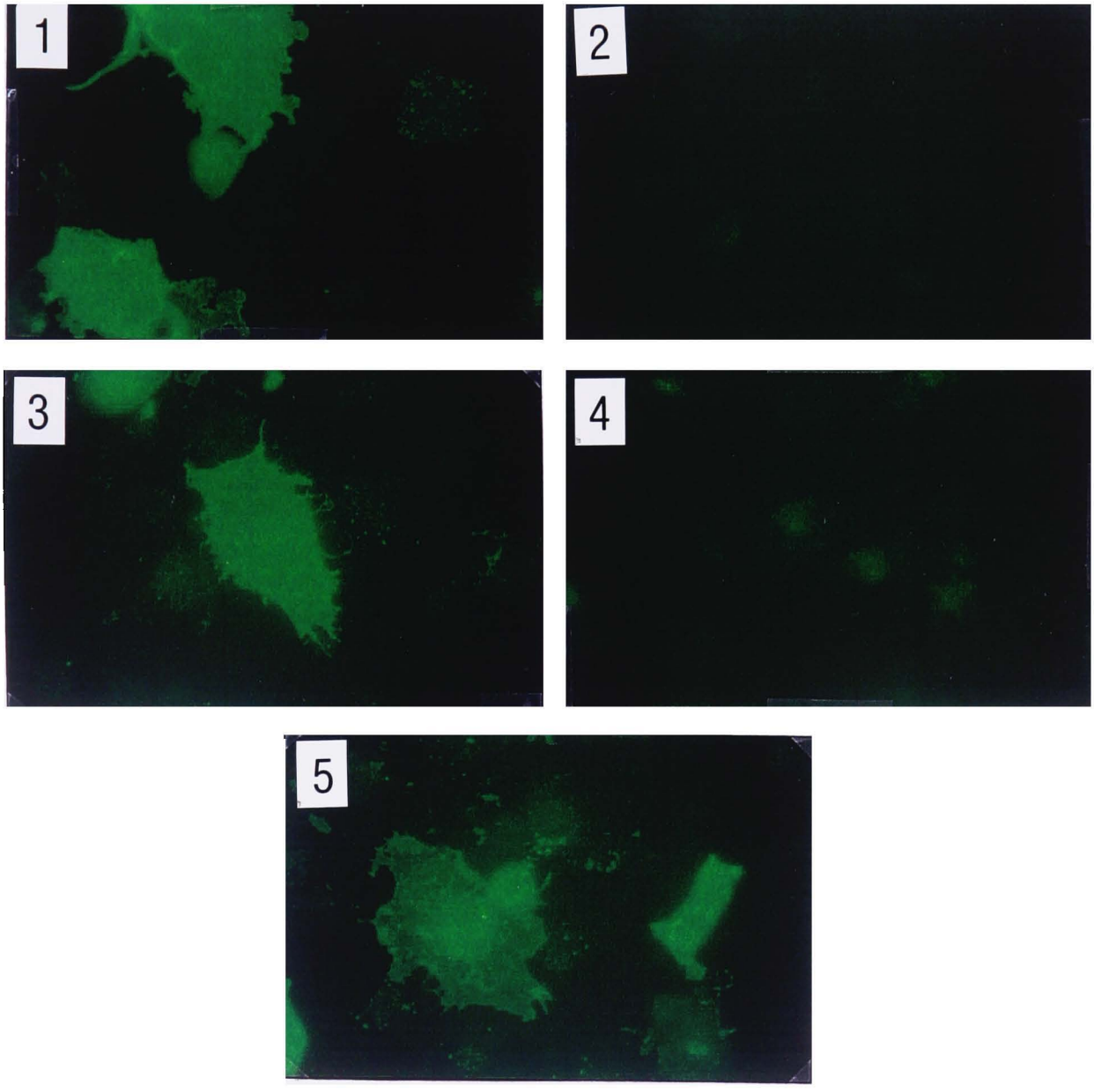


Figure 3.2b Demonstration of monospecificity of rabbit polyclonal anti-CD31 antibody. The monospecificity of the polyclonal antibody raised against the CD31 cytoplasmic tail peptide ETVYSEVRKAVPDAVESR was demonstrated by immunofluorescence staining of COS-1 cells transiently expressing full length human CD31 as follows: Panel 1 - 9G11 mouse monoclonal antibody, visualised with goat anti-mouse FITC (positive control for successful transfection). Panel 2 and 3 - Pre-immune and immune sera respectively, secondary reagents goat anti-rabbit biotin and streptavadin-FITC. Panels 2 and 3 demonstrate a CD31 specific response following immunisation with peptide coupled to keyhole limpet haemocyanin. Panels 4 and 5 - COS cells stained with immune sera and a 200-fold molar excess of either the immunising peptide (panel 4) or a second peptide (sequence NHAMKPINDNKE) derived from the cytoplasmic tail of CD31 (panel 5). Panels 4 and 5 demonstrate a specific response against the immunising peptide, but not a second non-immunising peptide.

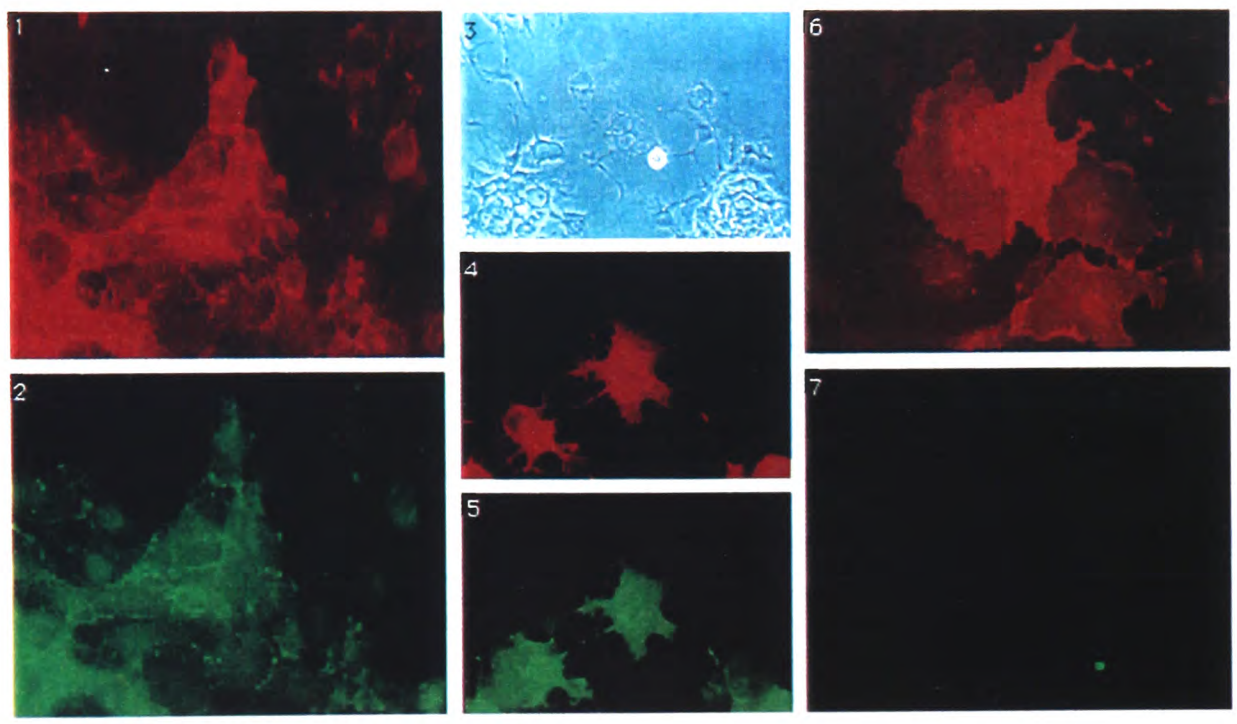


Figure 3.3 CD31-GPI constructs lack a cytoplasmic tail. COS cells expressing full length CD31 or CD31-GPI, and HUVEC endothelial monolayers were stained with 9G11, a mouse monoclonal antibody against the extracellular domain of CD31, and a rabbit polyclonal anti-serum against a peptide derived from the cytoplasmic tail of CD31. Panels 1 and 2 show HUVEC staining, panels 3, 4, and 5 are COS full length CD31 transfectants, and panels 6 and 7 show COS CD31-GPI transfectants. Panels 1,4 and 6 are stained with 9G11, goat anti-mouse TRITC secondary; panels 2, 5 and 7 are stained with anti-CD31 cytoplasmic tail polyclonal, goat anti-rabbit FITC secondary. Panel 3 is phase contrast. Staining shows specificity of polyclonal reagent in full length CD31 transfectants and HUVECs, and that no cytoplasmic tail is detectable in CD31-GPI transfectants.

Expression of both CD31-GPI and full length CD31 in COS-1 cells supported comparable binding in a homophilic adhesion assay to CD31Fc proteins immobilised on plastic compared to negative control protein MUC18 (D1-D5)Fc (Figure 3.4).

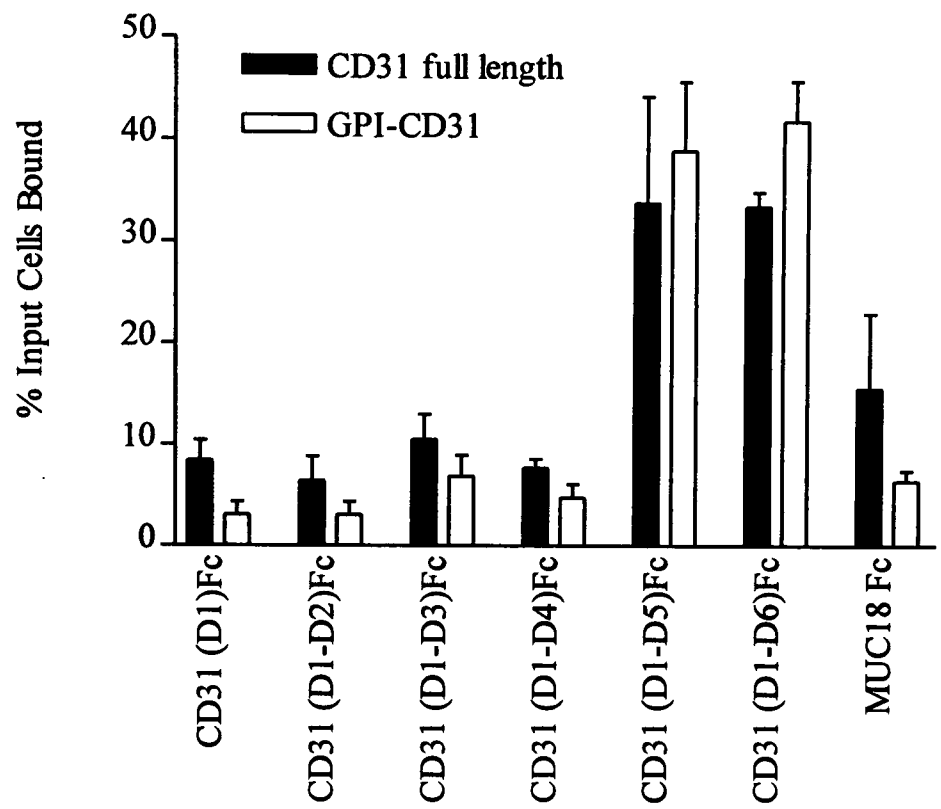


Figure 3.4. Adhesion of COS-1 cells expressing full length CD31 or glycosylphosphatidyl-inositol (GPI) anchored CD31 to CD31 domain deletion series. COS-1 cells transiently expressing either full length or GPI anchored CD31 were allowed to adhere to the CD31 domain deletion series. GPI-CD31 shows the same pattern of binding to the deletion series as full length CD31, and supports comparable levels of adhesion, indicating that the transmembrane and cytoplasmic tail of CD31 are not required in order to mediate homophilic adhesion. Results are expressed as % input cells bound ± 1 SD (n=3)

These results demonstrate that the extracellular domain of CD31 alone is sufficient to support homophilic adhesion and that adhesion is not dependent on transmembrane or cytoplasmic sequences, since neither sequences are present in either the soluble Fc protein or in the cell expressed GPI-linked protein. This validated our Fc chimera strategy, and allowed further dissection of the mechanism of homophilic adhesion using a range of Fc chimeras.

3.3 Mapping the CD31 homophilic binding site

3.3.1 Generation and characterisation of anti-CD31 monoclonal antibodies which affect CD31 homophilic adhesion.

Initial work from this laboratory identified both the membrane proximal and membrane distal immunoglobulin-like domains of CD31 as being involved in homophilic adhesion. Evidence for the role of the NH_2-terminal domains was obtained by the use of antibodies that were mapped to specific domains and which inhibited homophilic adhesion. Screening commercially available anti-CD31 antibodies identified antibodies (L133.1, and 5.6E) which inhibited homophilic adhesion and which mapped to domain 2. A significant limitation of this approach is paucity of antibodies available from commercial sources with functional effects, which may therefore bias the identification of interacting domains. We therefore set out to generate additional functional monoclonal antibodies against CD31 by immunising animals with recombinant CD31Fc proteins. Results of individual fusions are summarised in Table 3.1.

Host	Initial Immunogen	Boost Immunogen	CD31 specific mAbs	Functional mAbs
Female Balb/c mouse	CD31 (D1-D6)Fc	CD31 (D1-D6)Fc	9	0
Female Balb/c mouse	CD31 (D1-D6)Fc	CD31 (D1-D3)Fc	14	1
Female AO rat	CD31 (D1-D6)Fc	CD31 (D1-D6)Fc	64	7 (2 block, 5 enhance)

Table 3.1: Summary of hybridoma fusions to generate anti-CD31 monoclonal antibodies. Animals were immunised subcutaneously with the initial immunogen in complete adjuvant and boosted by intravenous injection in incomplete adjuvant before spleens were removed and hybridomas produced by standard protocols. Hybridoma supernatants were subsequently screened for specificity in ELISAs against CD31 (D1-D6)Fc and MUC18 (D1-D5)Fc to eliminate antibodies with specificity for the Fc portion of the immunogen. Antibodies raised against CD31 were assigned to specific domains and tested for functional effects in homophilic adhesion assays.

The initial fusion produced nine anti-CD31 monoclonal antibodies which mapped throughout the extracellular domain (data not shown), none of which blocked CD31 homophilic adhesion (data not shown). Since the previously characterised functional mAbs cluster at the NH_2-terminus, we initially decided to focus the immune response against this portion of the molecule by boosting with CD31 (D1-D3)Fc protein as immunogen. This produced a total of 14 monoclonal antibodies, one of which (clone 10B9) was found to be

effective in blocking CD31 homophilic adhesion (Figure 3.5). The epitope recognised by 10B9 was determined by ELISA against the CD31 domain deletion series (Figure 3.5), which demonstrated that 10B9 only recognised constructs containing domain 3 of CD31, indicating that 10B9 recognises an epitope contained within this domain.

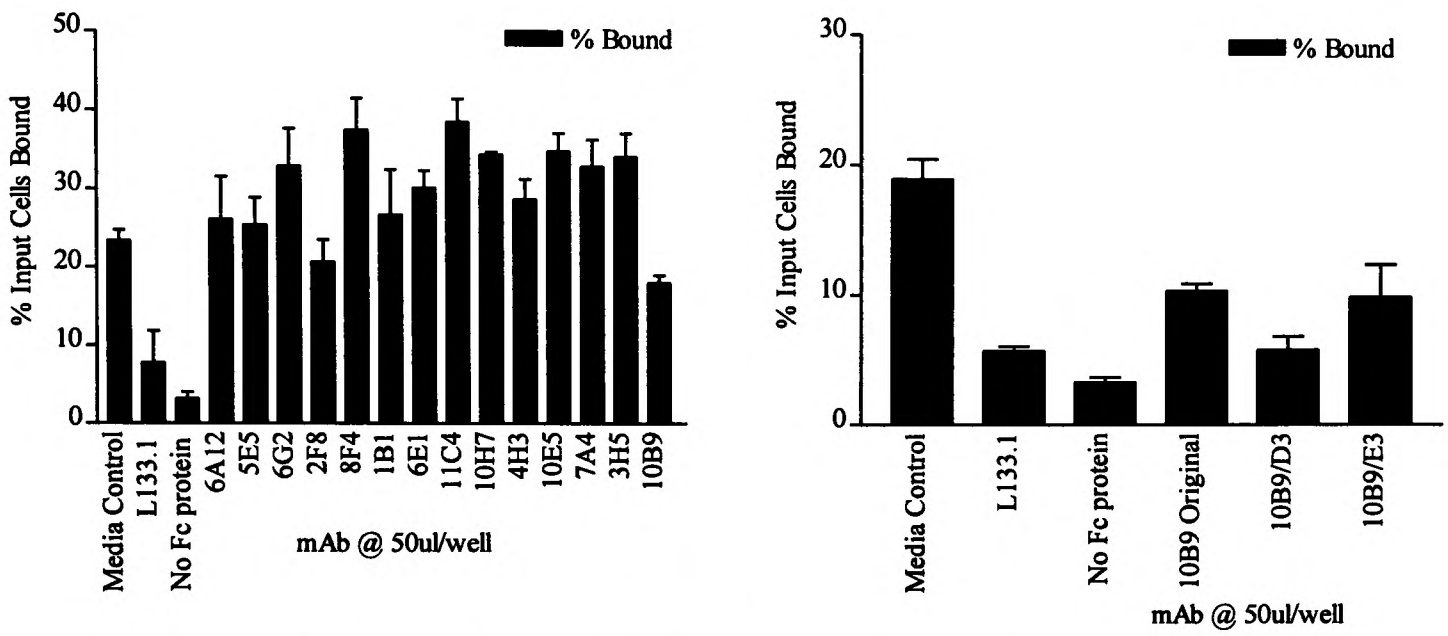


Figure 3.5 Generation and characterisation of an inhibitory anti-human CD31 monoclonal antibody, clone 10B9. Antibody supernatants from a panel of hybridomas raised against CD31 (D1-D3)Fc proteins were screened in an ELISA against CD31 (D1-D6)Fc and MUC18 (D1-D5)Fc proteins which identified 14 supernatants which reacted specifically with CD31. These 14 supernatants were screened for functional effects in homophilic adhesion assays. Adhesion assays were performed as per normal, except that 96-well plates were pre-incubated for 15 minutes with 50µl of each mAb supernatant to be tested prior to the addition of cells. Of the 14 monoclonal supernatants tested, two were initially identified as potential blockers of homophilic adhesion (clones 2F8 and 10B9). Of these supernatants, only clone 10B9 gave consistent inhibition, comparable to that obtained with the previously characterised blocking antibody L133.1, upon subsequent re-cloning (clones 10B9/D3 and 10B9/E3). ELISAs were performed on 10B9 supernatants against CD31 domain deletion series proteins to identify the domain containing the epitope recognised 10B9 (below). Only CD31 constructs containing domain 3 were recognised by 10B9, indicating that 10B9 recognises an epitope within that domain. Previously mapped antibodies (9G11 mapped to domain 1, and L133.1 mapped to domain 2) gave the expected binding patterns, indicating that the failure to bind to shorter constructs containing just NH_2-domains 1 and 2 was not due to gross misfolding of these constructs.

	Antibody supernatant		
	9G11	L133.1	10B9
CD31 (D1)Fc	0.844	0.344	0.256
CD31 (D1-D2)Fc	1.186	1.422	0.240
CD31 (D1-D3)Fc	1.227	0.927	1.184
MUC18 (D1-D5)Fc	0.314	0.390	0.297

This second fusion although successful in generating a novel functional mAb (10B9), was biased towards the NH_2-terminal domains of CD31 and therefore it was decided to carry

out an unbiased fusion using full length CD31 (D1-D6)Fc as immunogen, and to generate rat rather than mouse antibodies. It was hoped that changing the species might give rise to antibodies with novel specificities, and also potentially antibodies with dual specificity for both murine and human CD31. This final fusion was by far the most successful, generating 64 anti-CD31 monoclonal antibodies mapping throughout the extracellular domain (summarised Table 3.2).

CD31 Domain	Antibody clones recognised by
Domain 1	2-3-H11, 4-1-A9, 4-1-E10,, 4-1-F1, 4-2-A11, 4-2-B1, 4-2-D9, 4-3-C10, 4-3-D12, 4-3-F11, 4-3-G6, 4-3-G7, 4-3-H9, 2-1-C7-A7, 2-1-E9-B6, 2-1-E9-B6-H7, 2-1-E9-B6-G11, 4-1-E10-C5-A9,
Domain 2	2-1-F11, 2-2-E1, 2-3-F9, 3-3-A7, 4-1-A6, 4-1-C6, 4-1-H8, 4-2-B3, 4-2-H6, **4-3-C7**, 4-3-E11, 4-3-F10,
Domain 3	2-1-A10, 4-1-A11, 4-2-E3, 4-3-B2,
Domain 4	3-3-C1, *4-2-C3*, 2-1-F7-E12, 4-2-C3-E8-T25,
Domain 5	**2-2-B12**, *2-2-G11*, *2-2-H3*, 2-3-F2, *4-2-C2*, *4-2-F10*, 4-3-E7, 4-3-E9, 4-3-F8, 4-3-H2, 2-1-B2-G12, 2-1-C2-F12, 2-1-E8-G9, 2-1-F2-E8, 2-1-B2-C9-B12, 2-1-B2-C9-E9, 2-1-B2-C9-F11, 2-1-C2-F10-A7, 2-1-C2-F10-G11
Domain 6	4-1-H7, 4-2-F8, 4-3-E7-A10-G12
Unclear (low titre)	2-1-E11, 2-3-B8, 2-3-G2, 2-3-H7

Table 3.2: Summary of epitope mapping by ELISA. Antibodies recognising epitopes in particular domains were assigned by ELISA against the CD31 domain deletion series as previously described for 10B9. Clones in **bold** were found to inhibit CD31 homophilic adhesion, whilst clones in *italics* were identified as potential enhancers of homophilic adhesion

When tested in homophilic adhesion assays (Figure 3.6) two clones were found to block homophilic adhesion, clone 2-2-B12 and clone 4-3-C7. Epitope mapping by ELISA against the CD31 domain deletion series showed that the epitopes recognised by clone 2-2-B12 and clone 4-3-C7 were in domains 5 and 2 respectively.

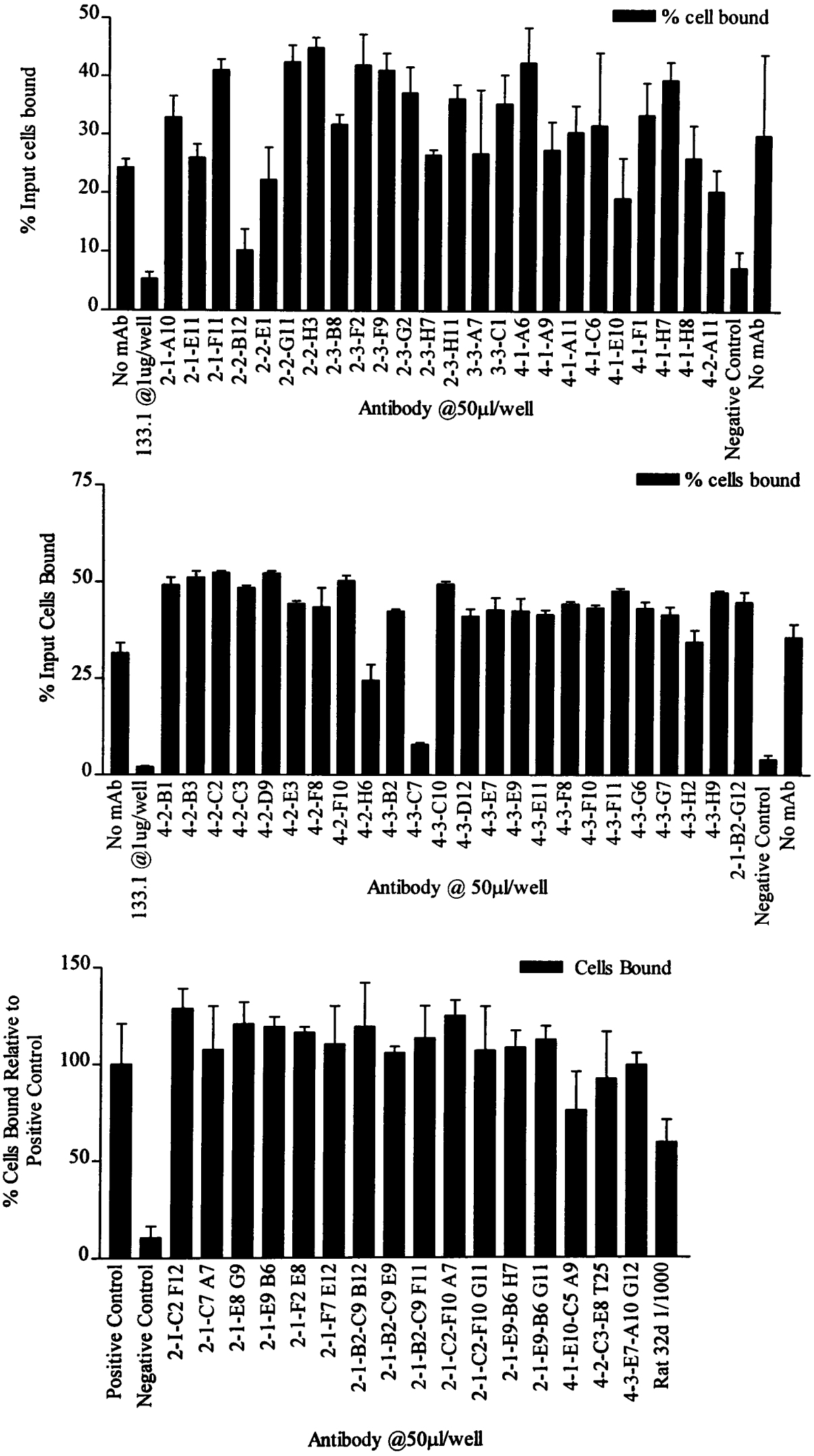


Figure 3.6 Screen of rat anti-human CD31 monoclonal antibody supernatants for functional effects. Assays were performed as described previously (see figure 3.5 legend), to identify 2 functional blocking antibody clones (2-2-B12 and 4-3-C7) and five potential stimulating antibodies (2-2-G11, 2-2-H3, 4-2-C2, 4-2-F10 and 4-2-C3).

In addition a large number of antibodies were identified which increased CD31-mediated adhesion in the homophilic COS assay. The majority of these antibodies mapped to the NH_2-terminal domain 1, and the apparent stimulation in adhesion was attributed to antibody cross-bridging of CD31 expressed on the surface of transfected COS cells and recombinant CD31 bound to plastic. However a subset of the stimulating antibodies recognised epitopes in domains 4 and 5, i.e. the membrane proximal region of CD31, which is less easy to rationalise by cross-bridging of recombinant and cell expressed protein on steric grounds. Previous work from others has shown that an antibody directed against membrane proximal domain 6 of CD31 is capable of stimulating CD31 mediated adhesion. Specifically Fab fragments of the antibody 4G6, which recognises the epitope CAVNEG in domain 6 of CD31 (Yan *et al.*, 1995) has been shown to enhance CD31 homophilic adhesion (Sun *et al.*,1996b). Clearly it will be necessary to produce Fab fragments of these antibodies to confirm that stimulation of adhesion is not due to cross-linking, and these experiments are currently underway.

Previous work from this laboratory identified two commercially available monoclonal antibodies which inhibited homophilic adhesion, all of which mapped to NH_2-terminal domain 2 of the extracellular domain. The present study has produced a large number of monoclonal antibodies raised in mouse and rat against every domain of human CD31. Moreover, antibodies recognising epitopes in domains 2,3 and 5 have been produced which inhibit homophilic adhesion, suggesting that a large portion of the extracellular domain is involved in mediating homophilic adhesion and is thus consistent with the two-site anti-parallel fully-interdigitating model originally proposed by Fawcett *et al.*, 1995. Interestingly a number of stimulating antibodies, have also been identified. Whilst further experiments are required to confirm that this is not a cross-bridging effect, these suggest that CD31 can be induced to undergo conformational changes which influence homophilic adhesion.

3.3.2 Use of ICAM-3 (CD50)/CD31 chimeras to investigate the role of the N-terminal extracellular immunoglobulin-like domains.

The antibody blockade studies described above indicate that both the membrane proximal and membrane distal immunoglobulin-like domains are involved in mediating CD31 homophilic adhesion, consistent with the two-site anti-parallel, fully interdigitating model of CD31 homophilic engagement. The data presented to date do not exclude the possibility

that rather than a direct association between membrane proximal and membrane distal domains of CD31 on apposing cell surfaces, some domains may play an accessory or enabling role, rather than a direct role in mediating homophilic adhesion. The identification of stimulating antibodies mapping to the membrane proximal domains is suggestive of this possibility. A prediction of a fully interdigitating model for CD31 homophilic adhesion is that two binding sites exist on each molecule, and as such, removal of one site would be expected to reduce rather than ablate binding. In order to directly test the anti-parallel interdigitating model of homophilic adhesion a series of chimeric ICAM-3/CD31 constructs were produced in which immunoglobulin domains from CD31 were replaced by the equivalent domains from ICAM-3 (CD50), as summarised in Figure 3.7. Chimeric constructs were generated as described in Materials and Methods, using either a recombinant PCR strategy with overlapping primers comprised of CD31 and ICAM-3 sequences, or by introducing restriction sites by PCR. COS cells expressing each construct were analysed by FACScan (Figure 3.8a) and immunoprecipitation (Figure 3.8b) to show expression of chimeras containing the appropriate domains (summarised Table 3.3). Transfectants were then allowed to adhere to plastic coated with CD31 (D1-D6)Fc or negative control MUC18 (D1-D5)Fc proteins (Figure 3.9). Replacement of the first NH_2-terminal domain of CD31 resulted in complete ablation of adhesion, indicating that domain 1 is necessary for homophilic adhesion. This is not consistent with the two-site anti-parallel model initially proposed, and indicates that there is a single homophilic binding site located at the NH_2-terminus of CD31, with domain 1 playing a dominant role.

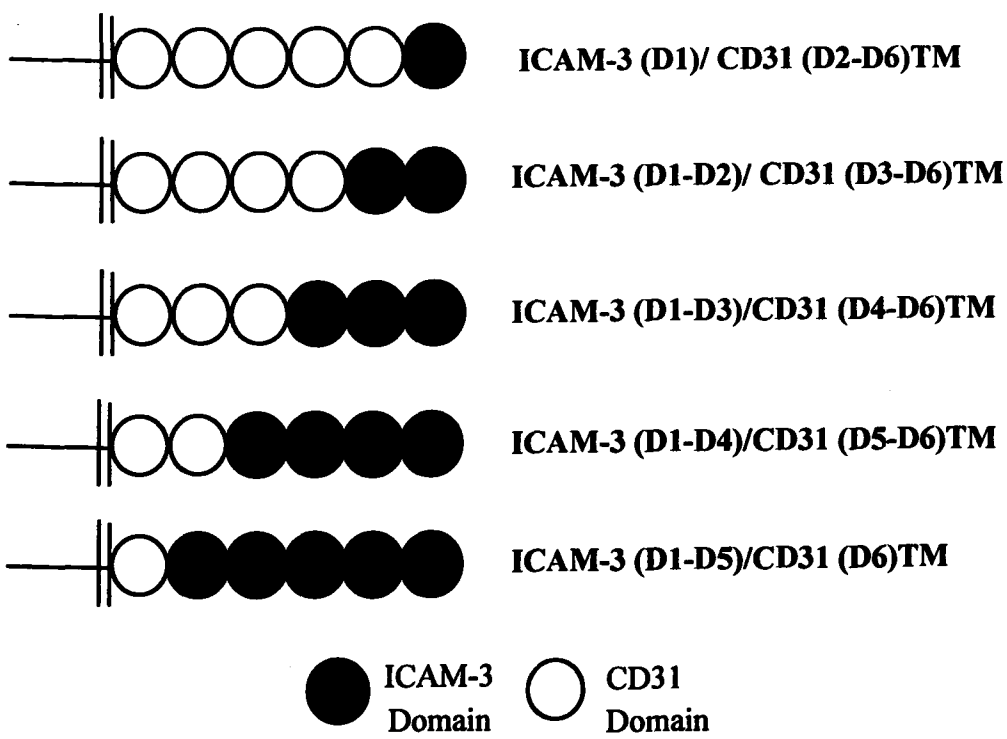


Figure 3.7 A series of ICAM-3 (CD50) and CD31 chimeric constructs were produced in which specific immunoglobulin-like domains of CD31 were replaced by equivalent domains from ICAM-3. D1 through D6 indicate the immunoglobulin folds of the extracellular domain, (numbering from the NH_2-terminus). TM indicates that the transmembrane and cytoplasmic tail of CD31 are present.

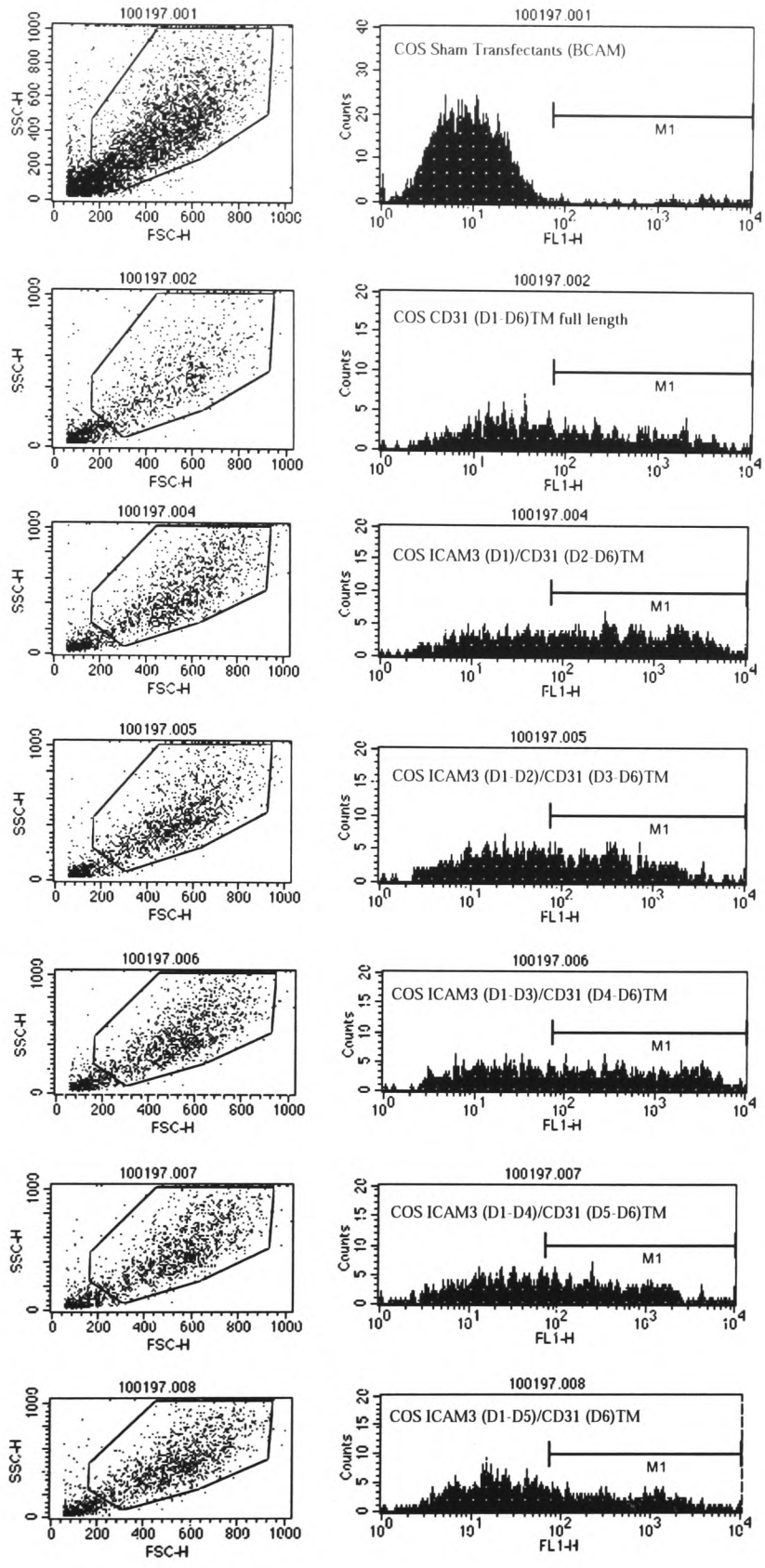
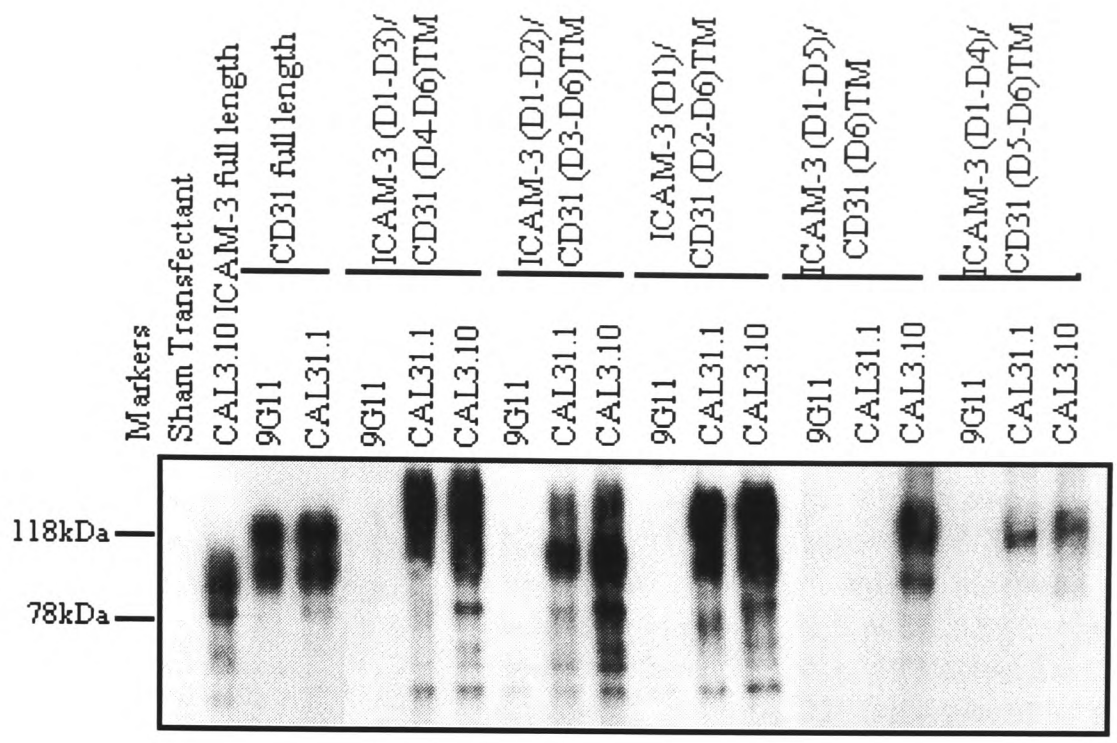


Figure 3.8a: FACScan profiles of COS-1 cells transiently transfected with CD31/ICAM-3 constructs. Cells were harvested 48 hours post-transfection with the various constructs in 2mM EDTA/PBS, washed, and resuspended in at 2 x 10^6 cells/ml in PBS containing 0.25% BSA. 100µl aliquots of cells were stained for 20 minutes on ice with 2µg of either mouse anti-CD31 monoclonal 9G11 (recognising NH_2-domain 1of CD31) or mouse anti-ICAM-3 monoclonal CAL3.10 (recognising NH_2-domain 1 of ICAM-3) as appropriate. For negative control, COS sham transfectants expressing BCAM, a cell surface molecule of unknown function, (gift Dr. Ian Campbell, University of Southampton) were stained with both 9G11 and CAL3.10 antibodies. Cells were washed and bound antibody detected by incubating with goat anti-mouse.FITC conjugated secondary antibody diluted 1:100 in PBS. Finally cells were washed and fixed in a 2% paraformaldehyde solution in PBS, before being analysed on a Becton Dickinson FACScan.



Source: Lab Book 1 p.121

Figure 3.8b Immunoprecipitation analysis of ICAM-3/CD31 chimeras expressed on COS-1 cells. COS-1 cells transiently expressing ICAM-3/CD31 chimeras were harvested in 2mM EDTA/PBS, washed and cell surface proteins biotinylated. Cells were lysed, and samples pre-cleared with anti-ICAM-1 mAb BBA-4. Samples were immunoprecipitated with anti-ICAM-3 antibody CAL3.10, anti-CD31 antibodies 9G11 and CAL31.1. Immunoprecipitated protein samples were run out on a 7.5% acrylamide gel, transferred onto HighBond-N nitrocellulose membrane, blocked with 5% non-fat milk powder and biotinylated protein detected with streptavadin-HRP, and visualised with the ECL-kit (according to the manufacturers protocol). All of the chimeras were recognised by the anti-ICAM-3 domain 1 specific antibody CAL 3.10 as expected, and are of a higher apparent molecular weight than full-length ICAM-3, consistent with the expected chimeric nature of these six Ig domain constructs. With the exception of ICAM-3 (D1-D5)/CD31(D6) all of the chimeras are recognised by CAL 31.1, an anti-CD31 antibody specific for domain 6 of CD31, which is consistent with the expected chimeric nature of the proteins. The failure of ICAM-3 (D1-D5)/CD31(D6)TM to be recognised by CAL31.1 may indicate that this construct is misfolded, or that the antibody recognises an epitope at the boundary between domains 5 and 6. None of the chimeras is recognised by 9G11, an anti-CD31 mAb specific for domain 1.

Construct	IP result with			FACScan profile	
	9G11	CAL 31.1	CAL 3.10	MFI	COS cells expressing construct
full length CD31	+	+	-	324	40.6%
ICAM-3 (D1)/CD31 (D2-D6)TM	-	+	+	654	63.2%
ICAM-3 (D1-D2)/CD31 (D3-D6)TM	-	+	+	191	43.1%
ICAM-3 (D1-D3)/CD31 (D4-D6)TM	-	+	+	594	55.1%
ICAM-3 (D1-D4)/CD31 (D5-D6)TM	-	+	+	305	48.5%
ICAM-3 (D1-D5)/CD31 (D6)TM	-	-	+	237	38.9%

Table 3.3 Summary of experiments to characterise cell surface expressed ICAM-3/CD31 chimeras. Each construct was expressed on the cell surface, and recognised by antibodies specific for the NH_2-terminal domain. In immunoprecipitations, each chimera was immunoprecipitated by the anti-ICAM-3 antibody CAL3.10 directed against the NH_2-terminal domain 1, and with the exception of ICAM-3 (D1-D5)/CD31 (D6)TM by the anti-CD31 antibody CAL31.1, recognising domain 6. None of the chimeras were recognised by 9G11, an anti-CD31 antibody recognising domain 1 of CD31.

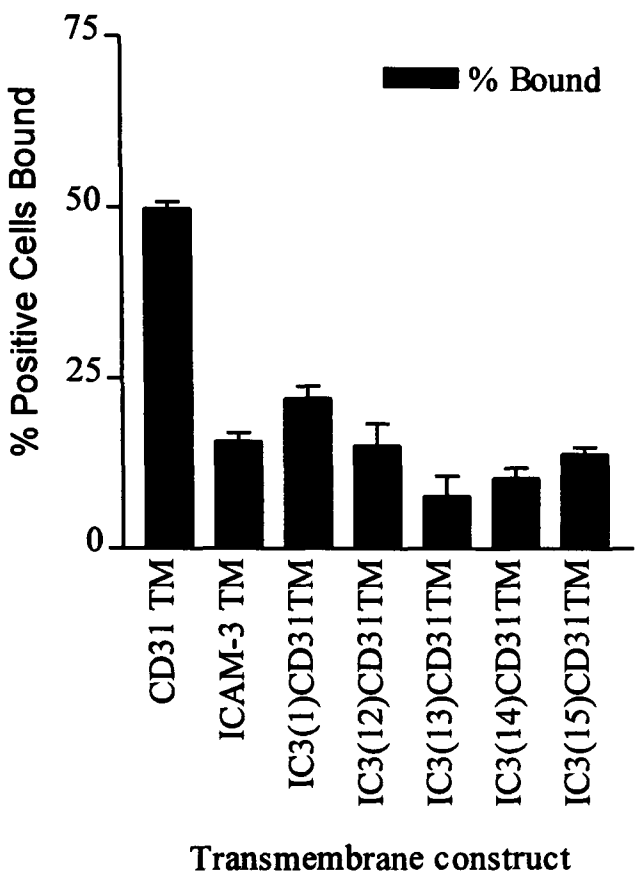


Figure 3.9 CD31 domain 1 is necessary to support homophilic adhesion. COS-1 cells transiently expressing the ICAM-3/CD31 transmembrane expressed chimeras described in Fig. 3.8 were allowed to adhere to plastic coated with CD31 (D1-D6)Fc or negative control ICAM-3 (D1-D5)Fc proteins. Replacement of NH_2-terminal domain 1 of CD31 with the equivalent domain of ICAM-3 results in complete ablation of CD31 homophilic adhesion, indicating that the homophilic binding site resides at least in part in domain 1 of CD31. IC3(1)CD31TM indicates that domain 1 of CD31 is replaced by domain 1 from ICAM-3. In IC3(12)CD31TM domains 1 and 2 of CD31 are replaced by equivalent domains from ICAM-3. IC3(13)CD31TM indicates domains 1 to 3 of DC31are replaced by equivalent domains from ICAM-3. IC3(D14)CD31TM indicates that domains 1 to 4 of CD31 are replaced by equivalent domains from CD31 IC3(15)CD31TM indicates that domains 1 to 5 of CD31 are replaced by domains 1 to 5 from ICAM-3. Results are corrected for transfection efficiency, assuming the values obtained from 9G11 staining (for wild type CD31) or CAL3.10 staining (for ICAM-3/CD31 chimeras) as shown in Table 3.3.

Source aa02/97 Plate 2

The identification of domains 5 and 6 as a component of the homophilic binding site was based upon the observation that in a series of nested deletion constructs, only those containing 5 or 6 domains supported homophilic adhesion. One possibility is that this arose because steric hindrance blocked the binding of cell expressed CD31 to truncated CD31Fc constructs when in proximity to plastic. Previous experience with similar constructs for CD66 (Watt *et al.*, 1993), ICAM-3 (Fawcett *et al.*, 1993, Holness *et al.*, 1995) and sialoadhesin (Nath *et al.*, 1995) would suggest that this is not the case. However, in order to completely eliminate this possibility two additional constructs in which the NH_2-terminal domains 1 and 2, and 1 to 3 of CD31 fused to an irrelevant ICAM-3 stalk, in all cases preserving the overall length of the extracellular portion as 6 Ig type doınains (Figure 3.10 and Table 3.4) were produced using the recombinant PCR strategy (see Methods and Materials for details). In an adhesion assay where COS cells expressing full length CD31 were allowed to adhere to each of these constructs (Figure 3.11), the three NH_2-terminal domains of CD31 did not support adhesion, even though the CD31 NH_2-terminal domains were presented in the context of a construct the same length as wild type CD31. The combined results from these constructs indicate that while the NH_2-terminal domains are

necessary for CD31 homophilic adhesion they are not sufficient. Significant homophilic binding occurs only in the context of a full length CD31 extracellular domain.

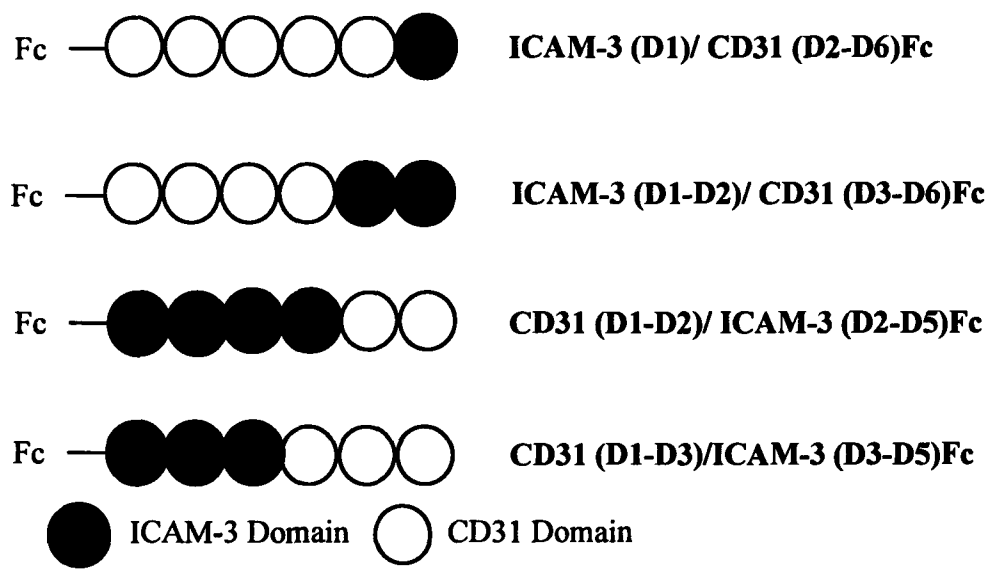
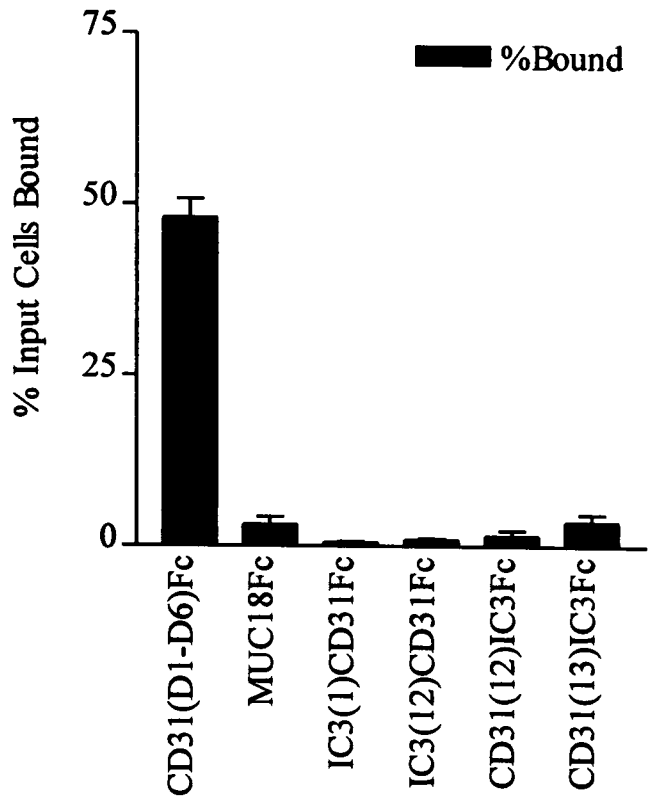


Figure 3.10. Schematic diagram of ICAM-3/CD31 Fc chimeric constructs. Chimeric constructs were produced in which specific domains of CD31 were replaced by equivalent immunoglobulin domains from ICAM-3. Initial replacements of the N-terminal domains recapitulates the ICAM-3/CD31 transmembrane constructs previously produced. In addition to further constructs were produced which consisted of the NH_2-terminal domains 1and 2, and 1 to 3 of CD31, expressed on an ICAM-3 stalk, preserving the overall length as six Ig domains. These were used to overcome any potential steric effects which might have blocked the binding of cell expressed CD31 to truncated CD31Fc proteins.

Construct	Anti-CD31 antibodies						Anti-ICAM-3 antibodies			
	9G11 (D1)	L133.1 (D2)	Hec7.2 (D2)	10B9 (D3)	10B5 (D5)	CAL31. 1 (D6)	CAL3. 10 (D1)	CAL3.24 (D1)	CH3. 2 (D1-2)	KS128 (D2)
ICAM-3 (D1)/CD31 (D2-D6)Fc	-	-	-	+++	++	++	++	++	+++	-
ICAM-3 (D1-D2)/CD31 (D3-D6)Fc	-	-	-	++	++	++	++	++	+	+
CD31 (D1-D2)/ICAM-3 (D2-D5)Fc	+	++	-	-	-	-	-	-	-	-
CD31 (D1-D3)/ICAM-3 (D3-D5)Fc	+++	+++	+++	++	-	-	-	-	-	-
ICAM-3 (D1-D5)Fc	-	-	ND	ND	-	-	+++	+++	+++	+++
CD31 (D1-D6)Fc	+++	+++	+++	+++	+++	+++	-	-	-	-

Source: ELISAs dated 01.02.96, 20.02.97 and 06.07.97

Table 3.4 ELISA Profile of ICAM-3/CD31 Fc chimeras. Solid phase ELISA's were performed on each construct using anti-CD31 and anti-ICAM-3 antibodies previously mapped to specific domains (24,28). ELISAs show the expected pattern of cross-reactivity with each construct, with the exception of L133.1 and Hec7.2(anti-CD31 domain 2) which fails to recognise ICAM-3 (D1)/CD31 (D2-D6)Fc, indicating that the epitope may reside in the boundary between domains 1 and 2. Hec7.2 also fails to recognise CD31 (D1-D2)/ICAM-3 (D2-D5)Fc. Broadly, the expected pattern of membrane proximal and membrane distal CD31 and ICAM-3 domains are present.



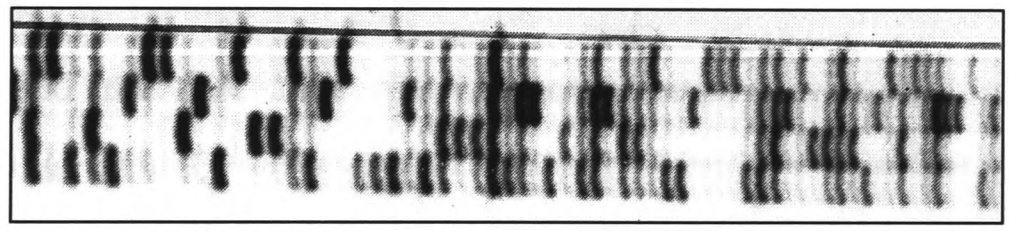
Source: yamaa08/96 wash 2

Figure 3.11 The NH_2-terminal domains of CD31 alone are not sufficient to support homophilic adhesion. COS-1 cells expressing full length CD31 were allowed to adhere to plastic coated with CD31/ICAM-3 Fc chimeras, in which either the NH_2-terminal domains of CD31 are replaced by equivalent domains from ICAM-3, or in which the NH_2-terminal domains of CD31 were expressed on an ICAM-3 stalk. Removal of NH_2-terminal domain 1 ablates binding, as noted previously, confirming that this is the case for both cell expressed (Figure 3.10) and soluble recombinant forms of CD31. Expression of the CD31 NH_2-terminal domains 1 and 2 or 1 to 3 on an ICAM-3 stalk preserving the overall length of the extracellular as six Ig domains, does not support homophilic adhesion. These results indicate that the failure of truncated NH_2-terminal domain deletion proteins to bind is not due to steric hindrance, and that the NH_2-terminal domains are not competent to mediate binding without the membrane proximal domains.

3.3.3 Use of mouse/human CD31 chimeras to identify the homophilic binding site.

Removal of the NH_2-terminal domain 1 of CD31 completely ablates homophilic adhesion, however, expressing the NH_2-terminal domains of CD31 in the context of a non-CD31 backbone (i.e. as CD31/ICAM-3 Fc chimeras) does not support adhesion, suggesting that the NH_2-terminal domains are necessary, but not sufficient to support homophilic adhesion. To test the hypothesis that the NH_2-terminal domains of CD31 are involved in mediating homophilic adhesion, but that the membrane proximal domains of CD31 play an important non-binding accessory role in adhesion, a human/mouse chimeric construct was made in which the two NH_2-terminal domains of murine CD31 were replaced by the equivalent domains from human CD31, utilising a shared unique *Bam*HI restriction site at the junction between domains 2 and 3. A murine CD31 (D1-D6)Fc immunoadhesin was initially generated as for human CD31 by PCR amplification from a murine CD31 template (gift of Professor William Müller, see Xie *et al* 1993) using forward amplification primer (5' ATAT AAGCTT CAGTCGGCAGCAAAG ATG 3') and reverse amplification primer (5' ATAT AGATCT ACTTACCTGT TTT CTT CCA TGG GGC AAG 3'). The resultant PCR product was digested with *Hind*III and *Bgl*II, and cloned into pIG_1 digested with *Hind*III and *Bam*HI to give murine CD31 (D1-D6)Fc in pIG_1. A human/mouse chimera was produced by digesting human CD31 in pCDM8 (Simmons *et al* 1989) with *Hind*III and

*Bam*HI to liberate a fragment corresponding to domains 1 and 2, and subcloning this fragment into murine CD31 (D1-D6)Fc in pIG_1 similarly digested with *Hind*III and *Bam*HI. The resulting chimera was sequenced across the junction between domains 2 and 3 (Figure 3.12) to confirm the presence of both mouse and human sequences. Chimeras were expressed in COS-1 cells and Fc proteins purified from conditioned media with Protein-A sepharose, and the presence of the expected domains confirmed by ELISA. (Table 3.5). In adhesion assays with COS-1 cells expressing either full length human or murine CD31 (Figure 3.13), human CD31 expressed on the surface of COS-1 cells failed to support adhesion to murine CD31 and *vice versa*, demonstrating species specificity. Replacement of murine domains 1 and 2 with the equivalent human domains resulted in loss of binding to murine CD31 expressed on COS-1 cells, but significantly gave rise to a "gain-of-function" phenotype in which COS-1 cells expressing human CD31 bound to the human/mouse chimera. Thus transfer of human CD31 domains 1 and 2 into a murine domain 3 to 6 background was sufficient to restore homophilic binding to human CD31. These findings strongly implicate the NH_2-terminal domains as forming the primary homophilic contact sites.



ATGTCAAGCTAGGATCATTTCAGGGATCCTGTCCGGATTCAAATTGCAGGAGT

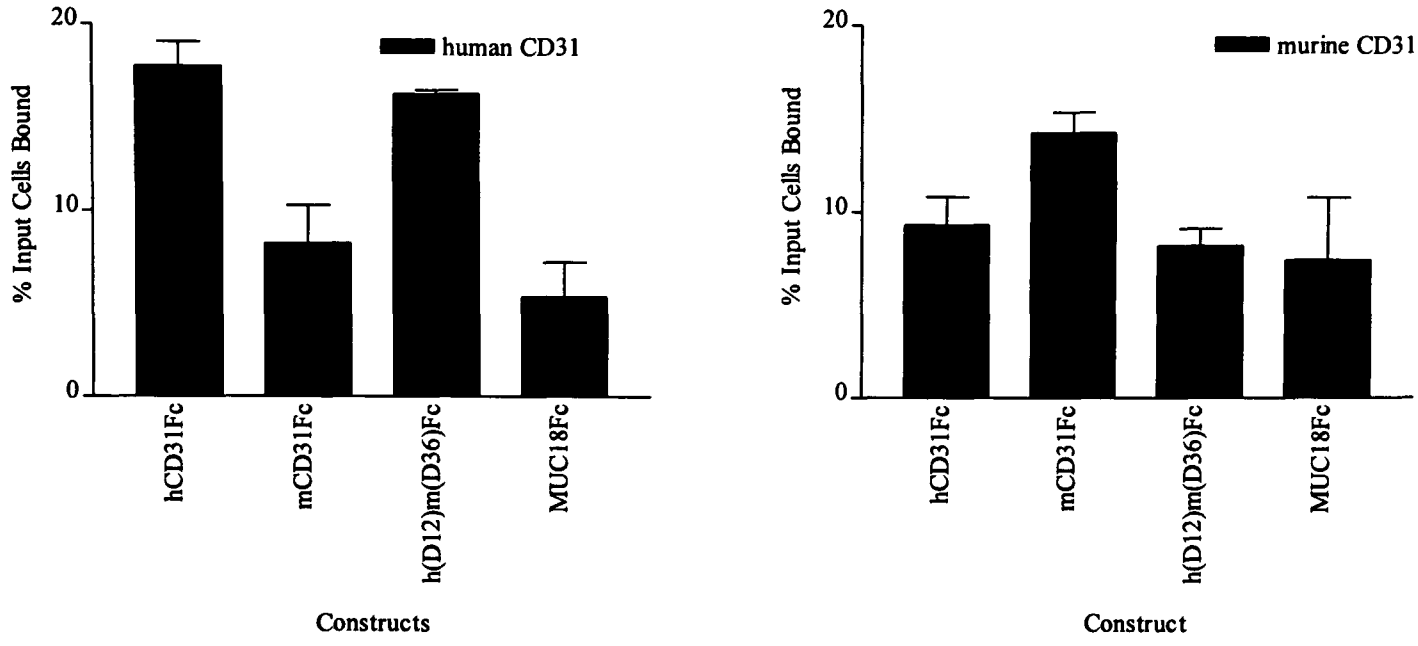
Human Sequences BamHI Site Murine Sequences

Figure 3.12 Chimeric human/murine CD31 construct sequence. Chimeric human/murine CD31 construct was produced utilising a unique endogenous BamHI restriction site at the boundary between domains 2 and 3 present in both murine and human CD31. Sequencing of this construct showed the expected human and murine CD31 sequences, including at the predicted BamHI site, as shown above.

Construct	9G11 (D1)	Hec7.2 (D2)	10B9 (D3)	CAL31.1 (D6)	Mec 13.3 (D2)	Clone 390 (D2)
Human CD31 (D1-D6)Fc	+++	+++	+++	+++	-	-
Murine CD31 (D1-D6)Fc	-	-	-	-	+++	+++
Human CD31 (D1-D2)/Murine CD31 (D3-D6)Fc	+++	-	-	-	-	-

Source: ELISA 06.07.97

Table 3.5. ELISA profile of human/mouse CD31 constructs.. Mouse and human CD31 show expected cross-reactivity with anti-mouse (MEC13.3 and Clone 390) and anti-human (9G11, Hec7.2, 10B9 and 2H8) monoclonals. In the human/mouse chimera, replacement of the first two NH_2-terminal domains with the equivalent domains from human CD31 prevents recognition by the two anti-murine monoclonals directed against domain 2 (Dr. Ian Bird, personal communication), and restores binding to 9G11 (anti-human CD31 monoclonal recognising domain 1 of CD31), although not binding to Hec7.2 (recognising domain 2 of human CD31)



Source: aa15/97 wash 1

Figure 3.13 Analysis of homophilic adhesion using human/murine CD31 chimeras. COS-1 cells expressing human and murine CD31 were allowed to adhere to plastic coated with human CD31 (D1-D6)Fc, murine CD31 (D1-D6)Fc, human CD31 (D1-D2)/murine CD31 (D3-D6)Fc and negative control protein MUC18 (D1-D5)Fc. Human CD31 expressed on the surface COS-1 cells bound to human CD31 (D1-D6)Fc, but not murine CD31 (D1-D6)Fc and *vice versa*, demonstrating species specificity. Significantly, replacement of the NH_2-terminal domains of murine CD31 by equivalent domains from human CD31 ablate binding to murine CD31, but gives rise to a "gain-of-function" phenotype by binding to COS-1 cells expressing human CD31. Collectively these results imply that the homophilic binding site is contained within the two NH_2-terminal domains 1 and 2.

3.3.4 Site-directed mutagenesis of CD31 immunoglobulin-like domains 1 and 2

Having established that the two NH_2-terminal domains of CD31 directly mediate homophilic binding, a mutagenesis screen of domains 1 and 2 was undertaken. The primary amino acid sequences of CD31, VCAM-1, and ICAM-1 were aligned using the Genetics Computer Group (Wisconsin University) PILEUP programme (Figure 3.14) and using the crystal structure co-ordinates for VCAM domain 1 as a representative immunoglobulin fold (Jones *et al.*, 1995), equivalent residues from CD31 were substituted in the place of residues from VCAM using the programme MUTATE (Robert Esnouf, Laboratory of Molecular Biophysics, Oxford), preserving the crystal structure Cα and Cβ main chain co-ordinates for each residue. Regions lacking homology, corresponding to loop regions between β-strands, were modelled using the interactive graphics programme FRODO (Jones, 1985). Modelled inserts of five, four and one additional residues at the NH_2-terminus, the BC loop and the FG loop respectively were included to generate a putative topology appropriate for residues 3 to 100 of CD31.

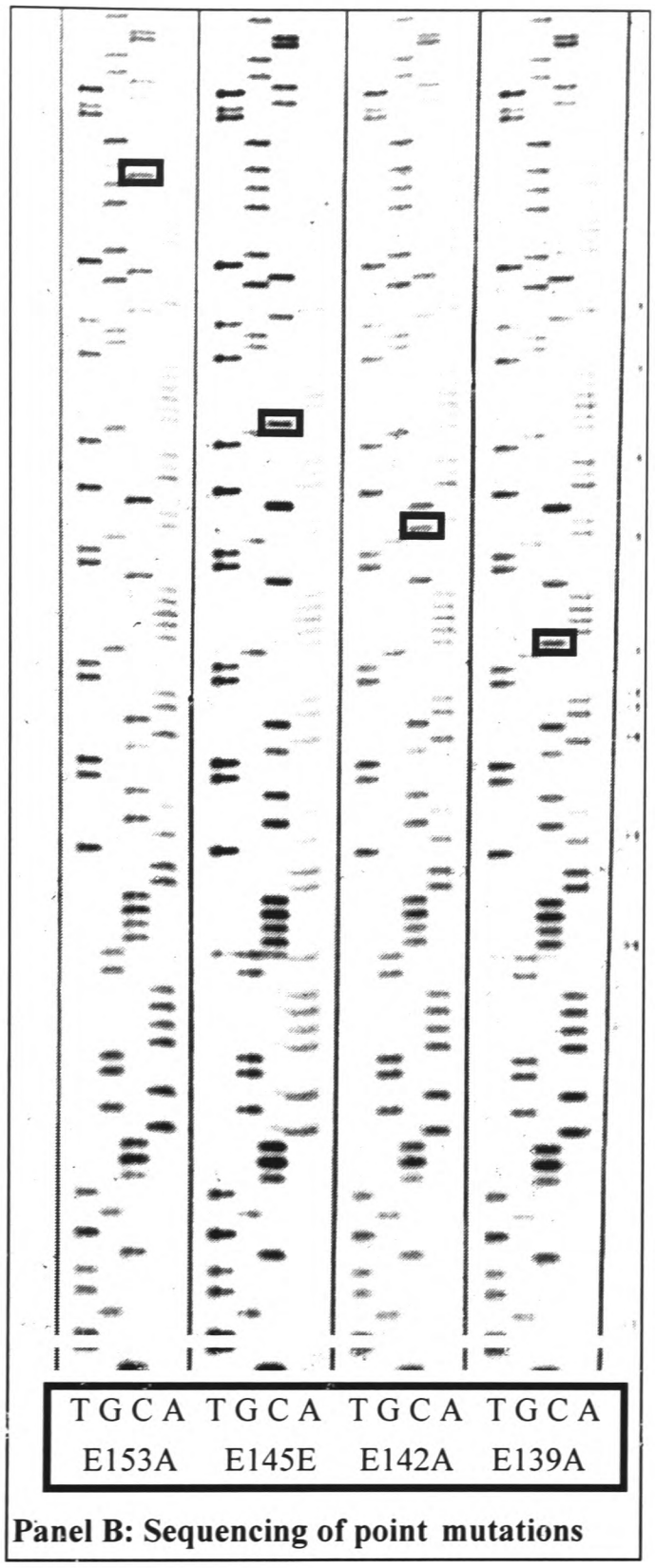
```
                    <----------A----------> <---------B--------> <--C--->
ICAM1  .......NAQ TSVSPSKVIL PRGGSVLVTC ....STSCDQ PKLLG....I
 VCAM  .......FKI ETTPESRYLA QIGDSVSLTC ....STTGCE SPFFSWRTQI
 CD31  QENSFTINSV DMKSLPDWTV QNGKNLTLQC FADVSTTSHV KPQHQMLFYK
        [ Insert ]                          [ Insert ]

                  <---D----> <--E--->           <-----F-------> <-------G-------->
ICAM1  ETPLPKKELL LPGNNRKVYE LSNVQEDSQP MCYSNCPDGQ STAKTFLTVY
 VCAM  DSPLNGKVTN EGTTSTLTMN PVSFGNEHSY LCTATCESR. KLEKGIQVEI
 CD31  DDVLFYNISS MKSTESYFIP EVRIYDSGTY KCTVIVNNKE KTTAEYQLLV
                                                    [Insert

ICAM1  WTPERVEL.. ..APLPSWQP VG.....
 VCAM  YSFPKDPEIH LSGPLEAGKP ITVKCSV
 CD31  EGVPSPRV.. .......... ......
```

Figure 3.14 Alignment of primary amino acid sequence for the NH2-terminal immunoglobulin C2-type domains from ICAM-1, VCAM-1 and CD31. Sequences (obtained from GenBank) were aligned using GCG PILEUP programme (Gapweight = 3.000, Extension penalty =0.100). Strand assignments are based upon the crystal structure of VCAM domains 1 and 2 previously solved by Jones *et al* 1995. Compared to VCAM-1 D1 there are three significant regions of non-homology, at the N-terminus, in the BC-loop region, and in the FG-loop. These loop regions were modelled using the interactive graphics programme FRODO, whilst the remaining residues were mapped onto the Cα and Cβ carbon positions of the equivalent residues in the VCAM-1 structure to generate a topology model for CD31 domain 1 (see figure 3.18).

Using this model as a guide, all of the predicted solvent exposed aspartate, glutamate, arginine and lysine residues in domain 1, and a subset of charged residues in domain 2 encompassing the putative heparin binding motif LKREKN (DeLisser *et al.*, 1993) were selected as targets for mutagenesis. For the most part, charged residues were substituted with alanine, using a two step recombinant PCR approach to generate 26 single point mutants in a CD31(D1-D6)Fc backbone (as described in Methods and Materials). This method proved to be extremely rapid and simple, and combined with the use of *Pwo* thermostable DNA polymerase, gave relatively few spontaneous PCR induced mutations. Each mutant was sequenced in its entirety (Figure 3.15) to confirm the presence of the expected mutation. Mutant proteins were produced in COS cells by transient expression and purified from culture supernatants with Protein-A sepharose.



Panel B: Sequencing of point mutations

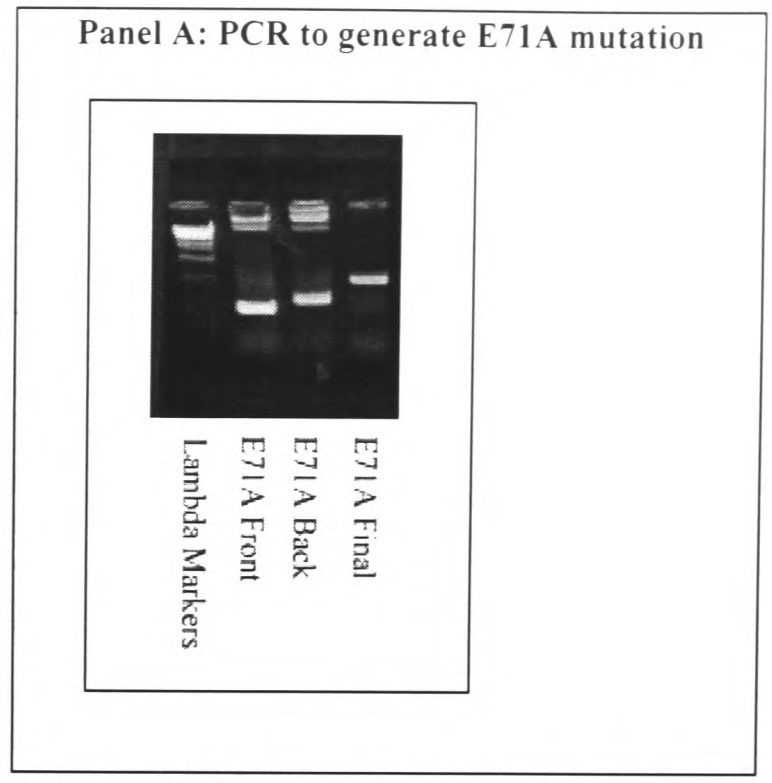


Figure 3.15 Generation of single point mutations in CD31 (D1-D6)Fc in pIG_1 vector. Single point mutations were introduced using an overlapping PCR protocol in which each mutant was synthesised as two overlapping fragments, where the overlap occurs between two complementary mutagenic primers (see Methods and Materials). Both fragments were subsequently used as self-priming templates in a second round of PCR using only the outer non-mutagenic primers to generate a single PCR fragment corresponding to domains 1 and 2 of CD31 (see panel *A*, above). Each mutant was manually sequenced by the dideoxy-terminator method to confirm the presence of the expected mutation and lack of adventitious PCR induced mutations (see panel *B* left), before being subcloned into the CD31 (D1-D6)Fc backbone.

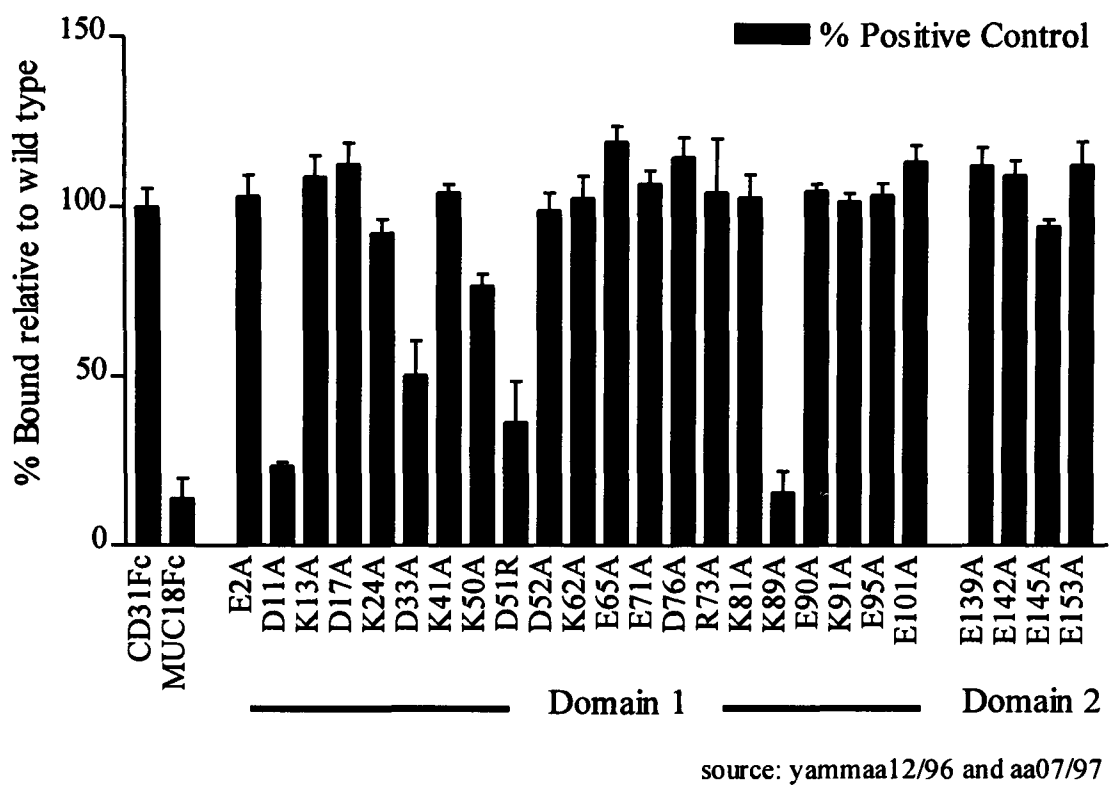
The structural integrity of the mutants was assessed by ELISA profile (Table 3.6) using a panel of 12 anti-CD31 monoclonal antibodies predominantly against epitopes in domains 1 and 2 (including blocking antibodies L133.1, Hec 7.2 and 5.6E) but also including antibodies mapping throughout the extracellular domain. Of the mutants examined, only one (K50E) was judged to be grossly misfolded, and subsequently excluded from further analysis.

Mutant (domain)	CLB-468 (D2)	VM64 (ND)	P2B1 (ND)	CLB-58 (D5)	5.6E (D2)	WM59 (D2)	CAL 31.1 (D6)	9G11 (D1)	Igi18 (ND)	L133.1 (D2)	10B8 (D5)	Hec 7.2 (D2)	-'ve control
E2A	+++	+++	+++	+++	+++	+++	+++	+++	+++	+++	++	+++	-
D11A	+++	+++	+++	+++	+++	+++	+++	+++	+++	+++	+++	+++	-
K13A	+++	+++	+++	+++	+++	+++	+++	+++	+++	+++	+++	+++	-
D17A	+++	+++	+++	+++	+++	+++	+++	+++	+++	+++	+++	+++	-
K24A	+++	+++	+++	+++	+++	+++	+++	+++	+++	+++	+++	+++	-
D33A	+++	++	+++	+++	+++	+++	++	++	+++	+++	++	+++	-
K41A	+++	+++	+++	+++	+++	+++	+++	+++	+++	+++	++	+++	-
K50A	+++	++	+++	++	++	+++	++	++	++	+	++	++	-
K50E	+	++	-	-	-	+	-	-	-	-	+	-	-
D51R	+++	+++	-	-	++	+++	+++	+++	+++	++	+++	+++	-
D52A	+++	+++	+++	+++	++	+++	++	+++	+++	++	+	++	-
K62A	+++	+++	++	+++	+++	+++	+++	+++	+++	++	++	++	-
E65A	+++	+++	+++	+++	+++	+++	+++	+++	+++	+++	+	+++	-
E71A	+++	+++	+++	-	++	++	+++	+++	++	++	+++	+++	-
R73A	+++	++	+++	+++	+++	+++	++	+++	+++	+++	++	+++	-
D76A	+++	+++	-	++	+++	+++	+++	+++	+++	+++	+++	+++	-
K81A	+++	+++	++	+++	+++	+++	++	+++	+++	++	++	++	-
K89A	+++	+++	+++	+++	+++	+++	+++	+++	+++	+++	++	+++	-
E90A	+++	+++	+++	+++	+++	+++	+++	+++	+++	+++	++	++	-
K91A	+++	+++	+++	+++	+++	++	++	+++	+++	+++	+++	++	-
E95A	+++	+++	+	+++	+++	+++	+++	+++	+++	+++	++	++	-
E101A	+++	+++	++	+++	+++	+++	+++	+++	+++	+++	+++	+++	-
E139A	+++	+++	+++	+++	+++	+++	+++	+++	+++	+++	++	++	-
E142A	+++	+++	++	+++	+++	+++	++	+++	+++	++	++	++	-
E145A	+++	+++	+++	+++	+++	+++	+++	+++	+++	+++	+++	+++	-
E153A	+++	+++	+++	+++	+++	+++	+++	+++	+++	+++	+++	+++	-

Table 3.6 ELISA Profile of CD31 (D1-D6)Fc mutants. Solid phase ELISAs were performed on each mutant with a panel of 12 anti-CD31 monoclonal antibodies. Antibodies recognising epitopes through out the extracellular domain were used. +++ indicates greater than 80% of wild type CD31 positive control, ++ indicates 60-80% of positive control, + represents 40-60% positive control, and - indicates less than 40% of positive control. On the basis of this profile K50E was judged to be grossly misfolded and excluded from subsequent analysis. Interestingly none of the known blocking antibodies were affected by the blocking mutations in domain 1.

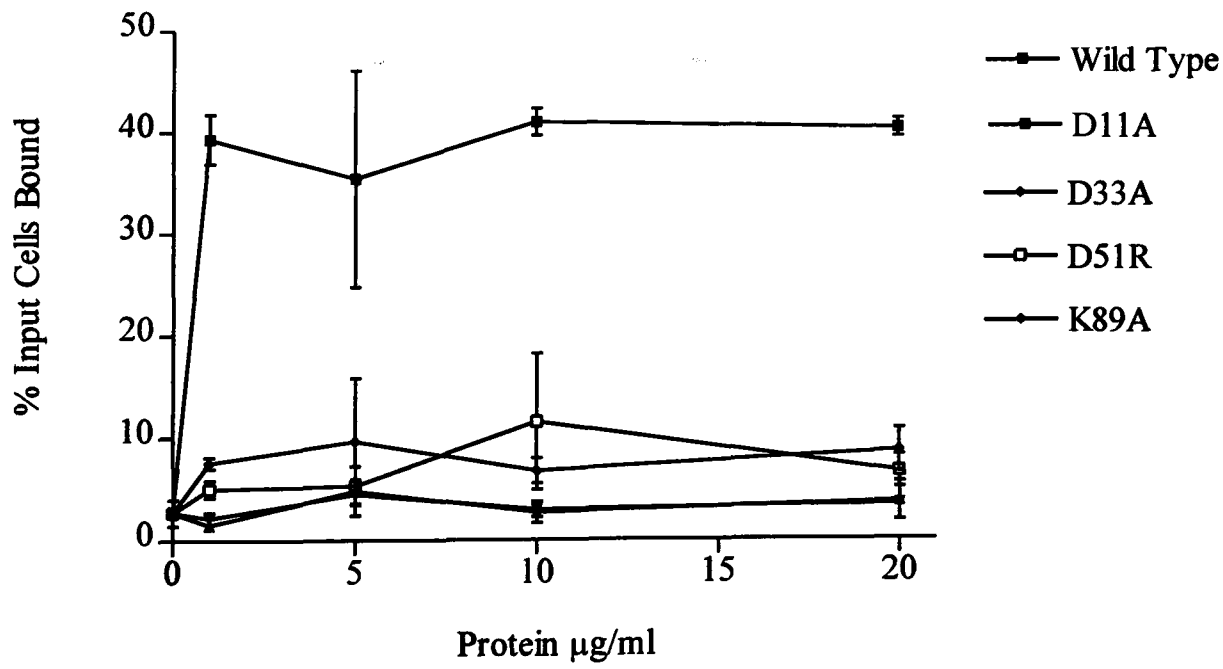
To address the effect of mutations of CD31 on homophilic adhesion, assays were performed to determine the adhesion of COS cells transiently expressing full length CD31 to plastic coated with mutant and wild type Fc-proteins at 0.5µg/well (a concentration determined to be saturating). When compared to wild type CD31(D1-D6)Fc, mutations D11A and K89A were found to abolish binding down to background levels observed with negative control protein MUC18 (D1-D5)Fc, whilst mutations D33A, K50A and D51R

significantly reduced binding (figure 3.16a). To verify these findings, mutant proteins D11A, D33A, D51R and K89A were titrated in the range 0.1μg/well to 2μg/well. There was no increase in cell binding with increasing concentration of protein (figure 3.16b), demonstrating that the assay was indeed saturating.



source: yammaa12/96 and aa07/97

Figure 3.16a Site directed mutagenesis dissection of the homophilic adhesion face. COS-1 cells transiently expressing wild type full length CD31 were allowed to adhere to plastic coated with CD31(D1-D6)Fc mutant and wild type proteins, or MUC18(D1-D5)Fc as a negative control. The percentage of input cells bound after two washes was calculated relative to the wild type positive control and results expressed as mean ± 1 SD (n=3). Results are representative of four experiments on two independently produced batches of protein.



source: yammaa14/96 plate 2

Figure 3.16b Titration of CD31 mutants. COS-1 cells transiently expressing CD31 were allowed to adhere to a concentration range (0-20μg/ml, 0-2ug/well) of CD31(D1-D6)-Fc mutant and wild type proteins. The concentration range was achieved by pre-coating 1μg/well anti-human Fc immunoglobulin, and then coating

with chimeric protein at the indicated concentration. Adhesion was quantified after two washes, and results are expressed as mean ± 1 S.D. (n=3).

The identification of residues involved in homophilic adhesion was further confirmed by inverting the assay, so that mutant proteins were cell expressed. Each mutant that exhibited a functional effect was subcloned from the CD31(D1-D6)Fc background into full length transmembrane expressed CD31. Briefly, domains 1 and 2 of CD31 containing the mutations of interest were excised from CD31 (D1-D6)Fc in pIG_1 with *Hind*III and *Bam*HI and subcloned into full length CD31 in pCDNA3 also digested with *Hind*III and *Bam*HI. The presence of the desired mutation was confirmed by sequencing of the mutated region. In adhesion assays where COS cells expressing cell surface mutant CD31 protein (Figure 3.17b) were allowed to bind to wild type CD31(D1-D6)Fc, significant inhibition of homophilic adhesion was observed (Figure 3.17a). Thus the mutant profile revealed using Fc-chimeras was fully confirmed in the context of cell expressed transmembrane bound forms of CD31.

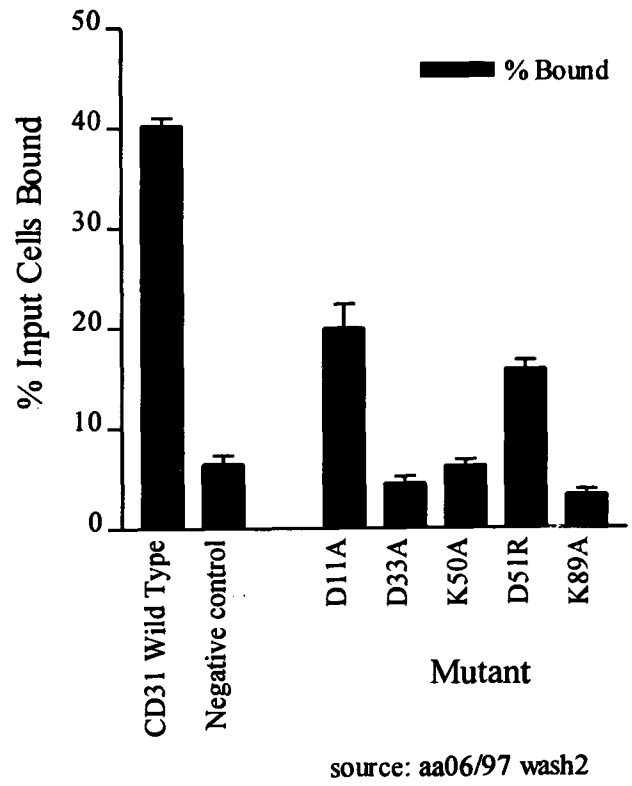
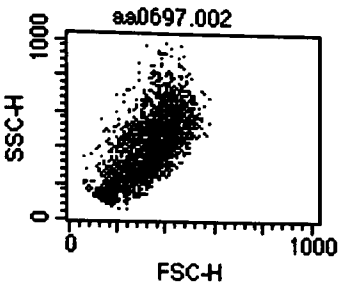
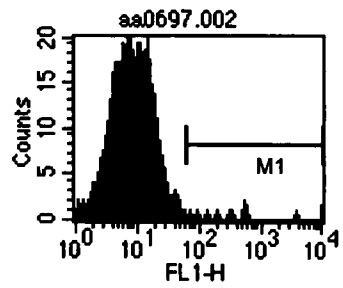


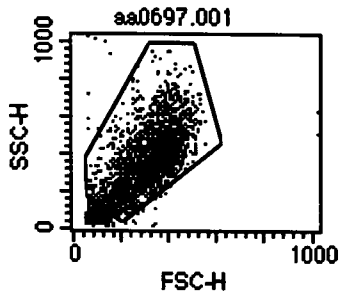
Figure 3.17a CD31 mutants expressed as transmembrane bound forms on the surface of COS-1 cells. Mutants identified by screening Fc-chimeras were subcloned from an Fc-chimera background into a full length transmembrane form of CD31 in pCDNA3. COS-1 cells expressing mutant CD31 were allowed to adhere to plastic coated with wild-type CD31(D1-D6)Fc or negative control MUC18(D1-D5)Fc protein and adhesion quantified after two washes. Results are expressed as means ± 1 SD (n=3) and are corrected for transfection efficiency (20-40% cells positive as determined by FACScan analysis in Figure 3.17b).

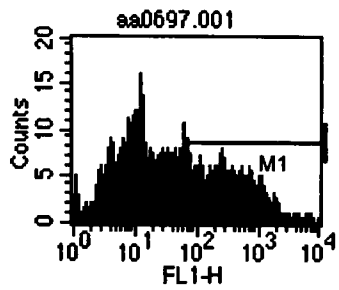




Sample ID: CD31 negative Gated Events: 2552
Total Events: 3000 X Parameter: FL1-H (Log)

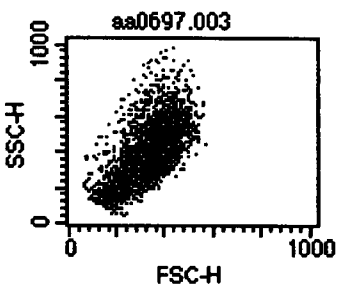
Marker	Left, Right	Events	% Gated	% Total	Mean
All	1, 9910	2552	100.00	85.07	23.54
M1	66, 9910	14	0.55	0.47	2556.03

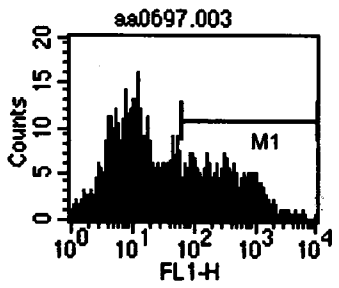




Sample ID: CD31 positive Gated Events: 2411
Total Events: 3000 X Parameter: FL1-H (Log)

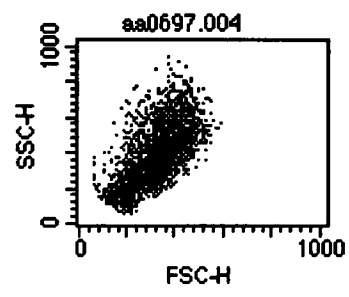
Marker	Left, Right	Events	% Gated	% Total	Mean
All	1, 9910	2411	100.00	80.37	182.84
M1	66, 9910	895	37.12	29.83	461.75

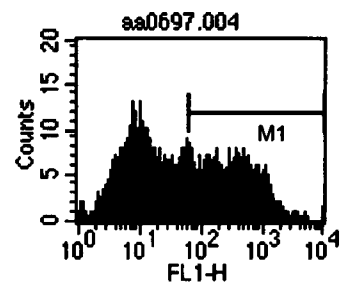




Sample ID: CD31 D11A Gated Events: 2523
Total Events: 3000 X Parameter: FL1-H (Log)

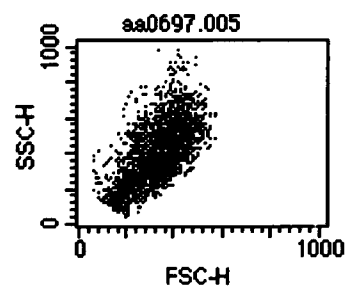
Marker	Left, Right	Events	% Gated	% Total	Mean
All	1, 9910	2523	100.00	84.10	158.92
M1	66, 9910	832	32.98	27.73	449.37

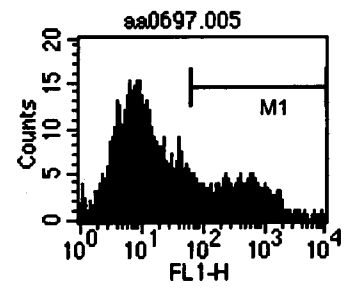




Sample ID: CD31 D30A Gated Events: 2508
Total Events: 3000 X Parameter: FL1-H (Log)

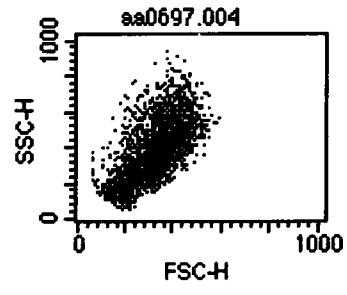
Marker	Left, Right	Events	% Gated	% Total	Mean
All	1, 9910	2508	100.00	83.60	204.72
M1	66, 9910	1036	41.31	34.53	469.27

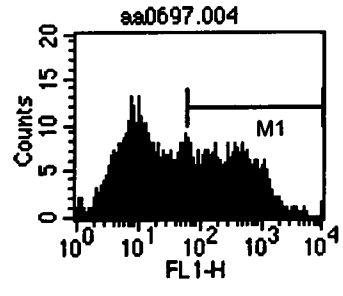




Sample ID: CD31 K50A Gated Events: 2547
Total Events: 3000 X Parameter: FL1-H (Log)

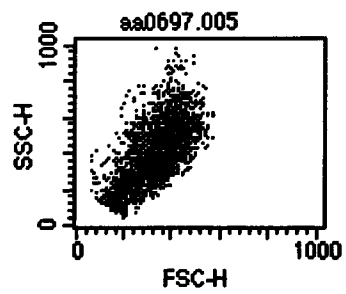
Marker	Left, Right	Events	% Gated	% Total	Mean
All	1, 9910	2547	100.00	84.90	128.15
M1	66, 9910	600	23.56	20.00	500.55

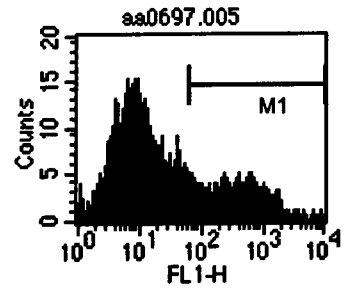




Sample ID: CD31 D51R Gated Events: 2444
Total Events: 3000 X Parameter: FL1-H (Log)

Marker	Left, Right	Events	% Gated	% Total	Mean
All	1, 9910	2444	100.00	81.47	204.56
M1	66, 9910	958	39.20	31.93	494.49





Sample ID: CD31 K89A Gated Events: 2604
Total Events: 3000 X Parameter: FL1-H (Log)

Marker	Left, Right	Events	% Gated	% Total	Mean
All	1, 9910	2604	100.00	86.80	127.60
M1	66, 9910	532	20.43	17.73	580.58

Figure 3.17b FACScan Profiles of COS-1 cells expressing full length transmembrane bound CD31 mutants. COS-1 cells were harvested in 2mM EDTA/PBS, washed and stained with mouse anti-human CD31 monoclonal antibody 9G11. Bound antibody was detected with goat anti-mouse FITC conjugated secondary reagent and FACS profiles collected on a Becton Dickinson FACScan running CELLQuest software. (Source aa06/97)

Based on the model of CD31, examination of the relative position of the residues identified by site directed mutagenesis shows both faces of immunoglobulin domain 1 to be involved in forming homophilic contacts (Figure 3.17). Residues D11 and D33 form a discrete acidic cluster on the A and B strands respectively, located on the ABDE face. K89 is located at the top of the inter-strand FG-loop, and K50 and D51 are located in the CD-loop, collectively indicating an extensive contact area on the CFG face.

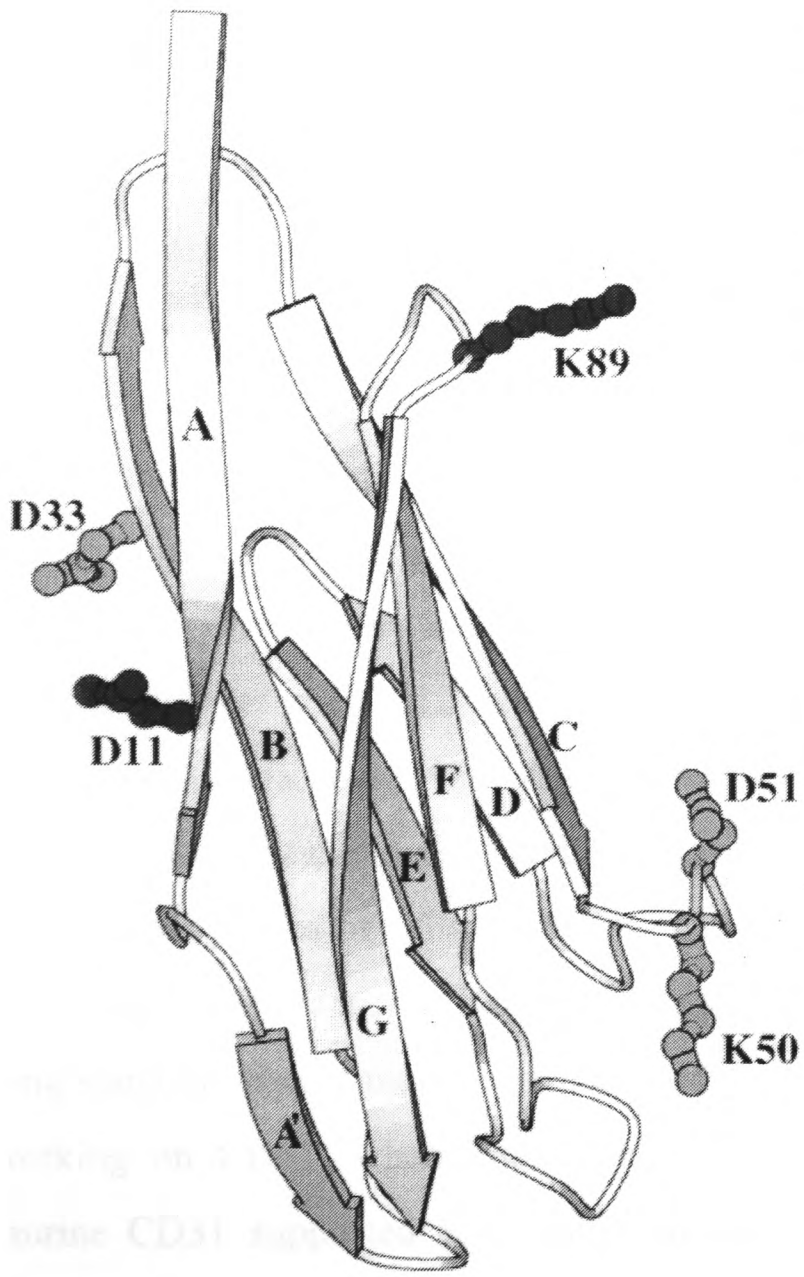


Figure 3.18 Distribution of the residues implicated in homophilic adhesion on an Ig-like fold. A schematic diagram of a representative adhesive immunoglobulin domain (based on the crystal structure of VCAM domain 1 (Jones *et al.*, 1995)) is shown. Modelled inserts of five, four and one additional residues at the NH_2-terminus, the BC loop and the FG loop respectively are included to indicate a putative topology appropriate for residues 3 to 100 of CD31. The residues implicated in homophilic CD31 adhesion when mapped in this three dimensional context cluster on two sides of the Ig fold. Inserts were modelled in the interactive graphics program FRODO (Jones 1985) and the figure was produced in the program MOLSCRIPT (Kraulis, 1991).

3.4 Discussion

In this chapter a well established and defined system of recombinant IgG chimeric constructs and heterologous COS cell adhesion assays have been used to dissect CD31 homophilic adhesion. The major findings may be summarised as follows: First, the extracellular domains 1 to 6 of CD31 are capable of supporting homophilic adhesion, independent of any contribution from either the transmembrane or the cytoplasmic tail

sequences. Second, CD31 extracellular domain 1 is necessary to mediate homophilic adhesion, but together with domains 2 and 3 it is not sufficient to support adhesion when expressed out of the context of the whole extracellular domain. Third, it is possible to confer the ability to bind human CD31 on mouse CD31 by replacing the first two NH_2-terminal domains with their equivalent domains from human CD31. Collectively these results indicate that the NH_2-terminal domains 1 and 2 form the primary homophilic binding sites, but these are not capable of forming stable homophilic contacts without the presence of the membrane proximal CD31 domain sequences. Finally, 5 residues in domain 1 have been identified which are involved in mediating homophilic adhesion.

Others have suggested that the transmembrane and cytoplasmic tail of CD31 are required to mediate homophilic adhesion (Sun *et al.*, 1996b). However the results presented in this chapter show that the extracellular domain alone, expressed as a GPI-anchored protein, is sufficient to support homophilic adhesion. These findings clearly demonstrate that neither transmembrane nor cytoplasmic tail sequences are required *per se* to mediate homophilic adhesion and are consistent with experiments performed by Zocchi *et al.*, 1997. The apparently contradictory results of Sun and co-workers may be explained by the finding that the cytoplasmic tail is required for the localisation of CD31 to areas of cell-cell contacts (Albelda *et al* 1991, Zocchi *et al* 1997). In the paper by Sun *et al.*, 1996b, the authors noted that the level of cell surface expression of CD31 is critical in determining the adhesive properties of cells expressing CD31, such that below a particular threshold cells do no support spontaneous homophilic aggregation. This observation was used to explain a long standing discrepancy in the literature between the results obtained by different groups working on CD31, where one group found that L-cell stable transfectants expressing murine CD31 supported homophilic adhesion (Xie and Muller, 1993), whilst a second group found that a similar CD31 expressing L-cell stable cell line did not (Yan *et al.*, 1995b). Closer examination of the relative levels of cell surface expression between the two stable cells lines revealed that the cell line which did not support homophilic aggregation used by Yan and co-workers had a significantly lower mean fluorescence intensity (MFI) than the cell line generated by Xie and Muller. By establishing cell lines with a range of MFI, Sun and colleagues were able to show that increasing cell surface expression gave the expected homophilic aggregation in cell lines expressing higher levels of human CD31. This effect may be more subtle in cells expressing constructs which lack the cytoplasmic

tail, since in these cell lines CD31 may not be sequestered to points of initial cell-cell contact and hence fail to form stable adhesive contacts. In contrast to the stable cell lines employed by these investigators, where MFIs in excess of 130 above background were required to give stable homophilic adhesion, the transiently transfected COS cells employed in our laboratory result in very high levels of cell surface expressed CD31 (MFI typically in the range 200-800 above background, see for example Table 3.3), such that the localisation of CD31 to cell-protein contacts may not be a significant factor in our experiments simply by virtue of the overall level of cell surface expression. Moreover in the COS transient system, the level of surface expression in the transfected population is quite heterogeneous, such that MFI measurements probably understate the level of cell surface expression for many of the cells .

The finding that the transmembrane and cytoplasmic tail of CD31 is not required to mediate homophilic adhesion is particularly significant since Goldberger *et al.*, 1994 have identified a soluble form of CD31 present in normal human plasma at levels of 10-25ng/ml, resulting from alternative splicing of the transmembrane domain. This form of CD31 is likely to be functional as a soluble homophilic ligand for cell expressed CD31 and may serve as a competitive endogenous regulator of leukocyte transmigration to restrict leukocyte transmigration under normal circumstances, or as a mechanism of down-regulating transmigration following inflammatory stimuli.

One of the key aims of this chapter was to test the anti-parallel fully interdigitating model proposed for CD31 mediated homophilic adhesion, which envisaged the membrane distal NH_2-terminal, domains of CD31 binding to the membrane proximal domains on an apposing cell surface and *vice versa.* The initial identification of the NH_2-terminal domains as being involved in the formation of homophilic contacts was based upon the observation that commercial antibodies which inhibited homophilic adhesion could be mapped to epitopes contained within domains 1 and 2. Due to the limited number of functional antibodies available commercially, a long term objective of our laboratory has been to raise new functional monoclonal antibodies against CD31. As reported, three new blocking monoclonal antibodies have been produced which intriguingly map to both the NH_2-terminal domains 2 and 3 (Clone 4-3-C7 and Clone 10B9 respectively) but also to domain 5 (Clone 2-2-B12), close to the membrane. Collectively these antibodies suggest that an

extensive face covering the whole extracellular domain is involved in mediating homophilic adhesion, which is consistent with the anti-parallel model initially proposed. However, in addition to blocking antibodies, a number of functional antibodies which appear to stimulate homophilic adhesion have also been identified which map to domains 4 and 5. This finding is consistent with the work of Sun *et al.*, 1996a, who have reported that Fab fragments of the antibody 4G6, which recognises the epitope CAVNEG in domain 6 of CD31 (Yan *et al.*, 1995) enhances CD31 homophilic adhesion.

The antibody studies presented here suggest that CD31 may undergo antibody-induced conformational changes which alter the ability of CD31 to engage homophilically. To date all of the stimulating antibodies have been identified as mapping to the membrane proximal domains, which in the anti-parallel model are presumed to form the second homophilic binding site on CD31. The finding that antibodies which bind to these domains can enhance homophilic adhesion, presumably by inducing conformational changes, suggests that these domains may play an indirect role in mediating homophilic engagement. The original intention was to raise functional blocking monoclonal antibodies, and use these to map the homophilic binding site. If CD31 can undergo conformational changes then interpretation of the results of antibody blockade must be treated with caution, since the assumption that blocking antibodies would reveal the homophilic binding site by direct blockade may not be correct. This scenario is similar to that seen amongst integrins where antibodies which map to locations distant from the binding site can both stimulate and inhibit adhesion (reviewed by Humphries, 1996; Mould, 1996). If CD31 can undergo conformational changes that influence its adhesive properties then this would be unique amongst members of the immunoglobulin superfamily. Although the antibody studies presented in this chapter may suggest that CD31 can *in principle* be induced to undergo conformational changes which can regulate its adhesive properties, the *physiological* significance of these findings, and the physiological regulators of conformational changes remain to be discovered. The finding that CD31 adhesion can be regulated by antibodies which enhance adhesion also suggests that earlier results may need re-interpreting. In the original extracellular domain deletion series (Fawcett *et al.*, 1995) constructs lacking domains 5 and 6 failed to support homophilic adhesion. In the light of the present findings that domains 4 and 5 (and also domain 6 from the data presented by Sun *et al* 1996b) are able to modulate the adhesive phenotype of CD31, it is possible that the Fc constructs lacking these

membrane proximal domains have a reduced affinity for cell surface CD31, hence the failure of these truncated constructs to support adhesion. Similarly a number of investigators have reported unexpected effects of anti-CD31 antibodies (both polyclonal and monoclonal) on the extravasation of monocytes and neutrophils through endothelial monolayers *in vivo* and *in vitro.* Initial observations showed that polyclonal antibodies with cross species reactivity were capable of inhibiting transmigration in both chronic (Murohara *et al.,* 1996) and acute (Vaporciyan *et al.,* 1993) *in vivo* models of inflammation, and that *in vitro* models, antibodies which inhibit homophilic adhesion could also inhibit monocyte transmigration (Muller *et al.*, 1993). In later studies, however Liao *et al.,* 1996 noted that a subset of antibodies which mapped to domain 6 prevented release of monocytes which had recently traversed the endothelial monolayer, but did not block transmigration itself. Similarly Wakelin *et al.*, 1996 found in a rat *in vivo* model of leukocyte transmigration into mesenteric capillaries that a polyclonal antibody against murine CD31 did not inhibit transmigration, but rather caused the accumulation of leukocytes in the perivascular space. In both cases these results may reflect an antibody induced increase in adhesion between leukocyte and endothelial CD31 rather than inhibition of homophilic adhesion.

The antibody studies described above suggest that although CD31 homophilic adhesion is mediated both by the NH_2-terminal and membrane proximal domains, the membrane proximal domains may play a regulatory role, rather than a direct binding role. This implies that the homophilic site may in fact be located in the NH_2-terminus. To further explore this hypothesis and establish the role of the NH_2-terminal domains, a series of chimeric ICAM-3/CD31 constructs were generated, in which a nested series of replacements of CD31 domains by the equivalent domains from ICAM-3 were produced. An important prediction of a fully interdigitating anti-parallel model for homophilic binding is that removal of one of the two binding sites on each molecule would be expected to reduce, rather than eliminate binding. Instead however, replacement of the NH_2-terminal domain 1 alone completely ablates binding, indicating that the homophilic binding site resides, at least in significant measure, in the NH_2-terminal domain of CD31. In principle this could arise because removing one binding site in a two site interaction reduces the affinity of the interaction below the detectable threshold of the assay employed. The obvious alternative interpretation is that homophilic binding results from a direct interaction between NH_2-

terminal domains, excluding a role for the membrane proximal portion of the molecule. This latter interpretation is consistent with the results obtained with mouse/human chimeras first reported by Sun *et al* 1996b using a complicated cell-cell aggregation assay, and repeated here using our Fc chimera strategy. These studies demonstrate that homophilic adhesion requires the presence of domains 1 and 2, and it is possible to confer the ability to bind human CD31 on mouse CD31 by replacing its first two domains with the equivalent domains from human CD31. Again implying that the homophilic binding site is contained within the first two NH_2-terminal domains. In order to determine whether the NH_2-terminal domains alone are homophilically competent in a non-CD31 backbone we produced constructs in which the NH_2-terminal domains of CD31 were expressed on a stalk consisting of ICAM-3 Ig domains. These chimeras preserved the overall length of the extracellular domain as compared to wild type CD31, thus removing any steric constraints arising from the use of truncated CD31-Fc chimeric proteins.

Importantly, these reagents revealed that while the NH_2-terminal domains are necessary, they are not sufficient to support stable homophilic adhesion. One potential model to explain these results is that stable homophilic contact between the NH_2-terminal domains of CD31 requires that these binding domains are held in the correct spatial orientation, and that this function is provided by the membrane proximal domains. This would explain the positive "gain-of-function" results obtained with the human/mouse chimera. In this construct the binding functions are provided by the human NH_2-terminal domains, whilst the murine domains maintain the human domains in the correct orientation.

The mechanism by which the membrane proximal domains modulate the binding domains is not clear, although evidence from the antibody studies presented in this chapter suggest that conformational changes are involved. These conformational changes in the membrane proximal domains may be directly translated into conformational shifts in the binding domains and consequent changes in affinity in a fashion analogous to integrin in-out signalling. Alternatively, different conformations may reflect the ability of these domains to mediate cis-interactions between CD31 on the same cell to dimerise or cluster multiple low affinity binding domains, resulting in an increase in overall avidity, as has been shown for ICAM-1 (Reilly *et al.*, 1995) and cadherins (Brieher *et al.*, 1996; Tomschy *et al.*, 1996). In the case of E- and N-cadherin, dimerisation is mediated via the NH_2-terminal domains,

so that the cadherin-zipper is made up of cis-interacting dimers, each half of which binds to a dimer in trans on the apposing cell surface. However, if CD31 does function as a dimer it is possible that immunoglobulin domains distinct from the ligand binding domains could mediate homodimerisation, as has been shown for the stem cell factor receptor *c-kit* which utilises the fourth immunoglobulin domain for dimerisation (Blechman *et al.*, 1995).

Such a model implies that CD31 homophilic engagement involves both cis- and trans-interactions, so that low affinity trans-interactions mediated by NH_2-terminal domains are clustered to achieve higher avidity by cis-interactions mediated by the membrane proximal domains, forming a zipper-like interaction (Figure 3.19). This model provides interesting regulatory possibilities. A puzzling aspect of CD31 biology is the fact that although CD31 is widely expressed on mature, circulating haematopoietic cells, $CD31^+$ cells do not undergo spontaneous CD31-mediated homotypic aggregation. This could be explained in terms of regulation of the cis-interactions of CD31, for example by cytoskeletal association and cell surface distribution. It has long been known that at least a fraction of CD31 expressed on endothelial cells is Triton-X100 insoluble and presumed to be associated with the cytoskeleton (Newman *et al.*, 1992). More recently it has been shown that CD31 associates with β-catenin and hence indirectly with F-actin at the adherens junctions of endothelial cells (Matsumura *et al.*, 1997), and that CD31 engagement by antibodies leads to cytoskeletal reorganisation (Poggi *et al.*, 1996). Furthermore, the recent finding that cytokine treatment of endothelial monolayers induces a re-distribution of CD31 from sites of cell-cell contact to the apical surface is particularly suggestive and could also provide a potential mechanism for switching between homophilic and heterophilic interactions (Romer *et al* 1995, Rival *et al* 1996).

The immunoglobulin fold has been identified as mediating a variety of interactions, for example antigen-antibody complexes (reviewed by Mariuzza *et al.*, 1993), heterophilic interactions with integrins such as ICAM-1,2,3/LFA-1, VCAM/VLA-4, MadCAM/a_4b_7 and CD31/a_vb_3, (reviewed Newham and Humphries, 1996) pseudo-homophilic interactions, e.g. CD2/CD48 (Van der Merwe *et al.*, 1995), and fully homophilic interactions such as CD31-CD31. The key feature of the immunoglobulin fold is a core structure formed by two β-sheets packed face to face. A comparison of structures solved at atomic resolution shows that the regions peripheral to the core, such as the edge strands of the β-sheets, and the loops that link the strands can have quite different conformations. Mirroring this structural

diversity different immunoglobulin-folds utilise different regions to interact with their ligands.

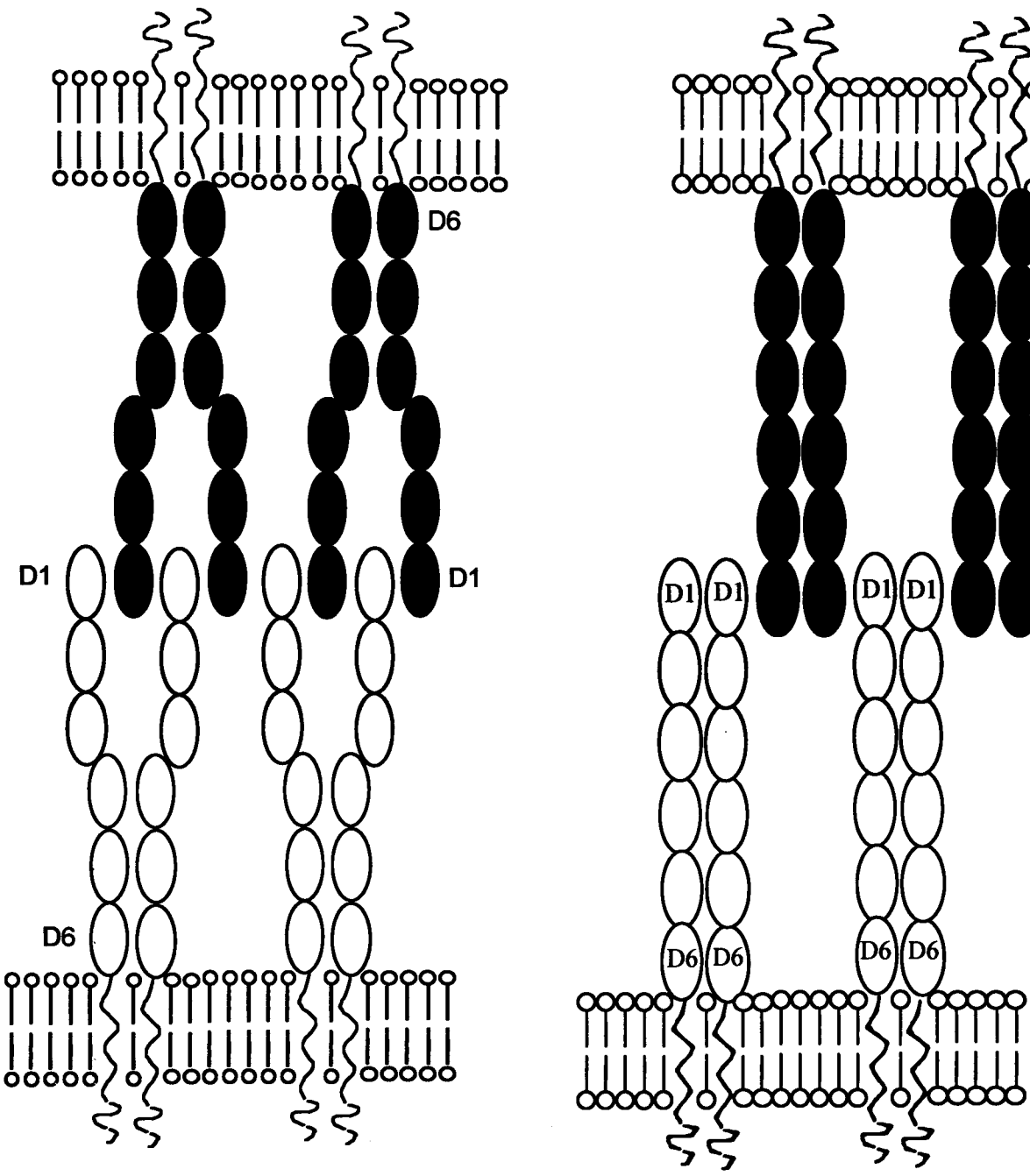


Figure 3.19 Zipper model of CD31 homophilic adhesion. The experiments presented in this chapter show that while the homophilic binding site is located in the NH_2-terminal domains 1 and 2, the entire extracellular domain is required to support stable homophilic adhesion. It is proposed that the membrane proximal domains perform a non-binding accessory role required to maintain the binding domains in the correct orientation. One possibility is that this accessory role involves clustering or dimerisation to achieve an increase in avidity. This is supported by the observation that residues which inhibit homophilic adhesion map to both faces of the immunoglobulin fold of domain 1, implying that each immunoglobulin fold interacts with two others. There are two possibilities, firstly that each NH_2-terminal region of CD31 interacts with two others on an apposing cell surface (left), or alternatively that each molecule of CD31 interacts with two others, one on the same cell (to form lateral associations), and a second on an apposing cell surface, to form a zipper composed of dimers of dimers (right). This later possibility is suggested by the pattern of residues identified by site direct mutagenesis compared to the N-cadherin structure. This shows that the residues on the ABDE face of CD31 identified by mutagenesis are in equivalent positions to the residues in N-cadherin forming contacts in laterally associated dimers observed in crystalline arrays (Shapiro *et al.*, 1995).

In antigen-antibody complexes, antigen recognition and binding is mediated by loops at the NH_2-terminal end of the fold. A recurring theme amongst integrin-IgSF interactions is the

utilisation of acidic residues presented either in the NH_2-terminal portion of the loop joining the CD β-strands on the CFG face of the Ig fold, for example the QIDS motif in VCAM (Renz *et al.*, 1994) or in the C strand itself, for example the LETS motif identified in the ICAMs (Holness *et al.*, 1995; Casanovas et al., 1997). In the case of CD2/CD48, a pseudo-homophilic interaction, mutagenesis data implicate an adhesive surface comprised of the equivalent GFCC'C'' faces of the immunoglobulin fold in both CD2 and CD48 (Van der Merwe *et al.*, 1995). To date, no systematic site-directed mutagenesis of any fully homophilic IgSF interaction has been undertaken. There is some limited data on the interaction of NCAM based on the ability of a decapeptide derived from its third immunoglobulin domain to block homophilic adhesion (Rao *et al.*, 1993; Rao *et al.*, 1994). Likewise spontaneous mutations in L1 give rise to neurological disease such as X-linked hydrocephalus (Jouet *et al.*, 1994). However many of these mutations result in frameshifts or premature truncations, and only 26 result in missense mutations. Of these, 13 are predicted to affect key structural residues or domain boundaries and destabilise the protein, whilst others introduce cysteines and may promote intermolecular disulphides (Bateman *et al.*, 1996). Hence spontaneous mutations have so far yielded few insights into the nature of homophilic interactions. The results presented in this chapter therefore represent the most extensive directed analysis of the structures mediating IgSF homophilic adhesion.

Significantly, site-directed mutagenesis of CD31 has identified residues on both faces of the immunoglobulin fold as being involved in the homophilic contact sites. Specifically a cluster of two acidic residues, D11 and D33, which lie on the predicted A and B strands, K89 which lies at the top of the FG loop, and two residues K50 and D51 on the CD-loop. This finding represents a novel mode of interaction between immunoglobulin folds. The use of two binding faces to bind the same ligand appears to be unique to CD31, although a number of IgSF members utilise different faces of the same immunoglobulin fold to mediate adhesion to different ligands. For example, ICAM-1 binds a number of ligands via its NH_2-terminal domain 1, including the leukocyte integrin LFA-1 (CD11a/CD18, a_Lb_2), fibrinogen (Languino *et al.*, 1993, Duperrary *et al.*, 1997), *Plasmodium falciparum*-infected erythrocytes (Berendt *et al.*, 1989, Smith *et al.*, 1995) and some serotypes of the major *Rhinovirus* serogroup (Greve *et al.*, 1989). Adhesion to the integrin LFA-1 is mediated in part by acidic residue, E37, on the CFG face, whilst *Plasmodium falciparum*-infected

erythrocytes and fibrinogen appear to share an overlapping binding site mapped to the apex of the molecule and the ABDE face.

The mutagenesis results for CD31 are consistent with the zipper model proposed above, where each CD31 molecule interacts with two others on an apposing cell surface, thus requiring two distinct binding faces. Attempts to align CD31 NH_2-terminal domain 1 monomers using FRODO such that charged residues identified by site-directed mutagenesis formed discrete salt-bridges did not produce an obvious model for homophilic interactions. This may reflect the fact that the full extent of the binding face is not known. Results from the mouse/human chimeras presented in this chapter indicate that the homophilic contact sites are located completely within the NH_2-terminal domains 1 and 2. Sun and colleagues (Sun *et al.*, 1996a) have made further chimeras in which only the NH_2-terminal domain 1 was swapped, however this failed to confer the ability to bind human CD31 on murine CD31, indicating that the homophilic contact site extends into domain 2. This would also fit the available antibody data, where antibodies mapping to domain 2 were found to inhibit homophilic adhesion, despite the limitations of antibody blockade to map binding sites eluded to earlier. Involvement of domain 2 may explain the failure of molecular modelling to align monomers of domain 1. Interestingly however, superpositioning of the predicted CD31 domain 1 fold onto the known crystal structure for N/E-cadherin (Collaboration with Andrew P. May, Laboratory of Molecular Biophysics, University of Oxford - Figure 3.20) positions the residues on the ABDE face of CD31 identified in the mutagenesis screen (i.e. D11 and D33) at positions equivalent to the points of contact between cadherin molecules interacting in cis, whilst the residues on the CFG face (i.e. K89 at the top of the FG loop, and residues K50 and D51 in the CD loop) occupy the positions identified as forming adhesive contacts between cadherin molecules interacting in trans. Hence the residues identified by the mutagenesis screen may reflect both residues required for homophilic adhesive contacts, and residues required to mediate lateral cis association in the membrane if dimerisation is required to generate stable homophilic adhesion. This would still be consistent with the zipper model proposed earlier, but would require the interaction of dimers with dimers (see Figure 3.19) as seen in the crystal structure of N- and E-cadherin (Shapiro *et al.*, 1995, Nagar *et al.*, 1996). This hypothesis would not explain the requirement for domains 5 and 6, but is nevertheless suggestive of lateral association between cell surface CD31.

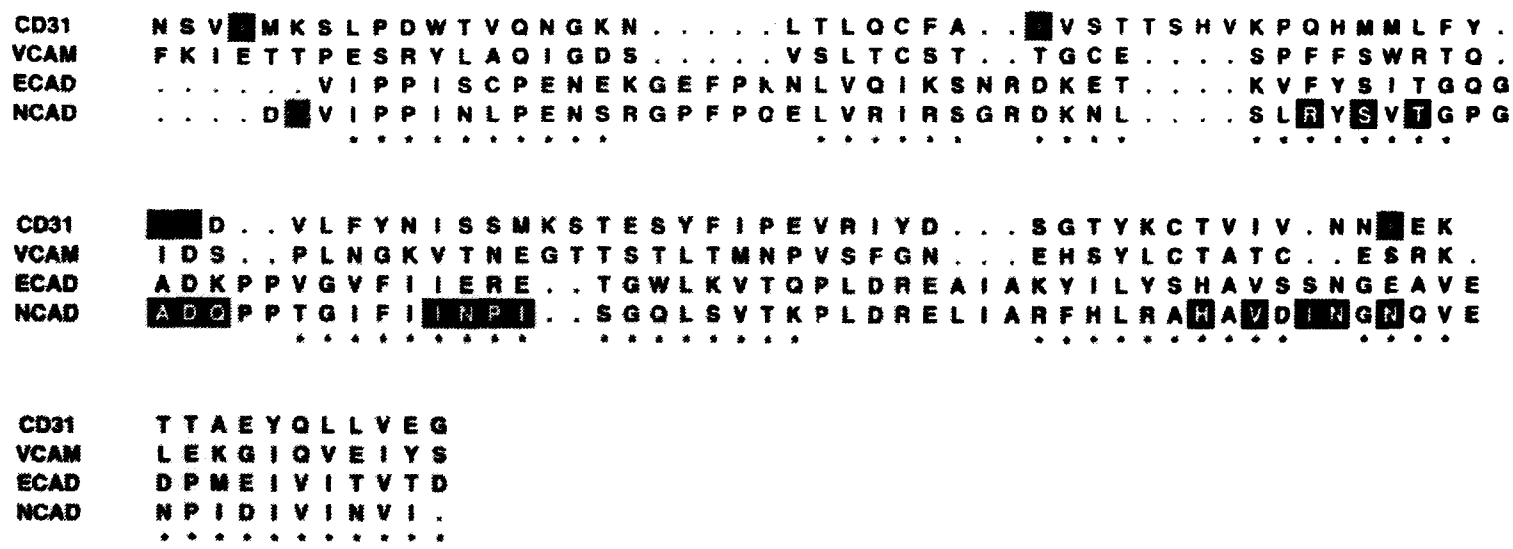


Figure 3.20 Structure based alignments of CD31 and cadherins. structural superpositions were performed with program SHP (Stuart *et al.* 1979) and the implications for CD31 homodimerisation assessed using the interactive graphics program O (Jones *et al.*, 1991). Residues implicated in the crystal contacts of E- and N-cadherin are highlighted, and the residues identified by site directed mutagenesis of CD31 are also shown.

Residues for mutagenesis were originally selected on the basis of predicted solvent accessibility of aspartate, glutamate, lysine and arginine residues in domain 1. Sequence alignments between the available species orthologues of CD31 (human, murine, ovine and bovine) show that of the five residues which have an effect on homophilic adhesion, four are absolutely conserved (D33, K50, D51, K89) across all species for which sequence data is available, whilst the fifth, (D11), although not itself conserved lies within a highly conserved region (Figure 3.21). It is gratifying to note therefore that an alternative strategy, often employed to select residues for mutagenesis, (i.e. conservation across species) would therefore have identified similar residues. One significant limitation of the present mutagenesis screen is that only charged residues were selected as targets for mutagenesis. Careful and highly detail mutagenesis and microcalorimetric analysis of the interaction between CD2 and CD48 (Van der Merwe *et al.*, 1995, Simon Davies, personal communication) has shown that whilst the binding specificity of adhesive interactions arises largely from charged and dipolar residues, these contribute little to the overall stability of the interaction. Instead much of the binding energy results from the interaction of hydrophobic surfaces, which have not been targeted in the present mutagenesis strategy. The present strategy is likely to have highlighted key areas involved in mediating adhesion, but is unlikely to have disclosed the full extent of the interacting face.

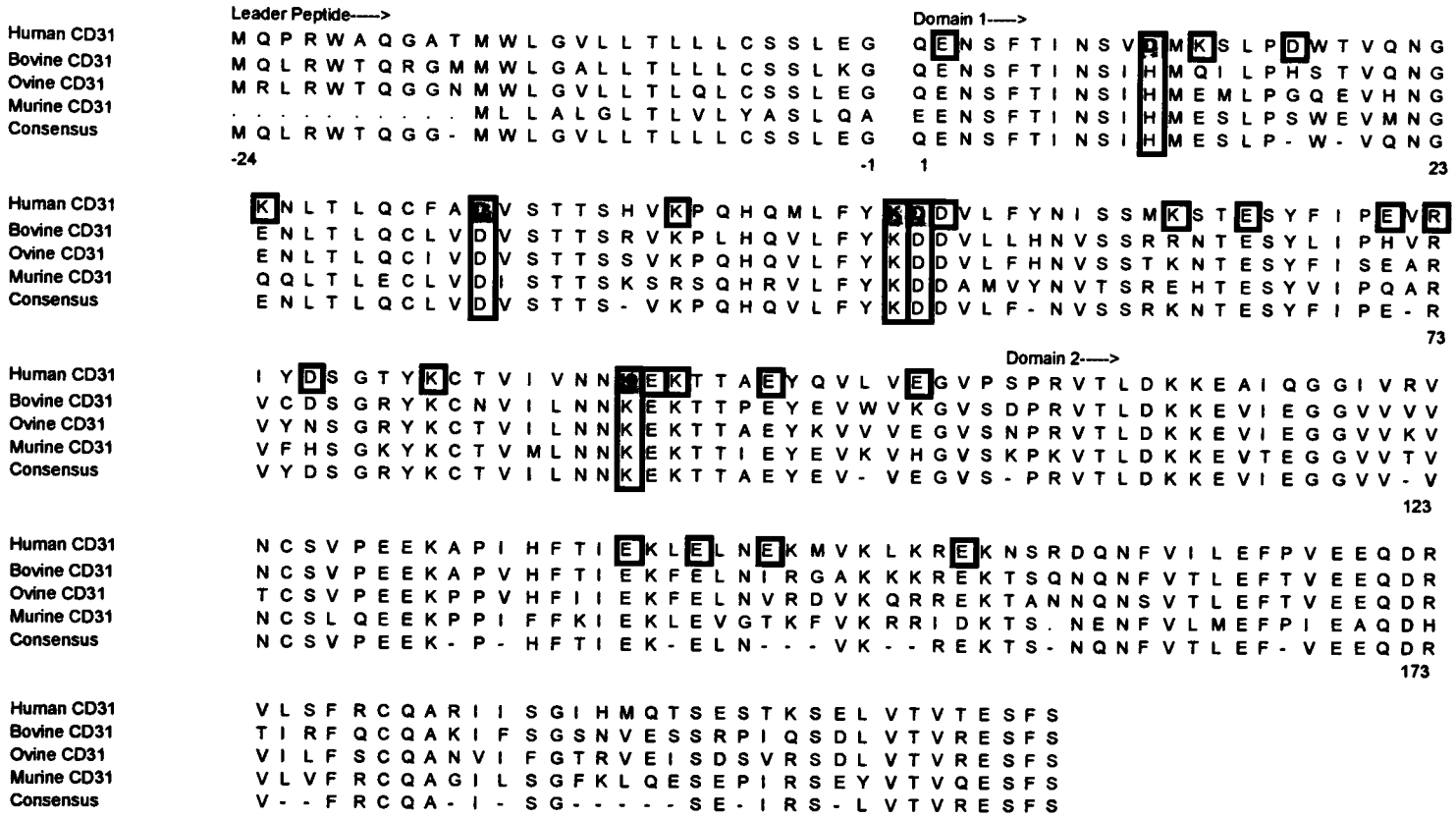


Figure 3.21 Alignment of human, bovine, ovine and murine CD31 sequences. The primary amino acid sequences of domains one and two of each species orthologue were aligned using GCG PILEUP and PRETTY programmes. Charged residues selected for mutagenesis in the human sequence are boxed, and residues effecting homophilic adhesion (D11, D33, K50, D51 and K89) are boxed and highlighted. The equivalent residues in each of the species orthologues to those residue identified in the mutagenesis screen are also boxed. Interestingly of the five residues identified in the mutagenesis screen, four (D33, K50, D51 and K89) are absolutely conserved across all species for which sequence data is available.

3.4.1 Summary

CD31 mediated adhesion is complex both in terms of the potential ligands, both homophilic and heterophilic, and in terms of the domains involved in each interaction. In this chapter, a role for both NH_2-terminal (domains 1 and 2) and membrane proximal domains of CD31 has been identified in mediating homophilic adhesion. In contrast to the original two-site anti-parallel interdigitating model of homophilic adhesion proposed by Fawcett *et al* 1995, it has been demonstrated that the direct homophilic binding site is located in the NH_2-terminal domains (consistent with the results of other investigators, see for example Sun *et al.*, 1996a, Sun *et al.*, 1996b, and Liao *et al.*, 1997) but that the NH_2-terminal domains are not sufficient to support stable homophilic adhesion outside of the context of an accessory function provided by the membrane proximal domains. Consistent with a role for the membrane proximal domains in regulating homophilic adhesion a number of stimulating antibodies have been identified which map to these domains. This chapter also describes the most extensive, site-directed analysis of the structures which mediate homophilic IgSF interactions to date. Uniquely, the results from the mutagenesis

study indicate that both faces of domain 1 are involved in the homophilic interaction, suggesting that each CD31 molecule contacts two others. One potential model which rationalises the above findings is one in which CD31 homophilic adhesion is mediated by a zipper-like interaction in which each CD31 molecule on the surface of one-cell interacts with two others on the surface of an apposing cell. The role of the membrane proximal domains may be to dimerise or cluster multiple low affinity interactions to achieve an increase in overall avidity. This possibility is investigated further in chapter four.

Chapter Four: CD31 Exists in both Monomeric and Dimeric Forms

4.1 Introduction

The analysis of the homophilic binding site on CD31 described in the preceding chapter, demonstrated that whilst the NH_2-terminal domains 1 and 2 contain the binding site, these two domains are not capable of supporting stable homophilic adhesion when expressed outside the context of the full length extracellular domain. It was speculated that the remaining domains might fulfil some other accessory role, either by directly modulating the affinity of the binding site in a fashion analogous to integrins, or by clustering multiple low affinity homophilic binding sites to increase avidity, by forming macromolecular zippers and leading to stable adhesive contacts as has been observed for cadherins (Shapiro *et al.*, 1995, Nagar *et al.*, 1996, Tomschy *et al.*, 1996, Brieher *et al.*, 1996).

Initial experiments with monomeric E-cadherin (Pokutta *et al.*, 1994) did not indicate that cadherins formed dimers, however the crystal structures of both the NH_2-terminal domain 1 of N-cadherin (Shapiro *et al.*, 1995) and the NH_2-terminal domains 1 and 2 of E-cadherin (Nagar *et al.*, 1996) showed that, at least in constrained crystalline arrays, cadherins formed dimeric lateral associations, in which the ABDE faces formed contacts equivalent to a lateral association, whilst the CFG face formed the homophilic contact points with two other dimers arranged in an anti-parallel fashion, to produce a macromolecular ribbon. The nature of the dimerisation contacts differ in the two crystal structures, in the N-cadherin structure the A-strands exchange between laterally associated protomers (monomeric repeating units within the crystal structure) to bury an aromatic tryptophan residue in the core of the partner protomer. In contrast to the N-cadherin structure, the dimer in the E-cadherin crystal is held together by shared co-ordination of a Ca^{2+} divalent cation. More recently other investigators have shown that monomeric C-cadherin forms stable self associating dimers in solution (Brieher *et al.*, 1996), and that pentameric E-cadherin self associates via a two step, co-operative mechanism, involving initial dimerisation of the NH_2-terminal domains on one pentamer, followed by homophilic contacts with a second pentamer between dimerised NH_2-terminal domains (Tomschy *et al.*, 1996).

One of the surprising features of the crystal structures of the cadherins is that each cadherin domain fold shares a very similar topology to that of the immunoglobulin-like molecules, and indeed the structures of the cadherins can be superimposed quite well on immunoglobulin-like domains, despite statistically insignificant sequence conservation and lack of core-defining residues. Structure based alignments (collaboration with Andrew P. May, Laboratory of Molecular Biophysics, Oxford University, see Chapter 3) showed that the regions implicated by mutagenesis as being involved in mediating CD31 homophilic adhesion are also utilised in cadherin interactions, both in the dimerisation ABDE face, and the adhesion CFG face.

Recently several investigators have provided evidence that a number of cell adhesion molecules exist as dimers, and also demonstrated a role for the dimeric forms in determining function, for example it has been shown that ICAM-1, but not ICAM-2, forms dimers on the cell surface, and that dimeric ICAM-1 has a significantly higher affinity for LFA-1 (CD11a/CD18) than does the monomeric form (8nM for dimeric ICAM-1, negligible affinity for monomeric ICAM-1, Miller *et al.*, 1995). Similarly, it has very recently been shown that human CD4 forms dimers when expressed as a soluble recombinant form, and this may be extremely significant *in vivo*, by positioning CD4 associated *Lck* tyrosine kinase subunits in close proximity, potentially allowing autophosphorlyation and downstream signal transduction.

Given the suggestion from structural comparisons with cadherins that residues which are involved in mediating CD31 homophilic adhesion are in an analogous position to residues mediating cadherin dimerisation, the aim of this chapter was to determine if CD31 exists in a dimeric form.

4.2 Results

4.2.1 Generation of soluble recombinant monomeric CD31 (D1-D6)STOP protein.

Previous work investigating CD31 mediated homophilic adhesion made extensive use of Fc tagged chimeric proteins. Whilst these construct were extremely convenient and useful, they are already dimeric (dimerisation via intermolecular disulphide bridges between the Fc region), such that they are of little direct use in investigating CD31 dimerisation/multimerisation. Studies with C-cadherin (Brieher *et al.*, 1996) and human

CD4 (Wu *et al.*, 1997) indicate that it is possible to detect self association from monomeric cell adhesion molecules expressed as soluble recombinant forms, in contrast to earlier findings with E-cadherin (Pokutta *et al.*, 1994). This emboldened us to produce a soluble monomeric form of the CD31 extracellular domain to begin these studies. Monomeric CD31 was generated by Dr. David Simmons by PCR amplification from full length CD31 template in pCDM8 (Simmons *et al.*, 1990), using a forward amplification primer at the initiating methionine, incorporating a *Hind*III site (5' GATC AAGCTT GTCTTCACTCTCAGG ATG 3'), and a reverse primer at the extracellular domain/transmembrane boundary introducing a stop codon, and incorporating a *Not*I restriction site (5' ATAT GCGGCCGC TCA TTT CTT CCA TGG GGC AAG 3'). PCR product was digested with *Hind*III and *Not*I, and cloned into the expression vector pCDNA3. This vector was used to stably transform CHO-K1 cells (collaboration with Ian Collins, R&D Systems Europe, Abingdon, Oxford, UK), and milligram quantities of protein were produced in a hollow fibre bioreactor operated in a continuous culture mode. CD31 (D1-D6)STOP protein was purified from conditioned culture supernatants by affinity chromatography with a column based on the anti-CD31 monoclonal antibody 9G11 (protein purification and cell culture performed by Ian Collins). After purification, 20mg of protein were available for subsequent experiments. The purified protein ran as a single band of approximately 80kDa on reducing and non-reducing SDS-PAGE gels, and reacted with a range of anti-CD31 monoclonal antibodies in ELISAs (Figure 4.1).

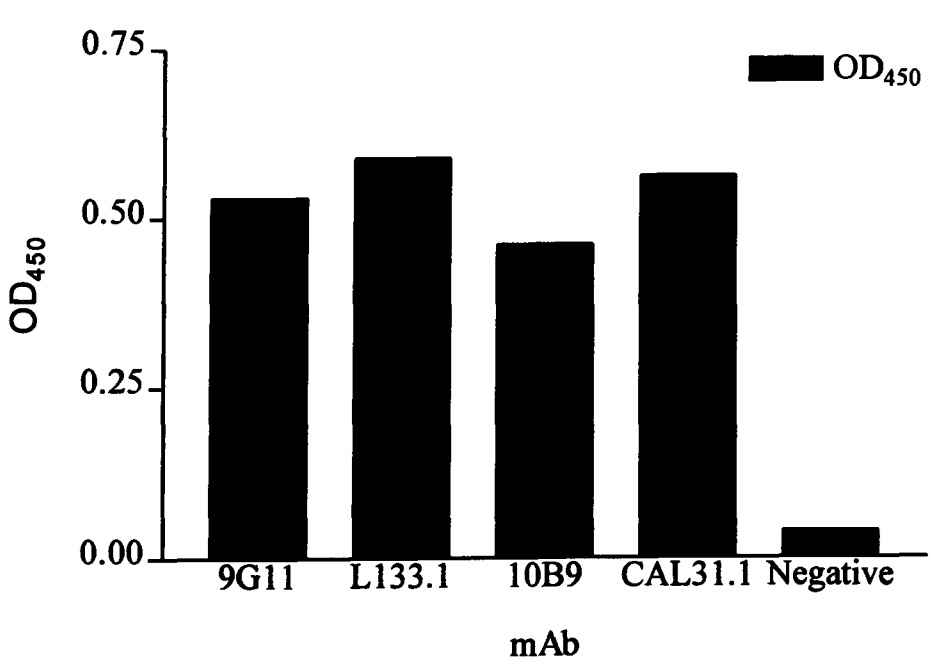


Figure 4.1 ELISA profile of CD31 (D1-D6)STOP protein. 0.5μg/well of purified CD31 (D1-D6)STOP protein were coated onto plastic in PBS overnight at 4°C. Plates were blocked with 5% BSA in PBS for 2 hours at room temperature. Primary antibodies (including negative control anti-integrin β3, F3) were added at 0.2μg/well and incubated for 30 minutes at room temperature. Bound antibody was detected with 1:2,000 dilution of sheep anti-mouse HRP and OPD substrate. CD31 (D1-D6)STOP protein was recognised by all of the anti-CD31 antibodies tested.

4.2.2 CD31 (D1-D6)STOP protein forms dimers in solution

The ability of CD31 (D1-D6)STOP protein to undergo self association was initially assessed using a number of complementary biophysical approaches, as outlined below:

4.2.2.1 Analytical Ultracentrifugation

Analytical ultracentrifugation is a classical technique for investigation of the hydrodynamic properties of macromolecules. With the appropriate mode of operation (sedimentation velocity and sedimentation equilibrium) and analysis, it can be used to determine sample purity, detect and characterise conformational changes, determine subunit stoichiometries, and measure equilibrium constants and thermodynamic parameters for associating systems (reviewed by Hansen *et al.*, 1994). Unfortunately in the past, the instrumentation required to perform these experiments has been both delicate and highly complex, and extremely expensive in terms of capital investment and maintenance, limiting its application to specialist centres. Consequently the use of ultracentrifugation has declined in recent decades, in favour of other hydrodynamic methods such as gel filtration and electrophoresis (for a historical review, see Schachman, 1992). More recently, the introduction of the Beckman XL-A analytical ultracentrifuge has greatly increased the accessibility of this technique to non-specialists. This instrumentation was used to investigate the ability of CD31 (D1-D6)STOP protein to self-associate in solution.

In order to facilitate interpretation of the experiments described in this chapter, the theory of sedimentation is briefly outlined below. Macromolecules in the cell of the ultracentrifuge move under the effect of three forces:

i. The centrifugal force, F_c

$$F_c = \omega^2 rM$$

where ω is the angular velocity (radians s^{-1}) of the rotor, r is distance of the macromolecule from the axis of rotation, and M is the molecular mass of the macromolecule.

ii. The buoyant force, F_b

$$F_b = -\omega^2 rM\bar{v}\rho$$

where $\bar{v}$ is the partial specific volume of the molecule, and ρ is the density of the solvent. This force, which is analogous to the upthrust of the Archimedes principle, opposes the centrifugal force due to displacement of solvent by the macromolecule.

iii. The frictional force, F

$$F = -fv$$

where f is the frictional coefficient, and v is the sedimentation velocity (usually measured by meniscus depletion).

When a particle is moving at constant velocity, the net sum of forces is zero (from Newton's First Law, F=ma, where m is the mass of the molecule, and a is the acceleration. Since a=0, F_{total}=0). Hence $F_b+F_c+F = 0$. By rearranging and substituting to separate intrinsic "molecular" parameters from "measurable" experimental parameters, where the measurable parameters, $v/\omega^2 r$, define the sedimentation coefficient, s:

$$\frac{M(1-\bar{v}\rho)}{f} = \frac{v}{\omega^2 r} = s$$

Macromolecules in the presence of a centrifugal field not only sediment, but also diffuse. The combination of sedimentation and diffusion in the cell is described in terms of the flow, *J*:

$$J = s\omega^2 rc - D\frac{dc}{dr}$$

where s is the sedimentation coefficient as described above, D is the diffusion coefficient, c is the solute concentration and dc/dr is the solute concentration gradient.

In sedimentation velocity experiments, the centrifugal force is so great that diffusion has negligible affect on the experiment, however if the centrifugal force is small enough to allow diffusion to significantly oppose the process of sedimentation, and sufficient time is allowed, an equilibrium concentration distribution of macromolecules is obtained throughout the system. Because the system is at equilibrium, there is no dependence on the shape of the solute or the viscosity of the solution, and the system can be analysed thermodynamically to calculate an accurate molecular weight. For an ideal, single component system, the concentration distribution is an exponential function of the buoyant mass of the macromolecule, $M(1-\bar{v}\rho)$, as described by:

$$c(r) = c(a)\exp[M(1-\bar{v}\rho)\omega^2(r^2 - a^2)/2RT]$$

where c(r) is the concentration at radial position r, c(a) is the concentration at a reference point, usually the meniscus, and R and T represent the gas constant and absolute temperature, respectively.

The molecular mass can be obtained by plotting Ln c(r) against r^2, which yields a slope of $M(1-\bar{v}\rho)$. By differentiation, the apparent weight averaged molecular weight (M_{app}) can be plotted against concentration. In an ideal, monodisperse system, M_{app} as a function of concentration is constant, however, in more complex self associating systems the relationship will vary. The equation above can be modified to allow for a variety of interactions (ranging from simple monomer-dimer to more complex interactions), and data fitted to these equations to test different models of association, and where appropriate to calculate equilibrium constants for each interaction (McRorie and Voelker, 1993).

In order to calculate M_{app}, the density (ρ) of the solution and the partial specific volume ($\bar{v}$) of the macromolecule must be known. The density is trivial, provided that the protein solution is relatively dilute, it can be assumed to be that of the solvent. The partial specific volume is defined as the volume change upon addition of 1g of a solute to a large volume of solution keeping all other parameters (temperature, pressure, etc.) constant. Reliable estimation of $\bar{v}$ is critical to accurate determination of molecular weights, since a 1% error in the estimation of $\bar{v}$ leads to a 3% error in molecular weight. The most accurate method of measuring $\bar{v}$ uses a pycnometer, but this requires large amounts of sample (g to mg quantities), alternatively the use of two solvents of different densities (such as hydrogen/deuterium labelled solvents) leads to two simultaneous equations which can be solved for $\bar{v}$ and M (Edelstein and Schachman, 1967), however this is expensive and often impractical. The simplest approach, and the method employed here, is based on the weight average of the partial specific volume of the component amino acids present, such that:

$$\bar{v} = \frac{\sum m_i v_i n_i}{\sum_i m_i n_i}$$

Where m is the molecular weight of the amino acids, v is the partial specific volume of the individual amino acid and n is the number of each amino acid present in the macromolecule.

The calculated and observed partial specific volumes of many proteins have been shown to be in good agreement (McMeekin *et al.*, 1952, Charlwood, 1957). For glycoproteins such as CD31 (D1-D6)STOP, a similar calculation can be used to determine the partial specific volume (Gibbons, 1972) provided the proportion of oligosaccharide as a function of molecular weight is known. The quantity of sugar present on the CD31 (D1-D6)STOP

protein was determined by comparing the theoretical molecular weight based on the primary amino acid sequence (Figure 4.3) with the actual molecular weight. Initial attempts to determine the molecular weight using electrospray mass spectrometry (ES-MS) were unsuccessful. This is a common problem for heavily glycosylated proteins since it can be difficult to ionise and accelerate the particles in the sample (collaboration with Dr. Robin Aplin, Oxford Centre for Molecular Sciences, Physical Chemistry, Oxford University). The alternative method Matrix-Assisted Laser Desorbtion/Ionisation (MALDI) mass-spectrometry was therefore employed (collaboration with Dr. David Harvey, Glycobiology Institute, Oxford University). In this method, the sample is mixed with a large excess of matrix material (in this case sinapinic acid) and bombarded with laser light. The matrix is volatile and is rapidly vaporised in the form of a jet in which intact analyte molecules are entrained and become ionised by proton transfer from the matrix. The principle ions seen in MALDI spectra are $(M+H)+$ "molecular" ion, however, doubly charged ions, $(M+2H)^{2+}$ and triply charged ions $(M+3H)^{3+}$ will also be detected, in addition to non-physiological ion clusters such as $(2M+H)^{+}$ (Figure 4.2).

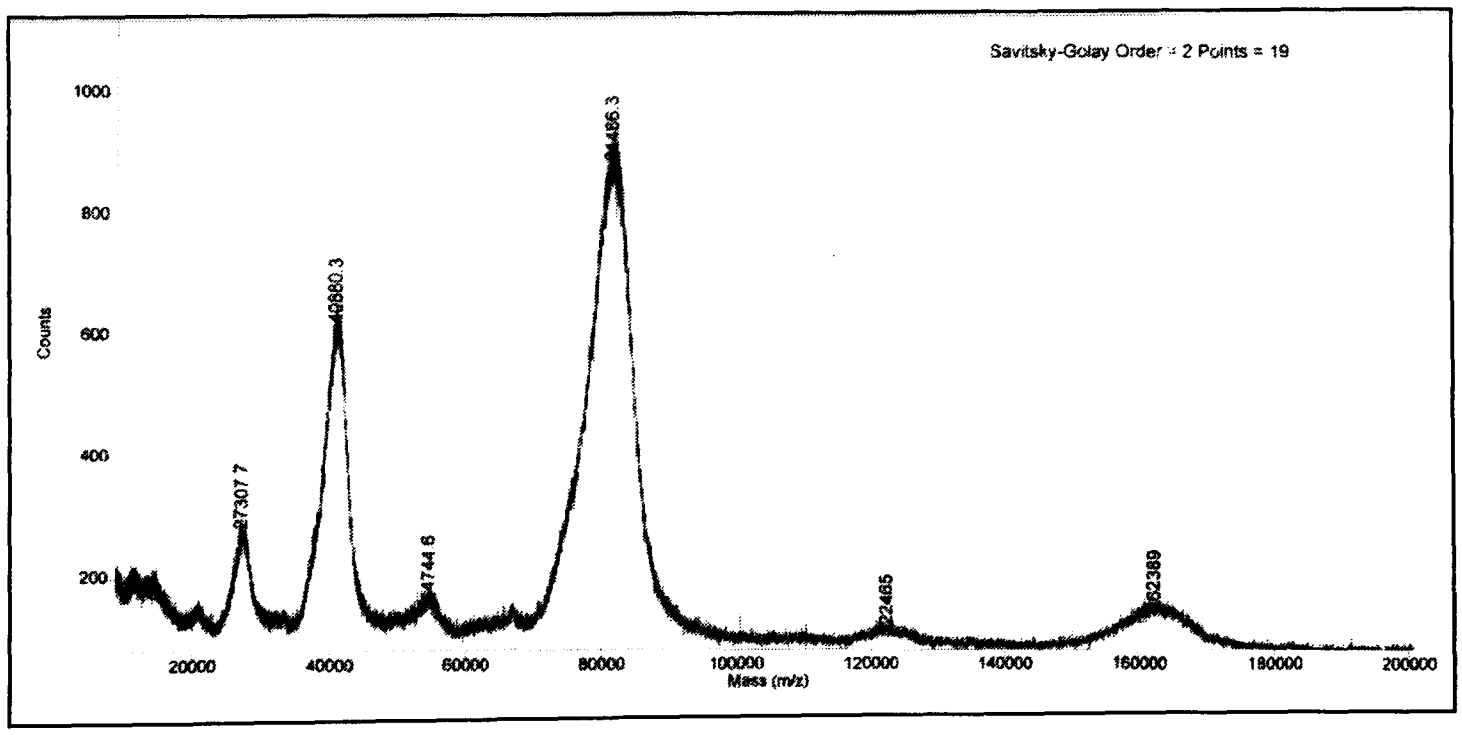


Figure 4.2 Sample MALDI-MS spectra for CD31 (D1-D6)STOP protein. Spectra shows the prominent "molecular" ion $(M+H)^{+}$ peak, corresponding to a molecular weight of 81456.3 Da.

Three independent measurements by MALDI-MS gave comparable results, with a mean of 81494.87 Da for the molecular ion, compared to the predicted molecular weight of 64483.80 Da from the primary amino acid sequence (Figure 4.3). The average molecular weight indicates that the oligosaccharide component contributed 17011.07 Da to the mass

of CD31(D1-D6)STOP protein. This allowed the partial specific volume of CD31 (D1-D6)STOP protein to be calculated (Table 4.1), assuming a partial specific volume of 0.63 for carbohydrates (Gibbons, 1972). The deduced partial specific volume for CD31 was 0.71486, which is close to the figure of 0.73 nominally assumed for proteins. Although the difference is small, had a value of 0.73 been assumed, this would have led to a systematic error in estimation of the molecular weight of around 6%.

Amino Acid	C	S	T	P	A	G	N	D	E	Q	B	Z	H
Number of Residues	14.	57.	41.	24.	28.	21.	28.	22.	46.	31.	0.	0.	14.
% of total Residues	2.4	9.9	7.1	4.2	4.9	3.7	4.9	3.8	8.0	5.4	0.0	0.0	2.4
Molecular weight	1444.	4963.	4145.	2331.	1990.	1198.	3195.	2532.	5939.	3972.	0.	0.	1920.

Amino Acid	R	K	M	I	L	V	F	Y	W	-	X	?	
Number of Residues	18.	48.	12.	43.	31.	54.	22.	17.	3.	0.	0.	0.	0.
% of total Residues	3.1	8.4	2.1	7.5	5.4	9.4	3.8	3.0	0.5	0.0	0.0	0.0	0.0
Molecular weight	2811.	6152.	1574.	4866.	3508.	5353.	3238.	2774.	559.	0.	0.	0.	0.

Total molecular weight = 64483.797

Figure 4.3 Theoretical molecular weight of mature CD31 (D1-D6)STOP protein. The theoretical molecular weight of CD31 (D1-D6)STOP protein was calculated (Staden, Protein Analysis suit of programmes, PIP), after cleavage of he predicted signal peptide sequence. The expected molecular weight from the primary amino acid sequence was found to be 64483.8 Da, assuming no glycosylation. This figure was used to estimate the molecular weight of carbohydrate present on CD31 D1-D6STOP protein by comparison to actual molecular weight as determined by mass spectrometry.

Amino Acid	Residues	Mw	v	C(Y)	A(Y)
Ala	28	71.08	0.74	1472.778	1990.24
Arg	18	156.2	0.7	1968.12	2811.6
Asn	28	114.11	0.62	1980.95	3195.08
Asp	22	115.09	0.6	1519.188	2531.98
Cys	14	103.14	0.63	909.6948	1443.96
Gln	31	128.14	0.67	2661.468	3972.34
Glu	46	129.12	0.66	3920.083	5939.52
Gly	21	57.06	0.64	766.8864	1198.26
His	14	137.15	0.67	1286.467	1920.1
Ile	43	113.17	0.9	4379.679	4866.31
Leu	31	113.17	0.9	3157.443	3508.27
Lys	48	128.18	0.82	5045.165	6152.64
Met	12	131.21	0.75	1180.89	1574.52
Phe	22	147.18	0.77	2493.229	3237.96
Pro	24	97.12	0.76	1771.469	2330.88
Ser	57	87.08	0.63	3127.043	4963.56
Thr	41	101.11	0.7	2901.857	4145.51
Trp	3	186.21	0.74	413.3862	558.63
Tyr	17	163.18	0.71	1969.583	2774.06
Val	54	99.14	0.86	4604.062	5353.56
Sugar	1	17011.07	0.63	10716.97	17011.07
Monomer Mw		81494.87	SUM	58246.41	81480.05
Theoretical Mw		64483.80	**v-bar**		**0.714855**
Carbohydrate Mw		17011.07			

Table 4.1 Calculation of the partial specific volume (v-bar) of CD31 (D1-D6)STOP protein. The partial specific volume of CD31 (D1-D6)STOP protein was calculated assuming a weighted average of the individual amino acid and oligosaccharide component. Partial specific volumes were take from Laue *et al.*, 1992. The calculated v-bar is 0.714855, which is close to the predicted v-bar of most unglycosylated proteins (0.72-0.73), but if uncorrected is sufficient to lead to a small, systematic error in the estimation of the apparent molecular weight during ultracentrifugation.

Sedimentation equilibrium experiments were performed in a Beckman XL-A analytical ultracentrifuge with a Yphantis 6-channel centrepiece in an AN-60Ti rotor to allow multiple concentrations of protein to be loaded simultaneously. Protein concentrations were determined by UV scanning at 230nm or 280nm in PBS. Equilibrium experiments were carried out from initial loading concentrations (120µl/sample) of 0.5-0.125 mg/ml or 0.2-0.05 mg/ml, and a rotor speed of 9000 rpm. Centrifugation was performed at 22°C, and

samples were allowed 40hr to attain equilibrium, and scans were taken every 9hr until 96 hours. Scans for analysis were selected such that there was no significant evidence for any change in radial concentration in the previous 18 hours (to ensure that equilibrium had been reached). The radial distances suitable for analysis were determined by comparison of optical density and intensity scans (the intensity drops at the cell boundary). Scans were corrected for optical imperfections or partial masking of light pulses by subtracting an OD_{360} reading, and by subtracting a scan taken at the end of the run after running the centrifuge at 48,000 rpm for 4 hours. This later procedure sediments the protein, and allows for any low molecular weight contaminants contributing to the observed spectra to be accounted for. Sample scans at equilibrium, are shown below (Figure 4.4 top panel).

Data were analysed by two methods, comparison of the apparent molecular weight (M_{app}) against concentration (M_{app} versus c) and by the Omega function (discussed below) using the SEDPROG sedimentation analysis suite of programmes developed by Greg Ralston (Ralston and Morris, 1992). A plot of the apparent molecular weight against concentration (Figure 4.4 middle panel, data smoothed by box-car averaging over 20 points) shows that the apparent molecular weight shifts upwards as the concentration increases, which is consistent with a self associating system. The nature of this oligomeric interaction was investigated by non-linear curve fitting (based on the Marquardt algorithm, as implemented by Duggleby, 1984) against a range of model associations, ranging from ideal non-associating through simple monomer-dimer to more complex, monomer-dimer-tetramer-hexamer models, calculating appropriate association constants, second virial coefficients (a measure of departure from ideality assuming that the chosen model actually applied) and monomer molecular weight. In initial modelling experiments the notional monomer molecular weight was allowed to "float" during the fitting process, since this is often a useful test of the accuracy of the model; a large discrepancy between the actual and fitted monomer molecular weight is usually an indication that the chosen model is inappropriate.

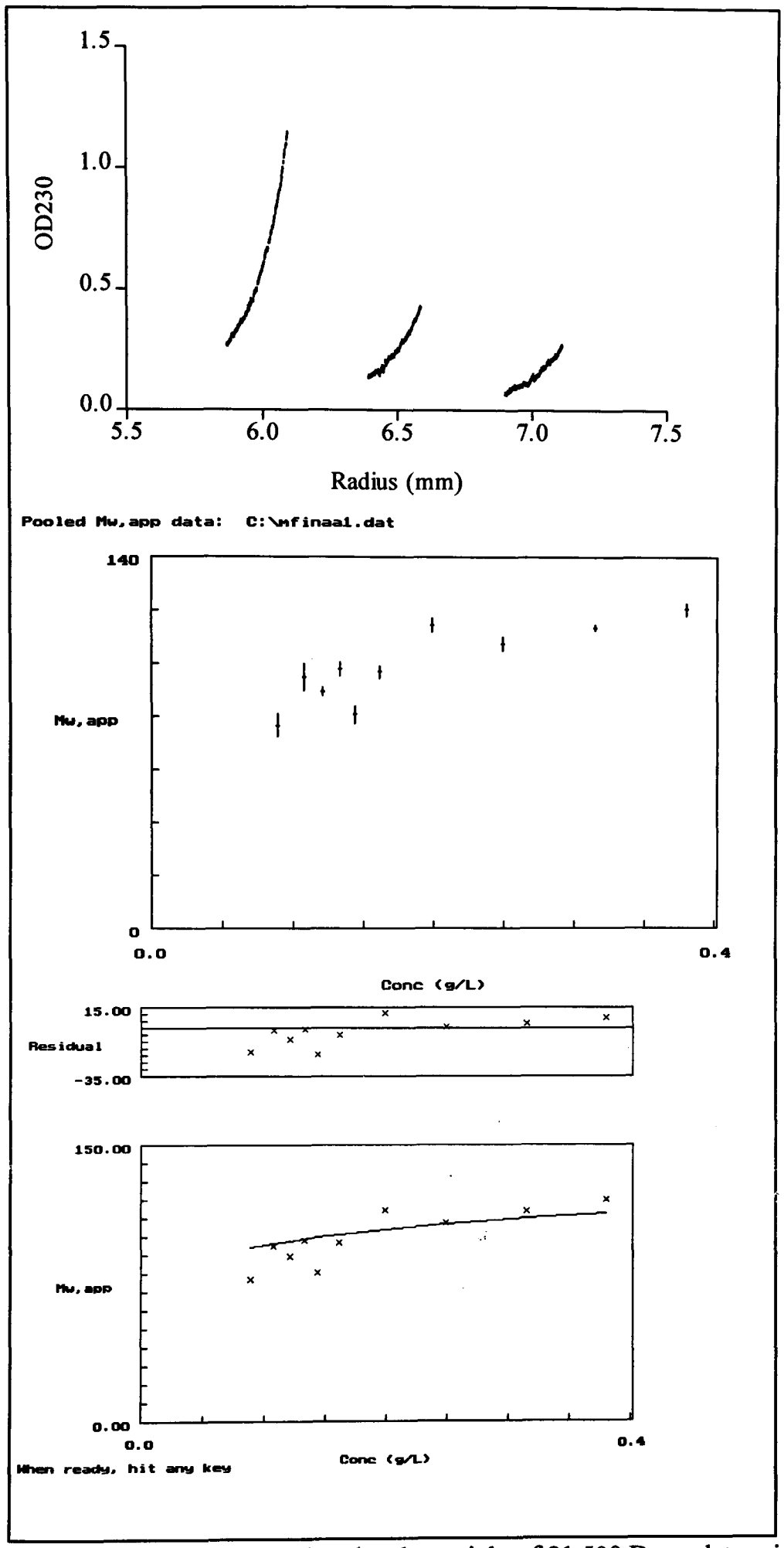


Figure 4.4 Initial analysis of sedimentation equilibrium experiments with CD31(D1-D6)STOP protein. Sedimentation equilibrium experiments were carried out on CD31 (D1-D6)STOP protein using a Beckman XL-A analytical ultracentrifuge with UV scanning optics as described. In each experiment three different initial loading concentrations of each sample were spun at 22°C and 9,000 rpm until equilibrium was reached (as determined by comparison of scans taken every nine hours). The optical density at 230nm against radial position for each of the three concentrations of protein (0.2, 0.1 and 0.05 mg/ml) is plotted (***top panel***), after correction for optical imperfections (subtraction of OD_{360}), and after depletion of protein by centrifugation at high speed. The apparent molecular weight at each radial position was calculated using the SEDPROG suite of programmes (***middle panel***), to show an increase in apparent molecular weight (M_{app}) with increasing concentration, which is characteristic of self-associating systems. In order to model the interaction between CD31 (D1-D6)STOP protein, the distribution of M_{app} against concentration was fitted by a non-linear iterative modelling programme (WTDUGMW) against a variety of different models ranging from simple monomer-dimer through to more complex interaction. Of the models tested (table 4.2), the data was most satisfactorily fitted by assuming a monomer-dimer interaction (***lower panel***), without competing higher order oligomers. Following a monomer-dimer assumption, the monomer molecular weight was predicted to be 77,700±1,400 Da, which is close to the actual molecular weight of 81,500 Da as determined by MALDI mass spectrometry. The association constant was calculated to be 8.0×10^4 M^{-1} (12.5μM dissociation constant).

Model tested	Estimated monomer molecular weight (kg/mol)	Association Constants (L/g)	Second virial coefficient (L mol g^{-2})
Single Species	99.0±0.06	-	-
monomer-dimer	77.7±1.4	k_1=+1.96	1 x 10^{-20}
monomer-dimer-trimer	56.5±0.4	k_{12}=-1.00 k_{13} = +19.9	1.91 x 10^{-3}
monomer-dimer-tetramer	58.6±0.02	k_{12}= +2.51 k_{14}=+9.90	4.11 x 10^{-3}
Monomer-dimer-trimer-tetramer	63.3±0.02	k_{12}=+1.83 k_{13}=+8.89 k_{14}=+0.915	1 x 10^{-2}
Monomer-dimer-teramer-hexamer	31.5±0.05	k_{12}=99.0 k= 9.14	6.44 x 10^{-3}

Table 4.2: Summary of non-linear curve fitting of M_{app} against concentration, using models of association. Non-linear curve fitting was performed using the SEDPROG suite of programmes to analyse potential interaction schemes. In these curve fitting experiments, all critical values were unrestrained (monomer molecular weight, association constants and virial coefficients) Of the different models tested, the data is most satisfactorily modelled by assuming a monomer-dimer interaction. Other models either inaccurately fit the monomer molecular weight, give non-physical (i.e. negative) association constants, or have unacceptably large virial coefficients.

Of the models tested, the data is most satisfactorily explained by a simple monomer-dimer model, (see figure 4.4 bottom panel and Table 4.2) other potential interaction schemes either fit the data poorly (as judged by large second virial coefficients), significantly underestimate/overestimate the monomer molecular weight (again indicating that the model is inappropriate), or give non physical association constants. For a monomer-dimer interaction, the estimated monomer molecular weight of 77,700±1,400 is close to the molecular weight determined by mass-spectrometry (81,500 Da), and the association constant is estimated to be 1.96 L/g. The equilibrium constant, *k*, estimated in this analysis, is the quantity K_i/M_1; i.e. the value in the molar scale, expressed on a g/L scale. These values are related to the quantities in the g/L scale, k (L/g):

$$k_i \text{ (L/g)} = i\, K_i/M_1$$

Such that for the monomer-dimer interaction above, where $k_{12} = 1.96$:

$$k_2 = +1.96 = \frac{2K_2}{81494}$$

$$K_2 = \frac{+1.96 \times 81494}{2}$$

$$K_2 = 79864 mol / L$$

$$K_2 \approx 8.0 \times 10^4 M^{-1}$$

Hence the affinity constant for the interaction between CD31 (D1-D6)STOP protein is 8.0 x 10^4 M^{-1}, or expressed as a dissociation constant, K_d is 12.5μM. Although this indicates that the affinity is not particularly high, relative to antibody-antigen interactions, or to the interaction between adhesion molecules (typical dissociation constants in the nM range), it is significantly greater than that observed (1.08mM) for the dimerisation of soluble recombinant CD4 (Wu *et al.*, 1997), and is likely to be substantially greater than the affinity of E-cadherin, where monomeric soluble E-cadherin does not self-associate free in solution, although pentameric E-cadherin will interact with other pentamers (Pokutta *et al.*, 1994, Tomschy *et al.*, 1996).

A second alternative method of data analysis was also employed, based on the Omega function (Milthorpe *et al.*, 1975; Morris and Ralston,1985; Ralston and Morris, 1992). The Omega function was introduced as a means of avoiding the differentiation required in computing M_{app}. This greatly enhances the signal to noise ratio, and allows potential artefacts, such as mixtures of non-interacting solutions of macromolecules, to be readily eliminated. Omega is defined as the ratio of the actual measured concentration at any point in the cell relative to the thermodynamic activity of a single non-associating real solute whose activity was equal to the concentration of the real solute at an arbitrary reference position, c(ref). Since the distribution of such an ideal species is given by :

$$a_1(r) = a_1(ref)\exp(\phi M_1(r^2-ref^2)), \text{ where } \phi = (1-v\rho)\omega^2/2RT$$

and when $a_1(ref)$ is set to c(ref), it follows that :

$$\Omega = c(r)/a_1(r)$$
$$= c(r) \exp(\phi M1 (ref^2-r^2)/c(ref)$$

Milthorpe *et al.*, (1975) showed that Ω_0, the value of Ω at zero concentration, yields a_1(ref)/c(ref). Since c(ref) is chosen arbitrarily, a_1(ref) may be calculated to give the thermodynamic activity of the monomer at the reference point, from which the thermodynamic activity of the monomer at any other point can be determined. Importantly, Morris and Ralston (1985) showed that the Omega distribution, like the distribution of M_{app}, is a continuous and unique function of the total concentration for a self-associating solute, and that the parameters of self association can be estimated from fitting the Ω versus concentration distribution. An initial analysis of the sedimentation data showed that Ω versus concentration for a range of different loading concentrations generated a continuous and overlapping distribution (Figure 4.5), indicating that CD31 (D1-D6)STOP protein exists as an equilibrium between self associating monomers and higher order oligomers. This result rules out the possibility of gross contamination giving rise to a fixed proportion of two non-interacting species, which can be difficult to deduce from M_{app} against concentration plots. By using the same non-linear curve fitting programmes, the association constant assuming a monomer-dimer interaction was estimated to be 1.73 L/g, which in molar equivalents is an association constant of 7.05×10^4 M^{-1}, or a dissociation constant of 14.2μM. Hence both methods of analysis (M_{app} versus concentration, and omega function fitting) give similar results.

Thus, analysis of the hydrodynamic properties of CD31 (D1-D6)STOP protein by analytical ultracentrifugation in sedimentation equilibrium mode is highly suggestive of a reversible equilibrium between monomeric and dimeric forms.

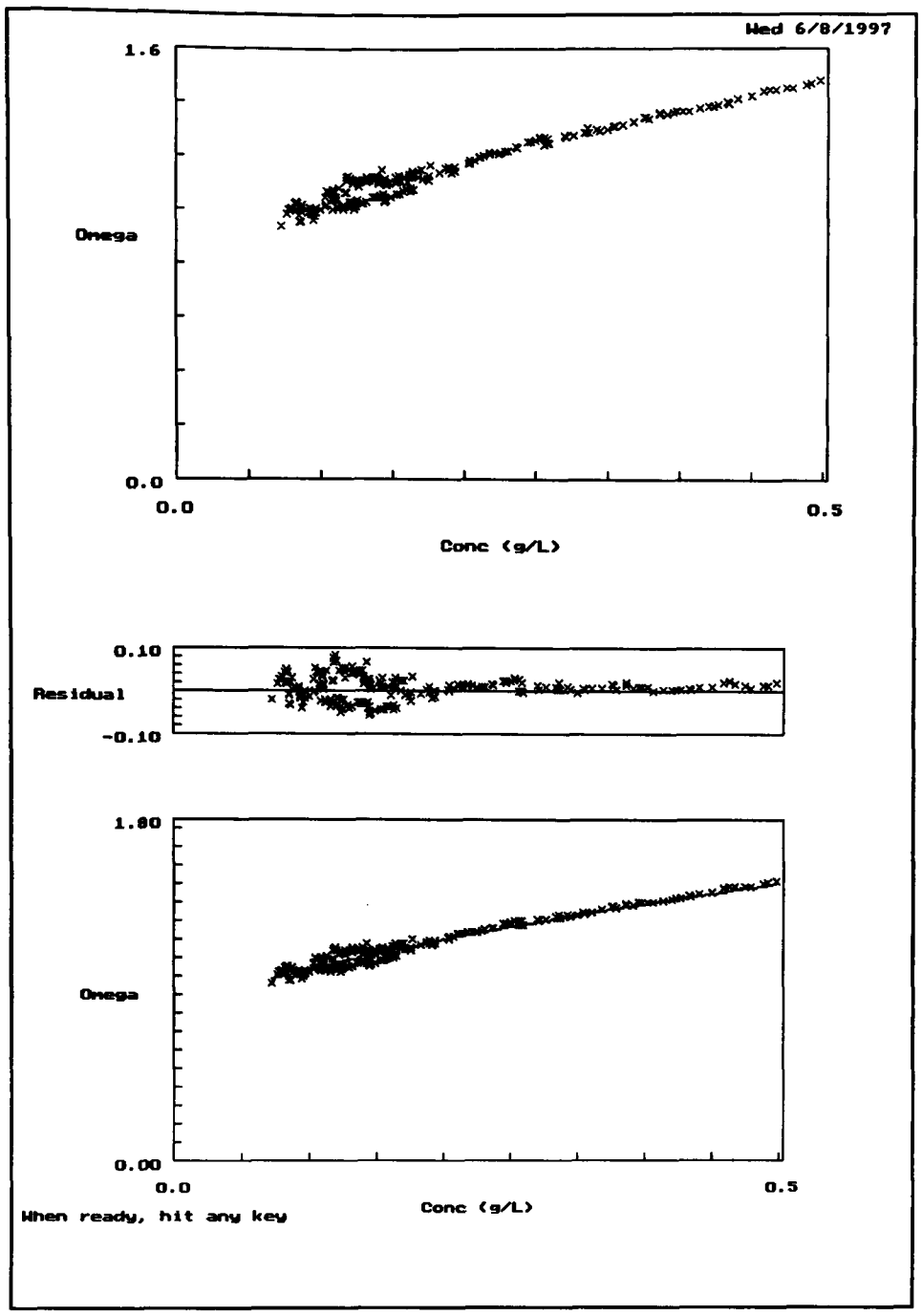


Figure 4.5 Analysis of sedimentation equilibrium experiment data by Omega function. Omega analysis was performed using the SEDPROG suite of programmes on the data shown above in Figure 4.4. Importantly, this shows that three independent loading concentrations of CD31 (D1-D6)STOP protein give rise to an overlapping omega distribution (***top panel***), indicating that the system has reached equilibrium, and that the changes in apparent molecular weight are not due to either contamination with a low molecular weight component, or to proteolysis of CD31 (D1-D6)STOP protein during the course of the experiment (which would result in a discontinuous distribution of Omega). The Omega function increases with concentration which is characteristic of a self-associating system (an ideal monomeric solution gives a constant omega value). Fitting the data to a monomer-dimer model (***bottom panel***), previously characterised as being most representative of the change in M_{app} with concentration, estimates the association constant to be 7.05 x 104 M-1 (Kd = 14.2μM), which is close to the value estimated previously.

4.2.2.2 Quasi-dynamic light scattering.

Dynamic light scattering (DLS) is a biophysical technique used to estimate molecular weights in solution, and to assess the tendency of molecules in solution to interact with one another. It utilises a beam of monochromatic light passed through a sample containing the protein of interest. When a single molecule is illuminated by a beam of light, the light incident on the molecule is re-radiated in all directions. For particles having dimensions less than five percent of the wavelength of the incident light, the scattering intensity from a single molecule suspended in a transparent medium and illuminated by a monochromatic, plane polarised light is given by the Rayleigh scattering relationship:

$$I_{s,o} = \frac{4\pi^2 M^2 \sin^2 \phi (dn/dc)^2 I_o}{N_A{}^2 \lambda^2 r^2}$$

Where the scattering angle ϕ is the angle between the direction of the incident beam and the direction of scatter, M is the molecular mass in Daltons, dn/dc is the dependence of the solvent refractive index upon the solute concentration, I_0 is the intensity of the incident light, N_A is Avogadro's number, λ is the wavelength of the light, and r is the distance from the molecule to the point of detection.

If a large number of such particles is illuminated simultaneously, the intensity of the scattered light at a distant point detector is given by the square of the vector sum of the scattered light from each particle. Where the incident light is a plane wave (e.g. from a laser), the amplitude of the detected signal will vary as the individual particles move randomly under Brownian motion. This effect arises because, as the particles move with respect to one another, the phases of their individual contributions to the scattered light field at the detector are constantly changing, and a whole range of optical interference conditions between maximum and minimum can arise, such that the observed intensity fluctuates about the time-averaged value with minima approaching zero intensity and maxima approaching twice the mean value. When analysed, the light scattering shows a large degree of short range order in the fluctuations which correlate to the translational diffusion coefficient of the particles, D_T. D_T is calculated by a mathematical technique known as autocorrelation using the Nelder Meade Simplex algorithm by the instrument (DYNAPRO-801). Under the assumption of Brownian motion, this coefficient is converted to the hydrodynamic radius, R_H, of the particles, using the Stokes-Einstein relationship, assuming a hard-sphere model for the particle:

$$R_H = \frac{k_b T}{6\pi\eta D_T}$$

Where k_b is Boltzman's constant, T is the absolute temperature in Kelvins, and η is the solvent viscosity. The molecular weight (MW) can then be calculated from the hydrodynamic radius using an empirically derived relationship between R_H and MW values for a number of well characterised proteins in buffered aqueous solution.

Initial dynamic scattering experiments performed with CD31 (D1-D6)STOP at 0.5mg/ml (results tabulated below, Table 4.3), showed that the population of macromolecules was slightly polydisperse, which is consistent with the hypothesis that the protein exists in an

equilibrium between monomers and dimers, and biased towards a high apparent molecular weight form (M_{app} = 321.8 kDa).

Amp	Diffn Coeff	Radius (nm)	Est. MW	Conc mg/ml	Polyd (nm)	Count Rate	Base Line	SOS
0.789	323	7.0	329k	0.553	1.438	159	1.001	0.590
0.785	327	6.9	322k	0.566	1.311	159	1.000	0.589
0.788	326	6.9	321k	0.561	1.140	157	0.999	0.325
0.781	328	6.9	316k	0.569	-----	157	1.000	0.353
0.784	327	6.9	318k	0.561	1.443	156	1.002	0.593
0.783	328	6.9	316k	0.533	1.236	147	1.001	0.560
0.770	327	6.9	322k	0.496	1.533	140	1.000	0.517
0.772	325	7.0	328k	0.469	-----	135	1.001	0.583
0.760	323	7.0	328k	0.422	1.256	122	1.000	0.468
0.766	329	6.9	318k	0.459	1.303	128	1.001	0.468

Table 4.3 Results from DynaPRO-801 dynamic light scattering experiments. Output from the DynaPRO-801 machine is recorded above. Output parameters are Amp (amplitude of the scattering component), Diffn Coeff (the translational diffusion coefficient), Radius (the hydrodynamic radius of the molecules in solution), Est. MW (the estimated molecular weight), Conc (concentration of protein in the sample cell), Polyd (the polydispersity value, in nanometers, which indicates the standard deviation of the spread of particle sizes about the reported average radius), Count Rate (photon count rate, '000s per second), Baseline (represents the completeness and fit of the analysis - 1.000 indicates a complete fit), SOS (sum of squares, a second measure of fit). Data are slightly polydisperse, which is consistent with the monomer-dimer equilibrium proposed previously, and well fitted as judged by baseline values close to 1.000 and small residual sum of squares. The mean molecular weight estimated from these ten measurements is 321.8kDa. Although the estimated molecular weigh is unlikely to be accurate (see text for discussion), it is considerably larger than the 80kDa predicted for monomeric CD31 (D1-D6)STOP protein.

Since the estimated molecular weight is unlikely to be accurate (most cell surface proteins comprised of immunoglobulin folds form relatively rigid rod-like structures as judged by rotary shadowing electron microscopy, and the M_{app} calculation is based on a hard-sphere assumption), it was hoped to use scattering to follow changes in association. Theoretically, one could dilute the CD31 (D1-D6)STOP protein, and follow changes in M_{app} against concentration, in a manner analogous to the analysis of the ultracentrifugation experiments reported above, however, in practice this is not possible since the scattering intensity falls off rapidly as the concentration decreases, so that the useful threshold of detection lies outside the concentration range of interest. An alternative approach is to use a constant concentration of protein which gives a strong scattering signal, and diffuse in salt to concentrations which would be expected to dissociate non-covalent quaternary

interactions, resulting in a drop in M_{app}, as has been used successfully to show self-association for CD4 (Wu *et al.*, 1997). When this approach was tried with CD31 (D1-D6)STOP protein, addition of NaCl to a concentration of 300-400mM had no effect, however, increasing the concentration of salt to 500mM or above induced gross protein aggregation to form MDa sized aggregates (data not shown). This technique was therefore not pursued any further.

4.2.2.3 Native non-denaturing gel electrophoresis

5% native, non-denaturing gels were prepared using fresh glass plates, and buffers of standard composition (see methods and materials), except that SDS was omitted. Running buffer was also prepared as per standard, without SDS, and gels were pre-run extensively for 4 hours to ensure that excess oxidising agents used in the polymerisation reaction (ammonium persulphate) were removed. Running buffer was replaced following the pre-run, and samples of CD31 (D1-D6)STOP protein in non-reducing sample buffer, lacking SDS were loaded on the gel. Under these conditions, migration of protein through the gel depends on the hydrodynamic properties of the macromolecule, including size, shape, subunit association, and charge. Thus, non-denaturing native gel electrophoresis is a simple technique to investigate potential interactions between proteins. Because of the lack of success in dissociating CD31 oligomers with elevated salt concentrations, samples were either run completely native, or following a brief 2 minute pulse at 100°C. (Figure 4.6).

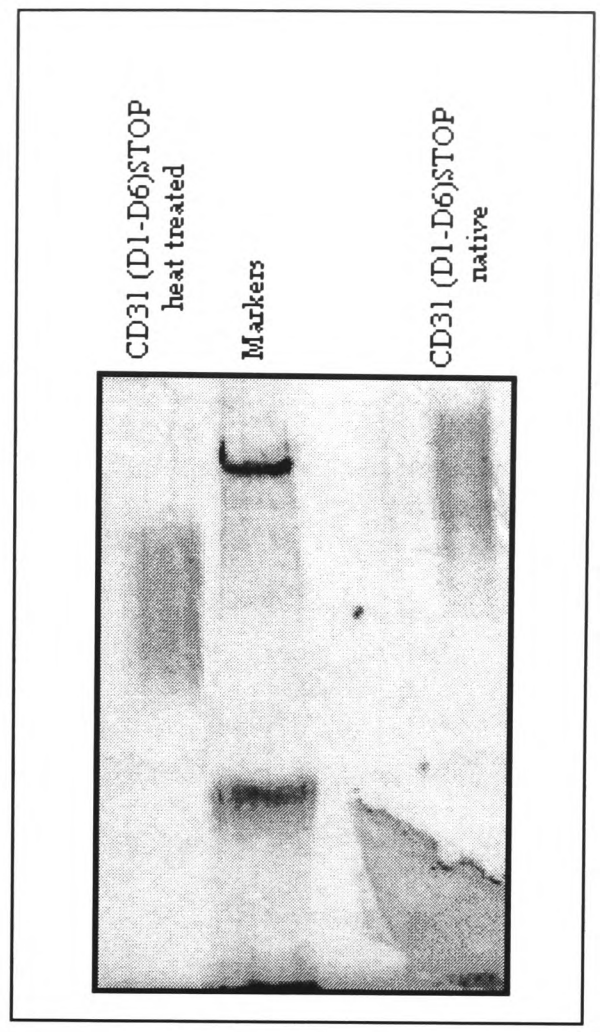


Figure 4.6 Native, non-denaturing gel electrophoresis on CD31 (D1-D6)STOP protein. 5% non-denaturing PAGE gels were run on native and heat pulsed CD31 (D1-D6)STOP proteins as described above. Both proteins run as broad bands consistent with heterogeneity noted from MALDI-MS data. Significantly, heat treated CD31 (D1-D6)STOP protein ran at much lower down the gel than native material, which is consistent with the hypothesis that in solution CD31 (D1-D6)STOP protein self associates. (Molecular weight standards visible are 250kDa and 98kDa)

Both native and heat pulsed CD31 (D1-D6)STOP protein run as broad smeared bands, which indicates some sample heterogeneity. Importantly, the native protein runs at considerably higher up the gel than the heat pulsed sample. Assuming that the brief heat pulse will dissociate any non-covalent interactions, this is also consistent with the hypothesis that CD31 (D1-D6)STOP protein undergoes spontaneous self association.

4.2.3 Chemical cross-linking studies with CD31 (D1-D6)STOP protein

A common approach to investigating the interaction between a receptor and its ligand is chemical cross-linking, and cross-linking studies have previously been used to show that ICAM-1 is present as a dimer on the cell surface (Reilly *et al.*, 1995, Miller *et al.*, 1995). In initial experiments, the wild type CD31 (D1-D6)STOP protein used previously for biophysical experiments was diluted in PBS (pH7.4) in the range 1.7mg/ml to 0.0625mg/ml, such that 10µl samples were used for each concentration, and cross-linking

performed as described in materials and methods using Bis(Sulphosuccinimidyl) suberate (BS_3) as the cross-linker. BS_3 is a homobifunctional cross-linker with a reactive NHS-ester groups which react with primary amines (i.e. NH_2-terminal primary α-amine and the ε-amine groups of lysine residues, Figure 4.7).

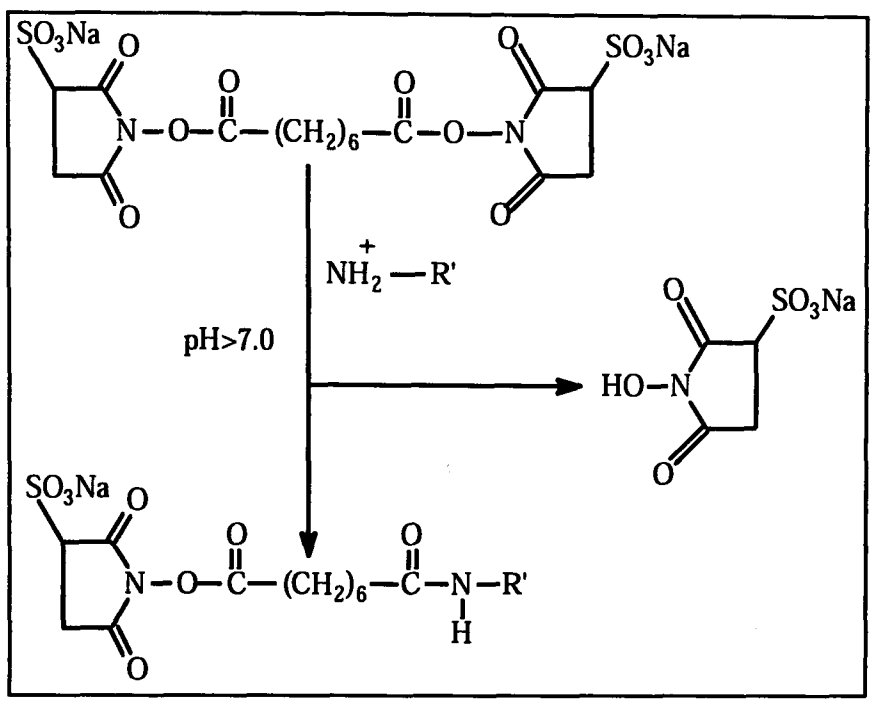


Figure 4.7 Scheme for succinimidyl ester based homobifunctional cross-linker Bis(Sulphsuccinimidyl) suberate (BS3) reacting with primary amines.

There are 48 lysine residues in the extracellular domain of CD31 (see figure 4.3), such that addition of a 50-fold molar excess at the highest concentration of protein, and considerably greater excess at lower concentrations would be expected to react with all the available NH_2 groups within the protein. Since the cross-linker is a low molecular weight (572.43 g/mol) compared with the CD31 (D1-D6)STOP protein, the cross-linker will diffuse much more rapidly than the protein, such that if the protein were a monomer, the available NH_2 groups would be blocked by reacting with the BS_3, before random diffusion allowed contact with another protein with free cross-linking NHS-ester group. If however, there are dimers, or higher order aggregates present, then initial reaction of NHS-ester homobifunctional cross-linker with a primary amine on one protein will position a second reactive group in close proximity to the second protein in the dimer, which will then favour cross-linking of the two proteins. After cross-linking, 200ng of protein were resolved on 4-20% Tris-glycine gradient gels, and CD31 detected by either Western blotting with a cocktail of anti-CD31 antibodies, or the gel directly silver stained (Figure 4.8).

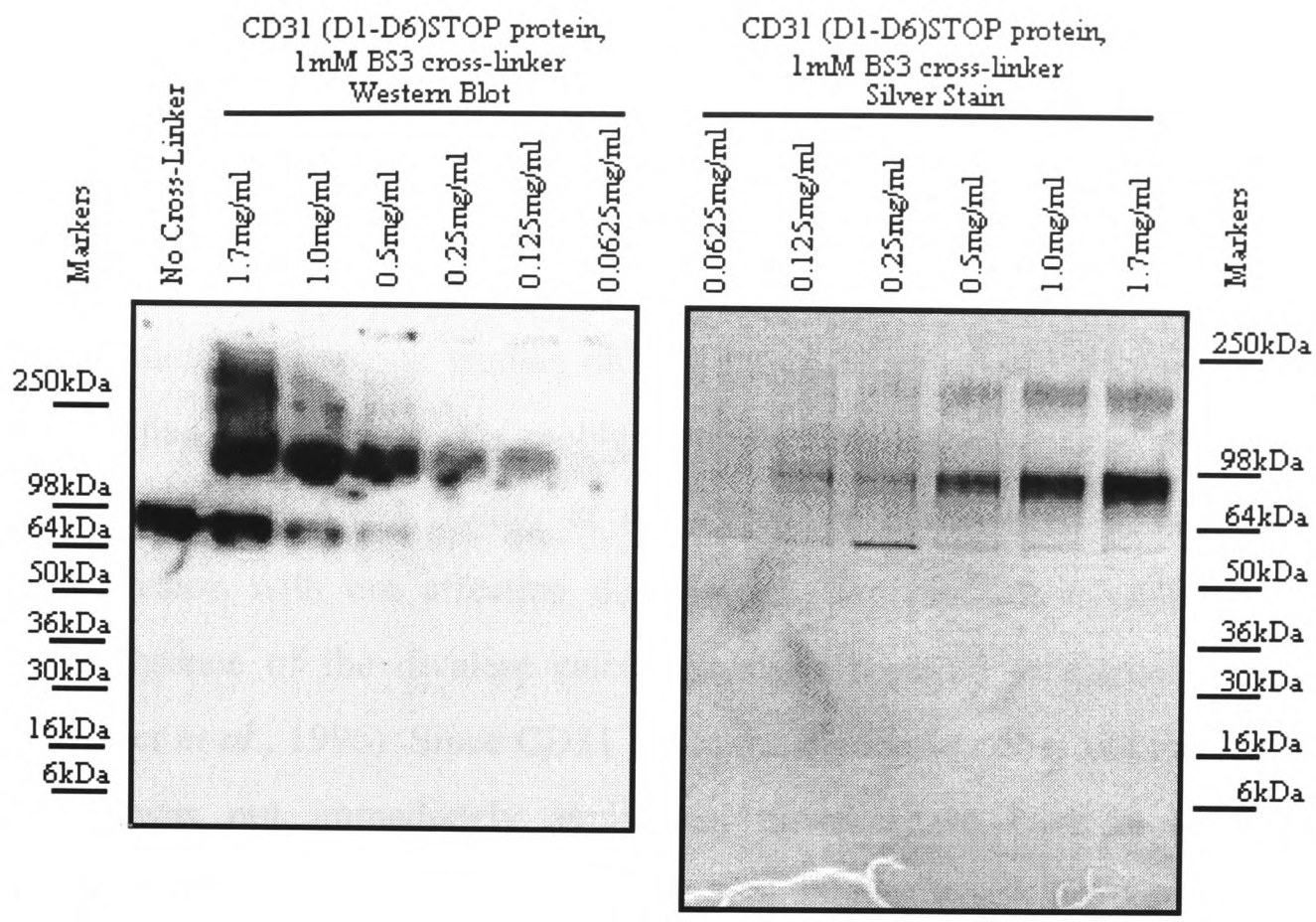


Figure 4.8 Chemical cross-linking of soluble CD31 (D1-D6)STOP protein shows the presence of monomers and dimers in solution. CD31 (D1-D6)STOP protein in the concentration range 1.7mg/ml to 0.0625mg/ml was subjected to chemical cross-linking with the homobifunctional cross-linker BS_3 at a final concentration of 1mM. 200ng protein samples were resolved under non-denaturing conditions with SDS-PAGE 4-20% gradient Tris-glycine gels, blotted onto nitrocellulose, and CD31 protein detected by Western blotting with a cocktail of anti-CD31 mAbs (9G11, CAL31.1 and 10B5). As expected, untreated CD31 runs as a monomer of apparent molecular weight 80kDa under non-reducing conditions. Addition of BS_3 to the samples produces a covalently linked protein migrating at approximately 160kDa, as expected for a dimer. Silver staining of cross-linked protein show bands equivalent to both monomers and dimers.

As expected, the untreated CD31 (D1-D6)STOP protein ran as a monomer with an apparent molecular weight of approximately 80kDa (close to the molecular weight established by mass spectrometry above). Importantly, because the gel was run under non-reducing conditions it was possible to state that no significant disulphide exchange resulting in covalent intermolecular disulphide bridges had occurred between CD31 (D1-D6)STOP protein monomers during the time course of the experiment. Therefore, any multimers present in the cross-linked structures were likely to have resulted from non-covalent interactions between monomers. Addition of BS_3 to the samples clearly identified bands corresponding to both a monomer and a dimer, suggesting that CD31 (D1-D6)STOP protein exists as an equilibrium between monomeric and dimeric forms in solution. Also at the highest concentrations of CD31 protein tested, higher order aggregates corresponding to trimers and tetramers were noted. These may represent homophilic interactions between dimers and monomers, and dimer-dimer interactions. However these represent only a tiny fraction of the total CD31 protein, since they are not visible on silver stained gels (see

figure 4.8), which is consistent with the non-linear modelling of data from the equilibrium density ultracentrifugation experiments, which fit a simple monomer-dimer model.

CD31 is a homophilic adhesion molecule, capable of binding to itself. One possibility is that the dimerisation observed simply reflects homophilic contacts between individual monomers in solution. Previous studies on the dimerisation of cell adhesion molecules either have not had to deal with this problem simply because either they do not mediate homophilic adhesion (ICAM-1, Reilly *et al.*, 1995), or it has been possible to block homophilic adhesion with out affecting dimerisation, for example C-cadherin forms a dimer in the absence of the divalent calcium cations required to mediate homophilic adhesion (Brieher *et al.*, 1996). Since CD31 homophilic adhesion does not require cations, this approach was not immediately applicable, however we have tools that block homophilic adhesion in the form of single point mutations which are known to ablate homophilic adhesion in cell-protein assays. In the previous chapter it was also speculated that some of the residues identified in the mutagenesis screen, particularly those on the ABDE face, may represent residues mediating dimerisation between individual monomers. In order to investigate the role of these residues in mediating *cis*-dimerisation versus *trans*-homophilic adhesion, four residues having the most significant effect on homophilic adhesion (D11A, D30A, D51R and K89A) have been subcloned from CD31(D1-D6)Fc in pIG1 vector into CD31 (D1-D6)STOP in pCDNA3 by using restriction enzyme sites *Hind*III and *Bam*HI to excise a fragment corresponding to CD31 domains 1 and 2, containing the mutation of interest, and subcloning this fragment into a CD31(D1-D6)STOP backbone. It is planned to express these mutant proteins in COS-1 cells, and to perform cross-linking with BS_3 performed as described above.

This experiment will allow the role of homophilic contacts in dimer formation to be addressed. One speculative suggestion from the structure based alignment of CD31 with E- and N-cadherin in the previous chapter was that the residues on the ABDE face might represent points of contact in laterally associated dimer pairs rather than true homophilic contacts, as in the cadherin structures (Shapiro *et al.*, 1995, Nagar *et al.*, 1996). Analysis of the affect of mutations known to block homophilic adhesion on dimerisation will give some insights into the physical basis of each interaction, however, resolution of the role of

individual amino acids involved in dimerisation versus homophilic adhesion is likely to require x-ray crystallographic studies which have been used to analyse cadherin interactions in detail.

4.2.4 CD31 cross-linking at the cell surface identifies CD31 dimers.

The biophysical and biochemical approaches described above, indicate that in solution CD31 (D1-D6)STOP protein forms dimers. However, this interaction may not be physiologically relevant, and it was important to determine if CD31 expressed on cells also formed dimers. This would also help to confirm that the interaction involved lateral association rather than homophilic contacts. Chemical cross-linking was used to analyse CD31 neighbours on the stable CD31 expressing cell line U937, and on transiently transfected COS-1 cells using the non-membrane permeant cross-linker BS_3. Cross-linking was performed on 10^6 cells with BS_3 at a final concentration of 1-2 mM and at 4°C whilst rotating end-on-end, since this has been shown to enhance specificity for cross-linking of oligomeric membrane proteins (Eanger *et al.*, 1986). After 30 minutes, cross-linking was quenched by the addition of 50mM Tris.HCl, pH8.0, and 5mM iodoacetamide added to alkylate free sulphydryl groups and prevent the formation of intermolecular disulphides on lysis. After 10 minutes on ice, cells were pelleted and lysed in 0.5ml lysis buffer and sonicated. The sonicate was centrifuged at 14,000g for 10 minutes and soluble proteins precipitated from the supernatant with 500µl of ice-cold acetone. Samples were centrifuged at 14,000g for 30 minutes, the pellet washed in 70% ethanol, resuspended in non-reducing sample buffer containing 50mM iodoacetamide, heated to 100°C for 5 minutes, and subjected to SDS-PAGE on 4-20% Tris-glycine gels. CD31 containing protein complexes were identified by Western blotting as described for the CD31 (D1-D6)STOP proteins (Figure 4.9). In the absence of cross-linking reagent, western blotting identified a band of 120kDa, typical of transmembrane expressed CD31. Chemical cross-linking of both cell lines and transfectants with BS_3 at 4°C resulted in a shift in a portion of the immunoreactive 120kDa CD31 to a band of approximately 250kDa corresponding to a dimeric form of CD31. In the case of transiently transfected COS-1 cells, the proportion of CD31 cross-linked was significantly greater than observed for U937 cells, such that for U937 cells the intensity of the cross-linked 250kDa band was 28% of the 120kDa band, compared with a figure of 48% for transiently transfected COS-1 cells (Figures based on

the band intensity determined from Paintshop Pro image manipulation programme). No other CD31 immunoreactive bands were observed upon cross-linking, indicating that CD31 does not form heterodimers with other cell surface molecules on the cells tested. No higher molecular weight bands were observed in either COS transients or U937 cells, indicating that higher order oligomeric CD31 clusters are not present. This is consistent with the hypothesis that CD31 dimerisation is specific, rather than merely representing a clustering of CD31 at the cell surface.

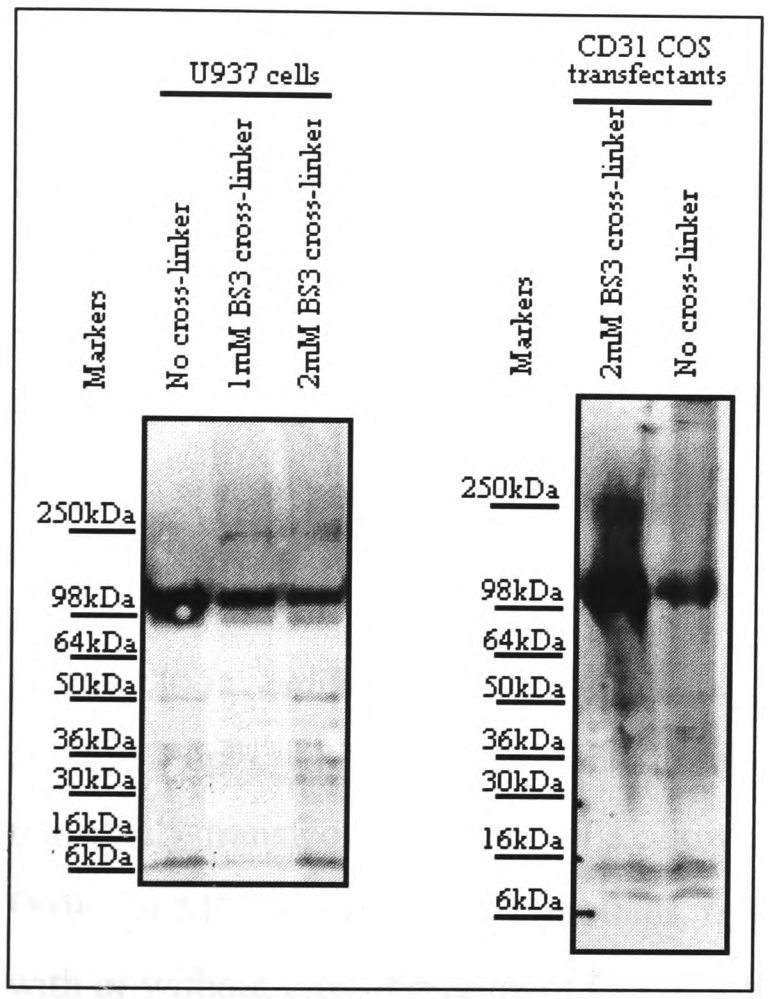


Figure 4.9 Chemical cross-linking with the membrane impermeant cross-linker BS_3 on COS-1 transients and U937 cells. 10^6 cells were cross-linked at 4°C with the indicated final concentrations of BS_3 for 30 minutes, cross-linking was quenched with 50mM Tris.HCl, pH8.0, 50mM iodoacetamide. Cells were pelleted and lysed by sonication, and protein precipitated from the soluble fraction with ice cold acetone. Protein pellets were washed in 70% ethanol, dried under vacuum, resuspended in non-reducing SDS sample buffer containing 50mM iodoacetamide, and resolved on 4-20% Tris-glycine gels. Immunoreactive CD31 was detected by Western blotting with a cocktail of anti-CD31 mAbs as described previously. In untreated samples a single CD31 specific band of 120kDa was observed as expected. Treatment with BS_3 resulted in a proportion of the CD31 120kDa band shifting upward to around 250kDa, corresponding to a dimer. These results indicate that CD31 is present on the cell surface both in monomeric and as dimeric form.

4.2.5 A CD31 extracellular domain/epidermal growth factor receptor cytoplasmic tyrosine kinase domain chimera is constitutively autophosphorylated.

The growth factor receptors are the prototypic examples of the tyrosine kinase family of receptors, which are characterised by an extracellular ligand binding domain, a single transmembrane portion, and a large intracellular catalytic domain. For these receptor types the key event following growth factor stimulation is autophosphorlyation within the intracellular domain induced by dimerisation of the receptor (Kazlauskas and Cooper, 1989), which in turn promotes interaction of the receptor with downstream target proteins and enzymes, including phosphoinositide-specific phospholipase Cγ, the 85kDa subunit of phosphatidylinositiol 3-kinase (PI3K), GTPase-activating protein (GAP), growth-factor-receptor binding protein 2 (Grb2), the phosphotyrosine phosphatase SHP-2, and members

of the non-receptor Src family of tyrosine kinases (for review see Marlarkey *et al.*, 1995). If CD31 exists as a dimer on the cell surface, then one would expect to see constitutive autophosphorlyation of a CD31/EGFr chimera, and co-immunoprecipitation of at least some of the associated cytosolic signalling proteins. A CD31/EGFr chimera was constructed in which the extracellular ligand binding domain of EGFr was replaced by the extracellular domain of CD31 (CD31 ECD/EGFr TM-TK in expression vector pCDM8 (see materials and methods) When transiently expressed in COS cells, this construct was expressed at the cell surface of COS-1 cells following transient transfection as judged by FACS analysis with anti-CD31 mAb 9G11 (Figure 4.10a) and following precipitation of total cell surface glycoproteins with Wheat Germ Agglutinin (WGA)-agarose, could be detected by Western blotting with 9G11 (Figure 4.10b). COS-1 cells transfected with CD31 ECD/EGFr TM-TK supported CD31 specific homophilic adhesion to full length CD31 (D1-D6)Fc protein immobilised on plastic, but not to MUC18 (D1-D5)Fc at levels comparable to full length wild type CD31 (Figure 4.10c). These results indicated that the chimera was expressed and was functional in terms of CD31 mediated homophilic adhesion.

In order to investigate the phosphorylation status of the chimera, CD31ECD/EGFr TM-TK and full length wild type CD31 were immunoprecipitated with anti-CD31 mAb 9G11 from transiently transfected COS-1 cells allowed to adhere to plastic coated with CD31 (D1-D6)Fc or MUC-18 (D1-D5)Fc proteins, or kept in solution by rotating end-on end at 37°C with or without cross-bridging of CD31 with mouse anti-CD31 mAb L133.1 and goat anti-mouse polyclonal. Cells were lysed in 1% Triton X-100 lysis buffer containing 1mM sodium orthovanadate, immunoprecipitated with anti-CD31 mAb 9G11, and the immunoprecipitated material resolved on 4-20% Tris-glycine gradient gels, blotted onto nitrocellulose, blocked with 3%BSA/1% ovalbumin, and phosphotyrosine containing proteins detected by Western blotting with horse-radish peroxidase conjugated anti-phosphotyrosine antibody PY-20.

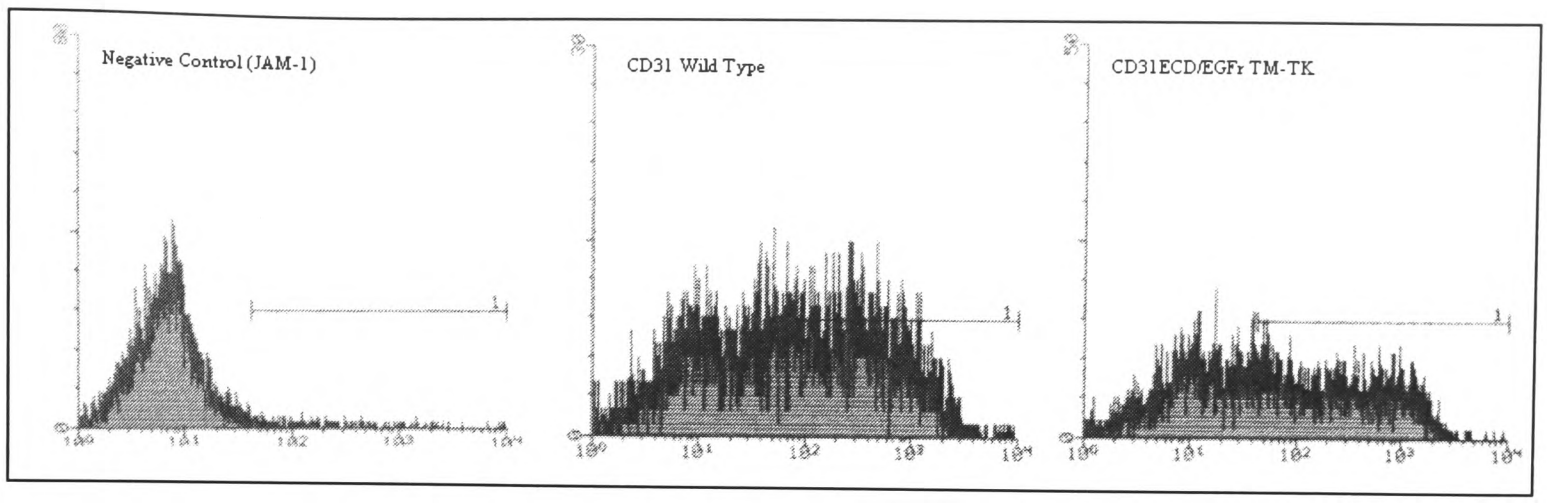


Figure 4.10a. FACScan profiles of COS-1 cells transiently expressed with JAM-1 (negative control), CD31 full length wild type and CD31 ECD/EGFr TM-TK chimera. Transiently transfected COS-1 cells were lifted in 2mM EDTA/PBS and 10^6 cells stained with 2μg of anti-CD31 mAb 9G11. Bound antibody was stained with goat anti-mouse FITC conjugated secondary, and labelled cells counted by FACScan and LYSIS II software. CD31 and CD31 ECD/EGFr TM-TK constructs were expressed on the cell surface at comparable levels (approximately 50% of cells judged to be positive), so that no further correction for transfection efficiency was made in the following experiments.

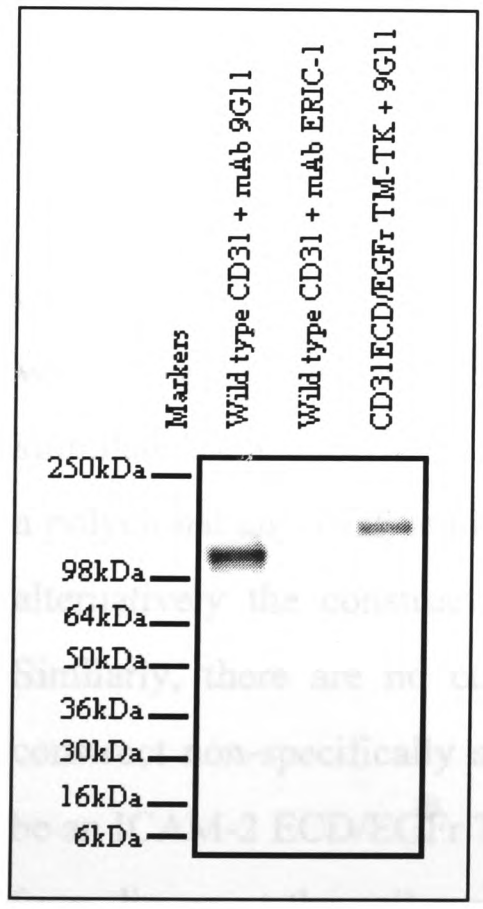


Figure 4.10b Immunoprecipitation of CD31 ECD/EGFr TM-TK from COS-1 cell transfectants. COS-1 cells transiently expressing either full length wild type CD31 of CD31 ECD/EGFr TM-TK were lifted in 2mM EDTA/PBS, washed in PBS, and cell surface proteins were labelled by biotinylation. Cells were lysed in buffer containing 1% Triton-X100 and general purpose protease inhibitor cocktail (Sigma). Lysates were spun to remove debris and were pre-cleared with anti-ICAM-3 mAb KS128 and cleared lysates were immunoprecipitated with either anti-CD31 mAb 9G11 or negative control anti-NCAM mAb ERIC-1. Samples were resolved on 4-20% Tris-glycine gradient gels, blotted onto nitrocellulose, blocked with 5% non-fat milk, and biotinylated proteins detected by streptavidin-HRP and ECL. Wild-type CD31 was immunoprecipitated by 9G11, but not negative control ERIC-1 mAb, and ran as expected at approximately 120kDa. The CD31 ECD/TM-TK chimera was also successful immunoprecipitated with anti-CD31 mAb 9G11, and as expected ran with a higher molecular weight, approximately 180-190kDa, again as expected.

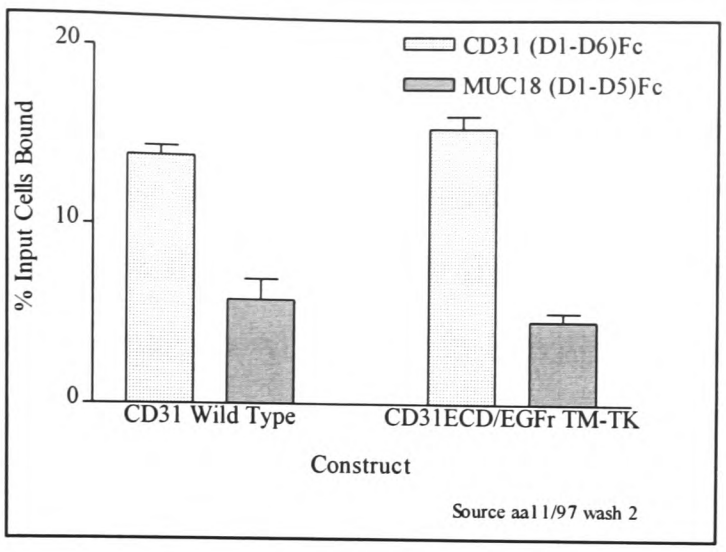


Figure 4.10c. CD31 ECD/EGFr TM-TK supports CD31 homophilic adhesion. Adhesion assays were performed in which COS-1 cells expressing either full length transmembrane CD31 or CD31 ECD/EGFr TM-TK were allowed to adhere to plastic coated with CD31 (D1-D6)Fc protein or negative control protein MUC18 (D1-D5)Fc. Both wild type and chimeric CD31 constructs support similar levels of homophilic adhesion to CD31Fc protein, but the EGFr containing chimera does not cause non-specific adhesion to negative control protein MUC18Fc.

Results from this tyrosine phosphate blots indicate that CD31 is normally tyrosine phosphorylated, which is consistent with the literature (Lu *et al.*, 1996). The CD31 ECD/EGFr TM-TK tyrosine kinase chimera was constitutively activated in COS cells, resulting in heavy autophosphorylation of the chimera, and co-immunoprecipitation of a large number of phosphotyrosine containing proteins. The extent of phosphorylation and pattern of bands observed did not change on exposure to CD31 (D1-D6)Fc relative to MUC18 (D1-D5)Fc, or when in solution, or when the CD31 component was artificially clustered with antibodies. This indicates that the receptor tyrosine kinase is constitutively active. These immunoprecipitation experiments are very preliminary, and are not fully controlled. Unfortunately, since COS cells are of fibroblast origin, and synthesise endogenous EGF, it was not possible to include a full length EGFr control, with and without stimulation by exogenous EGF, since the transfectants would be chronically stimulated in a autocrine fashion. One possibility to overcome this problem would be to use a polyclonal anti-EGF antibody to sequester/neutralise EGF produced by the COS cells, or alternatively the constructs could be expressed in a non-EGF expressing background. Similarly, there are no controls to determine whether the generation of the chimeric construct non-specifically activates the kinase domain. A suitable negative control would be an ICAM-2 ECD/EGFr TM-TK chimera, since ICAM-2 in contrast to ICAM-1 does not form dimers at the cell surface (Miller *et al.*, 1995). With an appropriate set of controls expressed in a EGF non-secreting cell line, it should be possible to rigorously control this experiment. However, given the limitations of the present analysis, it appears that the EGFr chimera is constitutively activated and autophosphorylated, leading to the recruitment and phosphorylation of other cytosolic proteins. This does not seem to be dependent on adhesion to CD31, and is not stimulated by artificially cross-linking CD31 on the cell

surface. Canonically, activation of receptor tyrosine kinases is though to be due to ligand induced-dimerisation, allowing the kinase domains of each receptor in the dimer to mutually autophosphorylate, leading to downstream signalling events. That a chimera between the extracellular domain of CD31 and the transmembrane kinase domain of the epidermal growth factor is constitutively activated, would suggest, and is consistent with the hypothesis that, CD31 exists on the cell surface as a dimer.

4.4 Discussion

The principle findings reported in this chapter may be summarised as follows. First, by a number of different biophysical techniques, including analytical ultracentrifugation and native gel electrophoresis, CD31 (D1-D6)STOP protein has been shown to form self-associating complexes. These have been most rigorously analysed by analytical ultracentrifugation, which demonstrates that the available data is most satisfactorily explained by a monomer-dimer equilibrium with apparent dissociation constant in the range 12-14μM depending upon the method of analysis used. Second, the presence of monomeric and dimeric forms of CD31 (D1-D6)STOP protein in solution was confirmed by chemical cross-linking with a homobifunctional cross-linker (BS_3). Third, mutations in domain 1 which have been shown to ablate homophilic adhesion, do not inhibit the formation of dimers in solution, suggesting that the dimers formed arose through lateral association, rather than NH_2-terminal mediated homophilic contacts. Finally, it is possible to cross-link wild type transmembrane expressed CD31 on the surface of both transiently transfected COS-1 cells or U937 cells which express CD31 to show that a proportion of the CD31 expressed is present as homodimers, but not higher order aggregates or heterodimers. Collectively, the biophysical and biochemical approaches outlined strongly support the hypothesis that CD31 exists in its native form as an equilibrium between monomeric and dimeric forms. This may have functional consequences for CD31 mediated adhesion.

Using a number of different biophysical approaches, it was shown that soluble recombinant CD31 (D1-D6)STOP protein, exists as a self-associating equilibrium between monomers and dimers. The most rigorous analysis was performed on data collected from the analytical ultracentrifuge run in sedimentation equilibrium mode. This has the advantage that because the system is at equilibrium, it can be analysed thermodynamically

to obtain association/dissociation constants, and because the analysis does not depend upon any external standards (unlike gel filtration), it is less likely to generate artifactual results. This is particularly a problem with glycoproteins because the molecular weight standards used to calibrate gel filtration chromatography columns are frequently globular, non-glycosylated proteins, so that the composition or content of carbohydrate on the analyte may significantly affect its behaviour on the gel chromatography media leading to errors in the determination of the apparent molecular weights of glycoproteins in solution (see for example Pennica *et al.*, 1992, and Shire, 1992 for illustration of this effect with recombinant TNF-α receptor). Results from analytical ultracentrifugation show a continuous distribution for both M_{app} and omega with respect to concentration, indicating that the system is at equilibrium, and that it is composed of self associating monomers and higher order oligomers, rather than two independent non-associating proteins of different molecular weights. By fitting the data to a number of different models of self-association by non-linear curve fitting, it was possible to show that the data was best explained by a monomer-dimer equilibrium. By two methods of analysis the dissociation constant was estimated to lie in the range 12-14μM. This is not a particularly high affinity interaction, as compared to the actual adhesive interactions mediated by adhesion molecules (the dissociation constant of dimeric ICAM-1 for LFA-1 has been estimated to be 8.0nM (Miller *et al.*, 1995), whilst the dissociation constant for the interaction of OX40 and OX40 ligand has been shown to be in the range 0.2-0.4nM (Al-Shamkhani *et al.*, 1997)). Nevertheless, this level of affinity is sufficient that at 1mg/ml around 50% of the total protein would be expected to be in the form of dimers (inspection of silver stained gels from chemical cross-linking suggests that this is something of an overestimate, although cross-linking may not efficiently trap all of the available dimers). This level of affinity is also comparable to that seen amongst other self-associating proteins, such as spectrin (Ralston *et al.*, 1996). It is also important to note that the affinity measurements are based upon association free in solution, rather than constrained within the membrane. When expressed as a membrane bound form, the tendency to form dimers is likely to be considerably greater than estimated by solution studies.

Self-association to form dimers was also supported by evidence from chemical-cross linking studies on the CD31 (D1-D6)STOP protein. In principle, the dimers observed could form through homophilic, head-to-head interactions, or through lateral interactions

analogous to those observed in cadherin crystal structures (Shapiro *et al.*, 1995; Nagar *et al.*, 1996). Several lines of evidence suggest that the later explanation is the case, first dimers of CD31 (D1-D6)STOP protein were detected even in proteins carrying mutations known to block homophilic adhesion in cell-protein assays (Figure 4.9). Second, cross-linking of CD31 expressed transiently on COS-1 cells, or on the cell line U937, identifies at least a proportion of the available CD31 in the form of homodimers, but not heterodimers or higher order aggregates. Since these assays were performed under conditions which do not favour cell adhesion (4°C, whilst rotating end-on-end), these dimers are unlikely to represent homophilic contacts. Finally, in preliminary experiments using an CD31/EGF receptor chimera, in which the cytoplasmic domain of CD31 was swapped with the tyrosine kinase domain of the EGF receptor, the cytoplasmic tail of the chimera was found to be constitutively tyrosine phosphorylated, and anti-CD31 mAb 9G11 was found to co-immunoprecipitate a large number of phosphotyrosine containing proteins. Canonically ligand induced dimerisation is thought to result in mutual autophosphorylation of the kinase domains in dimeric or oligomeric receptor tyrosine kinases. That a CD31/EGFr chimera appears to be constitutively activated is consistent with the hypothesis that CD31 is present as laterally associated dimers on the cell surface.

One of the major reasons for suspecting that CD31 might exist as a dimer was the observation that the residues on the ABDE face of CD31 which block homophilic adhesion (D11A and D33A) lie in structurally similar positions to the residues mediating lateral association in the cadherin crystal structures (Shapiro *et al.*, 1995, Nagar *et al.*, 1996). If this were the case then one would predict that mutation of these residues, if required for dimerisation, would prevent the formation of dimers whilst the mutations on the predicted CFG "adhesion" face (D51R and K89A) would not have such an effect. Preliminary results from such a cross-linking experiment show that none of the mutations which block homophilic adhesion have an effect on dimerisation (data not shown). This does not rule out the possibility that these residues are involved in part in mediating lateral association. Since the whole extracellular domain is necessary for homophilic adhesion (see Chapter 3), even though the binding site resides within domains 1 and 2, it may be that lateral contacts are distributed along the entire length of the extracellular domain. Mutations which affect the NH_2-teminal domain 1 lateral contacts might result in slight changes in the relative orientation of the binding domain, blocking homophilic adhesion, without necessarily

disrupting the dimer. This later possibility will probably require the structure to be solved at atomic resolution before progress is made definitively distinguishing between these possibilities. In the meantime, one further possibility is to use the analytical ultracentrifuge and sedimentation equilibrium experiments on each mutant protein. Since the method relies on the system coming to thermodynamic equilibrium, changes in temperature will also affect the position of equilibrium. By determining the change in association constants with temperature, for both wild type and mutant proteins, it may be possible to determine the stability of the interaction between protomers in the dimer, and if any of the mutations which block homophilic adhesion have an effect on dimerisation. If the residues involved in homophilic adhesion are not involved in mediating dimerisation, then the obvious candidate regions are the membrane proximal domains. This fits with the findings of others working with different members of the immunoglobulin superfamily, for human CD4 dimerisation is mediated by contacts in membrane proximal domain 4 (Wu *et al.*, 1997), homodimerisation of *c-kit* occurs via domain 4 (Blechman *et al.*, 1995), whilst dimerisation of ICAM-1 appears to involve domains 3 to 5, and possibly the transmembrane segment (Miller *et al.*, 1995). Since CD31 dimers can be trapped by chemical-cross linking on the surface of COS-1 cells, the domains responsible for mediating dimerisation could be investigated using the ICAM-3/CD31TM transmembrane expressed chimeric constructs generated in the previous chapter, assuming that ICAM-3 itself does not form dimers at the cell surface. To date there is no literature describing the native structure of ICAM-3 as being a dimer, and initial attempts at cross-linking of ICAM-3 transfected COS cells failed to show dimers, although I have not been able to repeat the cross-linking results reported by Miller *et al.*, 1995 and Reilly *et al.*, 1995 showing that ICAM-1 forms dimers (data not shown).

The functional significance of the ability of CD31 to dimerise has not been addressed in the present study, however a number of possibilities are immediately obvious. Firstly it may function to increase avidity of CD31 mediated interactions as has already been demonstrated for dimeric ICAM-1 (Miller *et al.*, 1995). By clustering multiple low affinity homophilic binding sites, for example, this might increase the avidity of homophilic interactions and lead to the formation of supramolecular assemblies of interacting dimers as has been postulated for cadherins in cell-cell junctions (Shapiro et al., 1995). Since the affinity of the interaction is relatively weak, monomers and dimers are likely to exist as a

dynamic equilibrium on the surface of cells, so that by changing the overall distribution of CD31, cells may be able to quite quickly change the strength of CD31 mediated adhesion. In this respect it is interesting to note that cells appear to be capable of regulating the localisation of CD31, for example in endothelial cells, CD31 is normally sequestered at the junctions between endothelial cells, and seems to play an important role in maintaining the integrity of endothelial monolayers (Fawcett *et al.*, 1995, Albelda *et al,*. 1991). However cytokine treatment of endothelial monolayers (with TNF-α and interferon γ) results in a redistribution of CD31 to the apical surface of the cells, and appears to be linked with changes in cytoskeletal association (Romer *et al.*, 1995). The recent finding that a fraction of CD31 appears to be associated with catenins (Matsumura *et al.*, 1997) suggests that CD31 homophilic contacts in the cell-cell junctions of endothelial cells may be subject to regulated assembly/disassembly as has been shown for cadherins (Dejana, 1996). Correct sub-cellular localisation appears to be important in the functional regulation of a large number of adhesion molecules, for example ICAM-2 clustering into uropods mediated by ezrin and cytoskeletal associations has been shown to be required for NK cell mediated cytotoxicity (Helander *et al.*, 1996), the distribution of PSGL-1 regulated by cytoskeletal association has been shown to determine the avidity of neutrophils for P-selectin (Lorant *et al.*, 1995), whilst the group of Sanchez-Madrid have shown that ICAM-1 and ICAM-3 are localised to uropod structures upon T-cell activation by chemokines such as RANTES, MCP-1, MIP-1α/β and IL-8, and that this allows CD45R0(+) peripheral blood memory T-cells to recruit bystander T-cells in an LFA-1 dependent interaction (Delpozo *et al.*, 1995; Delpozo *et al.*, 1997).

The function of dimerisation may be more central then simple changes in avidity, in that dimerisation may be necessary for CD31 to function as an adhesion molecule. As has been noted, the homophilic contact site is contained within the two NH_2-terminal domains of CD31, but these two domains are not capable of supporting homophilic adhesion when expressed either as a CD31 (D1-D2)Fc protein or even on an irrelevant ICAM-3 stalk as CD31 (D1-D2)/ICAM-3 (D2-D5)Fc in our standard adhesion assay. Since the Fc proteins are coated onto plastic at normalised levels via goat anti-human Fc antibodies, provided Fc proteins are added in saturating amounts, then density of the presented homophilic binding domains ought to be the same for both CD31 (D1-D2)Fc, CD31 (D1-D2)/ICAM-3(D2-D5)Fc and CD31 (D1-D6)Fc proteins, yet of these three constructs only CD31 (D1-D6)Fc

supports homophilic adhesion. This would argue that the function of dimerisation is more significant than mere clustering, and dimerisation may result in conformational changes which are necessary to position the binding domains in the correct orientation. The antibodies identified in the previous chapter which enhance homophilic adhesion may induce conformational changes which mimic those induced by dimerisation. A further corollary to this hypothesis is that dimerisation may also inhibit non-homophilic modes of CD31 mediated adhesion. A variety of non-CD31 heterophilic ligands have been proposed for CD31, of which the best characterised are glycosaminoglycan-decorated ligands (DeLisser *et al.*, 1994), and the integrin αvβ3 (Piali *et al.*, 1995, Buckley *et al.*, 1996, see also Chapter 6). Significantly, both of these interactions have been shown to be mediated by regions distinct from the homophilic binding site, in the case of GAG ligands to a region in domain 2, and for the αvβ3 interaction to involve domain 3 of CD31. It may be that dimerisation whilst promoting homophilic adhesion, simultaneously blocks heterophilic adhesion by obscuring the heterophilic binding site in the dimer interface. This might explain the results of Sun *et al.*, 1996 who showed that HUVECs, which express high levels of both CD31 and integrin αvβ3 can be stained with CD31 (D1-D6)Fc protein used as a surrogate antibody. Staining with their Fc protein was inhibited by anti-CD31 antibodies, but unaffected by treatment with LM609, a functional blocking antibody directed against αvβ3. From this they concluded that αvβ3 was not a ligand for CD31. An alternative explanation might be the dimerisation in the full length CD31 blocked the heterophilic binding site.

In summary, a range of biophysical, biochemical and molecular biology techniques have been used to show that CD31 exists as an equilibrium between monomeric and dimeric forms when expressed either as a soluble recombinant protein, or when expressed on the surface of cells.

Chapter Five: Structural Studies on CD31

5.1 Introduction.

Detailed knowledge of the structures of biological macromolecules has revolutionised our understanding of how biological processes occur, and have suggested further avenues of experimental work. Even for molecules which have been studied in detail for several years, atomic resolution structures can lead to significant new insights, for example the recently solved structure for ICAM-2 showed that the critical glutamate identified by site directed mutagenesis as mediating adhesion to LFA-1 was located in a flat region of the C-strand rather than exposed on the CD-loop as had been inferred from comparisons to VCAM-1 (Casanovas *et al.*, 1997). Similarly, the crystal structure of the complete src-kinase protein revealed a potentially novel regulatory interaction, which was subsequently shown to be physiologically significant (Sicheri *et al.*, 1997; Moarefi *et al.*, 1997). The results described in the proceeding two chapters have given some insights into how CD31 homophilic adhesion occurs, and how the process might be regulated in terms of dimerisation. However, many of the questions raised, such as the nature of the interaction between individual CD31 molecules in dimers are difficult to assess with molecular and cell biology techniques. In principle one could undertake a systematic mutagenesis approach to identify the residues/regions involved in dimerisation, however this would require an enormous commitment of resources. A detailed structure at atomic resolution would provide a start point to make detailed predictions about the underlying interactions, which could then be tested experimentally.

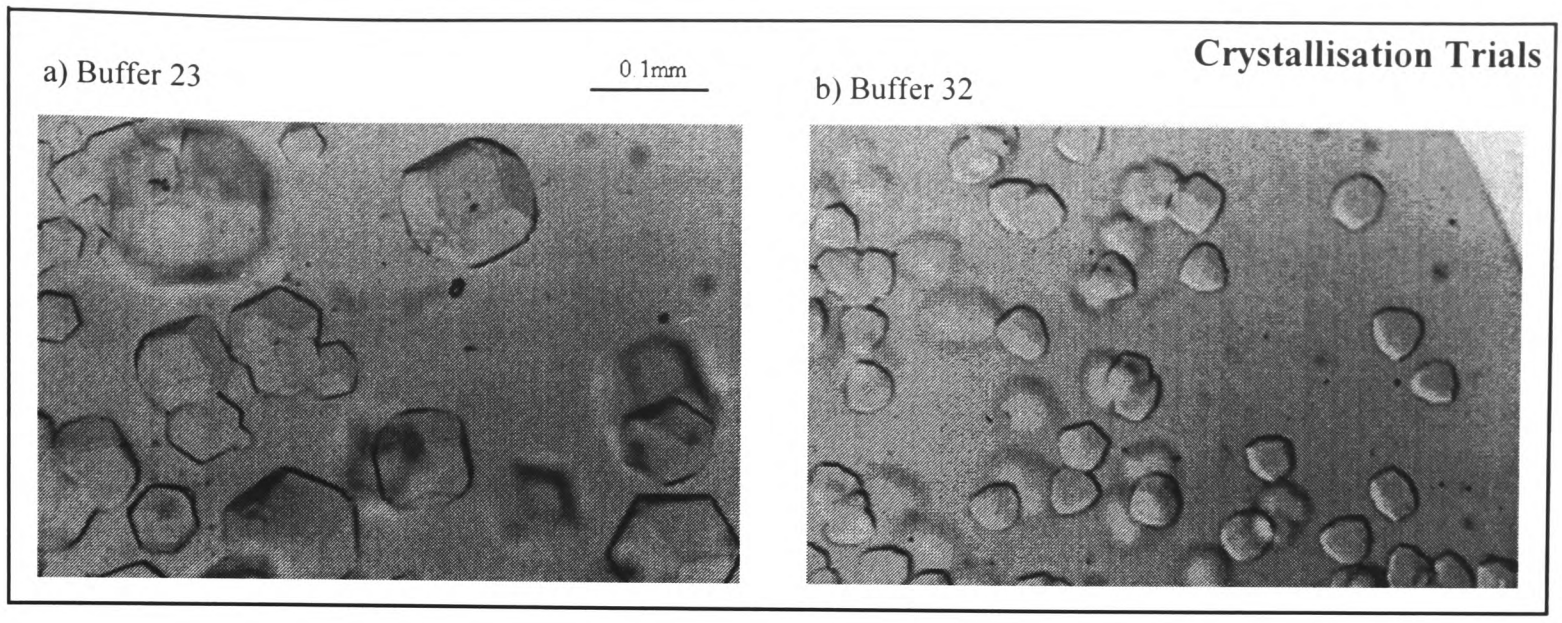
5.2 Results

5.2.1. Crystallisation trials with CD31 (D1-D6)STOP protein.

The results of hydrodynamic and biochemical analyses of CD31 (D1-D6)STOP protein in the forgoing chapter indicated that CD31 exists as an equilibrium between monomeric and dimeric forms. Since there is already a tendency to self-associate, it was hoped that this might predispose CD31 protein to form regular arrays of material during crystallisation trials, moreover lateral association may reduce the overall flexibility of the molecule, which would also favour crystallisation. The CD31 (D1-D6)STOP protein produced in CHO cells is fully glycosylated, and the MALDI mass-spectra peak shows that the molecular weight,

and hence the degree/type of glycosylation, is rather heterogeneous. Canonically, any sort of heterogeneity/glycosylation is thought to inhibit the process of forming ordered crystals, nevertheless there have been several major successes in crystallising glycosylated proteins, some of which have actually depended upon the presence of oligosaccharides to form stable crystals. For example the crystal structure of the murine T-cell receptor TCR C2 ($V_\alpha 3J_\alpha 58C_\alpha$;$V_\beta 8.2D_\beta 2J_\beta 2.4C_\beta 2$) and MHC class I co-complex was obtained from fully glycosylated TCR C2 material produced in *Drosophila melanogaster* cells. In the crystal structure, the interface between the Cα and Cβ subunits is stabilised by an ordered oligosaccharide (Garcia *et al.*, 1996).

For initial crystallisation trials, 2mg of CD31 (D1-D6)STOP protein was dialysed into 20mM Tris.HCl, pH8.0, and concentrated to approximately 10mg/ml using a Centricon-30 concentrator (Amicon). Concentrated protein samples were used to set up hanging drop crystallisation trials using the Crystal Scan I and II kits from Hampton Research according to manufacturers instructions (collaboration with Dr. Karl Harlos and Dr. Yvonne Jones, Laboratory of Molecular Biophysics, Oxford University). Crystals were observed after approximately 150 hours in two of the 96 conditions tested (figure 5.1a and b). Small crystals were observed when grown from buffer 32 (1.6M ammonium sulphate, 0.1M HEPES, pH7.5, 0.1M sodium chloride), whilst larger (up to 100μm in diameter) more regular crystals were grown from buffer 23 (1.6M ammonium sulphate, 10% dioxane, 0.1M MES, pH6.5). In order to confirm that the crystals were of CD31 protein, and not inorganic salts, a small sample of the crystal containing liquor (from buffer 23) was spun to pellet the crystals, these were re- dissolved in water, and run out on 7.5% reducing SDS-PAGE gels. Samples were blotted onto nitrocellulose and detected by Western blotting using CAL31.1 at 2μg/ml, and 1:10 dilution of JC70/A (gift, Dr. Kevin Gatter, John Radcliffe Hospital, Oxford University) as primary antibodies, and goat anti-mouse HRP as secondary reagent. Bound secondary antibodies were detected by ECL (Amersham International), according to manufacturers instructions (Figure 5.1c).



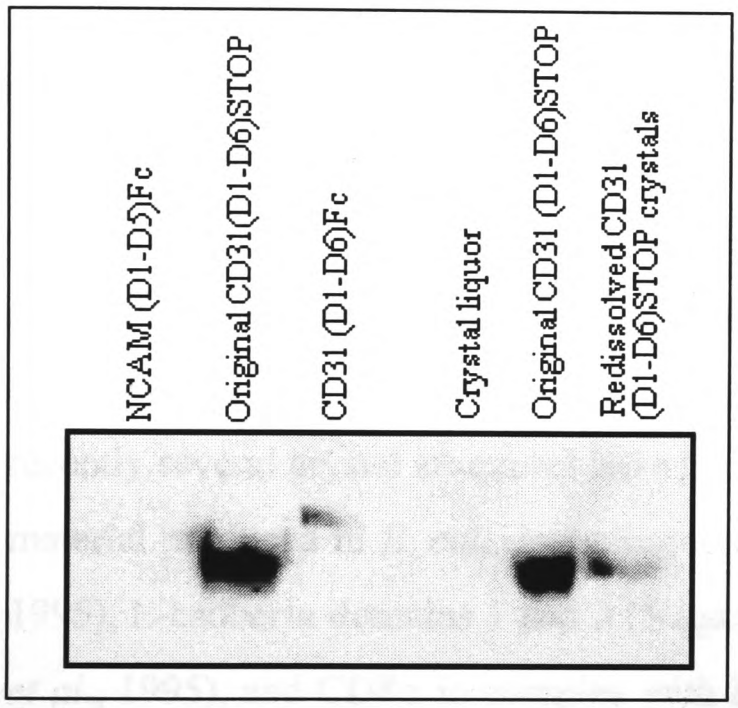


Figure 5.1 Crystallisation trials with CD31 (D1-D6)STOP protein. Soluble recombinant CD31 (D1-D6)STOP protein at a concentration of 10mg/ml was used to set up crystallisation trials using the Hampton Research Crystal Scan I and II kit. After approximately 150 hours crystals were observed under 2 of the 96 conditions tested (see panels a and b above). Crystals grown under buffer 23 conditions were re-dissolved in water, and analysed by Western blotting. The crystals were found to contain CD31 (D1-D6)STOP protein, and it was also shown that the crystal liquor was depleted of CD31 (D1-D6)STOP protein.

Western blotting showed that the crystals were of CD31 (D1-D6)STOP protein, rather than inorganic salts, and that the process of crystallisation depleted the crystal liquor of protein.

Unfortunately, the crystals failed to diffract X-rays under a variety of different conditions (Dr. Yvonne Jones, personal communication). As noted previously, heterogeneity is a major determinant in the quality of crystals, and their ability to diffract. Since the CD31 (D1-D6)STOP protein is fully glycosylated, this is likely to be the major source of heterogeneity in the sample. In order to produce a homogeneous sample, CD31 (D1-D6)STOP protein was treated with a combination of endoglycosidase F and endoglycosidase H (Boehringer Mannheim) to remove the oligosaccharide component. This treatment proved unsuccessful however, inducing the protein to precipitate from solution over a period of 48-72 hours. This finding was repeated by our collaborators at the Yamanouchi Research Institute (Joanne Saunders and Dr. Ian Bird), using CD31 (D1-

D6)STOP protein produced in CHO LecR cells. These cells are defective in the synthesis of sialic acid, translocation of CMP-sialic acid and of UDP-galactose into the Golgi, and in N-acetylglucosamine transisomerase. Hence proteins synthesised by these cells are uniformly N-glycosylated with minimal high-mannose type oligosaccharides and most O-linked carbohydrates are present as single N-acetylgalactosamine residues (Stanley, 1989). This approach has previously been used to generate material which crystallised and diffracted for fragments of CD2 (Davies *et al.*, 1993). CD31 (D1-D6)STOP protein produced in CHO LecR cells also crystallised quite readily, but again failed to diffract, and upon enzymatic removal of the oligosaccharide with endoglycosidase H, also precipitated.

5.2.2. Bacterial expression of CD31 fragments.

Since attempts to produce crystals which diffracted from the full length glycosylated CD31 (D1-D6)STOP protein produced in mammalian cells met with only limited success, other alternatives were explored. A large number of structures of different MHC class I proteins have been generated from crystals grown from material produced in bacteria, and more recently several crystal structures have been obtained for adhesion molecule domains using material produced in *E. coli,* including structures for N-cadherin domain 1 (Shapiro *et al.*, 1995), E-cadherin domains 1 and 2 (Nagar *et al.*, 1996), VCAM-1 domains 1 and 2 (Jones *et al.*, 1995), and CD8α in complex with MHC class I (Gao *et al.*, 1997). Since the CD31 homophilic binding site has been mapped to domains 1 and 2, it was feasible to produce fragments of CD31 which would still be of functional interest. In addition material produced in bacteria is not glycosylated, so that the removal of sugars will not be required. Evidence from the fully glycosylated material suggests that removal of sugars reduces the stability of the protein leading to aggregation and precipitation. In order to overcome this problem, a vector was selected in which the CD31 fragments would be produced as a fusion with a cytosolic bacterial protein. It was hope that this would increase the stability and solubility of bacterially produced recombinant proteins, whilst also providing a convenient purification tag. The vector selected was the PinPoint Xa-1 T-vector cloning system (Promega). This is an inducible vector which carries a segment encoding a peptide that becomes biotinylated in *E.coli* and subsequently functions as a purification tag for isolation with monomeric avidin resins, which allow for the elution of the protein under non-denaturing conditions. The vector also includes the preferred cleavage sequence for

Endoproteinase Factor Xa at the carboxyl terminus of the biotinylated region, providing a way to separate the purification tag from the native protein. Finally, the vector is supplied with single base T-overhangs allowing for the rapid and convenient cloning of PCR products provided that care is taken to design the primers to maintain the reading frame between the NH_2-terminal biotinylated tag and the CD31 protein following the addition of single non-template dependent adenosine residues by *Taq* DNA polymerase to CD31 fragments. Fusion proteins corresponding to CD31 domain 1 and domains 1 and 2 were produced by PCR amplification from the full length template in pCDM8 (Simmons *et al.*, 1990) using *Pwo* DNA polymerase and ten cycles of amplification with a common forward amplification primer beginning at the start of the mature protein (`5' A CAA GAA AAC TCT TTC ACA 3'`) and sequence specific reverse amplification primers at the ends of domains 1 and 2 respectively (domain 1: `5' GATC TCTAGA TCA GGG CAC TCC TTC CAC CAA 3'`; domain 2: `5' GATC TCTAGA TCA AGA GAA GGA TTC CGT CAC 3'`). PCR products produced with *Pwo* do not have A residues added in a non-template dependent fashion, so that the resultant PCR product was precipitated and A residues added with Taq polymerase, as described in methods and materials. PCR product was ligated into PinPoint Xa-1 T-vector and transformed into E.coli XL1-Blue. Positive colonies were selected on ampicillin plates, and screened for the presence of the desired insert by restriction digests with *Hind*III and *Bgl*II (restriction sites flanking the insertion point). Colonies with inserts were directly sequenced from miniprep DNA by fluorescent dye sequencing (ABI Prism) according to manufacturers instructions. The selected plasmids were found to contain the expected inserts and sequenced in their entirety to ensure that no adventitious PCR induced mutations were present, and that the insert was in the correct reading frame for expression.

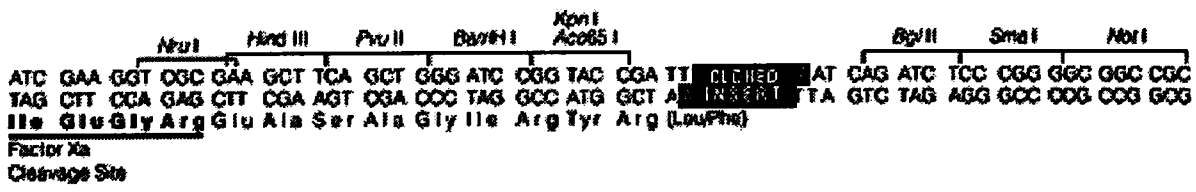


Figure 5.2: Reading frame across the multiple cloning region of the PinPoint Xa-1 T-vector. The amino acids in bold represent the Endoproteinase Factor Xa cleavage site. Direct amplification of the region of interest and cloning into the vector via the TA overhangs will produce a protein which is out of frame. An additional residue at the 5' end of the forward amplification primer is required to generate an inframe fusion, consequently an extra A residue was added to the complementary coding sequence of the forward amplification primer to give an additional leucine residue, prior to the CD31 specific sequence (Gln-Glu-Asn-Ser....etc).

Small scale induction experiments were performed to test for expression of protein. Fresh colonies were picked from LB agar plates supplemented with 100μg/ml ampicillin, and grown overnight at 37°C in 2.5ml LB medium containing 100μg/ml ampicillin. Overnight cultures were diluted 1:100 into 5ml LB broth containing ampicillin and 2μM biotin, and grown for 1hour with shaking. Expression was induced by the addition of 100μM IPTG (isopropyl beta-D-thiogalactopyranoside), and cultures were grown for a further 4-6 hours at 37°C. To determine the level of induction 100μl samples of the bacterial culture were spun down (1 minute at 14,000g) and resuspended in 50μl of reducing sample buffer. Bacteria were lysed by heating to 95°C for 5 minutes, and 5μl of lysate were resolved on 12% SDS-PAGE gels. Proteins were blotted onto nitrocellulose, and the membrane blocked TBS containing 1% non fat dried milk. The blot was washed with TBS containing 0.05% Tween-20, and biotinylated proteins detected with streptavidin directly conjugated to horse-radish peroxidase (Amersham International) diluted 1:1000 in TBS containing 0.05% Tween-20. Blots were washed and bound peroxidase visualised by ECL (Amersham International) according to manufacturers instructions (Figure 5.3). As expected the bacteria containing PinPoint Xa-1 plasmids produce specific band of the expected molecular weights on induction with IPTG, in addition to the major non-induced band at around 22kDa, corresponding to the biotinylated carboxyl carrier protein (BCCP).

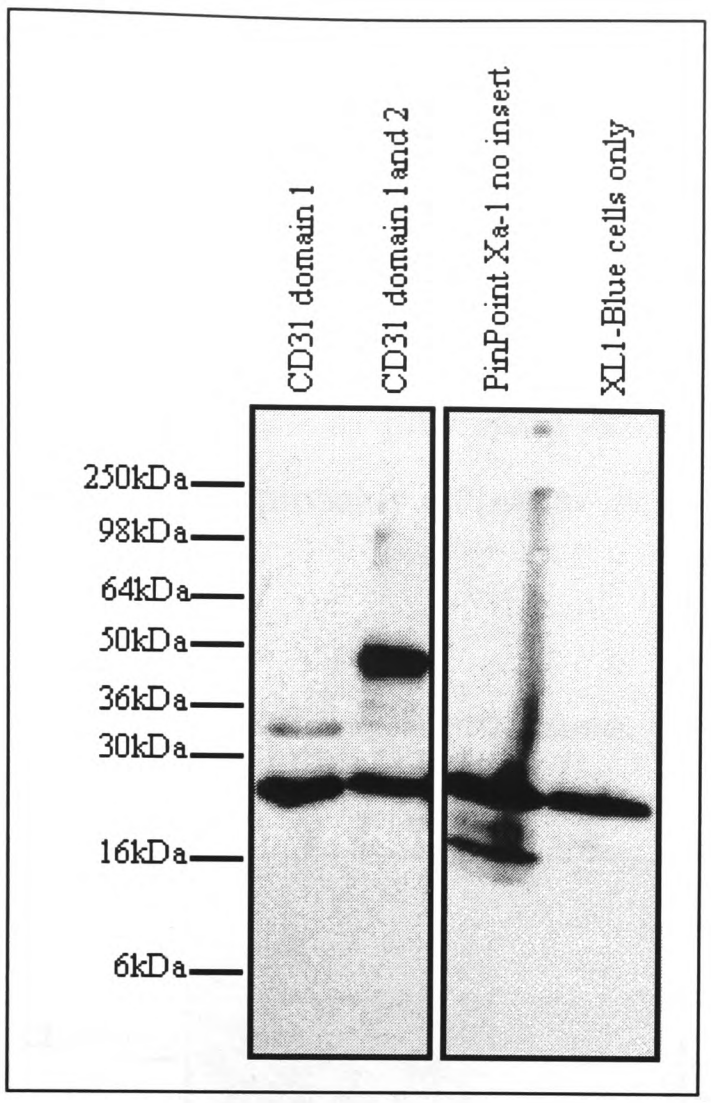


Figure 5.3 Induction of CD31 fusion proteins expressed in bacteria. *E.coli* XL1-blue cells transformed with PinPoint Xa-1 expression vector containing CD31 domain 1 and domains 1 and 2, were cultured and induced as described in the text. Bacteria were lysed and total proteins resolved by SDS-PAGE, and biotinylated proteins detected by Western blotting with Streptavidin.HRP. A common band at around 22kDa is visible in all samples corresponding to the major biotinylated species in E.coli, the biotinylated carboxyl carrier protein (BCCP), including the host cells. Induction of the PinPoint Xa-1 vector alone with no insert present gives a 14kDa band, also as expected, corresponding to the fusion tag alone. Finally CD31 domain 1 and CD31 domains 1 and 2 give additional bands at 32kDa and 45kDa. These are of the expected size for these constructs, allowing for the 14kDa fusion protein tag.

Western blotting is an extremely sensitive technique, and the actual amount of protein produced on induction will help to determine the subsequent purification protocol. In order to examine the amount of protein produced relative to endogenous *E.coli* proteins, and to determine the optimum time to harvest the protein, the small scale induction experiment described above was repeated for the CD31 Domains 1 and 2 construct except that samples were taken every hour, and gels were Coomassie Blue stained to examine total cellular protein content (Figure 5.4). As can been seen protein corresponding to CD31 domains 1 and 2 was clearly visible 3 hours post IPTG induction, showing that the protein was being produced in large amounts, without an obvious toxic effect upon the cells. Therefore large scale induction experiments were performed, essentially as described above, but scaling up to 1L bacterial cultures. Cells were harvested after 4 hours, spun down at 4,000 rpm in a Beckman J6 rotor, resuspended in lysis buffer (50mM Tris, pH7.5, 150mM NaCl, 5% glycerol, plus broad spectrum protease inhibitor cocktail (Sigma)) at a concentration of 10ml/g cell paste (assuming 4-5g cells/L culture) and cells lysed by sonication for 2 minutes, with alternating 15 second burst from the sonicator. The cell lysate was centrifuged at 10,000g for 30 minutes to pellet cellular debris, and the lysate affinity purified by applying to a column comprised of monomeric avidin coupled to a solid matrix

support (SoftLINK resin, Promega). The column was washed with 20mM Tris, pH7.5, and bound protein eluted with 20mM Tris, pH7.5 containing 5mM free biotin. This highly effectively purified cellular proteins containing biotin (aminotransferases, BCCP etc.), but failed to purify the CD31 fusion proteins except in trace amounts (data not shown). Resuspending the insoluble cellular debris in 1% SDS and western blotting with streptavidin HRP as previously described, revealed that the CD31 fusion proteins were insoluble, and probably present as inclusion bodies (data not shown).

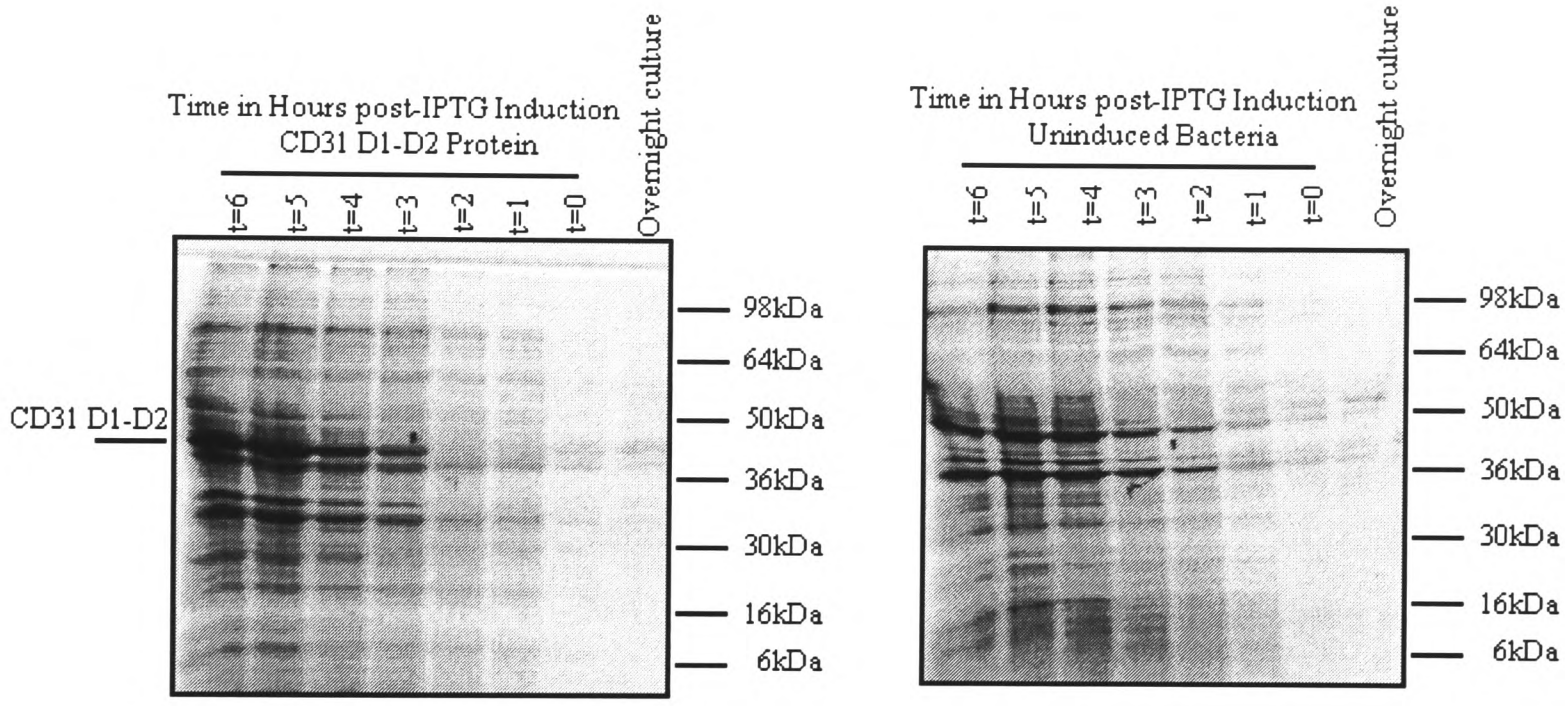


Figure 5.4 Induction of CD31 D1-D2 fusion protein in *E.coli* following treatment with IPTG. Small scale induction experiments were performed as previously described, except that samples were taken every hour post induction with IPTG, run on 12% gels and stained with Coomassie Blue. A specific band, not observed in uninduced bacteria transformed with the same plasmid, corresponding to CD31 domains 1 and 2 was visible approximately 3 hours post-induction, indicating that the protein was being expressed at high levels and with comparatively little ill effect upon the bacterial cells.

The formation of inclusion bodies is a common problem encountered when expressing heterologous proteins to high levels in bacteria. Attempts to slow the rate of protein production, thereby increasing solubility, by lowering the growth temperature, or inducing later, whilst cells were in late exponential growth phase did not significantly improve the yield of soluble material (data not shown). It is also possible to refold proteins from inclusion bodies, however it can be difficult to establish a suitable protocol on any rational basis, and this usually requires trial and error. Protocols are well established for refolding bacterially produced MHC class I proteins, and recently an IgSF family member, CD8α, has also been refolded from inclusion bodies using a modification of the protocol

developed for MHC class I proteins (Gao *et al.*, 1997). It was therefore decided to attempt to refold the CD31 fusion proteins from inclusion bodies following this modified protocol.

Briefly, 1L bacterial cultures were set and induced as before. Cells were harvested and resuspended in 10ml lysis buffer (10mM Tris.HCl, pH8.0, 150mM NaCl, 10% glycerol, 10mM EDTA pH8.0, 10mM DTT, 0.5mM PMSF and 400μg/ml lysozyme). DNAse I at 20μg/ml lysate and 10mM $MgCl_2$ (final concentration) were added, and cells were left on ice for 20 minutes. Samples were sonicated for 5 minutes in 15 second pulses, and 10ml Triton wash buffer added (50mM Tris.HCl pH8.0, 100mM NaCl, 0.5% Triton X-100, 10mM EDTA, 10mM DTT, 0.1% azide), and left on ice for a further 30 minutes. The bacterial slurry was centrifuged at 15,000 rpm in a Beckman JA20 rotor at 4°C for 20 minutes, the supernatant discarded, and the pellet washed three times with the Triton wash buffer. The pellet was washed once more in wash buffer omitting Triton X-100 and azide, and then resuspended in 10ml of a resolubilising Urea buffer (20mM Tris.HCl pH8.0, 8M urea, 10% glycerol, 500mM NaCl, 10mM EDTA, 10mM DTT). This urea suspension was left turning end-on-end overnight, centrifuged at 15,000rpm in a Beckman JA-20 rotor, and the solubilised protein stored at -20°C until refolding. This generated 30-40mg of protein per litre of bacterial culture. Running 5μg of total protein on a 4-20% Tris glycine gel showed that bands of the expected molecular weight were present and that these constituted the major proteins present (Figure 5.6). In order to refold the protein, 10mg of the protein in the Urea buffer were mixed with 15ml of 6M guanidine buffer (6M guanidine hydrochloride, 50mM Tris pH8.0, 100mM NaCl, 10mM EDTA, 10mM DTT) and left at room temperature before injecting into 1 litre of cold (4°C) refolding buffer (200mM Tris, pH8.0, 1M L-arginine hydrochloride, 10mM EDTA, 0.1mM PMSF, 6.5mM cysteamine, 3.7mM cystamine). This process was repeated over two or three days until the entire protein sample was refolded. After 72 hours of protein refolding, a white precipitate was visible in the refolding buffer, suggesting that the procedure had not been successful. The insoluble material was filtered out, and the filtrate subject to affinity purification with SoftLINK monomeric avidin resin. This failed to recover any material, indicating that the refolding protocol had not been successful, and that the CD31 fusion proteins had pre-precipitated once the denaturant was removed.

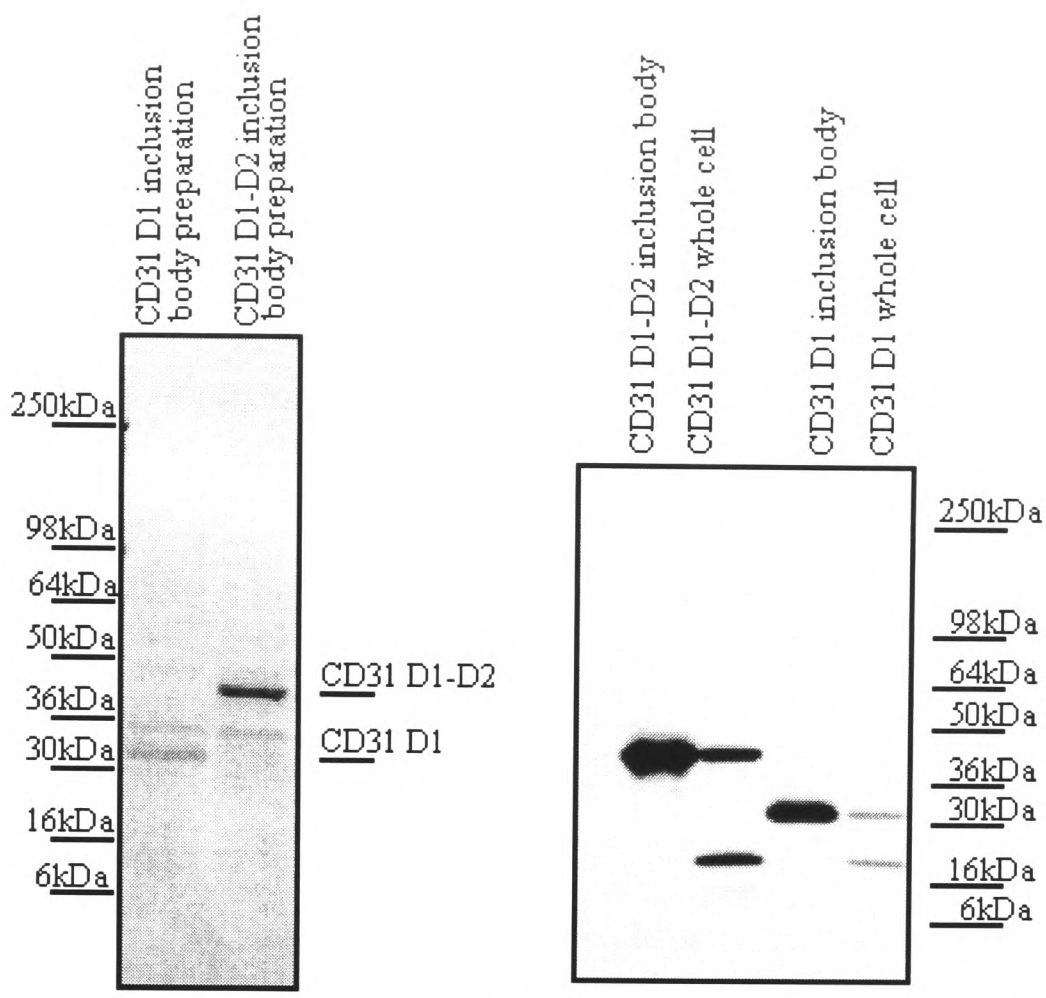


Figure 5.5 CD31 fusion proteins: Inclusion body preparation. Solubilised inclusion body proteins were resolved on 4-20% SDS PAGE Tris-glycine gradient gels and either stained with Coomassie Blue stain (left), or probed by Western blotting (right). The inclusion bodies contain biotin tagged proteins corresponding to CD31 D1 and CD31 D1-D2, and these are the major protein species present in the inclusion body.

5.3 Discussion

In order to obtain atomic resolution structures, two different techniques may be employed, NMR (nuclear magnetic resonance) or X-ray diffraction. NMR can be used to study macromolecules in solution, but is limited in terms of the size of proteins that can be analysed. As proteins become larger, peak broadening of the NMR spectra occurs due to slower tumbling in solution, and it is impossible to resolve the individual peaks required to determine the structure. The upper limit on the size of the structures which can be solved by NMR is around 20kDa (i.e. around one immunoglobulin-like fold), so that CD31 is too large to be studied by NMR without studying isolated individual domains (as has been done for fibronectin, for review see Campbell *et al.*, 1994). X-ray diffraction has the advantage that provided ordered crystals can be grown there is no size limit on the macromolecule that can be studied. For example, the structures of whole virus particles have been solved by X-ray crystallography. More importantly when constrained in a crystalline lattice, many molecules undergo interactions which are thought to be analogous to their *in vivo* interactions, for example in the CD2 structure, the individual CD2 monomers form head-to-head dimers which mimic the contacts between CD2 and CD48

inferred from site directed mutagenesis studies (Bodian *et al.*, 1994, Van der Merwe *et al.*, 1995). For these reasons it was decided to pursue a crystallographic approach. Initial attempts at crystallising CD31 (D1-D6)STOP protein were extremely encouraging, the protein rapidly formed crystals which were of a reasonable size, but unfortunately did not diffract. Attempts to improve the crystal order by removing the oligosaccharides by enzymatic treatment were not successful, resulting in large scale protein precipitation. This result has been mirrored by others using minimally glycosylated material produced in LecR CHO cells. This may indicate that the oligosaccharides play a role in maintaining the overall folding and stability of the protein in solution. A number of approaches are open to try and obtain diffraction patterns from these crystals, firstly the diffraction experiments were performed at room temperature, one common technique is to flash freeze crystals in liquid nitrogen, lowering the temperature to 100K, since this reduces the thermal energy leading to closer packing/increased order, and also reduces damage to the crystal caused by the X-rays. A second, related approach, is to slowly dehydrate the crystals by soaking them in gradually increasing concentrations of an organic solvent such as glycerol or polyethylene glycol (PEG). The removal of water is though to impose greater crystal order and improve diffraction This later approach has been used extremely successfully to obtain diffraction patterns and hence solve the structure to atomic resolution of HIV reverse transcriptase (Steitz *et al.*, 1992).

Due to the difficulties encountered with protein produced in mammalian cells, a second approach was also investigated using bacterially produced fragments of CD31 encompassing domains 1 and 2, which have been shown to contain the homophilic binding site (Chapter 3). Since removal of oligosaccharide from CD31 (D1-D6)STOP protein appeared to cause the protein to precipitate, a vector was chosen that incorporated a purification tag encoding a bacterial cytosolic protein. This was hoped to enhance the solubility of the fusion protein containing CD31. Bacterial expression of CD31 recombinant fusion proteins produced large amount of material (typically 30-40 mg/L of culture), however this was insoluble and formed inclusion bodies, from which it was not possible to recover soluble protein using a refolding protocol previously developed for CD8α, another member of the immunoglobulin superfamily. Further work modifying this protocol may lead to recovery of enough material to perform crystallisation trials, although

refolding of proteins is recognised as being an art form as much as a science, with few empirical rules. An alternative route may be to employ a different vector which either targets the protein to the periplasm or to the extracellular space so avoiding the tendency of cytosolic proteins to aggregate. This approach was employed for VCAM (Bottomley *et al.*, 1994), where the protein was produced as a fusion with the OmpR leader peptide (OmpR is a bacterial protein expressed in the outer membrane involved in osmoregulation).

In summary, CD31 recombinant proteins show an encouraging tendency to form crystals, which should allow detailed atomic resolution structural information to be obtained, provided existing technical problems can be overcome.

Chapter Six: Identification and Characterisation of Heterophilic Ligands for CD31

6.1 Introduction

Previous work to characterise the CD31 homophilic binding site (see Chapter 3) made extensive use of heterologous COS-1 cell transfectants. This system has many advantages, particularly that it is well controlled, allowing for the use of appropriate negative controls and sham transfectants. Moreover, this system also recapitulates many of the properties of more physiological models of CD31 homophilic adhesion seen in cell lines and primary isolates, for example the ability to upregulate β1 integrin mediated adhesion following CD31 homophilic engagement (Tanaka *et al.*, 1992, Fawcett *et al.*, 1995). In order to verify previous findings derived from heterologous COS-1 cell CD31 homophilic assays, it was decided to explore the binding modes of CD31 expressed on haematopoietic cells. In addition to a homophilic mode of adhesion, several groups have identified non-CD31 heterophilic ligands which bind to CD31 (DeLisser *et al.*, 1993, Piali *et al.*, 1995, Prager *et al.*, 1996), although at the time this work was initiated, the only heterophilic ligand for CD31 that had been identified was an uncharacterised glycosaminoglycan decorated ligand expressed on murine L-cells (DeLisser *et al.*, 1993) which is thought to bind to CD31 via sequences in domain 2. Since homophilic adhesion requires the full length extracellular domain, whilst GAG binding requires the NH_2-terminal domain 2, it was reasoned that homophilic and heterophilic, GAG-mediated, adhesion would show different binding patterns to the CD31 domain deletion series.

6.2 Results

6.2.1 Adhesion of a panel of cell lines representing stages of haematopoiesis

A panel of cell lines representing various stages of myeloid and lymphoid lineage development were examined for their ability to bind to recombinant chimeric forms of human CD31 (D1-D6)Fc and negative control protein MUC18 (D1-D5)Fc immobilised on plastic. Cell lines used were as follows: KG1, KG1a and KG1b (myeloblastic progenitors); Raji, Namalwa and Daudi (B-cell); Molt-4, Jurkat-J6 and HSB2 (T-cell); U937 (pro-monocyte), and K562 (erythroleukemia). Adhesion assays revealed two cell lines (KG1b

and U937) which bound constitutively and specifically to CD31 (D1-D6)Fc, but not to MUC18 (D1-D5)Fc (Figure 6.1).

Both cell lines were found to constitutively express CD31 on their cell surface by FACScan analysis (C. Buckley, personal communication). When adhesion assays to the CD31 domain deletion series were performed, KG1b bound in a fashion analogous to that previously observed for homophilic adhesion in heterologous COS-1 cell assays (i.e. significant adhesion above background binding to negative control protein only occurred for constructs containing domains 5 and 6), and consistent with earlier observations for adhesion to CD31 constructs exhibited by MIK-ALL, a pre-B cell line (Fawcett *et al.*, 1995, Buckley *et al.*, 1996). In contrast , U937 exhibited a radically different pattern of adhesion by binding to all of the truncation mutants of CD31, (Figure 6.2) including the minimal unit CD31 (D1)Fc, although for maximal binding the minimal unit was CD31 (D1-D3)Fc. This suggested that U937 interacted with CD31 via a different mechanism to KG1b and MIK-ALL, distinct from the homophilic mode of adhesion previously identified. Since homophilic adhesion requires the presence of the whole extracellular domain to achieve stable homophilic adhesion, this suggested that U937 bound CD31 in a predominantly heterophilic rather than homophilic manner, and that a novel CD31 counter-receptor was expressed by U937.

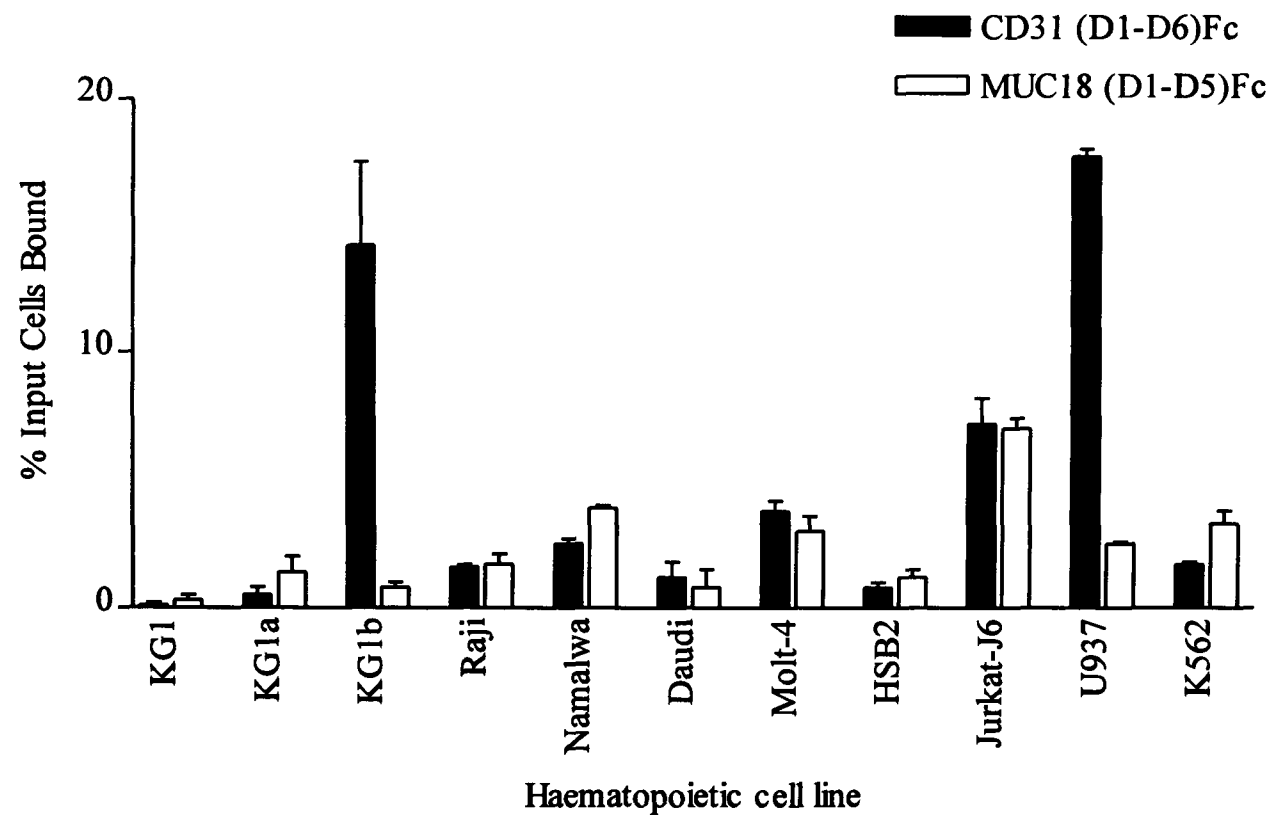


Figure 6.1 Cell-chimeric protein adhesion screen of haematopoietic cells lines. Adhesion of 11 haematopoietic cells lines (KG1, KG1a, KG1b, Raji, Namalwa, Daudi, MOLT-4, HSB2, Jurkat-J6, U937 and K562) to CD31 (D1-D6)Fc or negative control protein MUC18 (D1-D5)Fc, which represents the background level of adhesion in the assay. Results are expressed as the percentage of total input cells bound ± 1 SD (n=3).

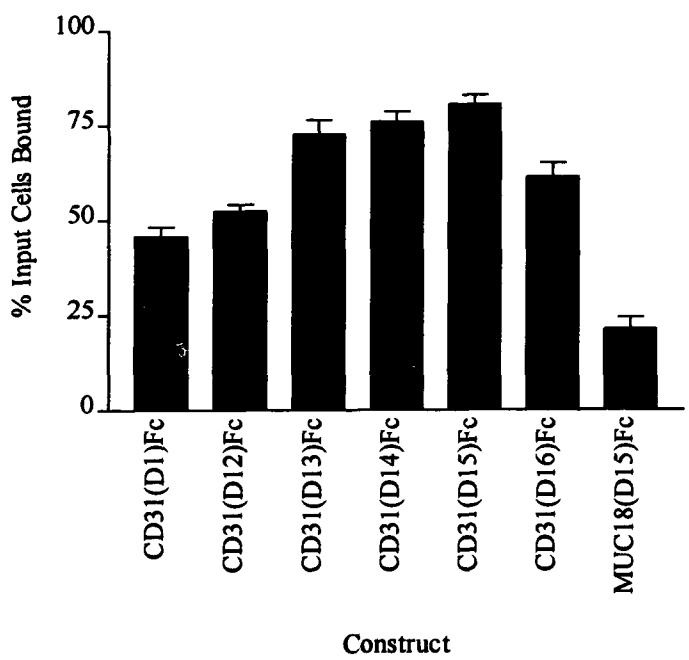


Figure 6.2 Adhesion of U937 cells to CD31 domain deletion series proteins. Pro-monocytic cell line U937 cells were allowed to adhere to plastic coated with CD31 domain deletion series proteins, or negative control protein MUC18 (D1-D5)Fc. All of the CD31 proteins bound above the background level of adhesion seen to MUC18 (D1-D5)Fc. CD31 (D1)Fc and CD31 (D1-D2)Fc bind at slightly lower levels than longer CD31 (D1-D3)Fc to CD31 (D1-D6)Fc. This pattern of adhesion is radically different to that seen in homophilic adhesion both in heterologous COS cells and in the cell lines KG1b and MIK-ALL, and suggests the existence of a novel heterophilic counter-receptor for CD31 on U937 cells.

A number of heterophilic ligands have been proposed for CD31 with varying degrees of credibility. A heterophilic adhesion mode has been reported that involves a site within the second immunoglobulin domain of CD31 binding to as yet uncharacterised cell associated glycosaminoglycans (GAGs) (Muller *et al.*, 1992, DeLisser *et al.*, 1993). This binding has been reported to be blocked both by heparin at 100μg/ml and a short linear peptide derived from domain 2 of CD31 (position 150-155 LKREKN), that is proposed to form the GAG binding site (DeLisser *et al.*, 1993). Given that the minimal unit capable of supporting U937 adhesion is CD31 (D1)Fc, it seemed unlikely that a GAG binding site in domain 2

was responsible for the heterophilic adhesion seen in U937 cells. This was confirmed by performing adhesion assays in the presence of heparin and peptides at the concentrations reported to inhibit GAG mediate heterophilic adhesion, which showed no effect on U937 adhesion. (Buckley *et al.*, 1996).

Recently, another laboratory examining the adhesion of murine lymphokine-activated killer (LAK) cells and pro-T-cells to recombinant forms of truncated *murine* CD31 reported that the integrin αvβ3 is an additional receptor for *murine* CD31 (Piali *et al.*, 1995). In order to investigate the possibility that U937 adhesion to CD31 was due to *human* CD31 binding to *human* integrin αvβ3, experiments were undertaken to examine whether U937 binding to CD31 was dependent on cations and temperature. The binding of U937 to CD31 (D1-D6)Fc was sensitive to both divalent cations (Buckley *et al.*, 1996) and temperature (Figure 6.3a). This cation and temperature dependence suggested that the heterophilic counter receptor for CD31 on U937 might be an integrin. This was further enforced by the observation that the addition of 0.5mM Mn^{2+} increased the binding of U937 to CD31 (D1-D6)Fc, however the same concentration of Mn^{2} had no effect on the binding of KG1b (Figure 6.3b). Mn^{2+} regulatability is a characteristic feature of integrin mediated binding (Dransfield *et al.*, 1992; Karecla *et al* 1995), and this strongly suggested that the counter-receptor on U937 was an integrin, whilst the lack of effect on KG1b adhesion is consistent with the results from binding to the domain deletion series proteins, which predicts a totally homophilic interaction.

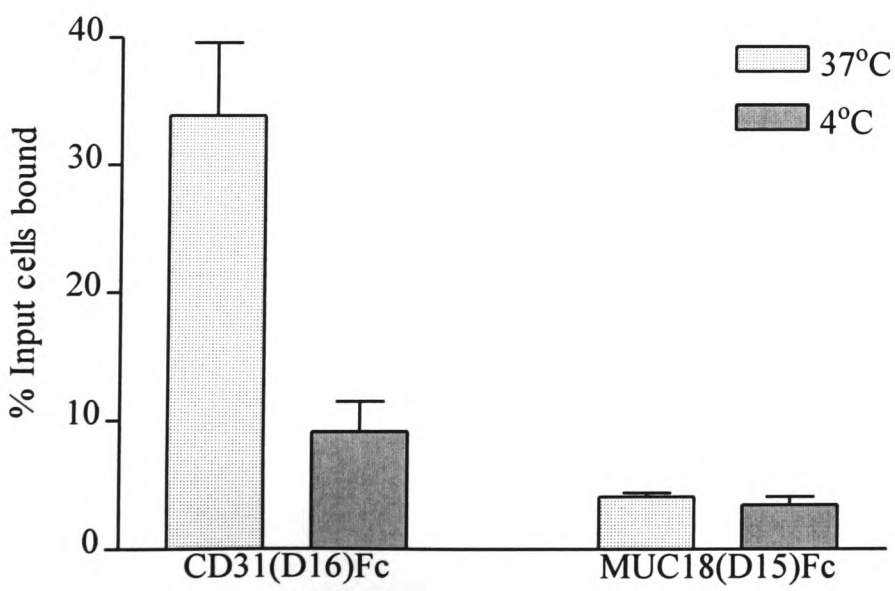


Figure 6.3a Temperature dependence of U937 adhesion. Adhesion of U937 to plastic coated with CD31 (D1-D6)Fc or negative control protein MUC18 (D1-D5)Fc at 37°C or 4°C Results are expressed as percentage of total input cells bound ± 1 SD (n=3). U937 cells bind specifically to CD31 (D1-D6)Fc compared to negative control MUC18 (D1-D5)Fc protein and shows strong temperature dependence.

Source aa29/96 wash 2

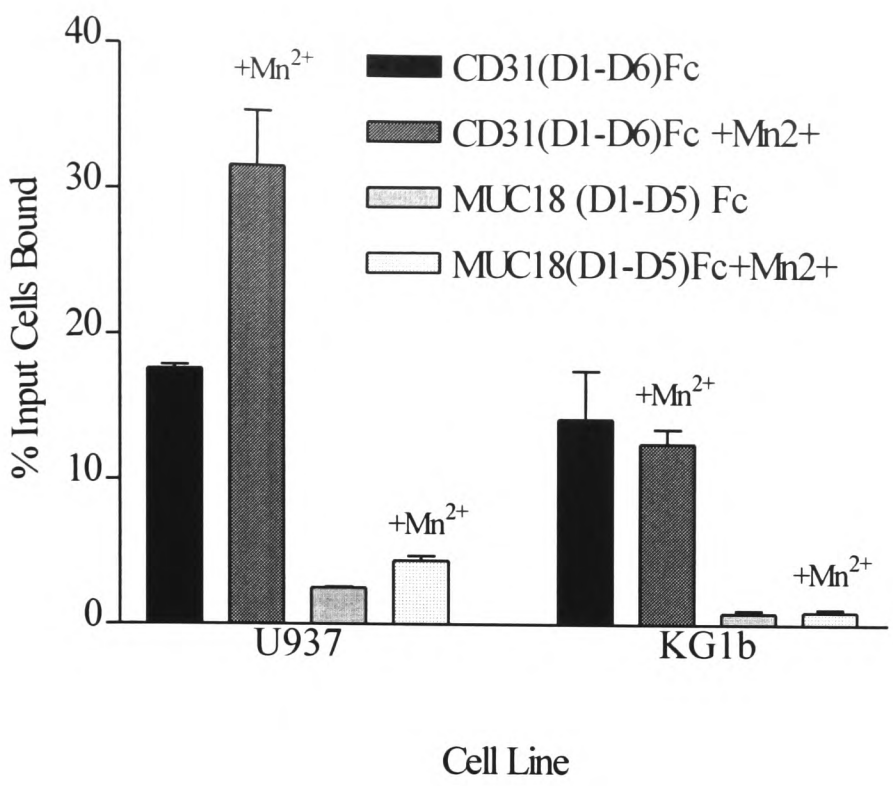


Figure 6.3b Manganese regulatability of U937 adhesion to CD31 (D1-D6)Fc. Adhesion of U937 to plastic coated with CD31 (D1-D6)Fc or negative control protein MUC18 (D1-D5)Fc, in the presence or absence of 0.5mM $MnCl_2$. Results are expressed as percentage of total input cells bound ± 1 SD (n=3). U937 cells bind specifically to CD31 (D1-D6)Fc compared to negative control MUC18 (D1-D5)Fc protein and shows enhancement of adhesion in the presence of Mn^{2+} divalent cations. In contrast, KG1b binds specifically to CD31 (D1-D6)Fc, but is not affected by the addition of Mn^{2+}. This is consistent with the results from the domain deletion series proteins, which indicated that KG1b adhesion is fully homophilic.

Source: ligand screen Summer 1995

In order to determine if the integrin αvβ3 does bind human CD31, adhesion assays were performed with functional blocking anti-αvβ3 antibody (clone LM609, Cheresh and Spiro, 1987) which was able to completely inhibit the adhesion of U937 cells to CD31 (Figure 6.4). In contrast, a non-blocking isotype controlled anti-αvβ3 antibody (clone 23C6) did not affect binding, suggesting that blockade by LM609 was not due to non-specific steric effects. mAbs directed against other integrins expressed on U937 cells and which are known to inhibit integrin function did not significantly affect adhesion of U937 cells to CD31, (Buckley *et al.*, 1996). Thus, antibody blockade studies identified the integrin αvβ3 as a heterophilic ligand for CD31.

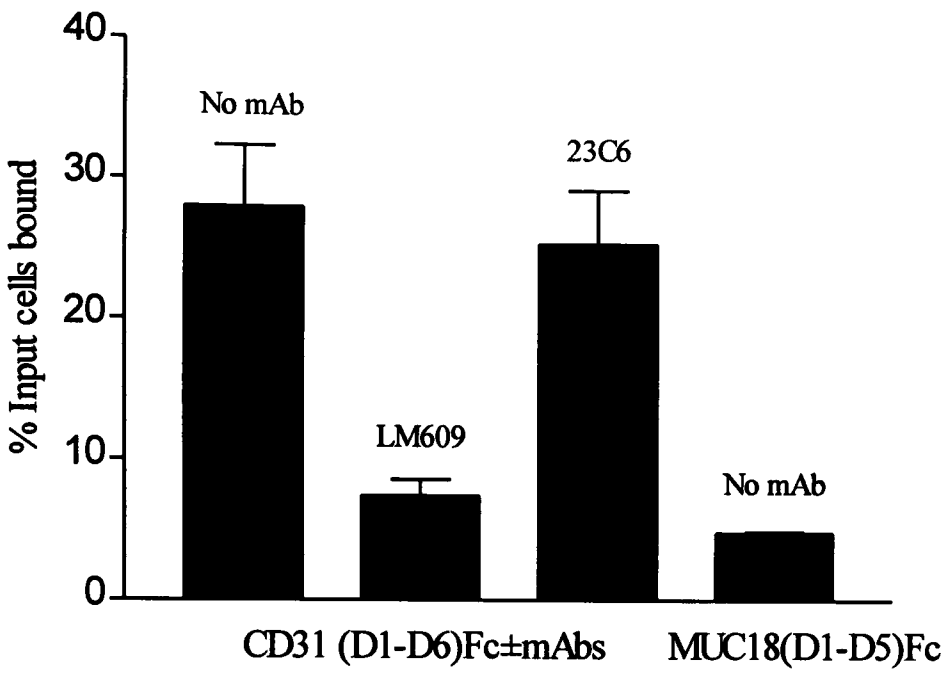


Figure 6.4. Inhibition of U937 cells to CD31 (D1-D6)Fc by anti-αvβ3 mAb LM609. Adhesion of U937 to CD31(D1-D6)Fc in the absence or presence of anti-αvβ3 antibodies. Cells were incubated with mAbs at 10μg/ml for 10 minutes at room temperature before the assay and then the cells were plated in 96-well plates coated with CD31 (D1-D6)Fc. mAbs were present throughout the assay. Results are expressed as percentage of total input cells bound ± 1 SD (n=3). Anti-αvβ3 mAb clone LM609, previously shown to block αvβ3 function, inhibited adhesion to U937, whilst a non-blocking mAb to αvβ3, clone 23C6, has no effect.

Source: aa06/96

It has been suggested that many of the proposed heterophilic ligands for CD31 are not heterophilic ligands *per se*, but that intracellular signalling induced by initial homophilic CD31 engagement leads to the upregulation of other adhesive pathways, a process known as "cross-talk" (see for example Sun *et al.*, 1996a and Jackson *et al.*, 1997). The aims of this chapter were to verify that the integrin αvβ3 was indeed a ligand for CD31 in both cell-protein and direct protein-protein systems, and to further dissect the interaction to identify the domains involved in regulating adhesion.

6.2.2 Mutational analysis of CD31 binding to pro-monocytic cell line U937.

From the initial pattern of binding observed with the CD31 domain deletion series, the minimal subunit that gave significant adhesion above negative control protein MUC18 (D1-D5)Fc was CD31 (D1)Fc. It was assumed, therefore, that the heterophilic binding site was contained within that domain. Previous studies identifying residues required for homophilic adhesion (Chapter 3) had produced 22 single-point mutations in domain 1, and generated these within a CD31 (D1-D2)Fc backbone prior to subcloning into CD31 (D1-D6)Fc for homophilic adhesion assays. These intermediate constructs were therefore expressed in COS-1 cells, and mutant CD31 (D1-D2)Fc purified from culture supernatants and tested in heterophilic adhesion assays to U937 cells (Figure 6.5).

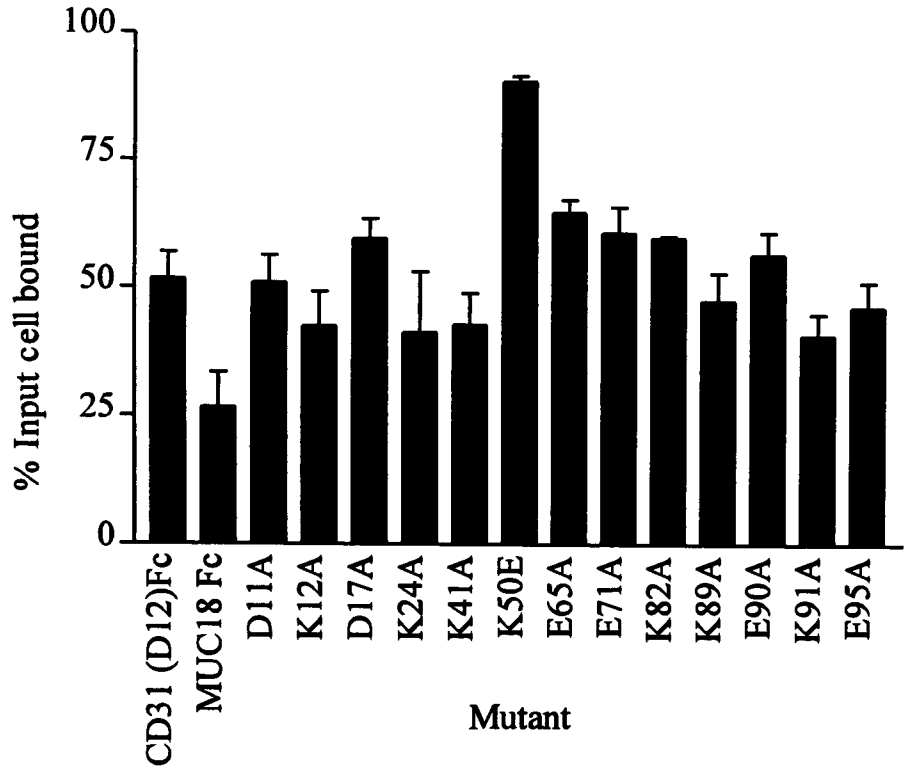


Figure 6.5 Initial screen of CD31 (D1-D2) mutants in a heterophilic adhesion assay with U937 cells. U937 cells were allowed to adhere to plastic coated with CD31 (D1-D2)Fc wild type and mutant proteins, or to MUC18 (D1-D5)Fc negative control protein. None of the mutations has any significant inhibitory affect on U937 cell adhesion, surprisingly however, one of the mutations, K50E, which had previously been shown to cause gross structural changes leading to a failure to be recognised by CD31-specific antibodies in an ELISA resulted in a significant increase in overall adhesion.

None of the mutations tested in the initial screen of 13 mutants had any inhibitory effect affect on U937 cell adhesion, however, one of the mutants which had previously been shown to be grossly misfolded as judged by an panel of anti-CD31 specific antibodies in an ELISA. (see Chapter 3, table 3.6) gave significantly higher levels of adhesion than the positive control . This mutation was routinely used as a negative control in homophilic adhesion assays, and the observation that this protein gives rise to enhanced adhesion was therefore a considerable surprise. Although this mutation caused a gross structural change, the Fc portion is at least folded correctly, since it is possible to purify the protein from conditioned media with protein-A sepharose. One possibility is that the adhesion is mediated by Fc receptors (FcRs) expressed on U937 cells (FcRγIIa and b, CD32A and B), and that by using an incorrectly folded protein the Fc tag was accessible to Fc receptors. Although MUC18 (D1-D5)Fc protein was included to control for non-specific Fc mediated effects, there are no size specific controls for each CD31 construct, such that the adhesion observed in the U937 assays may be mediated at least in part by Fc receptors (FcR). It is possible to hypothesise that for highly truncated CD31 constructs, cell expressed FcR may be able to access the Fc portion of the CD31 constructs when these are orientated and immobilised on plastic by goat anti-human Fc, however as the constructs become increasingly elongated accessibility to the Fc tag may decrease due to steric exclusion. If steric accessibility to Fc is a factor, then MUC18 (D1-D5)Fc is a poor control for Fc mediated effects, since of 6 potential N-glycosylation sites, 5 are located within domain 5, which is likely to further shield the Fc tag. Competition between FcR mediated and αvβ3-

mediated adhesion will obviously complicate the interpretation of which domains are involved in mediating heterophilic CD31 adhesion. Since there is a step up in binding between CD31 (D1-D2)Fc and CD31 (D1-D3)Fc constructs a tentative hypothesis is that the actual αvβ3 binding site is contained within domain 3, and that the binding of shorter constructs is FcR mediated. In order to investigate this possibility, it was decided to generate a series of appropriate non-binding size matched controls for the CD31 domain deletion series.

6.2.3 Comparison of U937 binding to CD31, MUC18 and NCAM domain deletion series.

In order to eliminate the possibility of, or control for, non-specific binding of truncated constructs, two non-binding size matched control domain deletion series were generated, a MUC18Fc and a NCAMFc domain deletion series. Deletion series were constructed as for the CD31 deletion series using PCR amplification with *Pwo* DNA polymerase, and subcloning into the pIG_1 expression vector (as described in methods and materials).

MUC18 Fc fusion plasmids were expressed in COS-1 cells, and protein isolated from tissue culture supernatants on protein A-sepharose. Protein run out on reducing 7.5% acrylamide gels and Coomassie Blue stained showed the expected apparent molecular weights, and were shown to be conformationally intact by ELISA with a panel of 28 anti-MUC18 mAbs obtained from the VIth Leukocyte Typing Workshop (Figure 6.6). These constructs were used to map the domains recognised by each antibody as part of the Leukocyte Typing Workshop.

Chimeric NCAMFc proteins were transiently expressed in COS-1 cells and purified from conditioned medium with protein-A sepharose. Unfortunately most of the available commercial antibodies to NCAM map to the membrane proximal fibronectin type III repeats, which are presumed to be most immunogenic region of the protein (Professor Pat Doherty, UMSD, London personal communication), so that it was not possible to test the NCAMFc chimeric proteins for structural integrity by an extensive ELISA screen as for the MUC18Fc deletion series. It was possible to show that one antibody, ERIC-1, reacted with NCAM (D1-D4)Fc and NCAM (D1-D5)Fc, indicating that ERIC-1 recognises an epitope in the fourth immunoglobulin like domain of NCAM-1 (data not shown).

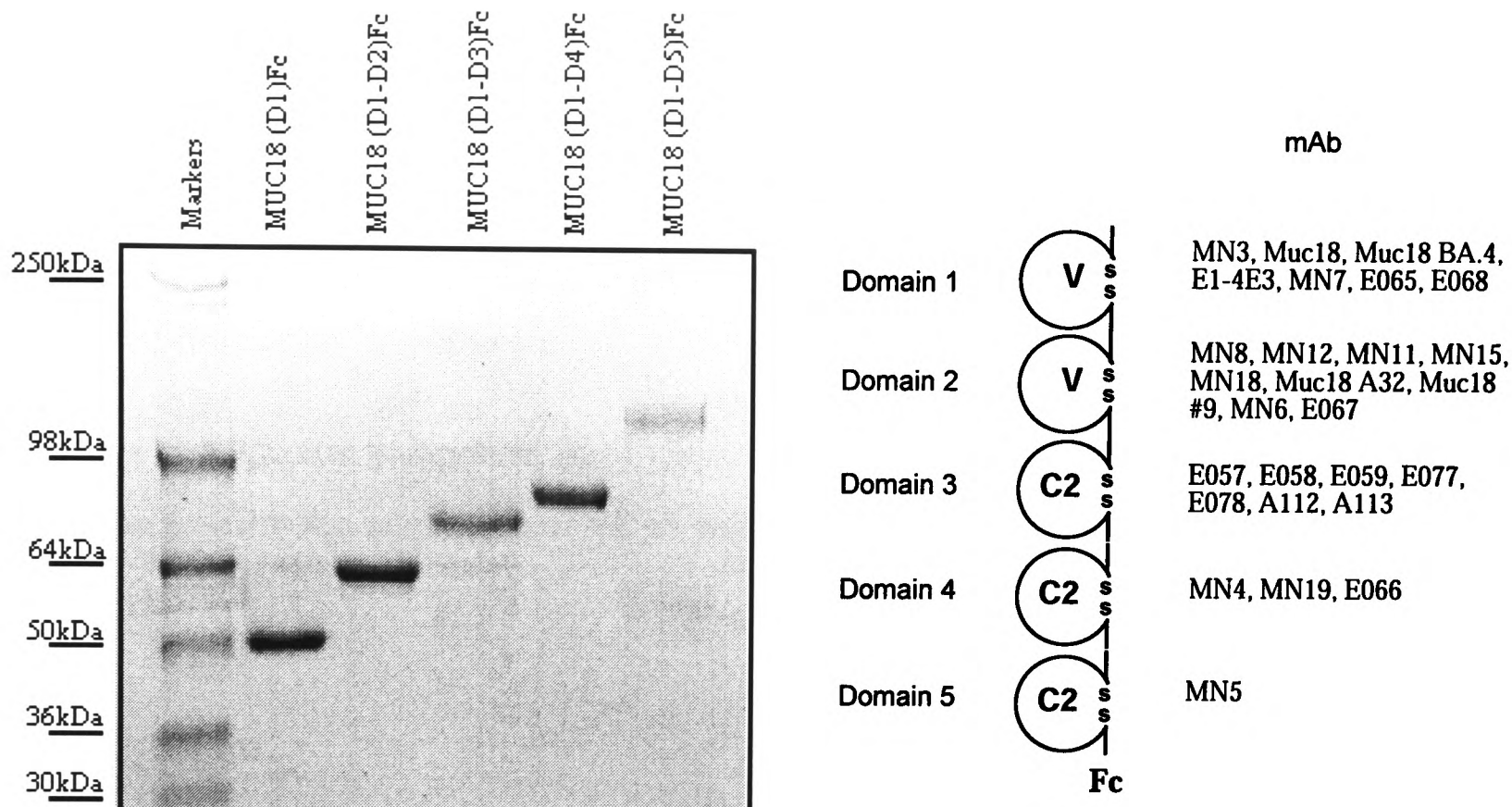


Figure 6.6 Characterisation of MUC-18Fc domain deletion series proteins. Proteins were purified from tissue culture supernatants by protein-A sepharose, 2μg of purified protein run on 7.5% SDS-PAGE gels, and stained with Coomassie Blue (above left). The apparent molecular weight for each chimeric construct was as expected, and showed the overall pattern of molecular weights expected for the domain deletion series. The presence of five of the six N-glycosylation sites of MUC18 in the fifth Ig domain results in a large shift in apparent molecular weight for MUC18 (D1-D5)Fc compared to MUC18 (D1-D4)Fc. The conformational integrity of each MUC18 chimeric protein was assessed with a panel of 28 monoclonal antibodies obtained from the VIth leukocyte typing workshop, allowing the domains recognised by each antibody to be assigned. Domain assignments were based on the minimal unit which gave mAb binding (as measured by OD_{450}) greater than 2-fold above ICAM-2Fc negative control protein in domain mapping ELISAs. Summary of the epitopes recognised by each monoclonal antibody is shown (above right).

Having generated two domain deletion series, these were used in adhesion assays with U937 cells to determine the extent of CD31 specific adhesion versus non-specific Fc mediated adhesion (Figure 6.7). These results show that there is a significant non-specific interaction of all Fc chimeric proteins with U937 cells when those proteins have less than three Ig domains in them, regardless of the particular IgSF member contributing those domains. This non-specific binding reduces as the constructs extend, which is consistent with the hypothesis that these constructs sterically exclude cell Fc receptor contact with the Fc tag.

That Fc receptors are involved in mediating adhesion to U937 was also suggested by the observation that pre-incubating U937 cells with 10μg/ml human IgG completely inhibits adhesion to all CD31 domain deletion series proteins (data not shown). This may be due to

steric effects of coating the cell with human IgG, but the obvious alternative explanation is that U937 cells use their Fc receptors to bind to Fc constructs. This also makes the interpretation of antibody based inhibition studies more complicated. Collectively results based on U937 cell binding to CD31 domain deletion series indicate that there is a non-homophilic binding component to CD31 mediated adhesion, however the extent to which adhesion is mediated by Fc receptors or other ligands for CD31 on U937 cells is not clear, and will require further investigation.

Given this non-specific component of binding, a more rigorous and controlled assay was required to confirm the interaction of CD31 with αvβ3, and to allow this interaction to be further dissected.

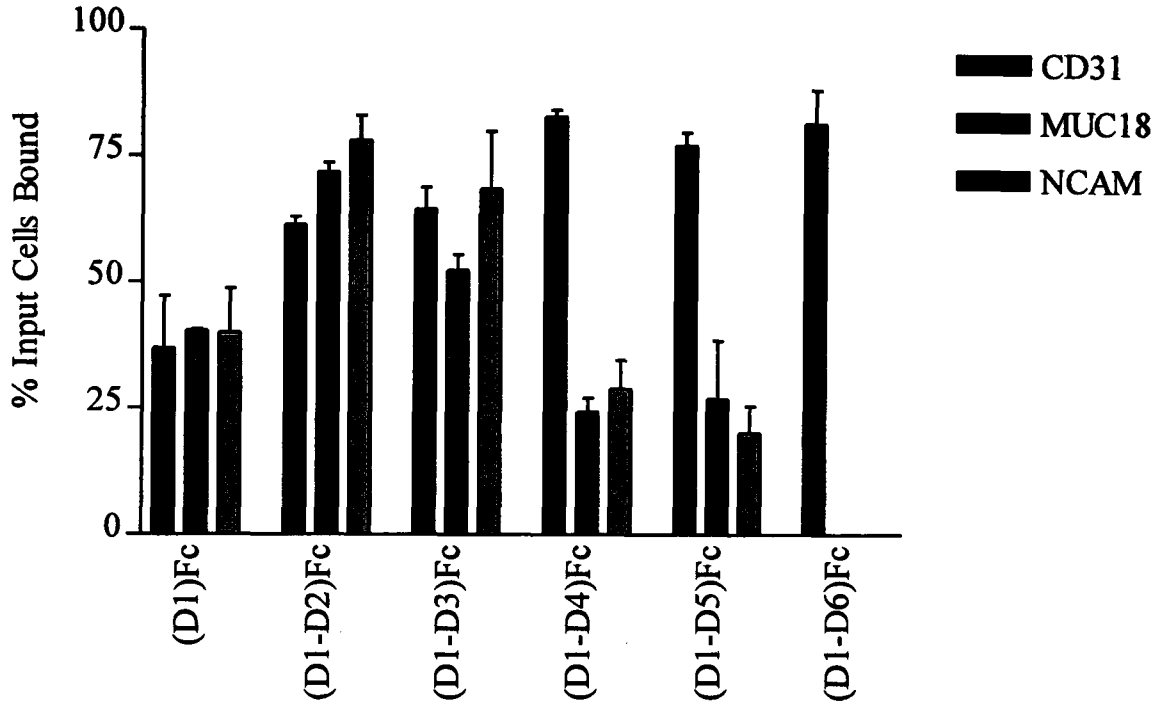
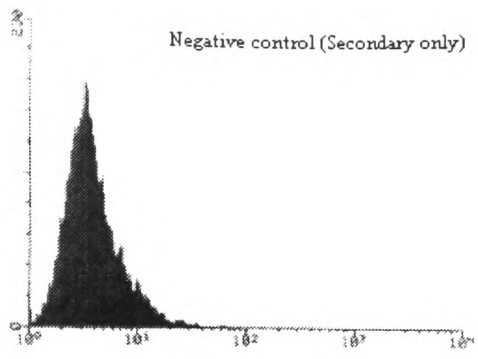


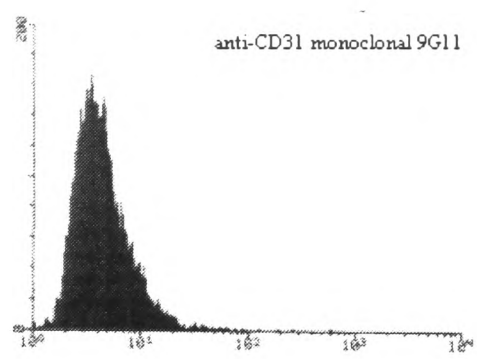
Figure 6.7 Comparison of U937 adhesion to CD31, NCAM, and MUC18 domain deletion series proteins. A. Adhesion assays were performed with U937 cells binding to plastic coated with the CD31, MUC18 and NCAM deletion series proteins to determine the specificity of U937 binding to CD31. These assays revealed that all domain deletion series proteins of 1,2, or 3 immunoglobulin-like domains bind non-specifically to U937, regardless of the particular IgSF member contributing those domains. These results indicate that the NH_2-terminal domains originally proposed to form the heterophilic binding site are unlikely to do so.

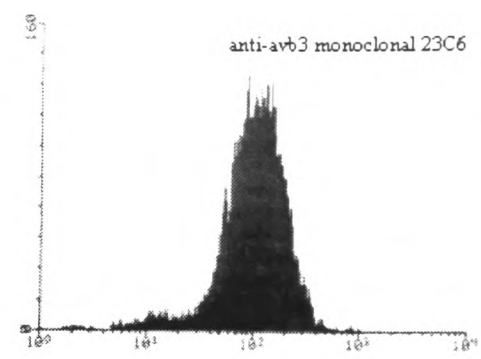
6.2.4 Development of a solid phase CD31- αvβ3 protein-protein interaction assay.

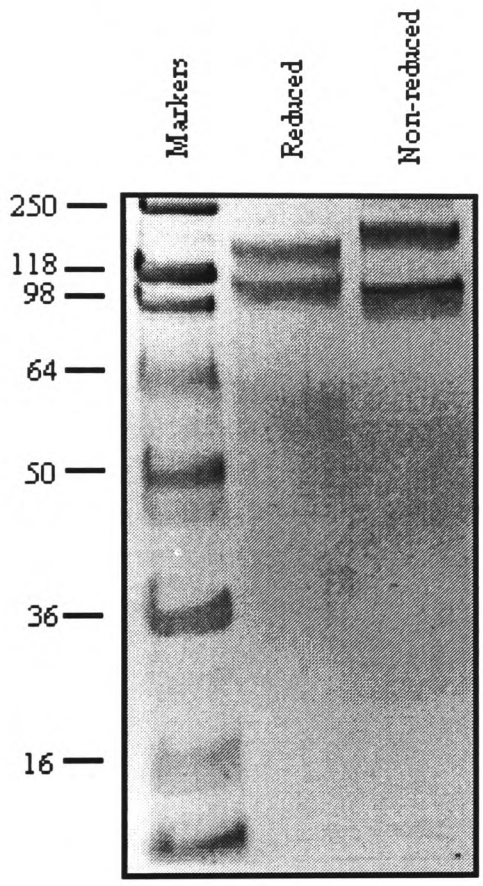
In order to overcome the problems of U937 cells binding non-specifically in cell-protein assays and the difficulty of dissociating homophilic from heterophilic adhesion, solid-phase protein-protein interaction assays were developed. This was intended to allow the interaction between CD31 and integrin αvβ3 to be studied directly and independently from

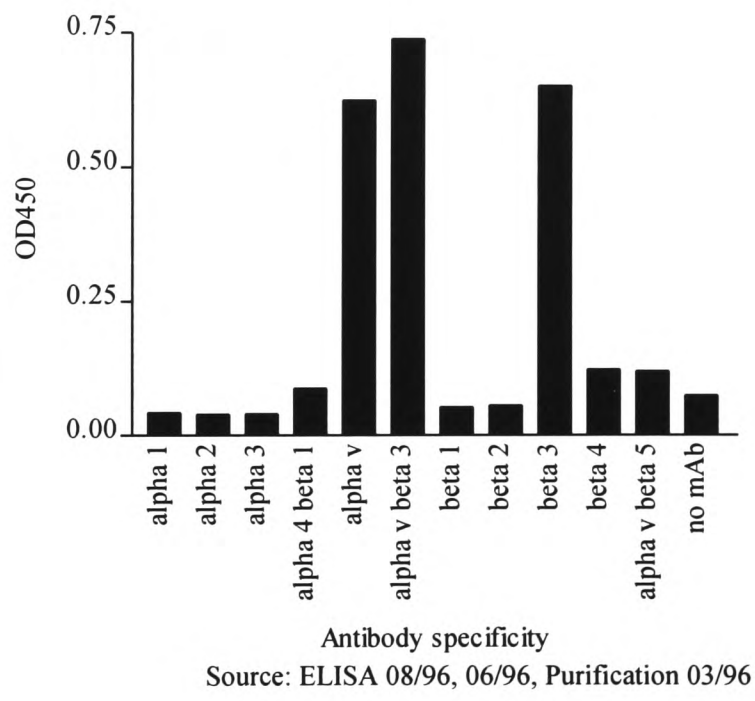
other adhesive interactions in a fully cell-free context. Several other investigators have utilised solid phase assays to study integrin mediated adhesion, both to extracellular matrix, for example the interaction between α5β1 and fibronectin (Mould *et al.*, 1995) , αvβ3 and fibronectin (Charo *et al.*, 1990), and the A-domain from the α1 subunit and laminin (Calderwood *et al.*, 1997), and between IgSF family members and integrins, for example MAC-1 and ICAM-1 (Vanstrijp *et al.*, 1993). Initial solid-phase binding was performed using a modification of the method originally developed by Charo and colleagues. Human integrin αvβ3 was purified from the melanoma cell line DX3 (a cell line which expresses high levels of αvβ3, but not CD31, see figure 6.8) and occasionally from full term placentas, as described in Chapter 2 (Methods and Materials). The integrin preparation was pure as judged by SDS-PAGE and ELISA using a panel of anti-integrin antibodies (Figure 6.8).











Source: ELISA 08/96, 06/96, Purification 03/96

Figure 6.8 Purification and characterisation of integrin αvβ3 from melanoma cell line DX3. The melanoma cell line DX3 expresses high levels of the integrin αvβ3, but not CD31 as determined by FACScan analysis, as shown above (primary antibodies used were anti-CD31 monoclonal 9G11, and anti-αvβ3 monoclonal 23C6). The DX3 cell line was therefore selected as a source of integrin αvβ3. Immunoaffinity purified protein was run out on 9.5% SDS-PAGE gels (above left) under both reducing and non-reducing conditions, and stained with Coomassie Blue. Molecular mass markers are indicated (in kDa). The αv and β3 chains run at 150 and 90kDa (non-reduced), and 125 and 105kDa (reduced), as expected from the literature (Cheresh and Spiro, 1987). In order to ensure that the purified αvβ3 was not contaminated with other integrins, ELISAs (above right) were performed. Antibodies used were as follows: anti-α1 clone 1, anti-α2 clone HAS-4, anti-α3 clone 11A3, anti-α4β1 clone TS2/16, anti-αv clone L230, anti-αvβ3 clone LM609, anti-β1 clone mAb 13, anti-β2 clone BBA11, anti-β3 clone RUU-PL7F12, anti-β4 clone ASC-3 and anti-αvβ5 clone P1F6. Purified αvβ3 material was recognised by anti-αv, anti-β3 and anti-αvβ3 monoclonal antibodies, as expected, but showed no cross-reactivity with any of the other anti-integrin antibodies tested.

Solid-phase binding assays were performed in two orientations, either with integrin αvβ3 bound to plastic or with integrin αvβ3 free in solution. This was to ensure that immobilisation of the integrin on plastic did not result in changes in the affinity of the immobilised integrin for ligands, which may give artifactual interactions, as it has been

suggested that this may represent significant problems in *in vitro* assays (Weitzman *et al.*, 1995). Initial solid phase assays were performed as described in Materials and Methods.

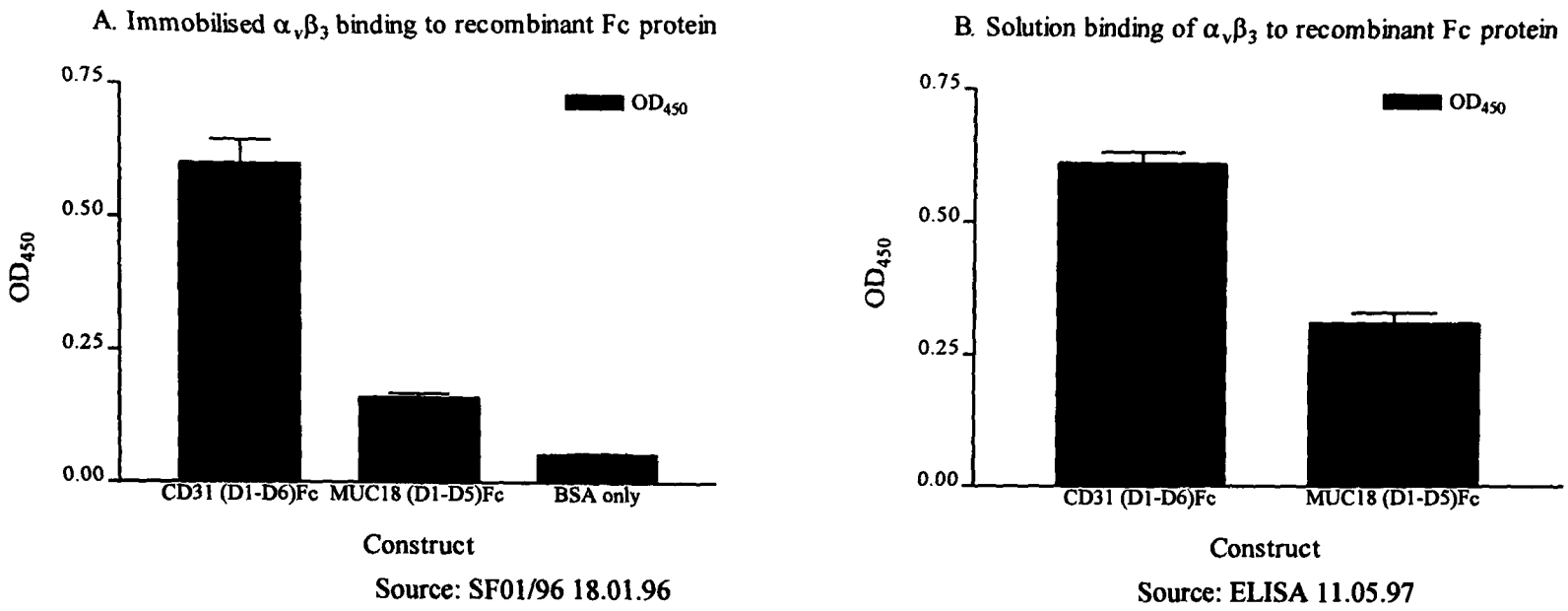


Figure 6.9a Integrin αvβ3 binds to CD31 (D1-D6)Fc when immobilised on plastic or free in solution. To provide evidence for a specific interaction between the integrin αvβ3 and CD31, the ability of purified CD31 (D1-D6)Fc to bind to purified αvβ3 was assessed using solid phase adhesion assays. In initial trial experiments, CD31 bound to αvβ3 significantly above background binding to BSA alone and MUC18 (D1-D5)Fc irrelevant control IgSF protein.

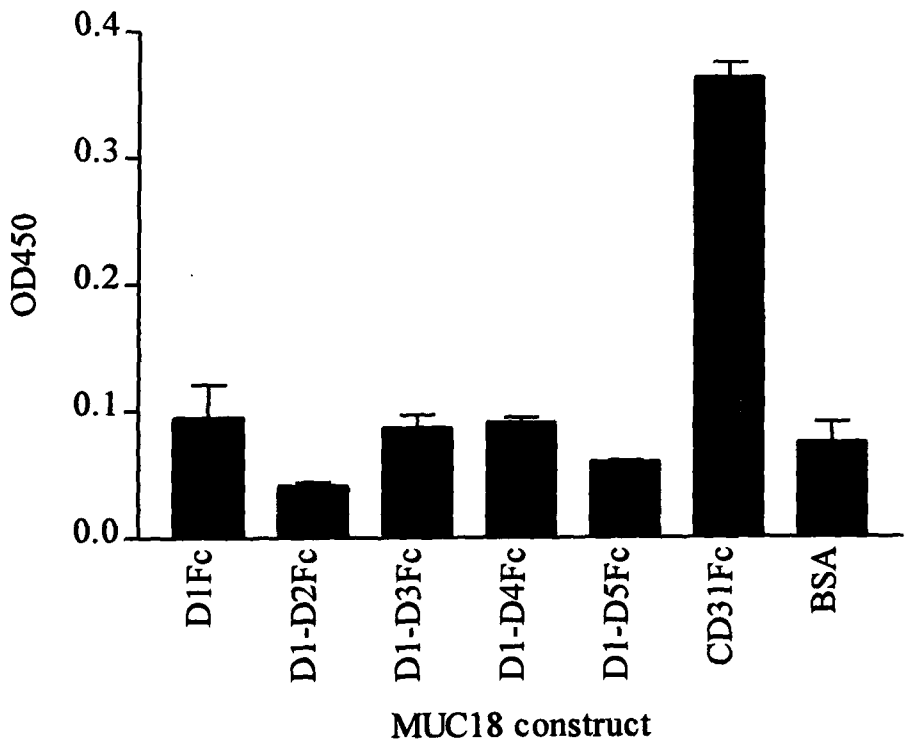


Figure 6.9b. Truncated MUC18 Fc proteins do not bind to αvβ3. None of the MUC-18 domain deletion series proteins supported binding to integrin αvβ3, compared to plastic treated with BSA alone, in contrast to the results with U937 cells and adhesion to this deletion series. CD31 (D1-D6)Fc protein bound specifically.

In initial trial experiments to provide evidence for a specific interaction between the integrin αvβ3 and CD31, solid phase assays between purified CD31 (D1-D6)Fc protein and purified integrin αvβ3 protein were performed, with both immobilised integrin and immobilised IgSF-Fc proteins. In both these assay formats, CD31 (D1-D6)Fc protein bound to a significantly greater extent than negative control proteins MUC18 (D1-D5)Fc (Figure 6.9a), indicating that the interaction between CD31 and αvβ3 was specific. This was further confirmed using the MUC-18 domain deletion series of proteins, which showed that truncated Fc constructs do not bind non-specifically to αvβ3 (Figure 6.9b)

6.2.5 Localisation of the heterophilic αvβ3 binding site on CD31 to domain 3.

Having established that purified recombinant CD31 binds to purified αvβ3, experiments were undertaken to map the domain(s) responsible for mediating this heterophilic interaction. Initially, the CD31 domain deletion series proteins were used to identify the domains involved in heterophilic adhesion. Binding of these domain deletion series proteins to αvβ3 immobilised on plastic showed little or no specific binding to CD31 (D1)Fc or CD31 (D1-D2)Fc proteins, and that the minimal CD31 unit capable of supporting adhesion was CD31 (D1-D3)Fc (Figure 6.10a to d). This suggests that the binding site resides in domain 3, which is consistent with the hypothesis that U937 cell binding to truncated Fc proteins was due to a non-specific interaction. This result was repeated with multiple batches of independently produced Fc proteins. Generally assays were reproducible between the same batch of proteins (Figure 6.10a and b), but there were differences in the absolute magnitude of the binding of CD31 (D1-D3)Fc to CD31 (D1-D6)Fc proteins to αvβ3 between batches of proteins (Figure 6.10c and d). This may be due to small errors in the determination of the total protein concentrations, contamination of the total protein with bovine immunoglobulins, or the presence of aggregates of CD31Fc proteins in the samples. In order to ensure that the failure of CD31 (D1)Fc to bind to αvβ3 was not due to an underestimation of the concentration of protein in the sample, CD31 (D1-D6)Fc and CD31 (D1)Fc protein binding to immobilised αvβ3 was titrated in the range 0-100μg/ml (Figure 6.11). Significantly, the binding of CD31 (D1-D6)Fc to αvβ3 was shown to be specific and saturable when compared to CD31 (D1)Fc protein. There was no evidence for the failure of CD31 (D1)Fc to bind to αvβ3 being due to an underestimation

of total Fc protein. This data is not suitable for Scatchard analysis since it is not possible to determine the absolute or relative levels of protein bound compared to total/unbound protein. Utilising the same assay and radio-iodine labelled CD31 (D1-D6)Fc protein this study was extended to show specific, saturatable binding of CD31 to αvβ3, which could be competed with a 250-fold molar excess of cold CD31 (D1-D6)Fc (C. Buckley and A. Sharma, personal communication). This data was suitable for Scatchard analysis, and revealed a value for the dissociation constant (Kd) of 4.1nM. Although CD31 (D1-D6)Fc is a dimer (dimerisation mediated by the hinge region of the C-terminal Fc affinity tag), the apparent binding constant is comparable for native dimeric ICAM-1 binding to its integrin counter receptor LFA-1 (Miller *et al.*, 1995). Collectively, data from both ELISA and RIA based assays are consistent with a specific interaction between CD31 and αvβ3, and that the minimal unit required for binding to αvβ3 was CD31 (D1-D3)Fc.

In order to prevent slight batch to batch variations in Fc proteins affecting future analyses, all subsequent assays were performed with the integrin in solution phase and with Fc proteins immobilised on plastic via anti-human Fc antibody, as this has previously been established to normalise the amount of protein bound to plastic, removing the need to correct for concentration effects (Holness et al., 1995). This also allows a single input protein (purified αvβ3 integrin) to be detected, which should improve intra-assay reproducibility.

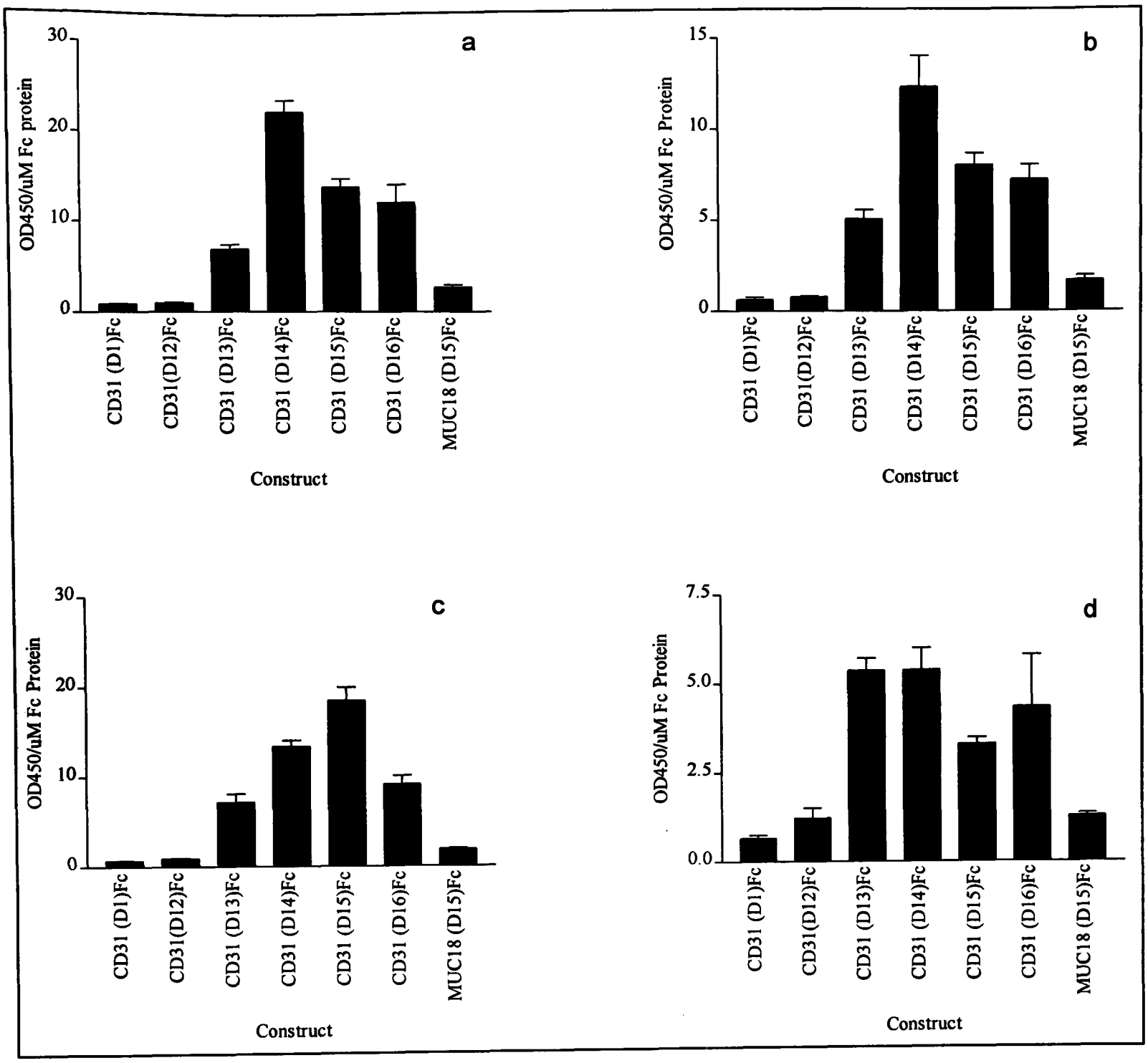


Figure 6.10 Binding of CD31 domain deletion series proteins to immobilised integrin $\alpha_v\beta_3$. Purified integrin αvβ3 was immobilised on plastic, and CD31 1μg/well domain deletion series proteins were allowed to bind to the immobilised integrin. Bound Fc proteins were detected with an anti-human Fc specific HRP conjugated antibody, and colour developed with OPD substrate. Fc protein bound was expressed as OD_{450} per μM Fc protein. In contrast to the binding of the cell line U937 to the domain deletion series, no significant adhesion was observed for CD31 domains 1 and 2, the minimal functional unit was CD31 (D1-D3)Fc. Results from four separate experiments are shown, a and b are assays on consecutive days with the same proteins, whilst c and d are with different batches of proteins.

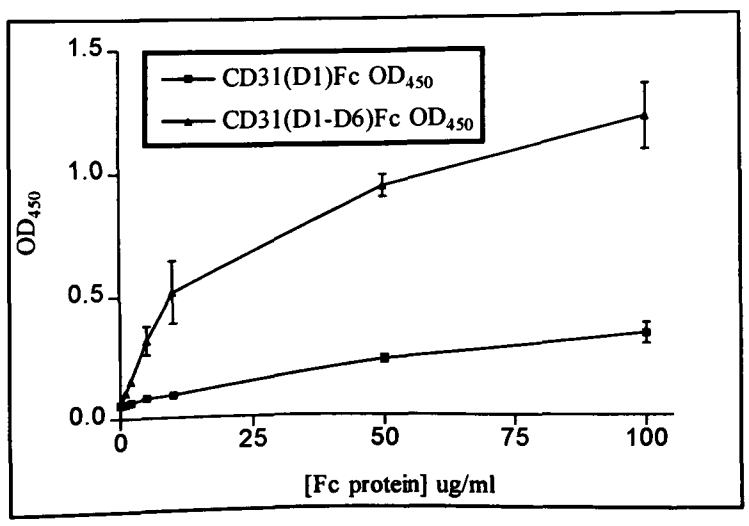


Figure 6.11 Titration of CD31 (D1-D6)Fc and CD31 (D1)Fc proteins binding to integrin αvβ3 immobilised on plastic. Titration of CD31 (D1-D6)Fc and CD31 (D1)Fc proteins in the range 0-100μg/ml to integrin αvβ3 immobilised on plastic. CD31 (D1-D6)Fc protein bound in a specific, saturatable fashion to the immobilised integrin αvβ3, in contrast to CD31 (D1)Fc protein, which showed only a slight increase in apparent binding with an increase in concentration.
Source: Solid Phase Assay 02/96 20.01.96

The role of domain 3 in mediating heterophilic adhesion to αvβ3 was further investigated by using the ICAM-3/CD31 chimeric Fc proteins previously developed to dissect homophilic adhesion (Chapter 3) and by generating an additional CD31 construct lacking domain 3 by recombinant overlapping PCR (See Methods and Materials). Each of these constructs was determined to be conformationally intact by ELISA using a range of domain specific mAbs (Table 6.1). In solid phase assays (Figure 6.12) ICAM-3 (D1)/CD31 (D2-D6)Fc and ICAM-3 (D1-D2)/CD31 (D3-D6)Fc, both of which contain domain 3, bind to αvβ3. Conversely, CD31 (D1-D2)/ICAM-3(D2-D5)Fc (lacking domain 3) does not bind to αvβ3 whereas, CD31 (D1-D3)/ICAM-3 (D3-D5)Fc (containing domain 3) yielded maximal levels of binding. These chimeras define a dominant role for domain 3 in mediating the heterophilic CD31-αvβ3 interaction. Moreover, they also show that the failure of the original short CD31 (D1)Fc and CD31 (D1-D2)Fc proteins is not due to steric hindrance from the plastic or inaccessibility of bound truncated CD31 proteins as the CD31/ICAM-3 chimeras preserve the normal length (six immunoglobulin-like domains) of native CD31. Finally to confirm the role for domain 3 in the interaction with integrin, a CD31Fc construct lacking only domain 3 but otherwise conformationally intact, CD31 (D1-2/D4-6)Fc, did not bind to αvβ3.

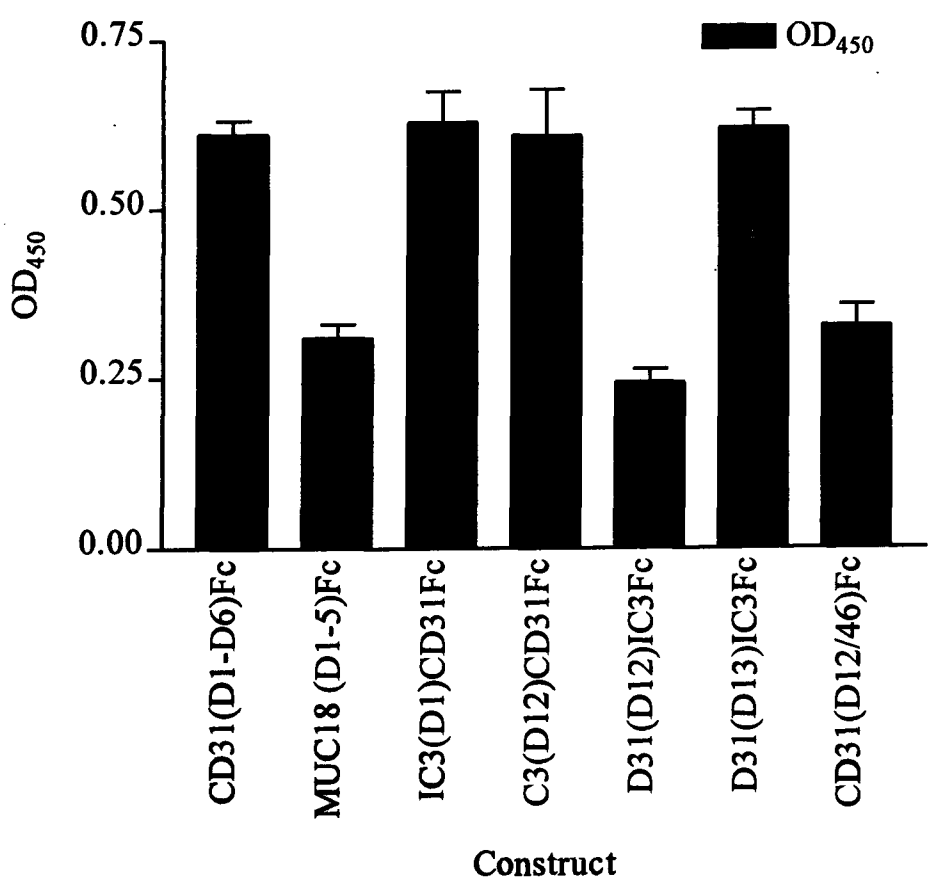


Figure 6.12 The heterophilic binding site for αvβ3 is contained in CD31 immunoglobulin-like domain 3. Binding of purified integrin to chimeric Fc proteins immobilised on plastic via goat anti-human Fc specific antibody. Bound integrin was quantified by ELISA with mouse anti-β3 integrin mAb, and bound antibody- integrin complex detected with sheep anti-mouse.HRP conjugated antibody and colour developed with OPD substrate. Constructs containing CD31 domain 3 (i.e. ICAM-3 (D1)/ CD31(D2-D6)Fc, ICAM-3(D1-D2)/CD31 (D3-D6)Fc and CD31(D1-D3)/ ICAM-3 (D3-D5)Fc), whereas constructs lacking domain 3 do not (i.e. CD31(D1-D2)/ICAM-3(D2-D5)Fc and CD31 (D1-D2/D4-D6)Fc).

Source: ELISA 11.05.97

Construct	9G11 (D1)	HEC7.2 (D2)	10B9 (D3)	CAL31.1 (D6)
CD31 (D1-D6)Fc	+++	+++	+++	+++
CD31 (D1-D2/D4-D6)Fc	+++	+++	-	+
ICAM-3 (D1)/CD31 (D2-D6)Fc	-	-	+++	+++
ICAM-3 (D1-D2)/CD31 (D3-D6)Fc	-	-	++	++
CD31 (D1-D2)/ICAM-3 (D2-5)Fc	+	++	-	-
CD31 (D1-D3)/ICAM-3 (D3-D6)Fc	+++	+++	+	-

Source: ELISA 06.07.97 and 19.02.97

Table 6.1 Chimeric constructs used to investigate the binding site for αvβ3 on CD31. ELISA screens were performed with a range of domain specific monoclonal antibodies. +++ indicates >80% wild type, ++ indicates 60-80% wild type, + indicates 40-60% wild type, and - is less then 40% wild type.

6.2.6 Binding to the integrin αvβ3 is not mediated by acidic residues in the CD-loop.

Having established that domain 3 of CD31 plays a major role in mediating heterophilic binding to αvβ3, a mutagenesis screen of domain 3 was undertaken. Mutations were focused on charged acidic residues in the C-strand and CD-loop region of domain 3. Such acidic residues have been identified as playing a key role in mediating integrin-ligand interactions for a wide range of ligands, including extracellular matrix ligands (classically via prototypic RGD sequences first identified by Pierschbacher and Ruoslahti, 1984), and members of the immunoglobulin superfamily, for example the QIDS motif in the CD-loop of VCAM (Renz *et al.*, 1994, Clements *et al.*, 1994, Chiu *et al.*, 1995 and Jones *et al.*, 1995) and the GIETS/LETS motifs identified in the C-strand amongst ICAMs (Staunton *et al.*, 1990, Sadhu *et al.*, 1994, Holness *et al.*, 1995, Klickstein *et al.*, 1996, Casasnovas *et al.*, 1997). Residues selected for mutagenesis in domain 3 were E239, E242, and D248, and these were generated by recombinant PCR with mutagenic primers to change the target residues to alanine (see Appendix A for sequences). Mutagenesis was performed as described for the earlier mutations generated in domains 1 and 2 by recombinant PCR. The resultant PCR product comprised of the NH_2-terminal domains 1 to 3 of CD31 containing the mutation of interest were digested with *Hind*III and *Bgl*II and subcloned directly into pIG_1 digested with *Hind*III and *Bam*HI. The mutations were constructed in a CD31 (D1-D3)Fc background since this represented the minimal functional unit required to give heterophilic adhesion to integrin αvβ3. Mutants were sequenced in their entirety to ensure

that the desired mutation was present, and that no adventitious PCR induced mutations were present. In addition to residues in domain 3, mutations in residues of domain 1 previously identified as forming part of the homophilic binding site (see chapter 3), i.e. D11A, D33A, D51R and K89A, and residues in domain 2 forming part of the putative heterophilic glycosaminoglycan (GAG) binding site (i.e. E139A, E142A, E145A and E153A) were subcloned from their original CD31 (D1-D6)Fc backbone into wild type CD31 (D1-D3)Fc utilising *Hind*III and *Bam*HI restriction sites as described previously. Mutant proteins were produced in COS-1 cells and purified from culture supernatants with protein-A sepharose.

The structural integrity of this panel of 11 mutants was assessed by ELISA profile (Table 6.2) using a panel of 4 anti-CD31 monoclonal antibodies mapping to epitopes contained within the first three NH_2-terminal domains of CD31. None of the mutations was judged to be grossly misfolded.

Mutant	9G11 (D1)	L133.1 (D2)	Hec7.2 (D2)	10B9 (D3)	CAL31.1 (D6)
CD31 (D1-D3)Fc WT	+++	+++	+++	+++	-
CD31 (D1-D3)Fc D11A	+++	+++	+++	+++	-
CD31 (D1-D3)Fc D30A	+++	+++	+++	+++	-
CD31 (D1-D3)Fc D51R	+	+	+++	+	-
CD31 (D1-D3)Fc K89A	++	+	+++	+++	-
CD31 (D1-D3)Fc E139A	+++	+	+	++	-
CD31 (D1-D3)Fc E142A	++	+	+	+	-
CD31 (D1-D3)Fc E145A	+	+	+	+++	-
CD31 (D1-D3)Fc E153A	+++	+++	+++	+++	-
CD31 (D1-D3)Fc E239A	+	++	++	+++	-
CD31 (D1-D3)Fc E242A	++	+	+++	+++	-
CD31 (D1-D3)Fc D248A	+	+	++	+++	-

Table 6.2. ELISA profile of CD31 (D1-D3)Fc mutant proteins. ELISAs were performed on the eleven mutant proteins to show that they were conformationally intact using four monoclonal antibodies directed against the three NH_2-terminal domains of CD31 and an anti-domain 6 mAb (CAL31.1) as negative control. +++ indicates >80% of wild type positive control, ++ indicates 60-80% of wild type, + indicates 40-60% of wild type, and - indicates <40% of wild type.

A heterophilic adhesion screen was performed using purified αvβ3 binding to mutant Fc proteins immobilised on plastic via anti-human IgG Fc. None of the mutated CD31 (D1-D3)Fc proteins affected binding to αvβ3 (Figure 6.13), including the mutations which had previously been shown to abolish homophilic binding or residues forming the putative

GAG binding site in domain 2. Thus, whilst the residues responsible for mediating the heterophilic interaction have not yet been defined, the heterophilic site is distinct from the homophilic site, and the CD-loop regions commonly used by other IgSF members which bind β1 and β2 integrin ligands are not used by CD31 to engage αvβ3.

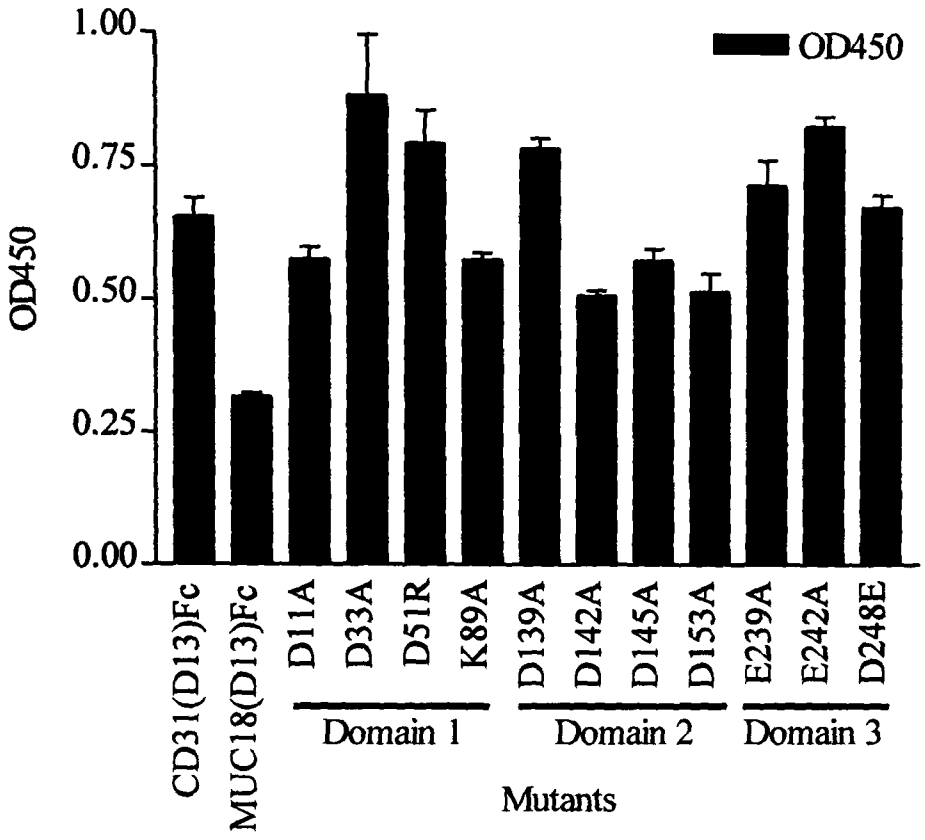


Figure 6.13. Analysis of heterophilic adhesion of CD31 to αvβ3 by site-directed mutagenesis. Binding of purified integrin αvβ3 to CD31 (D1-D3)Fc wild type and mutant proteins, and MUC18 (D1-D3)Fc negative control protein, was quantified by ELISA, using the anti-β3 integrin mAb F11 and anti-mouse HRP. Colour was developed with the OPD substrate. None of the residues targeting the CD-loop region of domain 3 had any effect on the binding of αvβ3 to CD31 indicating that the heterophilic site is not homologous to the residues identified in mediating adhesion of IgSF family members to β1 and β2 integrins. In addition, none of the residues identified previously as mediating homophilic adhesion had any effect on heterophilic adhesion, indicating that the homophilic and heterophilic binding sites are distinct. Source: ELISA 05.05.97

6.3 CD38 does not support adhesion via CD31.

Recently the group of Malavasi and co-workers have identified CD38 as a potential ligand for CD31. This work was based upon the finding that murine L-cells expressing human CD38 will bind to HUVEC (Human Umbilical Vein Endothelial Cell) monolayers. In an attempt to identify the ligand responsible for this adhesion, Malavasi's group screened monoclonal antibodies raised against HUVECs, and defined an antibody, Moon-1, which was capable of inhibiting the adhesion of L-cells expressing CD38 to endothelium (Deaglio et al., 1996). This antibody was shown to recognise a 120kDa highly glycosylated protein on endothelial cells, which was subsequently identified as human CD31 (Professor F. Malavasi, personal communication). Since work from others (Muller et al., 1992) has demonstrated that L-cells expressing human CD31 can bind to non-transfected L-cells in an apparently GAG-dependent fashion (DeLisser et al., 1993), we were interested to see if it were possible to verify these findings in our heterologous COS cell system.

CD38 cDNA in pCDM8 and mouse anti-CD38 mAbs 1B6 and OKT10 were a gift from Dr. David Jackson (Jackson *et al.*, 1992). CD38 was transiently expressed on COS-1 cells as per standard CD31 homophilic adhesion assays, and COS-1 cells expressing either CD31 or CD38 (Figure 6.14a) allowed to adhere to plastic coated with the CD31 domain deletion series (Figure 6.14b). In adhesion assays, cell expressed CD31 supported adhesion to full length CD31 (D1-D6)Fc protein as expected, however, cell expressed CD38 did not support adhesion above background binding to a MUC18 negative control protein. This data suggests that CD38 is not capable of supporting stable adhesive contacts via CD31 as a heterophilic ligand.

This contradicts the findings from Malavasi's group, and may be due to a number of factors. First, whilst performing the adhesion assays it was obvious from a visual inspection that CD38 over-expression has a profound effect on COS-1 cells; the cells showed a high propensity to aggregate, and required stringent washing conditions to remove cells from the negative control wells. This indicates that CD38 over-expression results in a non-specific adhesive phenotype. This is consistent with the observation that CD38 is an ecto-enzyme catalysing the conversion of NAD^+ to cyclic-ADP ribose (cADPR) (Sumerhill *et al.*, 1993, Howard *et al.*, 1993, and Takasawa *et al.*, 1993). In turn cADPR is a potent Ca^{2+}-mobilizing agent, and activator of downstream signal-transduction pathways, which may indirectly upregulate other adhesive pathways non-specifically. Second, the ability of Moon-1, an anti-CD31 mAb, to block the adhesion of CD38 expressing L-cells might be due to steric effects, since CD31 is highly expressed on endothelial cells (approximately 10^6 copies/cell). A cell highly decorated with antibody may not present a suitable adhesive substrate for L-cells to adhere to. Third, CD31 may not form stable adhesive contacts with CD38 *per se*, as tested here, but transient interaction between CD31 and CD38 may promote CD38 activity as a glycohydrolase and subsequent generation of cADPR, leading to adhesion via cross-talk to a second non-CD31 dependent pathway.

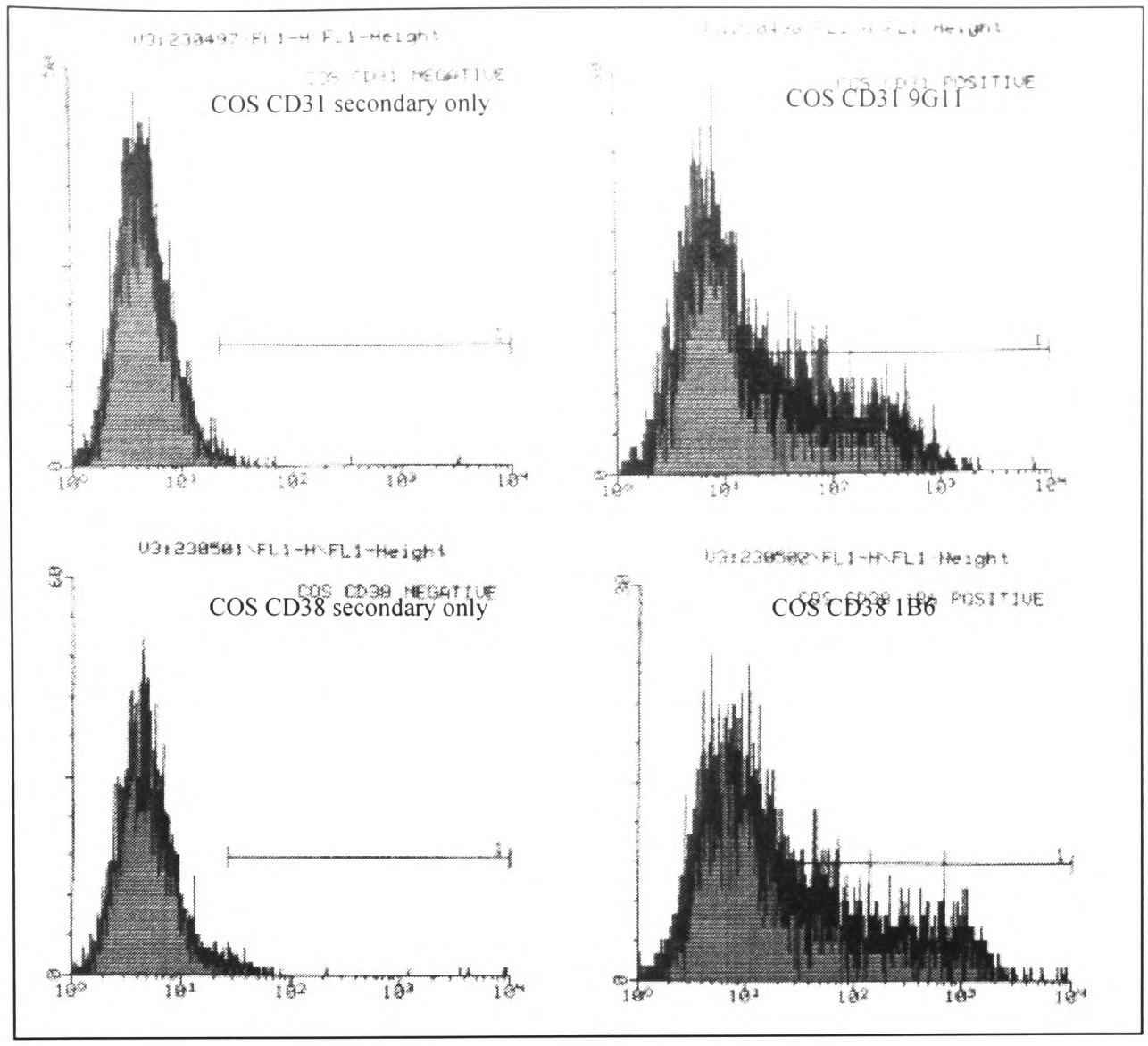


Figure 6.14a. Transient expression of CD38 and CD31 on the surface of COS-1 cells. COS-1 transiently expressing either CD31 or CD38 were stained with mAbs 9G11 (anti-CD31), 1B6 (anti-CD38) and OKT10 (anti-CD38 - data not shown) and goat anti-mouse.FITC conjugated secondary antibody, and analysed by FACScan with LYSIS II software. Both transient transfections results in expression of the appropriate CD antigen on the cell surface at comparable levels. (Approximately 34% of cells $CD31^+$ versus 35% of cells $CD38^+$).

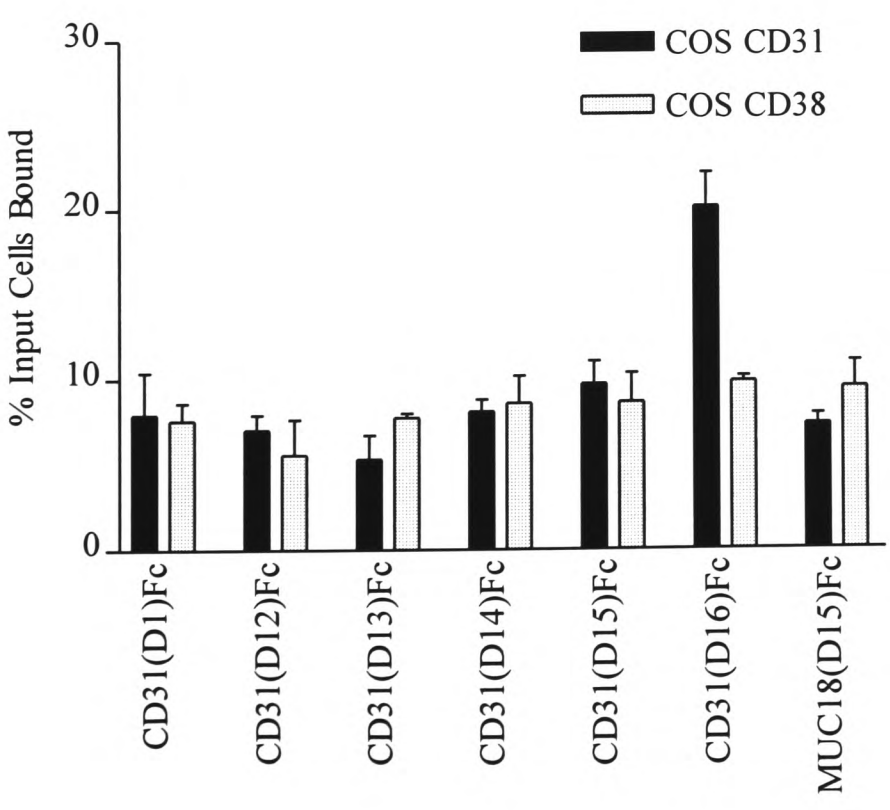


Figure 6.14b Adhesion of COS-1 cells expressing CD31 or CD38 to CD31Fc domain deletion series proteins. COS-1 cells transiently expressing either CD31 or CD38 (see figure 3.14a) were allowed to adhere to plastic coated with the CD31Fc domain deletion series of proteins. Cell expressed CD31 supported homophilic adhesion to full length CD31Fc protein as expected, however cell expressed CD38 did not support measurable adhesion to CD31 above background adhesion to negative control protein MUC18(D1-D5)Fc.

6.4 Discussion

The principle findings reported in this chapter may be summarised as follows: First, that U937 cells bind to CD31 in a manner very different from the pattern seen in homophilic adhesion in heterologous COS cells and other CD31 expressing cell lines. Adhesion of U937 to CD31 (D1-D6)Fc is temperature and divalent cation sensitive, suggestive of an integrin ligand, and this adhesion is blocked by functional antibodies directed against the integrin αvβ3, indicating that CD31 is a heterophilic ligand for the integrin αvβ3. Second, although U937 cells bind to all of the CD31Fc domain deletion series proteins, binding to constructs with either one, two, or three IgSF domains is non-specific. Third, using a protein-protein assay, the interaction between CD31 and αvβ3 was found to be a direct physical association, which exhibits specific and saturatable binding curves. Fourth, utilising the constructs previously generated to investigate homophilic adhesion (i.e. the domain deletion series, ICAM-3/CD31 chimeras) and a new CD31 construct lacking domain 3, the integrin binding site was mapped to domain 3 of CD31. Fifth, a series of single point mutations in domains 1, 2 and 3 showed that the αvβ3 binding site is independent of the homophilic binding site in domain 1 (see Chapter 3), the putative glycosaminoglycan (GAG) binding site in domain 2, and does not utilise any of the acidic residues in the C-strand or CD-loop of domain 3. Finally, in contrast to the findings of Malavasi and co-workers, it has not been possible to show that CD38 supports stable adhesion to CD31.

Much of the previously described work characterising CD31 homophilic adhesion (Chapter 3) relied upon the use of heterologous COS cell transfectants. In order to determine if these findings also applied in more physiological setting cell lines were screened for their ability to bind to CD31. In an initial screen of 11 cell lines representing different stages of haematopoiesis, two cell lines, KG1b and U937, both of which express CD31, were found to bind to CD31. KG1b adhesion to a nested series of CD31 domain deletion chimeras exhibited the same pattern as observed in homophilic adhesion assays with COS-1 cells transfected with CD31 and the previously characterised pre-B-cell line MIK-ALL . In contrast U937 cells bound in a very different manner to the previously characterised homophilic mode. Significant adhesion was observed with all CD31 proteins including CD31 (D1)Fc, with maximal binding requiring CD31 (D1-D3)Fc, but not with

negative control protein MUC18 (D1-D5)Fc. These findings suggested the existence of a novel counter receptor for CD31 on U937 cells.

Using a combination of biochemical and mAb blocking assays, U937 adhesion to CD31 was found to be dependent upon divalent cations and temperature, and inhibited by blocking antibodies raised against αvβ3, but not isotype matched control antibodies.

In addition to forming homophilic CD31-CD31 contacts, a number of heterophilic ligands have been proposed for CD31. The first suggestion that CD31 could mediate heterophilic adhesion came from studies which showed that L-cells expressing CD31 could bind in a cell-cell aggregation assay to non-transfected L-cells (Muller *et al.,* 1992), and that this aggregation could be blocked by heparin or peptides derived from CD31 corresponding to a putative glycosaminoglycan (GAG) binding site in domain 2 of CD31 (DeLisser *et al.*, 1993). This assay system has a number of significant weaknesses, principally that since it involves cell aggregation it is extremely difficult to control for post-receptor events such as signalling and triggering of other adhesive pathways. This latter possibility was not investigated or adequately controlled in the experiments reported by Muller *et al.*, 1992 and DeLisser *et al.*, 1993. It is well established that CD31 can function as a signalling molecule, by enhancing β1, β2 and β3 integrin mediated adhesion (Tanaka *et al.*, 1992, Piali *et al.*, 1992, Leavesley *et al.*, 1994, Fawcett *et al.*, 1995, Berman *et al.*, 1995, Jackson *et al.*, 1997), and by causing the release of pro-adhesive cytokines following co-ligation with FcRγII in monocytes (Chen *et al.*, 1994). The possibility that this GAG-mediated adhesion might not be due to direct CD31-GAG interaction was further suggested by the observation that truncation of the cytoplasmic tail (DeLisser *et al.*, 1994) of CD31 or removal of exon 14 (Yan *et al.,* 1995b) inhibits heterophilic adhesion. Exon 14 has recently been shown to be tyrosine phosphorylated on a TVYSEV motif by c-*src* kinase in response to a variety of physiological stimuli (Osawa *et al.*, 1997), and subsequently bound by the widely expressed tyrosine phosphatase SHP-2 (Jackson *et al.*, 1997) and also by the p85α subunit of PI3K (C. Buckley, personal communication). Given that the heterophilic GAG-mediated adhesion appears to be dependent upon sequences associated with the recruitment of signalling complexes, a model to explain the apparent heterophilic adhesion, is that initial homophilic CD31-CD31 adhesion between CD31 expressing L-cells results in phosphorylation of tyrosine 686 in exon 14 by *src* kinase and initiates downstream

signalling events which promote adhesion pathways (for example β1 integrin activation) which allow transfected L-cells to bind to non-transfectants. This explanation for the apparent GAG mediated heterophilic adhesion has now been accepted by some of the original authors (see for example, Jackson *et al* , 1997, and Sun *et al.*, 1996a), although this remains controversial.

Given the history of GAG mediated adhesion via CD31 outlined above, it was vital to show that CD31 physically interacted with αvβ3, and that the adhesion observed in U937 cells was not due to indirect signalling or cross-talk to αvβ3. Solid phase, protein-protein assays using both immobilised integrin and immobilised CD31, clearly demonstrate a specific, saturatable binding of CD31 to αvβ3 compared to negative control protein MUC18. Further studies using radiolabelled CD31, as dimeric CD31 (D1-D6)Fc protein, (C. Buckley and A. Sharma) allowed a fully quantitative measure of the interaction between CD31 and αvβ3. Scatchard analysis revealed an apparent dissociation constant of 4.1nM, which is comparable to that observed for dimeric ICAM-1 binding to LFA-1 (Miller *et al.*, 1995). Additional work (C. Buckley, personal communication) has also shown that the interaction of CD31 is highly specific to that integrin, as it does not bind to the related platelet integrin αIIbβ3 which shares a common β3 subunit with αvβ3. Collectively these results demonstrate a specific physical interaction between CD31 and αvβ3 which is independent of cell background, integrin activation state, post-integrin binding events such as cell spreading, and potential Fc receptor effects. This is consistent with the findings of Piali *et al.*, 1995, who were able to immunprecipitate αvβ3 from cell lysates using a CD31-kappa light chain fusion protein.

Initial evidence from U937 binding to the CD31 domain deletion series suggested that the minimal unit required for adhesion was domain 1, implying that this domain contained the heterophilic αvβ3 binding site. A more detailed analysis of U937 cells binding to a range of non-binding, size matched Fc proteins (MUC18 and NCAM domain deletion series), indicate that all IgSF-Fc constructs with 1, 2,or 3 IgSF domains bind non-specifically to U937. A specific element of CD31 binding only emerged in longer constructs of CD31. That non-specific adhesion occurred to truncated Fc proteins suggested that the heterophilic αvβ3 binding site was not contained within domain 1 as originally thought. Although not rigorously proven here, a plausible explanation for the non-specific adhesion of U937 cells

to short NH_2-terminal constructs is that in highly truncated Fc constructs, cell expressed Fc receptors may be able to access the Fc tag, whilst in longer constructs this is sterically blocked (U937 cells express FcRγIIa and b, CD32A and B). This hypothesis is supported by the observation that pre-incubation of U937 cells with human IgG inhibits adhesion to CD31 domain deletion series proteins. In order to verify this hypothesis a number of additional experiments are required, first and most obviously experiments with blocking antibodies against Fc receptors would directly address their role in U937 adhesion to Fc tagged proteins (a panel of anti-Fc receptor antibodies as monovalent Fab fragments is available from Medarix, New Hampshire, USA). Secondly, the cDNAs for the Fc receptors in expression vectors are available, and if Fc receptors were involved in adhesion to truncated forms of the domain deletion series then it ought to be possible to reconstitute this binding in heterologous COS cells expressing Fc receptors.

Due to complications arising from the non-specific adhesion to truncated Fc chimeras, studies to identify the domain(s) involved in mediating the interaction between CD31 and αvβ3 were limited to solid-phase protein-protein assays. The binding profile of purified αvβ3 to CD31Fc showed no specific adhesion of CD31 (D1)Fc or CD31 (D1-D2)Fc to αvβ3, however specific binding to CD31 (D1-D3)Fc and the other constructs of the deletion series was observed, which indicates that binding site is located in domain 3. This finding was confirmed using a range of ICAM-3/CD31 chimeras, which defined a dominant role for domain 3 in mediating adhesion to αvβ3. The use of an internal, rather than an NH_2-terminal immunoglobulin-like domain for integrin engagement is not unique, and has been observed in at least three other IgSF interactions, ICAM-1/Mac-1 (CD11b/CD18) which utilises ICAM-1 domain 3 (Diamond *et al.*, 1991), the VCAM/VLA-4 interaction which can be mediated by sequences in either domains 1 and 4 (Vonderheide *et al.*, 1994), and most recently the interaction between the NCAM-related adhesion molecule L1/NILE and the integrin αvβ3, which involves an RGD motif in domain 6 of L1 (Montgomery *et al.*, 1996).

The integrin αvβ3, although highly promiscuous in its ligand binding properties, is canonically thought of as being an RGD-dependent integrin, to date no ligands have been identified, either extracellular matrix (fibronectin, vitronectin, osteopontin, thrombospondin) or members of the immunoglobulin superfamily (L1/NILE), which do not

utilise an RGD-sequence. Examination of the primary amino acid sequence of CD31 shows no RGD sequences present in domain 3, or elsewhere in the extracellular domain. Although L1/NILE binding to αvβ3 is mediated by an RGD sequence (as shown by blocking with linear or cyclised RGD peptides and site-directed mutagenesis), this RGD motif is presented in the C-E' loop of domain 6, in a position equivalent to the QIDS motif in VCAM, and the GIETS/LETS motif identified in ICAMs. Examination of the putative CD-loop region and C-strand of CD31 domain 3 shows three acidic residues which might serve as an integrin binding site. Mutation of these three residues to alanine, showed no effect on the binding of CD31 (D1-D3)Fc to αvβ3 in solid phase binding assays. In addition mutations in domain 1 previously shown to affect homophilic adhesion (D11A, D33A, K50 and K89) had no effect confirming that the homophilic and heterophilic binding sites were distinct. These results indicate that CD31 binds the integrin αvβ3 by a novel mechanism which is not dependent on either an RGD-sequence, or an acidic residue in the CD-loop or C-strand as observed for VCAM and the ICAMs. Interestingly it has been shown that both RGD containing linear peptides and cyclised mimetics can inhibit the interaction between CD31 and αvβ3 (Piali *et al.*, 1995), and that RGD containing ligands such as fibronectin can displace bound CD31 from αvβ3, but not *vice versa* (A. Sharma, personal communication). There are two possible explanations for this, first that the interaction of RGD-containing ligands is of much greater affinity relative to CD31, so that it is not possible to directly compete off RGD based ligands, or second that the RGD-dependent ligands bind at a different site to CD31, and that the sites communicate allosterically via conformational changes. Clearly, more detailed classical kinetics studies will be required to distinguish between these possibilities, and to shed further light on the interaction of CD31 and RGD-containing ligands to αvβ3.

As noted, the integrin αvβ3 is highly promiscuous in its binding properties, binding to extracellular matrix proteins vitronectin, fibronectin, fibrinogen, von Willebrand factor, osteopontin and thrombospondin and also to IgSF-family members L1 and CD31. Moreover the αvβ3 heterodimer is widely expressed on endothelial cells, fibroblasts, smooth muscle cells, cells of the immune system, and some tumour cell lines (Cheresh, 1992; Brooks *et al.*, 1994). Similarly CD31 is widely expressed on vascular endothelium, platelets, leukocytes and some tumours, such that CD31-αvβ3 pairing may occur between multiple cell types, including cells of the immune system and vasculature. While CD31-

αvβ3 interactions may contribute to heterotypic or homotypic cell-cell adhesion, an additional role may be more related to the established role for αvβ3 engagement in regulating cell motility, survival and growth. For example αvβ3 has been shown to promote cell migration (Leaversley *et al.*, 1992), suppress apoptosis (Montgomery *et al.*, 1994), regulate angiogenesis (Brooks *et al.*, 1994), and stimulate mitogenesis (Sanders *et al.*, 1992).

Of particular note is the observation that monoclonal antibodies directed against both CD31 (see Chapter 7, Muller *et al.*, 1993, Vaporciyan *et al.*, 1993, Wakelin *et al.*, 1996), αvβ3 (Chapter 7), and the αvβ3 associated protein IAP/CD47 (Cooper *et al* ., 1995) all block the process of transendothelial migration during the inflammatory response. A fundamental characteristic of leukocyte migration through endothelial monolayers is the requirement to move through tight junctions. The electrical resistance of the endothelial monolayer is maintained during leukocyte extravasation, suggesting that even as the inter-endothelial junction is released to allow cell migration, new but transient junctions must be made between the migrating leukocytes and the endothelial cells between which it migrates. Leukocyte contact induces rearrangements and functional alterations in endothelial cadherins and catenins (Delmaschio *et al.*, 1996), as well as a $[Ca^{2+}]_i$ transient in these cells. Blocking changes in $[Ca^{2+}]_i$ in the endothelial cells inhibit leukocyte transmigration (Huang *et al.*, 1993). A hypothesis to explain the involvement of these molecules in transmigration is that CD31-αvβ3 contacts lead to a Ca^{2+} flux via CD47 associated with αvβ3 responsible for the dissociation of the cadherin-catenin complexes. CD31-αvβ3 heterophilic contacts, or CD31-CD31 homophilic contacts between leukocytes and endothelial cells might then serve to stabilise the integrity of the inter-endothelial junction. Since CD31 and αvβ3 are expressed on both leukocytes and endothelial cells, similar signalling effects might also occur in the leukocyte. It has been shown that engagement of αvβ3 enhances cell migration and motility. Of particular relevance is the observation that CD31-αvβ3 engagement leads to changes in mobility of leukocytes on VCAM-1 (B.A. Imhof, personal communication) with a parabolic dose dependence, such that increasing CD31 concentration co-coated at a fixed concentration of VCAM-1 results in an increase in mobility to a maximum, but this declines as the concentration of CD31 is further increased. The observation that certain cytokine treatments such as TNF-α and INF-γ result in a redistribution of CD31 from the inter-endothelial junctions to the apical surface of the endothelial cells (Romer *et al.*, 1995)

might provide a haptotactic gradient for leukocytes to migrate along to the endothelial junctions prior to transmigration. Thus, the αvβ3-CD31 complex may serve both as a direct adhesion complex and a signalling complex.

CD31 joins a group of cell adhesion molecules that are capable of mediating both homophilic and heterophilic adhesion to a range of different ligands, such as L1/αvβ3/axonin-1. Given that CD31 and αvβ3 are widely expressed on different cell types, potentially both homophilic and heterophilic adhesion could occur in parallel. The preferential usage of one adhesion pathway over another to regulate the adhesive properties of cells has been demonstrated for a variety of integrin/IgSF interactions. For example there appears to be a hierarchy of binding pathways for the integrins LFA-1 (Buckley *et al.*, 1997) and VLA-4 (Masumoto *et al.*, 1993). Similarly observations in both human and murine systems have shown that E-cadherin can mediate both homophilic, homotypic adhesion between epithelial cells, or heterophilic, heterotypic adhesion to the mucosal T cell integrin αEβ7 (Capek *et al.*, 1994; Karecla *et al.*, 1995). The regulation of homophilic versus heterophilic adhesion is likely to be complex. Whilst the ability of integrins to undergo changes in affinity is well established, IgSF members have not been noted to share this property until recently. Intriguingly there is now some evidence that CD31 can be induced to undergo conformational changes which affect homophilic adhesion (Sun *et al.*, 1996a, and Chapter 3),. In this respect it is probably important that CD31 exhibits a relatively low affinity for αvβ3, compared to extracellular matrix ligands, such that as cells pass through endothelial junctions, αvβ3 engages the basement matrix in preference to the endothelial CD31, allowing the cell to migrate into the tissue spaces.

The roles of CD31 and αvβ3 in mediating leukocyte transmigration are investigated further in the following chapter.

Chapter Seven: Functional consequences of CD31 engagement

7.1 Introduction

Previous chapters in this thesis have primarily addressed the structure-function relationships involved in different modes of CD31 mediated adhesion. This chapter describes experiments to investigate the functional consequences of CD31 engagement, and the role of CD31-αvβ3 contacts in leukocyte-endothelial interactions.

Previous studies have demonstrated that CD31 is normally localised to sites of cell-cell contact in confluent endothelial monolayers. However CD31 becomes diffusely distributed in cells at the leading edges of the migrating front during cell migration in wound healing assays (Schimmenti *et al.*, 1992). Ectopic expression of CD31 in fibroblast 3T3 cells reduces the rate at which the monolayer closes following the "wound", suggesting that CD31 may function to modulate cell migration. Cell migration on extracellular matrix components is mediated by integrins, primarily β1 integrins. Interestingly, several reports indicate that CD31 and integrin adhesive pathways cross-talk to one another, for example ligation of cell surface CD31 with antibodies increases β1-intregrin mediated adhesion in $CD8^+$ T lymphocytes (Tanaka *et al.*, 1992) and $CD34^+$ haematopoietic progenitor cells (Leavesley *et al.*, 1994). Similar antibody treatment also enhances β2 integrin mediated adhesion in murine LAK cells (Piali *et al.*, 1992), whilst Jackson *et al.*, 1997, have shown that β3 integrin engagement is accompanied by changes in the phosphorylation status of CD31 in platelets. Recently, Madri and co-workers (Lu *et al.*, 1996; Lu et al., 1997) have provided a mechanism to explain cross-talk with integrins by showing that CD31 tyrosine phosphorylation is regulated by β1 integrin engagement, and that the sites identified as being tyrosine phosphorylated are phosphorylatable by c-src and provide a docking site for SH2 domain containing proteins such as SHP-2 (see also Jackson *et al.*,1997).

To date, the effect of simultaneous engagement of both β1 integrins and CD31 on cell migration and motility has not been examined. On the basis of previous work (Tanaka *et al.*, 1992, Leavesley *et al.*, 1994), showing that CD31 engagement by mAbs leads to enhanced β1 adhesion, one might expect that this might inhibit migration.

7.2 Results

7.2.1 Engagement of CD31 on monocytes and endothelium enhances cell motility and induces changes in cell morphology

Several previous reports indicate that mAb cross-linking of CD31 induces enhanced adhesion mediated by integrins (Tanaka *et al.*, 1992; Piali *et al.*, 1992; Leaversley *et al.*, 1994). Rather than using antibodies to engage CD31, it was decided to use a more physiological stimulus and co-coat plastic with extracellular matrix and CD31 (D1-D6)Fc, since this would be expected to engage both homophilic and heterophilic ligands if present. Two cell types were selected, KG1b and HUVEC (Human Umbilical Vein Endothelial Cells). KG1b were selected since it is a motile cell type which has previously been shown to adhere to CD31 in an exclusively homophilic fashion (see Chapter 6, and Buckley *et al.*, 1996). HUVECs were used because endothelial cells are not normally mobile, cell migration is necessary under specific circumstances, for example during vasculogenesis, angiogenesis, and vessel repair following injury (Folkman 1995, Fan *et al.*, 1995).

24 well tissue culture plates (Nunc, Life technologies), were co-coated with goat anti-human Fc antibody and fibronectin, at 2.5µg/well and 5.0µg/well respectively, in PBS overnight at 4°C. Wells were washed with PBS and Fc proteins added at 12.5µg/well and incubated for 1 hour at 37°C (CD31 (D1-D6)Fc, MUC18 (D1-D5)Fc, NCAM (D1-D5)Fc or no Fc protein). Wells were washed once with PBS and once with cell culture media supplemented with 20mM HEPES. KG1b cells were harvested, spun down, and resuspended in fresh growth media supplemented with 20mM HEPES, whilst HUVECs were lifted in PBS containing 2mM EDTA, washed and resuspended in growth media containing 20mM HEPES. Cells were added to wells at $4x10^5$ cells/well, and adhesion followed by time lapse video microscopy for 10-60 minutes depending upon the experiment.

Initial exposure of KG1b to fibronectin alone showed that the cells did not adhere to, or spread on the substratum over the time course of the experiment, and that the cells were motile, although there was no evidence for chemotaxis or directed movement. KG1b cells exposed to surfaces co-coated with fibronectin and CD31 (D1-D6)Fc showed a number of significant differences to the fibronectin only control. First, the cells appeared much more motile, and second some cells appeared to undergo morphological changes. In fibronectin

only control experiments, the cells showed a rounded phenotype, with some evidence for cytoplasmic extension and retraction. When exposed to both CD31 and fibronectin the rate of movement of cells was notably increased, and a number of cells were visible (approximately 2-3%) with a flattened "amoeboid" morphology. These cells moved much more rapidly than the round phenotype, appearing to make contact with rounded cells via a series of uropod-like extensions, before moving off rapidly until contacting another cell. In similar experiments, HUVECs were found to adhere rapidly to fibronectin alone, moving from a rounded cell to becoming highly spread within 5-10 minutes of initial exposure to the extracellular matrix, as expected for adherent cells. Co-coating of fibronectin with CD31 had a profound effect on HUVECs; in contrast to initial predictions that CD31 engagement would enhance β1 integrin mediated adhesion to fibronectin, the cells remained rounded up and did not adhere and spread over the matrix. Moreover, almost all of the cells showed evidence for rapid cytoplasmic extension and retraction, often gyrating around a small area. This pattern was observed for 20-30 minutes before the cells eventually spread on the fibronectin, in contrast to fibronectin only exposed cells which were adherent within 5-10 minutes of plating. HUVECs exposed to fibronectin and an irrelevant IgSF-Fc protein, such as NCAMFc or MUC18Fc displayed the same rapid adhesion seen with fibronectin alone, indicating that the effect was not due to the Fc portion of the chimeric protein. CD31 (D1-D6)Fc alone without fibronectin did not support this effect, the cells remained rounded and only weakly adhered to the plastic.

It was clear from these initial observations that exposure of both KG1b and HUVEC to CD31 and fibronectin, compared to either fibronectin alone, or fibronectin plus an irrelevant Fc protein, had a profound effect on cell motility and morphology. This effect appears to be due to homophilic engagement of CD31, since KG1b cells have been shown to bind to CD31 in a homophilic fashion (see Chapter 6 and Buckley *et al.*, 1996), as have HUVECs (C. Buckley, personal communication). Moreover incubating HUVECs with blocking anti-αvβ3 mAb LM609 (at 5μg/well) did not inhibit the "gyrating" behaviour of HUVECs exposed to fibronectin and CD31 (data not shown).

7.2.2 Exposure of HUVEC to CD31 and fibronectin causes changes to cellular tyrosine phosphorylation status.

In the experiments reported above, changes in cell morphology and behaviour were observed within minutes of the cells settling on the plastic, suggesting that signalling events, rather than the induction of new gene expression, were involved. The rapid cytoplasmic extension and retraction require co-ordinated reorganisation of the cytoskeleton (reviewed by Bershadsky and Vasiliev, 1989), which is thought to involve small G-proteins of the Rac, Rho and cdc22 families (Hall, 1994) and focal adhesion kinase (FAK) amongst others (Hanks *et al.*, 1997). In order to begin investigating the signalling processes involved in regulating these changes, experiments were undertaken to determine the global status of phosphotyrosine containing proteins in cells exposed to fibronectin, fibronectin and CD31, and cells maintained in suspension in culture media alone. HUVECs were selected for investigation since the change from adherent to "gyrating" phenotype appears to involve a more significant variation in morphology than observed for KG1b cells. Plates were prepared as described above, and HUVECs were added to wells as before. Brief visual inspection confirmed that the HUVECs were "gyrating" in the CD31 treated wells, before cells were lysed *in situ* after 15 minutes by the addition of 1% SDS containing 1mM sodium orthovanadate. Lysates were rapidly collected and boiled for 5 minutes to inactivate phosphatases/proteases, and stored frozen at -20°C. Samples were thawed, warmed to re-dissolve precipitated SDS, and protein precipitated by adding ice cold (-20°C) acetone and spinning at 14,000g for 30minutes at 4°C. Pellets were washed, resuspended in reducing sample buffer, and resolved on 7.5% acrylamide gels. Gels were blotted onto nitrocellulose, blocked with 3% BSA/1% ovalbumin, and phosphotyrosine containing proteins directly detected with a HRP conjugated anti-phosphotyrosine antibody PY-20 and ECL (Figure 7.1)

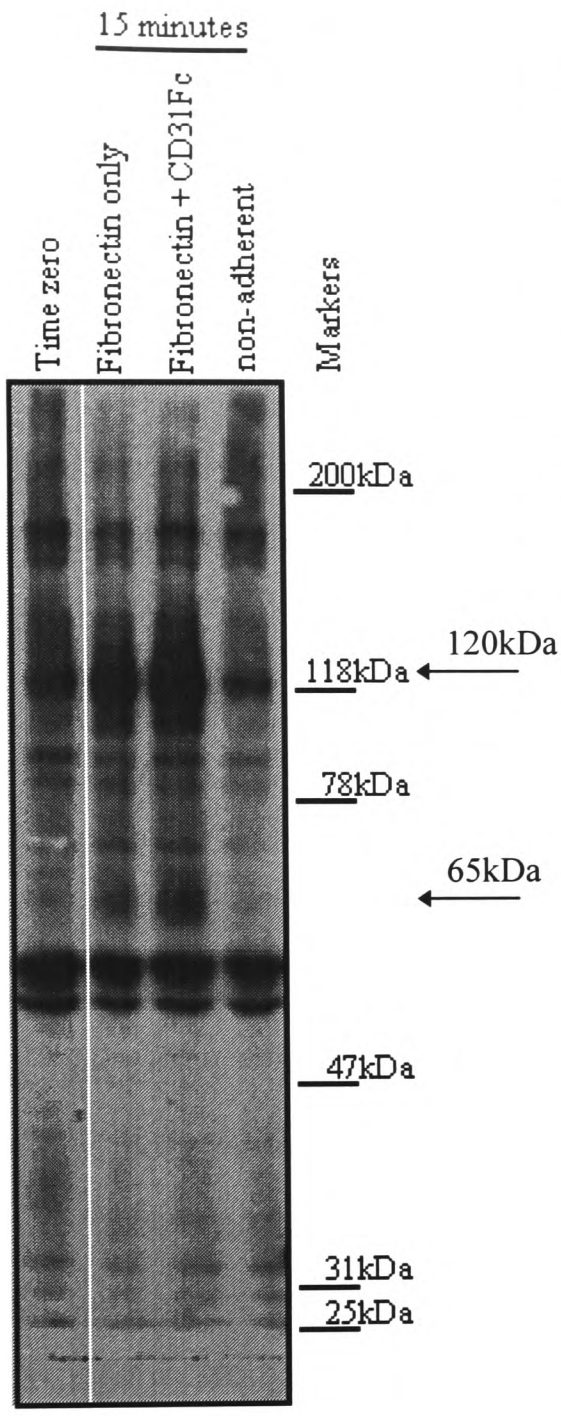


Figure 7.1 Cellular tyrosine phosphorylation status changes induced by exposure to CD31 and fibronectin compared to fibronectin and non-adherent cells. HUVEC exposed to fibronectin, fibronectin and CD31 and non-adherent HUVEC were lysed and total protein precipitated. The phosphotyrosine status was assessed by Western blot with PY-20, an anti-phosphotyrosine antibody. Adhesion causes an increase in intensity for several bands, whilst other proteins are unaffected and were used as a loading control. Comparison between fibronectin alone and fibronectin and CD31 shows that exposure to CD31 leads to an increase in tyrosine phosphorylation of protein(s) of apparent molecular weight 120kDa and 65kDa. Densitometry measurements show that the band intensity increased by 126% for the 65kDa band and 98% for the 120kDa band for cells exposed to fibronectin and CD31 compared to fibronectin alone.

As expected, HUVECs express a number of phosphotyrosine containing proteins, and the degree of tyrosine phosphorylation of several is increased by adhesion, and decreased when cells are maintained as non-adherent controls. Comparison of HUVEC lysates from cells exposed to fibronectin and CD31 against fibronectin alone shows increased tyrosine phosphorylation of protein(s) of apparent molecular weight 120kDa and 65kDa.

7.3 Role of CD31 and integrin αvβ3 in transmigration of monocytes across endothelial monolayers.

The importance of CD31 in leukocyte transmigration across endothelial monolayers is now well established both *in vitro* (Muller *et al.*, 1993; Liao *et al* 1996) and *in vivo* (Bogen *et al.*, 1993; Vaporciyan *et al.*, 1993), and in acute and chronic inflammation (Murohara *et al.*, 1996). The role of the integrin αvβ3 in transmigration is less well understood although the observation that antibodies against CD47/IAP, which forms a complex with αvβ3, inhibit neutrophil transmigration, point to a role for αvβ3 in leukocyte transmigration (Cooper *et al.*, 1995). Given the results reported in Chapter 6 (and Piali *et al.*, 1995; Buckley *et al.*, 1996), that CD31 is a ligand for the integrin αvβ3, it was of considerable interest to assess the role of both molecules during leukocyte transmigration. An *in vitro* model system was selected following the emigration of neutrophils from transwell chambers across an endothelial monolayer into the lower chamber (see Materials and Methods). This system is widely used to study inflammatory agonists/antagonists, is relatively robust, and utilises a cell type easily purified from the blood of healthy donors (Bird *et al.*, 1993). In order to investigate the roles of CD31 and αvβ3, functional blocking antibodies were generated. The generation and characterisation of a blocking anti-CD31 antibody (10B9) has been described previously (Chapter 3). A blocking anti-αvβ3 antibody clone 6C2 was generated in the laboratory by Dr. Christopher Buckley in collaboration with Mr. Ian Collins (R&D Systems Europe, Abingdon) using αvβ3 purified from the melanoma cell lines DX3 (purification as previously described, Chapter 6). 6C2 inhibits the adhesion of U937 cells to CD31 (D1-D6)Fc and K562/αvβ3 transfectant binding to vitronectin. Moreover, 6C2 recognises the αvβ3 heterodimer, but not the αv or β3 chains alone, as demonstrated by the fact that it does not recognise purified αIIbβ3 integrin in an ELISA, or K562/αvβ5 transfectants by FACS analysis (C. Buckley, personal communication).

Neutrophil adhesion/transmigration assays to IL-1β induced HUVEC monolayers were performed in collaboration with Mr. Matthew Wakelin and Dr. Sussan Nourshargh (National Heart and Lung Institute, Imperial College, London University) and Dr. Tim Stewart (Astra Charnwood, Loughborough, Leicestershire). In initial experiments, IL-1β stimulation gave a 5-fold increase in adhesion to endothelium, which was not affected by the presence of either anti-CD31 (10B9) or anti-αvβ3 (6C2) antibodies at 10μg/ml, but was partially inhibited by positive control anti-β2 (WT.3) antibody (Figure 7.4). This is consistent with earlier observations (Muller *et al.*, 1993), which showed that anti-CD31 antibodies do not inhibit the initial attachment and firm adhesion to endothelial monolayers, and that adhesion to endothelium of leukocytes involves the interaction of β2 integrins with ICAM-1 and ICAM-2 (Lo *et al.*, 1989). IL-1β stimulation enhanced the basal rate of transmigration by 9-10 fold. In contrast to the lack of effect of the anti-CD31 and anti-αvβ3 antibodies upon neutrophil adhesion to endothelium, both antibodies partially inhibited transmigration (Figure 7.4).

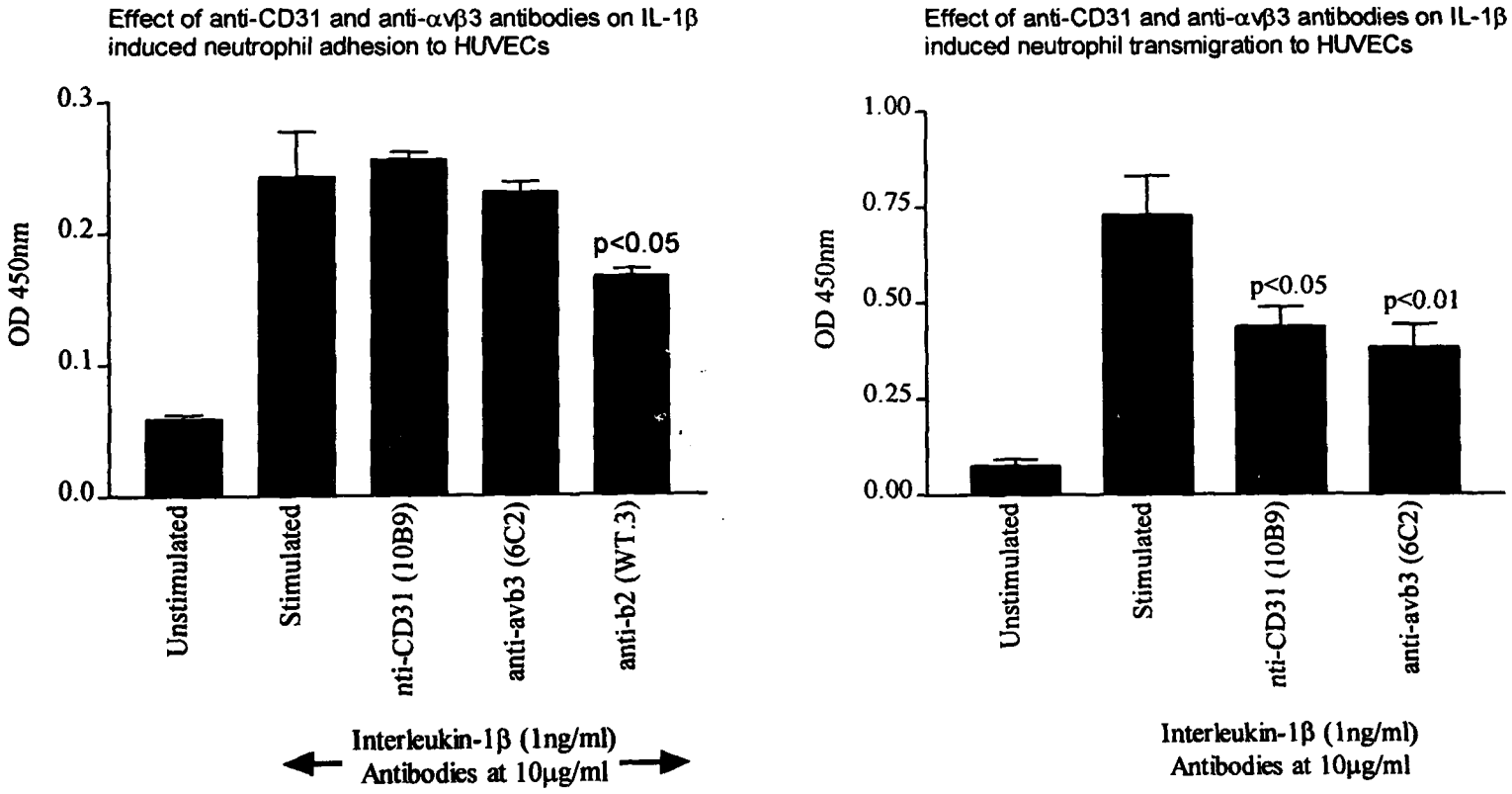


Figure 7.4 Effect of anti-CD31 and anti-αvβ3 antibodies on neutrophil adhesion and transmigration to HUVEC monolayers. The anti-CD31 and anti-αvβ3 antibodies (clones 10B9 and 6C2 respectively) were found to have no effect upon neutrophil adhesion to HUVEC endothelial monolayers (positive control anti-β2 antibody partially inhibited adhesion). In contrast both, anti-CD31 and anti-αvβ3 antibodies partially inhibit transmigration. The ability of anti-CD31 reagents to inhibit transmigration is well characterised (Muller *et al.*, 1993; Vaporciyan *et al.*, 1993), however there are no previous reports of integrin αvβ3 being involved in transmigration, although this possibility is strongly suggested by the observation that CD47, a molecule associated with αvβ3, also inhibit transmigration (Cooper *et al.*, 1995). Results are representative of three experiments, and results are expressed as mean OD ± 1 s.d. (n=3). Significance of antibody inhibition was determined by ANOVA with a Tukey post test.

The ability of anti-CD31 reagents to inhibit transmigration of leukocytes both *in vivo* and *in vitro* is well known and the results here confirm previous investigators findings, however there are no previous reports of anti-αvβ3 antibodies inhibiting transmigration, so this represents a novel and significant finding.

7.4 Discussion

In contrast to the earlier chapters in this thesis, which are largely concerned with dissecting the molecular basis of CD31 homophilic and heterophilic adhesion to αvβ3 using recombinant proteins and heterologous systems to reconstitute CD31 adhesion, this chapter describes experiments undertaken to investigate the functional significance of CD31 engagement. The findings may be summarised as follows: First, that CD31 homophilic engagement in parallel with exposure to fibronectin gives rise to a motile phenotype in both a promonocytic cell line and endothelial cell cultures. Second, this involves downstream signalling events leading to changes in the tyrosine phosphorylation status of the cell, indicating that CD31 functions as a signalling molecule as well as an adhesion molecule. Third, using anti-CD31 and anti-αvβ3 antibodies, it has been shown that CD31 is not required for neutrophil adhesion to endothelium, but is involved at the subsequent transmigration step. Intriguingly, anti-αvb3 antibody also partially inhibited transmigration. This is therefore the first direct evidence that αvβ3 is involved in transmigration.

Several previous investigators have shown that CD31 engagement by monoclonal antibody induces upregulation of integrin mediated adhesion, it was surprising to find that both KG1b cells (a motile, monocyte-like cell line) and HUVEC endothelial cells showed increased motility when exposed to plastic surfaces co-coated with fibronectin and CD31. This was a CD31 specific response, as MUC-18 and NCAM had no effect when substituted for CD31. The observed increase in cell motility appears to be due to homophilic engagement, since it is observed for in KG1b cells which have previously been shown to bind in a predominantly homophilic fashion (Chapter 6), and was not inhibited in HUVECs incubated with a functional blocking antibody against αvβ3. Changes in cell motility are associated with cytoskeletal changes and intracellular signalling pathways. Consistent with

this expectation, examination of the global cellular phosphotyrosine status shows changes induced by exposure to CD31 and fibronectin, compared to fibronectin alone, or cells maintained in suspension. Specifically protein(s) of apparent molecular weight 120kDa and 65kDa show increased tyrosine phosphorylation. These identity of these phosphoproteins is an area for future investigation, however several possibilities are suggested by recent reports that indicate CD31 can function as a signal transducing molecule itself becoming tyrosine phosphorylated by c-src kinase in response to physiological stimuli, such as platelet aggregation (Jackson et al., 1997), shear flow (Osawa *et al.*, 1997) and IgE receptor engagement (Sagawa *et al.*, 1997), resulting in the recruitment of SHP-2 tyrosine phosphatase via its SH-2 domain. The experiments presented here are preliminary, but define useful model systems for further investigation of the downstream signalling events induced by CD31 engagement. An initial method would be to take a candidate approach by immunoprecipitating CD31 and probing by western blot with antibodies against known signalling molecules such as SHP-2 or src-kinase. Also since the motile phenotype is a readily observed phenomenon, it ought to be possible to screen a large number of inhibitors of different signalling pathways for functional effects relatively quickly. This may then provide additional leads to inform the candidate approach outlined above.

The functional and physiological significance of these observations may be that cells use CD31 to promote motility in addition to a role in cell adhesion, for example during would healing or vascular remodelling, endothelial cells are required to migrate. A combination of extracellular matrix and CD31-CD31 contacts (provided either by other endothelial cells or by platelets) may help endothelial cells to migrate to the correct position and orientate themselves with respect to other endothelial cells. Similarly, during leukocyte recruitment to sites of inflammation, CD31 expressed on the apical surface of endothelial cells with appropriate integrin ligands (Romer *et al.*, 1995) may form a haptotactic gradient, promoting leukocyte motility towards endothelial cell-cell junctions thus increasing the rate of transmigration.

The role of CD31 and one of its heterotypic ligands, the integrin αvβ3, in neutrophil transmigration across endothelial monolayers was investigated in an *in vitro* model. This showed that CD31 and αvβ3 are not required for neutrophil adhesion to endothelium, but that antibodies against either CD31 or αvβ3 partially inhibit transmigration. These initial

experiments are tantalisingly suggestive of the possibility that CD31 might serve as a ligand for the integrin αvβ3 during transmigration, however additional experiments are required to confirm this hypothesis. Firstly, the anti-CD31 antibody (10B9) was originally characterised as an inhibitor of homophilic adhesion , recognising an epitope in domain 3 of CD31. Other anti-CD31 antibodies which block homophilic adhesion have been shown to inhibit heterophilic adhesion (Buckley *et al.*, 1996), however this has not yet been shown for 10B9; although anti-αvβ3 antibody clone 6C2 has been shown to block binding of αvβ3 to CD31. One obvious further experiment will be to assess the ability of both antibodies simultaneously to inhibit transmigration; if they show an additive effect then this would indicate that the antibodies are blocking different adhesive pathways, whereas if combined antibody treatment show a similar level of partial inhibition as found with the individual mAbs, this would support the hypothesis that they are counter ligands. These experiments are currently ongoing.

In the past, it has been assumed that transmigration of leukocytes across endothelium was dependent on interactions between endothelial cells and leukocytes mediated at least in part by homophilic CD31 contacts. This conclusion was based upon the observation that pre-treatment of either the neutrophils or endothelial monolayer with anti-CD31 monoclonals resulted in inhibition of transmigration (Muller *et al.*, 1993). This interpretation becomes more difficult to sustain as CD31 is a ligand for αvβ3, particularly since both are expressed on endothelium and leukocytes. Inhibition of CD31 heterophilic adhesion in either the endothelial cell or leukocyte may inhibit the process of transmigration either by reducing the strength of adhesive interactions between neutrophil and endothelial cell directly, or more subtly, since transmigration requires the active involvement of both the endothelial cells and leukocytes, by blocking the signalling events (for example calcium transient fluxes leading to cell-cell junction and cytoskeletal reorganisation) which are induced by cell-cell contact (for review see Brown, 1997). Alternatively, and invoking a further level of complexity, both homophilic and heterophilic interactions may be necessary to achieve transmigration, either sequentially or in parallel. A key future aim to investigate the possible role of CD31-αvβ3 contacts during transmigration will be to develop specific reagents which affect either homophilic or heterophilic adhesion.

Chapter Eight: General Conclusions and Suggestions for Further Work.

A. Conclusions and Discussion

CD31 (Platelet Endothelial Cell Adhesion Molecule, PECAM-1), a member of the immunoglobulin superfamily (IgSF), was amongst the first endothelial adhesion molecules to be cloned (Simmons *et al.*, 1990), along with VCAM-1 (Osborn *et al.*, 1989). Unlike VCAM-1 however, where the mechanism of adhesion to the integrins $\alpha4\beta1$ and $\alpha4\beta7$ have been extensively studied by various research groups with convergent conclusions, studies from different researchers on CD31 mediated adhesion have produced confusing and contradictory results.

This is in part because CD31 is an extremely versatile adhesion molecule mediating direct adhesive interactions to homophilic and heterophilic ligands in addition to indirect effects arising through signalling and "cross-talk" to integrins. It is well established that CD31 is capable of mediating homophilic adhesion however the domains involved have been subject to vigorous debate. The first attempt to map the interacting domains of CD31 was made by Fawcett *et al.*, 1995 using a series of truncated CD31Fc proteins (see also Chapter 3), which showed that the membrane proximal domains 5 and 6 were required to mediate homophilic adhesion in the context of the full length molecule. Using the same series of CD31Fc proteins, antibodies which blocked homophilic adhesion were mapped to the membrane distal domains. This data was explained in terms of an anti-parallel interdigitating model of adhesion, in which the membrane proximal domains of CD31 expressed on the surface of one cell bind to the membrane distal domains of CD31 expressed on an apposing cell surface and *vice versa,* in a model analogous to that proposed for the carcinoembyonic antigen (Zhou *et al.*, 1993).

In apparent contrast, Albelda and Newman's groups have implicated domains 1 and 2 as mediating homophilic adhesion using recombinant CD31 constructs lacking either of the membrane proximal domains 1 or 2, or chimeras between human and mouse CD31 (Yan *et al.*, 1995; Sun *et al.*, 1996a; Sun *et al.*, 1996b). Others have identified a role for the

membrane proximal domains on the basis of antibody and peptide blockade (Zehnder *et al.*, 1996).

In this thesis, I have confirmed that the homophilic binding site is contained within the NH_2-terminal domains using a combination of human/mouse CD31 chimeras and ICAM-3/CD31 chimeras. Importantly, results from the ICAM-3/CD31 chimeras show that the NH_2-terminal domains containing the homophilic binding site are not sufficient to support stable homophilic adhesion, and require the presence of the membrane proximal domains to perform a non-binding accessory role. This provides a consensus model which provides a conceptual framework that explains the results obtained by a number of different groups working independently over the past seven years.

The accessory role of the membrane proximal domains may be to mediate lateral associations between CD31 molecules in the same cell membrane clustering multiple homophilic binding sites. This may increase the avidity of CD31 interactions to achieve stable adhesive contacts between cells. There is a growing corpus of evidence that self association and clustering of adhesion molecules is a key mechanism controlling the adhesive properties of cells. For example, dimerisation of ICAM-1 increases the measured affinity with LFA-1 (Miller *et al.*, 1995), whilst clustering of ICAM-2 to uropods is necessary for natural killer cell cytotoxicity directed against melanoma cells (Helander *et al.*, 1996). This hypothesis is consistent with the observation that both soluble recombinant and cell expressed CD31 exist in an equilibrium between monomeric and dimeric forms (Chapter 4), and that homophilic adhesion is dependent upon the level of cell surface expression (Sun *et al.*, 1996b).

CD31 is widely expressed on the cells of the vasculature, including endothelia, platelets, and most leukocytes. One substantial difficulty in understanding the functional role of CD31 is to explain why CD31 expressing cells to not undergo spontaneous self association. Cells may be able to regulate their adhesive properties by regulating the cellular distribution of CD31, so that at high local concentrations of CD31 as observed at the endothelial cell-cell junctions, CD31 exists in a self-associated dimeric form capable of mediating homophilic adhesion, whilst if CD31 diffusely expressed on the cell surface (for example on the surface of leukocytes and platelets) then CD31 exists as a monomeric form

not competent to mediate homophilic adhesion. Importantly it has long been known that CD31 can become associated with the actin cytoskeleton (Newman *et al.*, 1992), and more recently that the cytoplasmic tail can associate with β-catenin (Matsumura *et al.*, 1997). An exciting possibility is that CD31 localisation and adhesive properties can be regulated in a fashion similar to cadherin/catenin complexes in endothelial/epithelial cells. This is also suggested by the observation that the cell distribution of CD31 is changed in endothelial cells following stimulation with inflammatory cytokines (Romer *et al.*, 1995).

One of the most interesting findings in this thesis is that although the homophilic binding site has been located in the NH_2-terminus, antibodies which block homophilic adhesion are located throughout the extracellular domain (domains 2, 3 and 5), whilst stimulatory antibodies are located in the membrane proximal domains, well away from the homophilic binding site. This is analogous to the situation in integrins where antibodies with stimulatory and inhibitory effects map throughout the extracellular domain, whereas ligand binding sites on integrins are located at the interface between NH_2-terminal domains of the α and β subunits. For integrins this has been interpreted in terms of conformational changes leading to changes in ligand binding (Mould *et al.*, 1996, Humpries *et al.*, 1996). If this is true for CD31, then this would be the first example seen outside of the integrin family of a cell adhesion molecule with binding properties regulated by conformational changes. One possibility is that these conformational changes are linked to the ability to CD31 to form monomers and dimers.

A large number of heterophilic ligands for CD31 have been proposed, including aglycosaminoglycan decorated ligand on murine L-cells (DeLisser *et al.*, 1993), a 120kDa ligand on T-cells (Prager *et al.*, 1996), the integrin αvβ3 (Piali *et al.*, 1995, Buckley *et al.*, 1996, Chapter 6), and CD38 (Professor Malavasi, personal communication). However, for many of these ligands is has not proved possible to show a direct adhesive interaction *per se*, and for a number, particularly glycosaminoglycans, it now appears that the apparent interaction may be due to indirect "cross-talk" mediated by signalling following homophilic interactions (Jackson *et al.*, 1997). Importantly, in Chapter 6, I have shown by solid phase protein-protein assays that the interaction between αvβ3 and CD31 is a direct physical association, and mapped the domain mediating CD31-αvβ3 interaction to domain 3. A preliminary mutagenesis screen showed that acidic residues in the C-strand and CD-

loop of this domain are not involved in mediating the interaction between CD31 and αvβ3, in contrast to the previously characterised interactions between IgSF family members and β1 (VCAM-1/VLA-4), β2 (ICAM/LFA-1) and β7 (MAdCAM-1/α4β7) integrins. One potentially informative interaction is the binding of E-cadherin to the integrin αEβ7, which has been shown to be mediated by a critical glutamate residue in the BC-loop of the NH_2-terminal domain of E-cadherin (Karecla *et al.*, 1996). The structure of E-cadherin (Nagar *et al.*, 1996) shows that cadherins and members of the immunoglobulin superfamily have a similar fold topology. Sequence alignment of individual immunoglobulin domains of CD31 (Watt *et al.*, 1995) shows that the BC-loop in domain 3 of CD31 is extended compared to the BC-loop region in the other CD31 immunoglobulin domains and contains an glutamate residue equivalent to the critical glutamate residue of E-cadherin. This clearly represents the next choice of target in a rational mutagenesis strategy.

The functional consequences of CD31 mediated adhesion has been tested in a number of *in vitro* assays (Chapter 7). In common with other research groups, antibodies against CD31 have been shown to block neutrophil transmigration across endothelial monolayers, and in the same assay that the integrin αvβ3 is also involved in transmigration. These are preliminary experiments, and the relationship between CD31 and αvβ3 in transmigration is not clear and will require substantial further experiments, since it is not clear that the antibodies used will block homophilic, heterophilic, or both forms of CD31 mediated adhesion.

In simple time-lapse video microscopy experiments, exposure of both endothelial cells and leukocytes to fibronectin and CD31 enhances cell motility, associated with changes in total tyrosine phosphorylation status of the cell. This finding was a surprise since CD31 engagement has previously been shown to result in enhanced β1 integrin mediated adhesion. This suggests that the role of CD31 may be to promote cell migration in addition to cell adhesion.

B. Suggestions for further work/areas of investigation.

In this thesis I have already analysed and discussed the significance of the results obtained in the appropriate chapters within the context of the associated discussion sections. As part of this discussion, limitations of the experiments performed and suggestions for further

experiments to clarify and incrementally advance understanding of CD31 structure and function were proposed. I do not intend to re-iterate these comments here, and instead suggest some broader areas of future research.

1. **Functional significance of monomeric and dimeric forms of CD31**

   In this thesis I have shown that CD31 exists in an equilibrium between monomeric and dimeric forms. It is proposed that this might regulate the adhesive properties of CD31 in a fashion analogous to other adhesion molecules such as ICAM-1 and E-cadherin. One of the major limitations to investigating this possibility is the lack of specific reagents against one or other form. In the case of ICAM-1, the antibody CA7 binds preferentially to monomeric ICAM-1 (Miller *et al.*, 1995). CA7 was generated fortuitously, however a strategy to generate antibodies specific to monomers or dimers of CD31 would be to "trap" dimeric CD31 by chemical cross-linking, and use this as an immunogen to generate anti-CD31 antibodies. Cross-linked protein may be resolved into monomeric and dimeric fractions by gel filtration, and the resolved fractions used to screen for differential binding of monoclonal antibodies to identify those specific for monomeric or dimeric forms. Such reagents might then be used to examine the specific location of different forms of CD31 and to test some of the predictions outlined previously. For example, if CD31 dimerisation is necessary for homophilic adhesion, then one would expect that antibodies specific for dimeric CD31 would preferentially stain cell-cell contacts between CD31 expressing cells. Similarly, if the antibodies which stimulated homophilic adhesion identified in Chapter 3 cause conformational changes favouring dimerisation, these ought to induce the binding of antibodies specific for CD31 dimers.

2. **Functional significance of CD31 homophilic and CD31-αvβ3 heterophilic interactions.**

   Recent work from several groups has produced a consensus model for CD31 homophilic adhesion, which emphasises the role of the NH_2-terminal domains in mediating direct homophilic adhesion, but that the membrane proximal domains of CD31 are involved in regulating adhesion mediated by CD31. Whilst this consensus has emerged for homophilic adhesion, the functional significance of the various heterophilic ligands proposed for CD31 remains highly controversial. For example several groups have identified the integrin αvβ3 as a ligand for CD31 (Piali *et al.*, 1995, Buckley *et al.*,

1996, see Chapter 6), but others have found no evidence for an interaction between CD31 and αvβ3 (Sun *et al.*, 1996a). Whilst the results in this thesis demonstrate in an *in vitro* protein-protein assay that CD31 is capable interacting directly with αvβ3, and that in transmigration assays that both CD31 and αvβ3 are involved in transmigration, further work is required to confirm the physiological significance of the interaction. An obvious approach is to screen for antibodies with a specific functional effect on either homophilic or heterophilic adhesion (in this context it would be interesting to determine the effect of antibodies observed to enhance homophilic adhesion on heterophilic adhesion). A less direct approach which may be informative is to examine the distribution of CD31 in neutrophils undergoing transmigration across endothelial monolayers. During transmigration the endothelial cells and neutrophils are in close proximity, and the amount of CD31 expressed by endothelial cells so large that it would not be possible to examine the location of CD31 expressed by neutrophils relative to CD31 expressed by endothelial cells. One possible way to avoid this difficulty would be to exploit the fact that there are at least two alleles of CD31 present in the population, caused by a single amino acid difference in domain 2 (leucine to isoleucine), a difference which can be detected with monoclonal antibodies (Behar *et al.*, 1996). By careful choice of donors with different CD31 alleles it should be possible to stain CD31 expressed by endothelial and neutrophil independently, which when combined with the distribution of αvβ3 may give qualitative information on the role of homophilic and heterophilic adhesion mediated by CD31.

3. **Are there novel endothelial and leukocyte adhesion molecules to be discovered?**

   CD31 is of particular interest as a potential target for anti-inflammatory therapeutics, since its involvement in the immune system appears to be limited to leukocyte transmigration, rather than other aspects of the initiation of an immune response. The process of transmigration is poorly understood and the first step in understanding a process is to determine the nature of the molecules involved. Historically, following an initial period of discovery/cloning in the late 1980's and early 1990's, relatively few new endothelial adhesion molecules have been cloned. The recent implication of a novel member of the immunoglobulin superfamily (JAM-1) in transmigration suggests that there are other adhesion molecules to be identified. One future area of investigation will be to undertake a saturation cloning effort of all endothelial cell surface molecules. In

the past expression cloning has proved an extremely powerful technique, but requires the generation of specific monoclonal antibodies. Recent work carried out in this laboratory has shown that it is possible to clone cDNAs using the supernatants from 96-well primary fusion plates (D. Simmons, personal communication), so that it will be possible to greatly speed-up the process of cloning. By iterative application of this technique, screening the supernatants against previously isolated cDNAs, it should be possible to clone most cell surface proteins relatively quickly, subject to the limitations of the experimental technique (size of cDNA, single chain molecules, etc.). Once the molecular players have been identified, the role of these cell surface molecules can be assessed in parallel to the roles of the known adhesion molecules during leukocyte recruitment and transmigration.

Despite having been studied for more than a decade, CD31 continues to be an active area of research. Recent work has begun to clarify the mechanisms by which CD31 mediates adhesion, however the physiological significance and integration of the different modes of CD31 adhesion are likely to be key areas of future research.

References

Ager, A. (1987) Isolation and culture of high endothelial cells from rat endothelial cells from lymph nodes. *Journal of Cell Science*87 133-144.

Airas, L., Salmi, M., Jalkanen, S. (1993) Lymphocyte-vascular adhesion protein-2 is a novel 70-kda molecule involved in lymphocyte adhesion to vascular endothelium. *Journal of Immunology* 151 4228-4238

Albelda, S.M., Muller, W.A., Buck, C.A. and Newman, P.J. (1991). Molecular and cellular properties of PECAM-1 (endoCAM/CD31): a novel vascular cell-cell adhesion molecule. *Journal of Cell Biology*. 114: 1059-1068.

Alemany, M., Concord, E., Garin, J., Vinçon, M., Marguerie, G., Guilino, D. (1996) Sequence 274-368 in the β3 subunit of the integrin αIIbβ3 provides a ligand recognition and binding domain for the γ chain of fibrinogen that is independent of platelet activation. *Blood* 87 592-601.

Allport, J.R., Ding, H.T., Ager, A., Steeber, D.A., Tedder, T.F., Luscinskas, F.W. (1997) L-selectin shedding does not regulate human neutrophil attachment, rolling, or transmigration across human vascular endothelium in-vitro. *Journal of Immunology* 158 4365-4372.

Alon, R., Hammer, D.A., Springer, T.A. (1995) Lifetime of the P-selectin-carbohydrate bond and its response to tensile force in hydrodynamic flow. *Nature* 374 539-542.

Al-Shamkhani, A., Mallett, S., Brown, M.H., James, W., Barclay, A.N. (1997) Affinity and Kinetics of the Interaction between Soluble Trimeric OX40 Ligand, a Member of the Tumor Necrosis Factor Superfamily, and Its Receptor OX40 on Activated T Cells *Journal of Biological Chemistry* 272 5275-5282.

Arbones, M.L., Ord, D.C., Ley, K., Ratech, H., Maynardcurry, C., Otten, G., Capon, D.J., Tedder, T.F. (1994) Lymphocyte homing and leukocyte rolling and migration are impaired in L-selectin-deficient mice. *Immunity* 1 247-260

Aruffo, A., Stamenkovic, I., Melnick, M., Underhill, C.B., Seed, B. CD44 is the principle cell surface receptor for hylaluronate (1990) *Cell* 61 1303-1313.

Arvilommi, A.M., Salmi, M., Kailmo, K. and Jalkanen, S. (1996). Lymphocyte binding to vascular endothelium in inflamed skin revisited: a central role for vascular adhesion protein 1 (VAP-1). *European Journal of Immunology* 26 825-833.

Ayalon, O., Sabanai, H., Lampugnani, M-G., Dejana, E., Geiger, B. (1994) Spatial and temporal relationships between cadherins and PECAM-1 in cell-cell junctions of human endothelial cells. *Journal of Cell Biology* 126 247-258.

Bailly, P., Hermand, P., Callebaut, I., Sonneborn, H.H., Khamlichi, S., Mornon, J.P., Cartron, J.P. (1994) The LW blood-group glycoprotein is homologous to intercellular-adhesion molecules. *Proceedings of The National Academy of Sciences (USA)* 91 5306-5310.

Bailly, P., Tontti, E., Hermand, P., Cartron, J.P., Gahmberg, C.G. (1995) The red-cell LW blood-group protein is an intercellular-adhesion molecule which binds to CD11/CD18 leukocyte integrins. *European Journal of Immunology* 25 3316-3320.

Bajt, M.L., Goodman, T., McGuire, S.L. (1995) β2 (CD18) mutations abolish ligand recognition by I domain integrins LFA-1 (αLβ2, CD11a/CD18) and Mac-1 (αMβ2, CD11b/CD18) *Journal of Biological Chemistry* 270 94-98.

Baldwin, H.S., Shen, H.M., Yan, H-C., DeLisser, H.M., Chong, A., Mickanin, C., Trask, T., Kirschbaum, N.E., Newman, P.J., Albelda, S.M. and Buck, C.A. (1994). Platelet endothelial cell adhesion molecule-1 (PECAM-1/CD31): alternatively spliced, functionally distinct isoforms expressed during mammalian cardiovascular development. *Development* 120 2539-2553.

Barclay, A.N., Birkeland, M.L., Brown, M.H., Beyers, A.D., Davis, S.D., Somoza, C., Williams, A.F. (1993) The leukocyte antigen FactsBook. Academic Press, London.

Bargatze, R. F. and Butcher, E. C. (1993). Rapid G protein-regulated activation event involved in lymphocyte binding to high endothelial venules. *Journal of Experimental Medicine*. 178 367-372.

Bargatze R.F., Kurk S., Butcher E.C., Jutila M.A. (1994) Neutrophils roll on adherent neutrophils bound to cytokine-induced endothelial-cells via l-selectin on the rolling cells. *Journal of Experimental Medicine* 180 1785-1792

Bartolazzi, A., Jackson, D., Bennett, K., Aruffo, A., Dickinson, R., Shields, J., Whittle, N., Stamenkovic, I. (1995) Regulation of growth acid dissemination of a human lymphoma by CD44 splice variants. *Journal of Cell Science* 108 1723-1733.

Bartolazzi, A., Nocks, A., Aruffo, A., Spring, F., Stamenkovic, I. (1996) Glycosylation of CD44 is implicated in CD44-mediated cell-adhesion to hyaluronan. *Journal of Cell Biology* 132 1199-1208.

Bateman A, Jouet M, MacFarlane J, Du JS, Kenwrick S, Chothia C (1996) Outline structure of the human L1 cell adhesion molecule and the sites where mutations cause neurological disorders. *EMBO Journal* 15 6050-6059.

Bazan, J.F., Bacon, K.B., Hardiman, G., Wang, W., Soo, K., Rossi, D., Greaves, D.R., Zlotnik, A., Schall, T.J. (1997) A new class of membrane-bound chemokine with a CX_3C motif. *Nature* 385 640-644.

Behar, E., Chao, N.J., Hiraki, D.D., Krishnaswamy, S., Brown, B.W., Zehender, J.L. and Grumet, C. (1996). Polymorphism of adhesion molecule CD31 and its role in acute graft versus host disease. *New England Journal of Medicine*. 334: 286-291.

Bennett, K.L., Jackson, D.G., Simon, J.C., Tanczos, E., Peach, R., Modrell, B., Stamenkovic, I., Plowman, G., Aruffo, A. (1995a) CD44 isoforms containing exon v3 are responsible for the presentation of heparin-binding growth-factor. *Journal of Cell Biology* 128 687-698.

Bennett, K.L., Modrell, B., Greenfield, B., Bartolazzi, A., Stamenkovic, I., Peach, R., Jackson, D.G., Spring, F., Aruffo, A. (1995b) Regulation of CD44 binding to hyaluronan by glycosylation of variably spliced exons. *Journal of Cell Biology* 1311623-1633

Berendt, A. R., Simmons, D. L., Tansey, J., Newbold, C. I., and Marsh, K. (1989) Intercellular adhesion molecule-1 is an endothelial cell adhesion receptor for *Plasmodium falciparum*. *Nature* 341, 57-59

Berg, E.L., McEvoy, L.M., Berlin, C., Bargatze, R.F., Butcher, E.C. (1993) L-selectin-mediated lymphocyte rolling on MAdCAM-1. *Nature* 366 695-698.

Berg, E.L., Yoshino, T., Rott, L.S., Robinson, M.K., Warnock, R.A., Kishimoto, T.K., Picker, L.J. and Butcher, E.C. (1991). The cutaneous lymphocyte antigen is a skin lymphocyte homing receptor for the vascular lectin endothelial cell-leukocyte adhesion molecule-1. *Journal of Experimental Medicine*. 174 1461-1466

Berlin, C., Berg, E.L., Briskin, M.J., Andrew, D.P., Kilshaw, P.J., Holzmann, B., Weissman, I.L., Hamann, A., Butcher, E.C. (1993) Alpha-4-beta-7-integrin mediates lymphocyte binding to the mucosal vascular addressin MAdCAM-1. *Cell* 74 185-195.

Berman, M.E., Muller, W.A. (1995) Ligation of platelet endothelial-cell adhesion molecule-1 (pecam-1/CD31) on monocytes and neutrophils increases binding-capacity of leukocyte CR3 (CD11b/CD18). *Journal of Immunology* 154 299-307.

Bershadsky, A.D., and Vasiliev, J.M. in *Cytoskeleton.* Cellular Organelles Series Edited by P. Siekevitz. Published by Plenum Press (New York) 1989

Beug, H., Katz, F.E., Gerisch, G. (1973) *Journal of Cell Biology*. 56 647-658

Bevilacqua, M.P., Stengelin, S., Gimbrone, M.A., and Seed, B. (1989). Endothelial leukocyte adhesion molecule 1: An inducible receptor for neutrophils related to complement regulatory proteins and lectins. *Science* 243 1160-1165.

Blechman, J.M., Lev, S., Barg, J., Eisenstein, M., Vaks, B., Vogel, Z., Givol, D., Yarden, Y.M. (1995) The 4th immunoglobulin domain of the stem-cell factor-receptor couples ligand-binding to signal-transduction. *Cell* 80, 103-113.

Bodian, D.L., Jones, E.Y., Harlos, K., Stuart, D.I., Davis, S.J. (1994) Crystal-structure of the extracellular region of the human cell-adhesion molecule CD2 at 2.5-angstrom resolution. *Structure* 2: 755-766

Bogen, S., Pak, J., Garifallou, M., Deng, X.H., Muller, W.A. (1994) Monoclonal-antibody to murine pecam-1 (CD31) blocks acute-inflammation in-vivo. *Journal of Experimental Medicine* 179 1059-1064.

Bossy, D., Mattei, M.G. and Simmons, D.L. (1994). The human intercellular adhesion molecule 3 (ICAM-3) gene is located in the 19p13.2-p13.3 region, close to the ICAM-1 gene. *Genomics* 23 712-713.

Brackenbury, R., THiery, J.P., Rutishauser, U., Edelman, G.M. (1977) Adhesion among neural cells of the chick embryo *Journal of Biological Chemistry* 252 6835-6840.

Brieher, W.M., Yap, A.S., Gumbiner, B.M. (1996) Lateral dimerisation is required for the homophilic binding activity of C-cadherin. *Journal of Cell Biology* 135 487-496.

Briskin MJ, McEvoy LM, Butcher EC (1993) MAdCAM-1 has homology to immunoglobulin and mucin-like adhesion receptors and to IgA1.Nature 363 461-464.

Brooks, P.C., Clark, R.A.F., Cheresh, D.A. (1994) Requirement of vascular integrin alpha(v)beta(3) for angiogenesis. *Science* 264 569-571.

Brooks, P.C., Montgomery, A.M.P., Rosenfeld, R.A., Reisfeld, T., Hu, G., Klier, G., Cheresh, D.A. (1994) Integrin avb3 antagonists promote tumour regression by inducing apoptosis of angiogenic vessels. *Cell* 79 1-20.

Brown, E.J. (1997) Adhesive interactions in the immune system. *Trends in Cell Biology* 7 289-295.

Brummendorf, T., Rathjen, F. (1994) Cell Adhesion Molecules 1: Immunoglobulin Superfamily. In *Protein Profile* series of publications (Volume 1, Issue 9), Edited by Sheterline, P. Academic Press Limited, London, UK.

Buchstaller, A., Kunz, S., Berger, P., Kunz, B., Ziegler, U., Rader, C., Sonderegger, P. (1996) Cell-adhesion molecules Ng-cam and axonin-1 form heterodimers in the neuronal membrane and co-operate in neurite outgrowth promotion. *Journal of Cell Biology* 135 1593-1607.

Buckley, C.D., Doyonnas, R., Newton, J.P., Blystone, S.D., Brown, E.J.,Watt, S.M., Simmons, D.L. (1996) Identification of alpha(v)beta(3) as a heterotypic ligand for CD31/pecam-1. *Journal of Cell Science* 109 437-445.

Buckley, C.D., Ferguson, E.D., Littler, A.J., Bossy, D., Simmons, D.L. (1997) Role of ligands in the activation of LFA-1. *European Journal of Immunology* 27 957-962.

Butcher, E. C. (1991).Leukocyte-endothelial cell recognition: three (or more) steps to specificity and diversity. *Cell* 67 1033-1036.

Butcher, E.C. and Picker, L.J. (1996). Lymphocyte homing and homeostasis. *Science* 272 60-66.

Buttrum, S.M., Hatton, R. and Nash, G.B. (1993). Selectin mediated rolling of neutrophils on immobilised platelets. *Blood* 82 1165-74.

Calderwood, D.A., Tuckwell, D.S., Eble, J., Kühn, K., Humphries, M.J. (1997) The integrin α1 A-domain is a ligand binding site for collagens and laminin. *Journal of Biological Chemistry* 272 12311-12317.

Calvete J.J. (1994) Clues for understanding the structure and function of a prototypic integrin: the platelet glycoprotein IIb/IIIa complex. *Thrombosis and Haemostasis* 72 1-15.

Calvete, J.J., Mann, K., Alvarez, M.V., Lopez, M.V. Gonalez-Rodriguez, J. (1992) Proteolytic dissection of the isolated fibrinogen receptor, integrin gpIIb/IIIa. Localisation of gpIIa and gpIIIa sequences putatively involved in the subunit interface and in intrasubunit and intrachain contacts. *Biochemical Journal* 282 523-532

Camerini, D., James, S.P., Stamenkovic, I., Seed, B. (1989) Leu-8/TQ1 is the human equivalent of the Mel-14 lymph node homing receptor. *Nature* 342 78-82.

Campbell, I.D., Downing, A.K. (1994) Building protein structure and function from modular units. *Trends in Biotechnology* 12 168-172

Campbell, I.D., Spitzfaden, C. (1994) Building proteins with fibronectin type-III modules. *Structure* 2 333-337.

Capek, K.L., Shaw, S.K., Parker, C.M., Russel, G.J., Morrow, J.S., Rimm, D.L., and Brenner, M.B. (1994) Adheson between epithelial cells and T lymphocytes mediated by E-cadherin and the αEβ7 integrin. *Nature* 372 190-193.

Casasnovas JM, Springer TA, Liu JH, Harrison SC, Wang JH (1997) Crystal structure of ICAM-2 reveals a distinctive integrin recognition surface. *Nature* 387 312-315.

Charlwood, P.A. (1957) Partial specific volumes of proteins in relation to composition and environment. *Journal of the American Chemical Society* 79, 776-781.

Charo, I.F., Nannizzi, L., Smith, J.W. and Cheresh, D.A. (1990). The vitronectin receptor αvβ3 binds fibronectin and acts in concert with α5β1 in promoting cellular attachment and spreading on fibronectin. J. Cell Biol. 111: 2795-2800.

Chen, W., Knapp, W., Majdic, O., Stockinger, H., Bohmig, G., and Zlabinger, G.J. (1994). Co-ligation of CD31 and FcRgII induces cytokine production in human monocytes. *Journal of Immunology.* 152, 3991-3997.

Cheresh, D.A. (1992) Structural and biological properties of integrin mediate cell adhesion. *Laboratory Immunology* 12 217-236.

Cheresh, D.A., and Spiro, R.C. (1987) Biosynthetic and functional properties of an Arg-Gly-Asp-directed receptor involved in human melanoma cell attachment to vitronectin, fibrinogen and von Willebrand factor. *Journal of Biological Chemistry* 262:17703-17711

Chiu, H.H., Crowe, D.T., Renz, M.E., Presta, L.G., Jones, S., Weissman, I.L., Fong, S. (1995) Similar but non-identical amino-acid-residues on vascular cell-adhesion molecule-1 are involved in the interaction with alpha(4)beta(1) and alpha(4)beta(7) under different activity states. *Journal of Immunology* 155 5257-5267.

Clements JM, Newham P, Shepherd M, Gilbert R, Dudgeon TJ, Needham LA, Edwards RM, Berry L, Brass A, Humphries MJ (1994) Identification of a key integrin-binding sequence in vcam-1homologous to the LDV active-site in fibronectin. *Journal of Cell Science* 104 2127-2135.

Cooper D, Lindberg FP, Gamble JR, Brown EJ, Vadas MA (1995) Transendothelial migration of neutrophils involves integrin-associated protein (CD47). *Proceedings of The National Academy of Sciences* 92 3978-3982.

D'Souza, S.E., Ginsberg, M.H., Burke, T.A., Plow, E.F. (1988). Localisation of an RGD recognition site within an integrin adhesion receptor. *Science* 242 91-93.

Davies, S.J., Puklavec, M.J., Ashford, D.A., Harlos, K., Jones, E.Y., Stuart, D.I., Williams, A.F. (1993) Expression of soluble recombinant glycoproteins with predefined glycosylation: application to the crystallisation of the T-cell glycoprotein CD2. *Protein Engineering* 6 229-232.

de Fougerolles, A.R., Qin, X. and Springer, T.A. (1994). Characterisation of the function of intercellular adhesion molecule (ICAM)-3 and comparison with ICAM-1 and ICAM-2 in immune responses. *Journal of Experimental Medicine* 179 619-629.

Deaglio S, Dianzani U, Horenstein A, Morra M, Pragher E, Banchereau J, Stockinger H, Malavasi F. (1996) Cloning and identification of a ligand of human CD38 (CD38l).*Tissue Antigens* 48 AS409-AS409 (Meeting Abstract).

Dedhar, S., Hannigan, G.E. (1996) Integrin cytoplasmic interactions and bidirectional transmembrane signalling. *Current Opinion in Cell Biology* 8 657-669.

Dejana, E. (1996) Endothelial adherens junctions: Implications in the control of vascular permeability and angiogenesis. *Journal of Clinical Investigation* 9 1949-1953

Dejana, E., Corada, M., Lampugnani, M.G. (1994) Endothelial cell-to cell junctions. *FASEB Journal* 9 910-918.

DeLisser, H.M., Chilkowtowsky, J., Yan, H.C., Daise, M.L., Buck, C.A. and Albelda, S.M. (1994). Deletions in the cytoplasmic domain of platelet-endothelial cell adhesion molecule-1 (PECAM-1, CD31) result in changes in ligand binding properties. *Journal of Cell Biology*. 124 195-203.

DeLisser, H.M., Chilkotowsky, J., Yan, H.C., Daise, M.L., Buck, C.A., Albelda, S.M. (1994) Deletions in the cytoplasmic domain of platelet-endothelial cell-adhesion molecule-1 (pecam-1, CD31) result in changes in ligand-binding properties. *Journal of Cell Biology* 124 195-203.

DeLisser, H.M., Yan, H.C., Newman, P.J., Muller, W.A., Buck, C.A., Albelda, S.M. (1993) Platelet endothelial-cell adhesion molecule-1 (CD31)-mediated cellular aggregation involves cell-surface glycosaminoglycans. *Journal of Biological Chemistry* 268 16037-16046.

Delmaschio, A., Zanetti, A., Corada, M., Rival, Y., Ruco, L., Lampugnani, M.G., Dejana, E. (1996) Polymorphonuclear leukocyte adhesion triggers the disorganisation of endothelial cell-to-cell adherens junctions. *Journal of Cell Biology* 135 497-510.

Delpozo, M.A., Cabanas, C., Montoya, M.C., Ager, A., Sanchezmateos, P., Sanchezmadrid, F. (1997) ICAMs redistributed by chemokines to cellular uropods as a mechanism for recruitment of T-lymphocytes. *Journal of Cell Biology* 137 493-508.

Delpozo, M.A., Sanchezmateos, P., Nieto, M., Sanchezmadrid, F. (1995) Chemokines regulate cellular-polarization and adhesion receptor redistribution during lymphocyte interaction with endothelium and extracellular-matrix - involvement of cAMP signaling pathway. *Journal of Cell Biology* 131 495-508.

Diacovo, T.G., Roth, S.J. Buccola, J.M., Bainton, D.F. and Springer, T.A. (1996a). Neutrophil rolling, arrest and transmigration across activated, surface-adherent platelets via sequential action of P-selectin and the β2 integrin CD11b/CD18. *Blood* 88 146-157.

Diacovo, T.G., Puri, K.D., Warnock, R.A. Springer, T.A. and von Andrian, U.H. (1996b). Platelet-mediated lymphocyte delivery to high endothelial venules. *Science* 273 252-255.

Diamond, M.S., Staunton, D.E., Marlin, S.D., Springer, T.A. (1991) *Cell* 65 961-971

Dransfield, I., Cabanas, C., Craig, A. and Hogg, N. (1992). Divalent cation regulation of the function of the leukocyte integrin LFA-1. *Journal of Cell Biology* 166 219-226.

Duggleby, R.G. (1984) Regression analysis of nonlinear Arrhenius plots: an empirical model and a computer program. *Computational Biology and Medicine*14 447-455.

Dunon, D., Piali, L., Imhof, B.A. (1996) To stick or not to stick: the new leukocyte homing paradigm. *Current Opinion in Cell Biology* 8 714-723.

Duperray, A., Languino, L.R., Plescia. J. McDowall. A. Hogg, N., Craig, A.G., Berendt, A.R., and Altieri, D.C. (1997) Molecular identification of a novel fibrinogen binding site on the first domain of ICAM-1 regulating leukocyte-endothelium bridging. *Journal of Biological Chemistry* 272, 435-441.

Eanger, B.O., Austin, K.S., Earp, H.S., and Cidlowski, J.A. (1986) Cross-linking of epidermal growth factor receptors in intact cells: detection of initial stages of receptor clustering and determination of molecular weight of high affinity receptors. *Biochemistry* 25 6414-6420.

Edelstein, S.J., Schachman, H.K. (1967) The simultaneous determination of partial specific volumes and molecular weights with microgram quantities. *Journal of Biological Chemistry* 242 306-311

Elices, M.J., Osborn, L., Takada, Y., Crouse, C., Luhowsky, S., Hemler, M. and Lobb, R.R. (1990). VCAM-1 on activated endothelium interacts with the leukocyte integrin VLA-4 at a site distinct from the VLA-4/fibronectin binding site. *Cell.* 60 577-584.

Fan, T-P.D., Jaggar R., Bicknell, R. (1995) Controlling the vasculature:angiogenesis, anti-angiogenesis and vascular targeting of gene therapy. *Trends in Pharmacological Sciences* 16 57-66.

Fassler, R., Georges-Labouesse, E. and Hirsch, E. (1996). Genetic analysis of integrin function in mice. *Current Opinion in Cell Biology.* 8: 641-646.

Fawcett, D.W. (1994) *A Textbook of Histology* 12th edition pp964 (Chapman and Hall, New York)

Feizi, T. (1994) Evidence for carbohydrate-mediated interactions between the neural-cell-adhesion molecules NCAM and L1.*Trends In Biochemical Sciences* 233-234.

Folkman, J. (1995) Angiogenesis in cancer, vascular, rheumatoid and other disease. *Nature Medicine* 1 27-31.

Frenette, P.S., Johnson, R.C., Hynes, R.O., Wagner, D.D. (1995) Platelets roll on stimulated endothelium in-vivo - an interaction mediated by endothelial p-selectin. *Proceedings of The National Academy of Sciences (USA)* 92 7450-7454

Frenette, P.S., Mayadas, T.N., Rayburn, H., Hynes, R.O., Wagner, D.D. (1996) Susceptibility to infection and altered hematopoiesis in mice deficient in both P-selectin and E-selectin. *Cell* 84 563-574.

Furuse, M., Itoh, M., Hirase, T., Nagafuchi, A., Yonemura, S., Tsukita, S., and Tsukita, S. (1994) Direct association of occludin with ZO-1 and its possible involvement in the localisation of occludin at tight junctions. *Journal of Cell Biology* 127 1617-1626.

Gallatin, W. M., Weissman, I. L. and Butcher, E. C. (1983). A cell surface molecule involved in organ-specific homing of lymphocytes. *Nature* 304 30-34.

Gao, G.F., Tormo, J., Gerth, U.C., Wyer, J.R., McMichael, A.J., Stuart, D.I., Bell, J.I., Jones, E.Y., Jakobsen, B.K. (1997) Crystal-structure of the complex between human CD8-alpha and HLA-a2. *Nature* 387 630-634.

Garcia, K.C., Degano, M., Stanfield, R.L., Brunmark, A., Michael, M.R., Peterson, P.A., Teyton, L., Wilson I.A. (1996) An αβ T-cell receptor structure at 2.5Å and its orientation in the TCR-MHC complex. *Science* 274 p209-219.

Geng, J.G., Bevilaqua, M.P., Moore, K.L., McIntyre, T.M., Prescott, S.M., Kim, J.M., Bliss, G.A., Zimmerman, G.A., McEver, R.P. (1990). Rapid neutrophil adhesion to activated endothelium mediated by GMP-140. *Nature*343 757-760.

Gibbons, R.A. (1972) Physico-chemical methods for the determination of the purity, molecular size and shape of glycoproteins. *Glycoproteins, Part A,* pp128-140. Edited by A. Gottschalk, 2ndl edition. Amsterdam, Elsevier Publication Company.

Gluzman, Y. (1981). SV40-transformed simian cells support the replication of early SV40 mutants. *Cell* 23 175-182.

Goldberger, A., Middleton, K.A., Oliver, J.A., Paddock, C., Yan, H.C., Delisser, H.M., Albelda, S.M., Newman, P.J. (1994) Biosynthesis and processing of the cell-adhesion molecule PECAM-1 includes production of a soluble form. *Journal of Biological Chemistry* 269 17183-17191.

Graves, B.J., Crowther, R.L., Chandran, C., Rumberger, J.M., Li, S., Huang, K-S, Presky, D.H., Familletti, P.C., Wolitzky, Burns, D.K. (1994) Insights into E-selectin/ligand interactions from the crystal structure and mutagenesis of the lec/EGF domains. *Nature* 367 532-538.

Greve, J. M., Davis, G., Meyer, A. M., Forte, C. P., Yost, S. C., Marlor, C. W., Kamarck, M. E., and McClelland, A. (1989) *Cell* 56, 839-847

Gumbiner , B.M. (1996) Cell adhesion: The molecular basis of tissue architecture and morphogenesis. *Cell* 84 345-357.

Guyer, D.A., Moore, K.L., Lynam, E.B., Schammel, C.M.G., Rogelj, S., McEver, R.P., Sklar, L.A. (1996) P-selectin glycoprotein ligand-1 (PSGL-11) is a ligand for L-selectin in neutrophil aggregation. *Blood* 88 2415-2421.

Hall A (1994) Small GTP-binding proteins and the regulation of the actin cytoskeleton. *Annual Review of Cell Biology* 10 31-54.

Hanahan, D. (1983) Studies on transformation of *Escherichia coli* with plasmids. *Journal of Molecular Biology* 166 557-580.

Hancock, D.C., Evan, G.I. (1992) Synthesis of peptides for use as immunogens. From *Methods in Molecular Biology, Vol.10: Immunochemical Protocols*, Ed. M.Manson, The Humana Press, Inc, Totowa, NJ.

Hanks SK, Polte TR (1997) Signalling through focal adhesion kinase. *Bioessays* 19 137-145.

Hannigan, G.E., Leung-Hagesteijn, C., Fitz-Gibbon, L., Coppolino, M., Radeva, G., Filmus, J., Bell, J. and Dedhar, S. (1996). Regulation of cell adhesion and anchorage dependent growth by a new β1 integrin linked protein kinase. *Nature* 379 91-96.

Hansen J.C., Lebowitz, J., Demeler, B. (1994) Analytical ultracentrifugation of complex macromolecular systems. *Biochemistry* 33 13155-13163.

Harpaz, Y., Chothia, C. (1994) Many of the immunoglobulin superfamily domains in cell-adhesion molecules and surface-receptors belong to a new structural set which is close to that containing variable domains. *Journal of Molecular Biology* 238 528-539.

Helander, T.S., Carpen, O., Turunen, O., Kovanen, P.E., Vaheri, A., Timonen, T. (1996) ICAM-2 redistributed by ezrin as a target for killer-cells. *Nature* 382 265-268.

Higuchi R., Krummel B., and Saiki RH (1988) A general method of *in vitro* preparation and specific mutagenesis of DNA fragments: a study of protein and DNA interactions. *Nucleic Acids Research* 16 p7351-7367.

Ho, S.N., Hunt, H.D., Horton, R.M., Pullen, J.K., and Pease, L.R. (1989) Site-directed mutagenesis by overlap extension using the polymerase chain reaction. *Gene* 77 51-59.

Holm, J., Appel, F., Schachner, M. (1995) Several extracellular domains of the neural cell-adhesion molecule L1 are involved in homophilic interactions. *Journal of Neuroscience Research* 42 9-20.

Holness, C.L., Bates, P.A., Littler, A.J., Buckley, C.D., McDowall, A., Bossy, D., Hogg, N., Simmons, D.L. (1995) Analysis of the binding-site on intercellular-adhesion molecule-3 for the leukocyte integrin lymphocyte function-associated antigen-1. *Journal of Biological Chemistry* 270 877-884.

Hotchin, N.A., Hall, A: The assembly of integrin adhesion complexes requires both extracellular matrix and rho/rac GTPases. *Journal of Cell Biology* 131 1857-1865.

Howard, M., Grimaldi, J.C., Bazan, J.F., Lund, F.E., Santos-Argumedo, L., Parkhouse, R.M., Walseth, T.F., Lee, H.C. (1993) Formation and hydrolysis of cyclic ADP-ribose catalysed by lymphocyte antigen CD38. *Science* 262 1056-1059.

Huang, A.J., Manning, J.E., Bandak, T.M., Ratau, M.C., Hanser, K.R., Silverstein, S.C. (1993) Endothelial-cell cytosolic free calcium regulates neutrophil migration across monolayers of endothelial-cells. *Journal of Cell Biology* 120 1371-1380.

Hubbe M, Kowitz A, Schirrmacher V, Schachner M, Altevogt P (1993) L1 adhesion molecule on mouse leukocytes - regulation and involvement in endothelial-cell binding. *European Journal of Immunology* 23 2927-2931.

Huber, O., Bierkamp, C., Kemler, R. (1996) Cadherins and catenins in development. *Current Opinion in Cell Biology* 8 685-691.

Hughes, P.E., Diaz-Gonzalez, F., Leong, L., Wu, C., McDonald, J.A., Shattil, S.J. Ginsberg, M.H. (1996) Breaking the Integrin Hinge *Journal of Biological Chemistry* 271 6571-6574.

Humphries, M.J. (1996) Integrin activation: The link between ligand binding and signal transduction. *Current Opinion in Cell Biology* 8 632-640.

Hwang, S.T., Singer, M.S., Giblin, P.A., Yednock, T.A., Bacon, K.B., Simon, S.I., Rosen, S.D.(1996) Glycam-1, a physiological ligand for L-selectin, activates beta-2 integrins on naive peripheral lymphocytes. Journal of Experimental Medicine 184 1343-1348

Hynes, R.O. (1992). Integrins: Versatility, modulation, and signalling in cell adhesion. *Cell* 69:11-25.

Imai, Y., Lasky, L.A., Rosen, S.D. (1993) Sulphation requirement for glycam-1, an endothelial ligand for L-selectin. *Nature* 361 555-557.

Imhof, B.A., Dunon, D. (1995) Leukocyte migration and adhesion. *Advances in Immunology* 58 345-416.

Jackson DE, Ward CM, Wang RG, Newman PJ (1997) The protein-tyrosine-phosphatase shp-2 binds platelet/endothelial cell-adhesion molecule-1 (pecam-1) and forms a distinct signalling complex during platelet-aggregation - evidence for a mechanistic link between pecam-1-mediated and integrin-mediated cellular signalling *Journal of Biological Chemistry* 272 6986-6993.

Jackson, D.G., Bell, J.I., Dickinson, R., Timans, J., Shields, J., Whittle, N. (1995) Proteoglycan forms of the lymphocyte homing receptor CD44 are alternatively spliced variants containing the v3 exon. *Journal of Cell Biology* 128 673-685.

Johnston, G.I., Cook, R.G., McEver, R.P. (1989) Cloning of GMP-140, a granule membrane protein of platelets and endothelium: Sequence similarity to proteins invovled in cell adhesion and inflammation. *Cell* 56 1033-1044

Jones EY, Harlos K, Bottomley MJ, Robinson RC, Driscoll PC, Edwards RM, Clements JM, Dudgeon TJ, Stuart DI (1995) Crystal-structure of an integrin-binding fragment of vascular cell-adhesion molecule-1 at 1.8 angstrom resolution. *Nature* 373 539-544.

Jones, T.A., Jou, J.W., Cowan, S.W. and Kjeldgaard, M. (1991) Improved methods for building proteinmodels in electron density maps and the location of errors in these models. *Acta Crystallographa* 47 110-119.

Jouet, M., Rosenthal, A., Armstrong, G., MacFarlane, J., Stevenson, R., Paterson, J., Metzenberg, A., Ionasescu, V., Temple, K., Kenwrick, S. (1994) X-linked spastic paraplegia (SPG1), MASA syndrome and X-linked hydrocephalus result from mutations in the L1 gene. *Nature Genetics* 7 402-407.

Kahn, J., Ingraham, R.H., Shirley, F., Migaki, G.I. and Kishimoto, T.K. (1994). Membrane proximal cleavage of L-selectin: Identification of the cleavage site and a 6-kD transmembrane peptide fragment of L-selectin. *Journal of Cell Biology* 125 461-470.

Karecla, P.I., Bowden, S.J., Green, S.J., and Kilshaw, P.J. (1995) Recognition of E-cadherin on epithelial cells by the mucosal T cell integrin $a_{m290}b_7$ (a_Eb_7). *European Journal of Immunology* 25, 852-856.

Karelcla, P.I., Green, S.J., Bowden, S.J., Coadwell, J., Kilshaw, P.J. (1996) Identification of a binding site for integrin αEβ7 in the N-terminal domain of E-cadherin. *Journal of Biological Chemistry* 271 30909-30915.

Keiffer D, Fuhlbrigge R, Amerding D, Rossiter H, Kupper TS (1997) Molecular-identification of cutaneous lymphocyte associated antigen (CLA) - CLA is an isoform of P-selectin glycoprotein ligand-1 (PSGL-1). *Journal of Investigative Dermatology* 108 107-107.

Kilger G, Needham LA, Nielsen PJ, Clements J, Vestweber D, Holzmann B (1995) Differential regulation of alpha(4)-integrin-dependent binding to domain-1 and domain-4 of vascular cell-adhesion molecule-1. *Journal of Biological Chemistry* 270 5979-5984.

Kirschbaum, N.E., Gumina, R.J., Newman, P.J. (1994) Organisation of the gene for human platelet endothelial-cell adhesion molecule-1 shows alternatively spliced isoforms and a functionally complex cytoplasmic domain. *Blood* 84 4028-4037.

Kishimoto, T.K., Warnock, R.A., Jutila, M.A., Butcher, E.C., Lane, C., Anderson, D.C., Smith, C.W. (1991) Antibodies against human neutrophil LECAM-1 (LAM-1/Leu-8/Dreg-56 antigen) and endothelial cell ELAM-1 inhibit a common CD18-independent adhesion pathway in vitro. *Blood* 78 805-

Klickstein, L.B., York, M.B., de Fourgrtolles, A.R., and Springer, T.A. (1996) Localisation of the binding site on intercellular adhesion molecule-3 (ICAM-3) for lymphocyte function-associated antigen-1 (LFA-1) *Journal of Biological Chemistry* 271 23920-23927.

Kolanus, W., Nagel, W., Schiller, B., Zeitlmann, L., Godar, S., Stockinger, H., Seed, B. (1996) Alpha-l-beta-2 integrin/LFA-1 binding to ICAM-1 induced by cytohesin-1, a cytoplasmic regulatory molecule. Cell 1996 86 233-242.

Kotovuori, P., Tontti, E., Pigott, R., Sheperd, M., Kiso, M., Hasegawa, A., Renkonen, R., Nortamo, P., Alteiri, D.C., Gahmberg, C.G. (1993) The vascular E-selectin binds to the leukocyte integrins CD11/CD18. *Glycobiology* 3 131

Kuijpers, T.W., Hoogerwerf, M., van der Laan, L.J.W., Nagel, G., van der Schoot, C.E., Grunert, F., Roos, D.(1992) CD66 nonspecific cross-reacing antigens are involved in neutrophil adherence to cytokine activated endothelial cells. *Journal of Cell Biology* 118 457-

Labow, M.A., Norton, C.R., Rumberger, J.M., Lombardgillooly, K.M., Shuster, D.J., Hubbard, J., Bertko, R., Knaack, P.A., Terry, R.W., Harbison, M.L., Kontgen, F., Stewart, C.L., McIntyre, K.W., Will, P.C., Burns, D.K., Wolitzky, B.A. (1994) Characterisation of E-selectin-deficient mice - demonstration of overlapping function of the endothelial selectins. *Immunity* 1 709-720

Languino, L. R., Plescia, J., Duperray, A., Brian, A. A., Plow, E. F., Geltosky, J. E., and Altieri, D. C. (1993) Fibrinogen mediates leukocyte adhesion to vascular endothelium through an ICAM-1-dependent pathway *Cell* 73 1423-1434.

Lasky, L.A., Singer, M.S., Yednock, T.A., Dowbenko, D., Fennie, C., Rodriguez, H., Nguyen, T., Stachel, S., Rosen, S.D. (1989) Cloning of a lymphocyte homing receptor reveals a lectin domain. *Cell* 56 1045-1055

Laue, T. M., Shah, B. D., Ridgeway, T. M., Pelletier, S. L. Computer-aided interpretation of analytical sedimentation data for proteins. *Analytical Ultracentrifugation in Biochemistry and Polymer Science*, pp. 90-125.Edited by S. E. Harding, A. J. Rowe and J. C. Horton. Cambridge, Royal Society of Chemistry, 1992.

Lawrence, M.B. and Springer, T. A. (1991). Leukocytes roll on a selectin at physiologic flow rates: distinction from and prerequisite for adhesion through integrins. *Cell* 65 859-873.

Leaveseley, D.I., Ferguson, G.D., Wayner, E.A., and Cheresh D.A. (1992) Requirement of the integrin b3 subunit for carcinoma cell spreading or migration on vitronectin and fibrinogen. *Journal of Cell Biology* 117 1101-1107.

Leavesley, D.I., Oliver, J.M., Swart, B.W., Berndt, M.C., Haylock, D.N., Simmons, P.J. (1994) Signals from platelet endothelial-cell adhesion molecule enhance the adhesive activity of the very late antigen-4 integrin of human CD34(+) haematopoietic progenitor cells. *Journal of Immunology* 153 4673-4683.

Lee, J.O., Bankston, L.A., Arnaout, M.A., Liddington, R.C. (1995b) 2 conformations of the integrin A-domain (I-domain) - a pathway for activation. *Structure* 3 1333-1340.

Lee, J.O., Reiu P, Arnaout, M.A., Liddington, R. (1995a) Crystal structure of the A domain from the a subunit of integrin CR3 (CD11b/CD18). *Cell* 155 3619-3628.

Lesley J, Howes N, Perschl A, Hyman R (1994) Hyaluronan-binding function of CD44 is transiently activated on T-cells during an *in-vivo* immune-response. *Journal of Experimental Medicine* 180 383-387.

Lesley, J., Hyman, R., Kincade, P.W. (1993) CD44 and its interaction with extracellular-matrix. *Advances In Immunology* 54 271-335.

Li, R., Nortamo, P., Valmu, L., Tolvanen, M., Huuskonen, J., Kantor, C., Gahmberg, C.G. (1993). A peptide from ICAM-2 binds to the leukocyte integrin CD11a/CD18 and inhibits endothelial cell adhesion. *Journal of Biological Chemistry* 268 17513-17518.

Liao, F., Ali, J., Greene, T., Muller, W.A. (1997) Soluble domain 1 of platelet-endothelial cell adhesion molecule (PECAM-1) is sufficient to block transendothelial migration in vitro and in vivo. *Journal of Experimental Medicine* 185 1349-1357.

Lo, S.K., van Seventer, G.A., Levin, S.M., Wright, S.D. (1989) Two leukocyte receptors (CD11a/CD18 and CD11b/CD18) mediate transient adhesion to endothelium by binding to different ligands. *Journal of Immunology* 143 3325-3335.

Loftus, J.C., O'Toole, T.E., Plow. E.F., Glass, A., Frelinger, A.L., Ginsberg, M.H. (1990) A β3 integrin mutation abolisges ligand binding and alters a divalent-cation dependent conformation. *Science* 249 915-918.

Lorant, D.E., McEver, R.P., McIntyre, T.M., Moore, K.L., Prescott, S.M. and Zimmerman, G.A. (1995). Activation of polymorphonuclear leukocytes reduces their adhesion to P-selectin and causes redistribution of ligands for P-selectin on their surfaces. *Journal of Clinical Investigation* 96: 171-182.

Lu, T.T., Barreuther, M., Davis, S., Madri, J.A. (1997) Platelet endothelial cell adhesion molecule-1 is phosphorylatable by c-src, binds src src-homology 2 domain, and exhibits immunoreceptor tyrosine based activation motif-like properties. *Journal of Biological Chemistry* 272 14442-14446.

Lu, T.T., Yan, L.G., Madri, J.A. (1996) Integrin engagement mediates tyrosine dephosphorylation on platelet-endothelial cell adhesion molecule 1. *Proceedings of the National Academy of Science (USA)* 93 11808-11813

Mackay, C.R., Marston, W.L., Dudler, L., Spertini, O., Tedder, T.F., Hein, W.R. (1992) Tissue-specific migration pathways by phenotypically distinct subpopulations of memory T-cells. *European Journal of Immunology* 22 887-895.

Malarkey K, Belham CM, Paul A, Graham A, McLees A, Scott PH, Plevin R (1995) The regulation of tyrosine kinase signaling pathways by growth-factor and g-protein-coupled receptors. *Biochemical Journal* 309 361-375.

Mariuzza RA, Poljak RJ (1993) The basics of binding - mechanisms of antigen recognition and mimicry by antibodies. *Current Opinion In Immunology* 550-55.

Martin-Padura, I., Lostaglio, S., Schneeman, M., Williams L., Romano, M., Fruscalla, P., Panzeri, C., Stoppacciaro A., Ruco, L., Villa, A., Simmons, D.L., Dejana E. (1997) JAM, a novel member of the immunoglobulin superfamily which codistributes with tight junction components and controls monocyte transmigration. *Submitted.*

Masumoto, A., and Hemler, M.E. (1993) Multiple activation states of VLA-4 - mechanistic differences between adhesion to CS1 fibronectin and to vascular cell-adhesion molecule-1. *Journal of Biological Chemistry* 268 228-234

Matsumura T, Wolff K, Petzelbauer P (1997) Endothelial-cell tube formation depends on cadherin-5 and CD31 interactions with filamentous actin. *Journal of Immunology* 158 3408-3416.

Mayadas, T.N., Johnson, R.C., Rayburn, H., Hynes, R.O., Wagner, D.D. (1993) Leukocyte rolling and extravasation are severely compromised in P-selectin-deficient mice. *Cell* 74 541-554

McCourt, P.A.C., Ek, B., Forsenberg, N. and Gustafson, S. (1994). Intercellular adhesion molecule 1 is a surface receptor for hyaluronan. *Journal of Biological Chemistry*. 269 30081- 30084.

McMeekin, T.L., Marshall, K. (1952) Specific volumes of proteins and the relationship to their amino acid contents *Science* 116 142-143

McRorie, D.K., and Voelker, P.J. (1993) *Self-Associating Systems in the Analytical Ultracentrifuge* Beckman Instruments, Inc., Fullerton, California, USA.

Miller, J., Knorr, R., Ferrone, M., Houdei, R., Carron, C.P., and Dustin, M.L. (1995) Intercellular adhesion molecule-1 dimerisation and its consequences for adhesion mediated by lymphocyte function associated-1. *Journal of Experimental Medicine.* 182, 1231-1241.

Milthorpe, B.K., Jeffrey, P.D., Nichol, L.W. (1975) The direct analysis of sedimentation equilibrium results obtained with polymerising systems. *Biophysical Chemistry* 3 169-176

Mizuno, T., Yoshihara, Y., Inazawa, J., Kagamiyama, H., Mori, K. (1997) cDNA cloning and chromosomal localisation of the human telencephalin and its distinctive interaction with lymphocyte function-associated antigen-1. *Journal of Biological Chemistry* 272 1156-1163.

Moarefi I, Lafevrebernt M, Sicheri F, Huse M, Lee CH, Kuriyan J, Miller WT (1997) Activation of the src-family tyrosine kinase hck by SH3 domain displacement. *Nature* 385 650-653.

Montgomery, A.M.P., Bekcer, J.C., Siu, C-H., Lemmon, V.P., Cheresh, D.A., Pancook, J.D., Zhao, X., and Reisfeld, R.A. (1996) Human neural cell adhesion molecule L1 and rat homologue NILE are ligands for integrin avb3 *Journal of Cell Biology* 132, 475-485.

Montgomery, A.M.P., Reisfield, R.A., and Cheresh, D.A. (1994) Integrin avb3 rescues melanoma cells from apoptosis in three-dimensional dermal collagen. *Proceedings of the National Academy of Sciences* 91 8856-8860.

Moos, M., Tackle, R., Scherer, H., Teplow, D., Fruh, K., Schachner, M (1988) Neural adhesion molecule L1 as a member of the immunoglobulin superfamily with binding domains similar to fibronectin. *Nature* 334, 701-703.

Morris, M.B., and Ralston, G.B. (1985) Analysis of sedimentation equilibrium through direct fitting of the Omega function. *Biophysical Chemistry* 23 49-61.

Mould, A.P. (1996) Getting integrins into shape: Recent insights into how integrin activity is regulated by conformational changes. *Journal of Cell Science* 109 2613-2618.

Muller, W.A., Weigl, S.A., Deng, X. and Philips, D.M. (1993). PECAM-1 is required for transendothelial migration of leukocytes. *Journal of Experimental Medicine* 178 449-460.

Murohara, T., Delyani, J.A., Albelda, S.M., Lefer, A.M. (1996) Blockade of platelet endothelial-cell adhesion molecule-1 protects against myocardial-ischemia and reperfusion injury in cats. *Journal of Immunology* 156 3550-3557.

Murphy, P.M. (1994). The molecular biology of leukocyte chemoattractant receptors. *Annual Review of Immunology.* 12 593-633.

Nagar, B., Overduin, M., Ikura, M., Rini, J.M. (1996) Structural basis of calcium induced E-cadherin rigidification and dimerisation *Nature* 380 360-364.

Nath, D., Van der Merwe, P.A., Kelm, S., Bradfield, P., Crocker, P.R. (1995) The amino-terminal immunoglobulin-like domain of sialoadhesin contains the sialic-acid binding-site - comparison with CD22. *Journal of Biological Chemistry* 270 26184-26191.

Needham, L.A., Vandijk, S., Pigott, R., Edwards, R.M., Shepherd, M., Hemingway, I., Jack, L., Clements, J.M. (1994) Activation-dependent and independent VLA-4 binding-sites on vascular cell-adhesion molecule-1. *Cell Adhesion and Communication* 2 87-99.

Newham, P., Humphries, M.J. (1996) Integrin adhesion receptors: structure, function and implications for biomedicine *Molecular Medicine Today* 2 304-313

Newman PJ (1997) The biology of PECAM-1 *Journal of Clinical Investigation* 99 3-7

Newman, P.J., Berndt, M.C., Gorski, J. White II G.C., Lyman, S., Paddock, C. and Muller, W.A. (1990) PECAM-1 (CD31) cloning and relation to adhesion molecules of the immunoglobulin gene superfamily *Science* 247, 1219-1222.

Newman, P.J., Hillery, C.A., Albrecht, R., Parise, L.V., Berndt, M.C., Mazurov, A.V., Dunlop, L.C., Zhang, J., Rittenhouse, S.E. (1992) Activation-dependent changes in human platelet PECAM-1:Phosphorylation, cytoskeletal association, and surface membrane redistribution. *Journal of Cell Biology* 119 239-246.

Ortlepp S, Stephens PE, Hogg N, Figdor CG, Robinson MK (1995) Antibodies that activate beta-2 integrins can generate different-ligand binding states. *European Journal of Immunology* 25 637-643

Osawa, M., Masuda, M., Harada, N., Lopes, R.B., Fujiwara, K. (1997) Tyrosine phosphorylation of platelet endothelial-cell adhesion molecule-1 (pecam-1, CD31) in mechanically stimulated vascular endothelial-cells. *European Journal of Cell Biology* 1997 72 229-237.

Osborn, L., Hession, C., Tizard, R., Vassallo, C., Luhowskyj, S., Chi-Rosso, G., Lobb, R. (1989) Direct expression cloning of vascular cell adhesion molecule-1, a cytokine-induced endothelial protein that binds to lymphocytes. *Cell* 59 1203-1211.

Pasqualini, R., Koivunen, E., Ruoslahti, E. (1995) A peptide isolated from phage display libraries is a structural and functional mimic of an RGD binding site on integrins. *Journal of Cell Biology* 130 1189-1196.

Patel, K.D., Nollert, M.U., McEver, R.P. (1995) P-selectin must extend a sufficient length from the plasma-membrane to mediate rolling of neutrophils. *Journal of Cell Biology* 131 1893-1902.

Peifer, M. 1995. Cell adhesion and signal transduction: The Armadillo connection. *Trends in Cell Biology* 5 224-229.

Pennica, D., Kohr, W.J., Fendly, B.M., Shire, S.J., Raab, H.E., Borchardt, P.E., Lewis, M., Goeddel, D.V. (1992) Characterisation of a recombinant extracellular domain of the type I tumor necrosis factor receptor. Eidence for tumor necrosis factor-a induced receptor aggregation. *Biochemistry* 31 1134-1141.

Piali, L., Albelda, S.M, Baldwin, H.S., Hammel, P, Gisler, R.H. and Imhof B.A. (1993). Murine platelet endothelial cell adhesion molecule (PECAM-1)/CD31 modulates b2 integrins on lymphokine-activated killer cells. European Journal of Immunology. 23: 2464-2471.

Piali, L., Hammel, P., Uherek, C., Bachmann, F., Gisler, R.H., Dunon, D., Imhof, B.A. (1995) CD31/pecam-1 is a ligand for alpha(v)beta(3) integrin involved in adhesion of leukocytes to endothelium. *Journal of Cell Biology* 130 451-460.

Picker, L.J., Warnock, R.A., Burns, A.R., Doerschuk, C.M., Berg, E.L., Butcher, E.C. (1991) The neutrophil selectin LECAM-1 presents carbohydrate ligands to the vascular selectins ELAM-1 and GMP-140. *Cell* 66 921-935

Pierschbacher, M.D., and Rouslahti, E. (1984) *Nature* 309, 30-

Pokutta, S., Herrenknecht, K., Kemler, R., and Engel, J. (1994) Conformational changes of the recombinant extracellular domain of E-cadherin upon calcium binding. *European Journal of Biochemistry* 223 1019-1026.

Pouyani, T., Seed, B. (1995) PSGL-1 recognition of P-selectin is controlled by a tyrosine sulfation consensus at the psgl-1 amino-terminus. *Cell* 83 333-343.

Prager, E., Sunderplassmann, R., Hansmann, C., Koch, C., Holter, W., Knapp, W., Stockinger, H. (1996) Interaction of CD31 with a heterophilic counter receptor involved in down-regulation of human T-cell responses. *Journal of Experimental Medicine* 184 41-50

Puzon-McLaughlin, W., Takada, Y. (1997) Critical residues for ligand binding in an I domain-like structure of the integrin β1 subunit. *Journal of Biological Chemistry* 271 20438-20443.

Qu AD, Leahy DJ (1996) The role of the divalent-cation in the structure of the I-domain from the CD11a/CD18 integrin. *Structure* 4 931-942.

Qu, A.D., Leahy, D.J. (1995) Crystal-structure of the I-domain from the CD11a/CD18 (lfa-1, alpha(l)beta-2) integrin. *Proceedings of The National Academy of Sciences* (USA) 92 10277-10281.

Ralston, G., Cronin, T.J., Branton, D.(1996) Self-association of spectrin's repeating segments. *Biochemistry* 35 5257-5263.

Ralston, G.B., and Morris, M.B. (1992) The use of the Omega function for sedimentation equilibrium analysis. In *Analytical Ultracentrifugation in Biochemistry and Polymer Science* (Harding, S.E., Rowe, A.J., and Horton, J.C., Eds. Royal Society of Chemistry, Cambridge) pp253-274.

Randi, A.M., Hogg, N. (1994) I domain of β2 integrin lymphocyte function-associated antigen-1 contains a binding site for ligand intercellular adhesion molecule-1. *Journal of Biological Chemistry* 269 12395-12398.

Rao Y, Wu XF, Yip P, Gariepy J, Siu CH (1993) Structural characterization of a homophilic binding-site in the neural cell-adhesion molecule. *Journal of Biological Chemistry* 268 20630-20638.

Rao Y, Zhao XN, Siu CH (1994) Mechanism of hemophilic binding mediated by the neural cell-adhesion molecule NCAM - evidence for isologous interaction. *Journal of Biological Chemistry* 269 27540-27548.

Rao, Y., Wu, X.F., Yip, P., Gariepy, J., Siu, C.H. (1993) *Journal of Biological Chemistry* 268 20630-20638.

Rathjen, F.G., Schachner, M. (1984) Immunocytological and biochemical characterisation of a new neuronal cell surface component (L1 antigen) which is involved in cell adhesion. *EMBO Journal* 3 1-10.

Reilly, P.L., Woska, J.R., Jeanfavre, D.D., McNally, E., Rothlein, R., and Bormann, B-J. (1995) The native structure of intercellular adhesion molecule-1 (ICAM-1) is a dimer. Correlation with binding to LFA-1. *Journal of Immunology* 155, 529-532.

Renz, M.E., Chin, H.H., Jones, S., Fox, J., Kim, K.J., Presta, L.G., Fong, S. (1994) Structural requirements for adhesion of soluble recombinant murine vascular cell-adhesion molecule-1 to alpha-4-beta-1 *Journal of Cell Biology* 125 1395-1406.

Romer, L.H., McLean, N.V., Yan, H.C., Daise, M., Sun, J., Delisser, H.M. (1995) Interferon-gamma and TNF-alpha induce redistribution of PECAM-1 (CD31) on human endothelial-cells. *Journal of Immunology* 154 6582-6592.

Ropers, H.H. and Mohrenweiser, H. (1993). Report of the committee on the genetic construction of chromosome 19. *Genetic Priority Report* 1 524-547.

Rosen, S.D. and Bertozzi, C.R. (1996). Leukocyte adhesion: Two selectins converge on sulphate. *Current Biology* 6 261-264.

Rosenstein, Y., Park, J.K., Hahn, W.C., Rosen, F.S., Bierer, B.E., Burakoff, S.J. (1991). CD43, a molecule defective in Wiskott-Aldrich syndrome, binds ICAM-1. Nature 354: 233-235.

Rosenthal, A., Coutelle, O. (1993) The complete sequence and genomic structure of the human gene for the neural cell adhesion molecule L1: X-linked hydrocephalus locus. *Cytogenetics and Cell Genetics* 64 185.

Ross, F.P., Chappel, J., Alvarez, J.I., Sander, D., Butler, W.T., Farachcarson, M.C., Mintz, K.A., Robey, P.G., Teitelbaum, S.L., Cheresh, D.A. (1993) Interactions between the bone-matrix proteins osteopontin and bone sialoprotein and the osteoclast integrin alpha-v-beta-3 potentiate bone-resorption. *Journal of Biological Chemistry* 268 9901-9907.

Ruppert, M., Aigner, S., Hubbe, M., Yagita, H., Altevogt, P. (1995) The l1 adhesion molecule is a cellular ligand for VLA-5. Journal of Cell Biology 131 1881-1891.

Sadhu C, Lipsky B, Erickson HP, Hayflick J, Dick KO,Gallatin WM, Staunton DE (1994) LFA-1 binding-site in ICAM-3 contains a conserved motif and non-contiguous amino-acids. *Cell Adhesion and Communication* 2 429-440.

Sagawa K, Swaim W, Zhang J, Unsworth E, Siraganian RP (1997) Aggregation of the high-affinity IgE receptor results in the tyrosine phosphorylation of the surface-adhesion protein pecam-1 (CD31). *Journal of Biological Chemistry* 272 13412-13418.

Salmi, M. and Jalkanen, S. (1992). A 90-kilodalton endothelial cell molecule mediating lymphocyte binding in humans. *Science* 257 1407-1409.

Salmi, M. and Jalkanen, S. (1996). Human vascular adhesion protein 1 (VAP-1) is a unique sialoglycoprotein that mediates carbohydrate-dependent binding of lymphocytes to endothelial cells. *Journal of Experimental Medicine*. 183 569-579.

Sanders, L., Felding-Habermann, C.B., Mueller, B.M., Cheresh, D.A. (1992) Role of av integrins and vitronectin in human melanoma cell growth. *Cold Spring Harbour Symposium on Quantitative Biology* LVII 233-240b

Sansom, D., Borrow, J., Solomon, E. and Trowsdale, J. (1991). The ICAM-2 gene maps to 17q23-25. *Genomics*. 11 462-464.

Satmper, H.B., and Woodruff, J.J. (1976). Lymphocyte homing to lymph nodes: In vitro demonstration of selective affinity of recirculating lymphocyes for high endothelial venules. *Journal of Experimental Medicine* 144 828-833

Scachman, H.K., (1992) Is there a future for the ultracentrifuge? in *Analytical Ultracentrifugation in Biochemistry and Polymer Science* (Harding, S.E., Rowe, A.J., and Horton, J.C., Eds.) pp3-15

Schimmenti, L.A., Yan, H., Madri, J.A., Albelda, S.M. (1992) The role of PECAM-1 in cell migration and wound healing. *Journal of Cell Physiology* 153 417-428.

Screaton, G.R., Bell, M.V., Bell, J.I., Jackson, D.G. (1993) The identification of a new alternative exon with highly restricted tissue expression in transcripts encoding the mouse pgp-1 (CD44) homing receptor - comparison of all 10 variable exons between mouse, human, and rat. *Journal of Biological Chemistry* 268 12235-12238.

Seed, B. (1995) Developments in expression cloning. *Current Opinion In Biotechnology* 6 567-573.

Shapiro, L., Fannon, A.M., Kwong, P.D., Thompson, A., Lehmann, M.S., Grubel, G., Legrand, J-F., Als-Nielsen, J., Colman, D.R., Hendrickson, W.A. (1995) Structural basis of cell-cell adhesion by cadherins. *Nature* 364 327-337.

Shattil, S.J., O'Toole, T., Eigenthaler, M., Thon, V., Williams, M., Babior, B.M. and Ginsberg, M.H. (1995). β3 endonexin, a novel polypeptide that interacts specifically with the cytoplasmic tail of the integrin β3 subunit. *Journal of Cell Biology*. 131 807-816.

Shimizu ,Y. and Shaw, S. (1993) Mucins in the mainstream. *Nature* 366: 630-631.

Shire, S.J. (1992) Determination of molecular weights of glycoproteins by analytical ultracentrifugation. In *Beckman Technical Information: Ultracentrifugation - update DS-837.*

Shyjan, A.M., Bertagnolli, M., Kenney, C.J., Briskin, M.J. (1996) Human mucosal addressin cell-adhesion molecule-1 (MAdCAM-1) demonstrates structural and functional similarities to the alpha(4)beta(7)-integrin binding domains of murine MAdCAM-1, but extreme divergence of mucin-like sequences. *Journal of Immunology* 156 2851-2857.

Sicheri F, Moarefi I, Kuriyan J (1997) Crystal-structure of the src family tyrosine kinase hck. *Nature* 385 602-609.

Siegelman, H.M., van den Rijn, M., Weissman, I.L. (1989) Mouse lymphnode homing receptor cDNA clone encodes a glycoprotein revealing tandem interaction domains. *Science* 243, 1165-1172

Sikorski, M.A., Staunton, D.E., Mier, J.W. (1996) L-selectin cross-linking induces integrin-dependent adhesion - evidence for a signalling pathway involving ptk but not PKC. *Cell Adhesion and Communication* 4 355-367.

Simmons, D.L. (1993). Cloning cell surface molecules by transient expression in mammalian cells. In Cellular Interactions In Development. D. Hartley, editor. Oxford University Press, Oxford. 93-128.

Simmons, D.L., Satterthwaite, A.B., Tenen, D.G., Seed, B. (1992) Molecular cloning of a cDNA encoding CD34, a sialomucin of human haematopoietic stem cells. *Journal of Immunology* 148 267-271

Simmons, D.L., Tan, S., Tenen, D.G., Nicholson-Weller, A., Seed, B. (1989) Monocyte antigen CD14 is a phospholipid anchored membrane protein. *Blood* 73 284-289

Simmons, D.L., Walker, C., Power, C. and Pigott, R. (1990) *Journal of Experimental Medicine* 171, 2147-2152.

Simon, S.I., Burns, A.R., Taylor, A.D., Gopalan, P.K., Lynam, E.B., Sklar, L.A., Smith, C.W. (1995) L-selectin (CD62l) cross-linking signals neutrophil adhesive functions via the Mac-1 (CD11b/CD18) beta(2)-integrin. *Journal of Immunology* 155 1502-1514.

Sims, P.J., Ginsberg, M.H., Plow, E.F., Shattil, S.J. (1991) Effect of platelet activation on the conformation of the plasma membrane glycoprotein IIb, IIIa complex. *Journal of Biological Chemistry* 266 7345-7352.

Sligh, J.E., Ballantyne, C.M. Rich, S.S., Hawkins, H.K., Smith, C.W., Bradley, A. and Beaudet, A.L. (1993). Inflammatory and immune responses are impaired in mice deficient in intercellular adhesion molecule 1. *Proceedings of the National Academy of Sciences (USA)* 90 8529-8533.

Smith, C.H., Barker, J.N., Morris, R.W., MacDonald, D.M., Lee, T.H. (1993) Neuropeptides induce rapid expression of endothelial cell adhesion molecules and elicit granulocyte infiltration in human skin. *Journal of Immunology* 151 3274-3782.

Smith, J. D., Chitnis, C. E., Craig, A. G., Roberts, D. J., Hudson-Taylor, D. E., Peterson, D. S., Pinches, R., Newbold, C. I., and Miller, L. H. (1995) *Cell* 82 101-110.

Smith, J.W., Cheresh, D.A. (1988) The RGD binding domain of the vitronectin receptor. Photoaffinity cross-linking implicates amino acid residues 61-203 of the β subunit. *Journal of Biological Chemistry* 263 18726-18731.

Springer, T.A. (1988) Adhesion receptors of the immune system. *Nature* 346 425-433.

Springer, T.A., Lasky L.A. (1991) Sticky sugars for selectins. *Nature* 349 196-197.

Springer, T.A. (1995) Traffic signals on endothelium for lymphocyte recirculation and leukocyte emigration. *Annual Review of Physiology* 57 827-872

Stanley, P. (1989) Transfection of a human gene that corrects the Lec1 glycosylation defect *Molecular and Cellular Biology* 9 377-383.

Starling, G.C., McLellan, A.D., Egner, W., Sorg, R.V., Fawcett, J., Simmons, D.L. and Hart, D.N.J. (1995). Intercellular adhesion molecule-3 is the predominant co-stimulatory ligand for leukocyte function antigen-1 on human blood dendritic cells. *European Journal of Immunology*. 29 2528-2532.

Staunton, D.E., Dustin, M.L., Erikson, H.P., and Springer T.A. (1990) The arrangement of the immunoglobulin-like domains of ICAM-1 and the binding sites for LFA-1 and rhinovirus. *Cell* 61 243-254 (1990).

Steegmaier, M., Levinovitz, A., Isenmann, S., Borges, E., Lenter, M., Kocher, H.P., Kleuser, B., Vestweber, D. (1995) The E-selectin-ligand ESL-1 is a variant of a receptor for fibroblast growth-factor. *Nature* 373 615-620.

Steitz, T.A., Kohlstaedt, L.A., Wang, J., Friedman, J.M., Rice, P.A. (1992) Crystal-structure at 3.5 angstrom resolution of HIV-1 reverse-transcriptase complexed with an inhibitor *Science* 256 1783-1786.

Stewart, M., Thiel, M. and Hogg, N. (1995). Leukocyte integrins. *Current Opinion in Cell Biology* 7: 690-696.

Stewart, M.P., Cabanas, C., Hogg, N. (1996) T-cell adhesion to intercellular-adhesion molecule-1 (ICAM-1) is controlled by cell spreading and the activation of integrin LFA-1. *Journal of Immunology* 156 1810-1817.

Stockinger, H., Gadd, S.J., Eher, R., Majdic, O., Schreiber, W., Kasinreck, W. Strass, B., Schnabl, E. and Knapp, W. (1990) *Journal of Immunology* 145, 3889-3897.

Stuart, D.I., Levine, M., Muirhead, H. and Stammers, D. (1979) The crystal structure of cat pyruvate kinase at a resolution of 2.6A. *Journal of Molecular Biology*. 134 109-142.

Subramaniam M, Frenette PS, Saffaripour S, Johnson RC, Hynes RO, Wagner DD (1996) Defects in haemostasis in P-selectin-deficient mice. *Blood* 87 1238-1242

Sugama, Y., Tiruppathi, C., Janakididevi, K., Anderson, T.T., Fenton, J.W., Malik, A.B. (1992) Thrombin-induced expression of endothelial P-selectin and intercellular adhesion molecule -1: A mechanism for stabilising neutrophil adhesion. *Journal of Cell Biology* 119 935-944.

Summerhill RJ, Jackson DG, Galione A (1993) Human lymphocyte antigen CD38 catalyses the production of cyclic ADP-ribose. FEBS Letters 335 231-233.

Sun, J., Williams, J., Yan, H-C., Amin, K.M., Albelda, S.M. and DeLisser, H.M. (1996b). Platelet endothelial cell adhesion molecule-1 (PECAM-1) homophilic adhesion is mediated by immunoglobulin-like domains 1 and 2 and depends on the cytoplasmic domain and level of surface expression. *Journal of Biological Chemistry*. 271 18561-18570.

Sun, Q.H., Delisser, H.M., Zukowski, M.M., Paddock, C., Albelda, S.M., Newman, P.J. (1996a) Individually distinct Ig homology domains in PECAM-1 regulate homophilic binding and modulate receptor affinity. *Journal of Biological Chemistry* 271 11090-11098.

Takagi, J., Kamata, T., Meredith, J., Puzon-McLaughlin, W., Takada, T. (1997) Changing Ligand Specificities of αvβ1 and αvβ3 Integrins by Swapping a Short Diverse Sequence of the β Subunit . *Journal of Biological Chemistry* 272 19794-19800.

Takasawa, S., Tohgo, A., Noguchi, N., Koguma, T., Nata, K., Sugimoto, T., Yonekura, H., Okamoto, H. (1993) Synthesis and hydrolysis of cyclic ADP-ribose by human leukocyte antigen CD38 and inhibition of the hydrolysis by ATP. *Journal of Biological Chemistry* 268 26052-26054.

Tanaka, Y., Albelda, S.M., Horgan, K.J., van Seventer, G.A., Newman, W. Hallam, J., Newman, P.J., Buck, C.A., Shaw, S. (1992) CD31 expressed on distinctive T-cell subsets is a preferential amplifier of b1 integrin-mediated adhesion. *Journal of Experimental Medicine* 176 245-253.

Tedder, T.F., Issacs, C.M., Ernst, T.J., Demetri, G.D., Alder, D.A., Disteche, C.M. (1989) Isolation and chromosomal localisation of cDNAs encoding a novel human lymphocyte cell surface molecule, LAM-1. Homology with the mouse lymphocyte homing receptor and other human adhesion proteins. *Journal of Experimental Medicine* 170 123-133.

Terry RW, Kwee L, Levine JF, Labow MA (1993) Cytokine induction of an alternatively spliced murine vascular cell-adhesion molecule (VCAM) messenger-RNA encoding a glycosyl phosphatidylinositol-anchored VCAM protein. *Proceedings of The National Academy of Sciences (USA)* 90 5919-5923.

Thiery, J.P., Brackenbury, R., Rutishauser, U., Edelman, G.M. (1977) Adhesion among neural cells of the chick embryo II. Purification and characterisation of a cell adhesion molecule from neural retina. *Journal of Biological Chemistry* 252 6841-6845.

Tian, L., Yoshihara, Y., Mizuno, T., Mori, K., Gahmberg, C.G. (1997) The neuronal glycoprotein telencephalin is a cellular ligand for the CD11a/CD18 leukocyte integrin. *Journal of Immunology* 158 928-936.

Tomschy, A., Fauser, C., Landwehr, R., Engel, J. (1996) Homophilic adhesion of E-cadherin occurs by a co-operative two step interaction of N-terminal domains. *EMBO Journal* 15 3507-3514.

Van der Merwe, P.A., McNamee, P.N., Davies, E.A., Barclay, A.N., Davis, S.J. (1995) Topology of the CD2-CD48 cell-adhesion molecule complex -implications for antigen recognition by T-cells. *Current Biology* 5 74-84

Vandervieren M., Letrong H., Wood C.L., Moore P.F., Stjohn T., Staunton D.E., Gallatin W.M. (1995) A novel leukointegrin, alpha-d-beta-2, binds preferentially to icam-3. *Immunity* 3 683-690

Vankooyk Y, Weder P, Heije K, Figdor CG (1994) Extracellular ca2+ modulates leukocyte function-associated antigen-1 cell-surface distribution on T-lymphocytes and consequently affects cell-adhesion. *Journal of Cell Biology* 124 1061-1070.

Vanstrijp J.A.G., Russell D.G., Tuomanen E., Brown E.J., Wright S.D. (1993) Ligand specificity of purified complement receptor type-3 (CD11b CD18, alpha(m)beta(2), mac-1) - indirect effects of an arg-gly-asp (rgd) sequence. *Journal of Immunology* 151 3324-3336

Vaporciyan, A.A., DeLisser, H.M., Yan, H.C., Mendiguren, I.I., Thorn, S.R., Jones, M.L., Ward, P.A. and Albelda S.M. (1993). Involvement of platelet-endothelial cell adhesion molecule-1 in neutrophil recruitment in vivo. *Science* 262 1580-1582.

Viney, J.L., Jones, S., Chiu, H.H., Lagrimas, B., Renz, M.E., Presta, L.G., Jackson, D., Hillan, K.J., Lew, S., Fong, S.(1996) Mucosal addressin cell-adhesion molecule-1 - a structural and functional-analysis demarcates the integrin binding motif. *Journal of Immunology* 157 2488-2497.

Vits, L., van Camp, G., Coucke, P., Fransen, E., De Boulle, K.D., Reyniers, E., Korn, B., Poustka, A., Wilson, G., Schrander-Stumpel, C., Winter, R., Schwartz, C., Willems, P.J. (1994) MASA syndrome is due to mutations in the neural cell adhesion gene L1CAM *Nature Genetics*7 408-413.

Von Andrian U.H., Hasslen S.R., Nelson R.D., Erlandsen S.L., Butcher E.C. (1995) A central role for microvillous receptor presentation in leukocyte adhesion under flow. *Cell* 82 989-999

Vonderheide, R.H., Tedder, T.F., Springer, T.A., and Staunton, D.E. (1994) Residues within a conserved amino-acid motif of domain-1and domain-4 of VCAM-1 are required for binding to VLA-4. *Journal of Cell Biology* 125 215-222.

Wakelin, M.W., Sank, M-J., Dewar, A., Albelda, S.M., Larkin, S.W., Boughton-Smith, N., Williams,T.J. and Nourshargh, S. (1996). An anti-platelet-endothelial cell adhesion molecule -1

antibody inhibits leukocyte extravasation from mesenteric microvessels in vivo by blocking the passage through the basement membrane. *Journal of Experimental Medicine*. 184 229-239.

Walcheck, B., Kahn, J., Fisher, J.M., Wang, B.B., Fisk, R.S., Payan, D.G., Feehan, C., Betageri, R., Darlak, K., Spatola, A.F., Kishimoto, T.K. (1996) Neutrophil rolling altered by inhibition of L-selectin shedding in-vitro. *Nature* 380 720-723.

Wassarman PM (1995) Towards molecular mechanisms for gamete adhesion and fusion during mammalian fertilization. *Current Opinion In Cell Biology* 7 658-664

Watson, S.R., Fennie, C., Lasky L.A. (1991) Neutrophil influx into an inflammatory site inhibited by a soluble homing receptor -IgG chimera. *Nature* 349 164-167.

Watson, S.R., Imai, Y., Fennie, C., Geoffroy, J.S., Rosen, S.D., Lasky, L.A. (1990). A homing receptor-IgG chimera as a probe for adhesive ligands of lymph node high endothelial venules. *Journal of Cell Biology* 110 2221-2229.

Watt, S.M., Gschmeissner, S.E., Bates, P.A. (1995) PECAM-1: Its expression and function as a cell adhesion molecule on haematopoietic and endothelial cells. *Leukemia and Lymphoma* 17 229-244.

Watt, S.M., Williamson, J., Genevier, H., Fawcett, J., Simmons, D.L., Hatzfeld, A., Nesbitt, S.A., and Coombe, D.R. (1993) The heparin-binding pecam-1 adhesion molecule is expressed by CD34+ hematopoietic precursor cells with early myeloid and B-lymphoid cell phenotypes. *Blood* 82 2649-2663.

Weitzman, J.B., Chen, A., and Hemler, M.E. (1995) Investigation of the role of b1 integrins in cell-cell adhesion. *Journal of Cell Science* 108, 3635-3644.

Wilkins, P.P., Moore, K.L., McEver, R.P., Cummings, R.D. (1995) Tyrosine sulfation of P-selectin glycoprotein ligand-1 is required for high-affinity binding to P-selectin. *Journal of Biological Chemistry* 270 22677-22680

Williams, A.F. and Barclay, A.N. (1988). The immunoglobulin superfamily-domains for cell surface recognition. *Annual Review of Immunology* 6 381-405.

Wilson, H.V. (1907) On some phenomena of coalescence and regeneration in sponges. *Journal of Experimental Zoology* 5 245-258

Wu, H., Kwon, P.D., Hendrickson, W.A. (1997) Dimeric association and segmental variability in the structure of human CD4. *Nature* 387 527-530.

Xie, Y. and Muller, W.A. (1993). Molecular cloning and adhesive properties of murine platelet/endothelial cell adhesion molecule-1. *Proceedings of the National Academy of Science*. (USA). 90: 5569-5573.

Yan, H.C., Baldwin, H.S., Sun, J., Buck, C.A., Albelda, S.M., DeLisser, H.M. (1995b) Alternative splicing of a specific cytoplasmic exon alters the binding characteristics of murine platelet endothelial-cell adhesion molecule-1 (PECAM-1). *Journal of Biological Chemistry* 270 23672-23680

Yan, H.C., Pilewski, J.M., Zhang, Q., Delisser, H.M., Romer, L., and Albelda, S.M. (1995a) Localisation of multiple functional domains on human PECAM-1 (CD31) by monoclonal-antibody epitope mapping. *Cell Adhesion and Communication*. 3 45-66.

Yoshihara, Y., Oka, S., Nemoto, Y., Watanabe, Y., Nagata, S., Kagamiyama, H., Mori, K. (1994) An ICAM-related neuronal glycoprotein, telencephalin, with brain segment-specific expression. *Neuron* 12 541-553.

Zehnder, J.L., Shatsky, M., Leung, L.L.K., Butcher, E.C, McGregor, J.L. and Levitt, L.J. (1995). Involvement of CD31 in lymphocyte-mediated immune responses: importance of the membrane proximal immunoglobulin domain and identification of an inhibiting CD31 peptide. *Blood* 85 1282-1288.

Zhang, Z.H., Vuori, K., Wang, H.G., Reed, J.C., Ruoslahti, E. (1996) Integrin activation by R-Ras. *Cell* 85 61-69.

Zhou, H., Fuks, A., Alcaraz, G., Bolling, T.J. and Stanners, C.P. (1993). Homophilic adhesion between Ig superfamily carcinoembryonic antigen molecules involves double reciprocal bonds. *Journal of Cell Biology* 122 951-960.

Zhou, L., Lee, D.H.S., Plescia, J., Lau, C.Y., Altieri, D.C. (1994) Differential ligand binding specificities of recombinant CD11b/CD18 integrin I-domain. *Journal of Biological Chemistry.* 269 17075-17079.

Zocchi M.R., Ferrero E., Leone B.E., Rovere P., Bianchi E., Toninelli E., Pardi R. (1997) CD31/pecam-1-driven chemokine-independent transmigration of human T-lymphocytes. *European Journal of Immunology* 26 759-767

APPENDIX A

The following primers were used to generate the point mutations described in this thesis:

Primers for site-directed mutagenesis.

Residues in domain 1

A. Lysines

1. K13A (AAG TO GCG)
FAMP 5' ATC AAC AGT GTT GAC ATG GCG AGC CTG CCG GAC TGG ACG 3'
RAMP 5' CGT CCA GTC CGG CAG GCT CGC CAT GTC AAC ACT GTT GAT 3'

2. K24A (AAG TO GCG)
FAMP 5' TGG ACG GTG CAA AAT GGG GCG AAC CTG ACC CTG CAG TGC 3'
RAMP 5' GCA CTG CAG GGT CAG GTT CGC CCC ATT TTG CAC CGT CCA 3'

3. K41A (AAG TO GCG)
FAMP 5' AGC ACC ACC TCT CAC GTC GCG CCT CAG CAC CAG ATG CTG 3'
RAMP 5' CAG CAT CTG GTG CTG AGG CGC GAC GTG AGA GGT GGT GCT 3'

4. K50A (AAG to GCG)
FAMP 5' CAC CAG ATG CTG TTC TAT GCG GAT GAC GTG CTG TTT TAC 3'
RAMP 5' GTA AAA CAG CAC GTC ATC CGC ATA GAA CAG CAT CTG GTG 3'

5. K50E (AAG to GAG):
FAMP 5' CAC CAG ATG CTG TTC TAT GAG GAT GAC GTG CTG TTT TAC 3'
RAMP 5' GTA AAA CAG CAC GTC ATC CTC ATA GAA CAG CAT CTG GTG 3'

6. K62A (AAG TO GCG)
FAMP 5' TAC AAC ATC TCC TCC ATG GCG AGC ACA GAG AGT TAT TTT 3'
RAMP 5' AAA ATA ACT CTC TGT GCT CGC CAT GGA GGA GAT GTT GTA 3'

7. K81A (AAA TO GCA)
FAMP 5' TAT GAC TCA GGG ACA TAT GCA TGT ACT GTG ATT GTG AAC 3'
RAMP 5' GTT CAC AAT CAC AGT ACA TGC ATA TGT CCC TGA GTC ATA 3'

8. K89A (AAA TO GCA)
FAMP 5' ACT GTG ATT GTG AAC AAC GCA GAG AAA ACC ACT GCA GAG 3'
RAMP 5' CTC TGC AGT GGT TTT CTC TGC GTT GTT CAC AAT CAC AGT 3'

9. K91A (AAA TO GCA)
FAMP 5' ATT GTG AAC AAC AAA GAG GCA ACC ACT GCA GAG TAC CAG 3'
RAMP 5' CTG GTA CTC TGC AGT GGT TGC GAG AAA ACC ACT GCA GAG 5'

B.Arginine

10. R73A (CGG TO GCG)
FAMP 5' TAT TTT ATT CCT GAA GTC GCG ATC TAT GAC TCA GGG ACA 3'
RAMP 5' TGT CCC TGA GTC ATA GAT GGC GAC TTC AGG AAT AAA ATA 3'

C. Aspartates:

11. Q2A (GAA to GCA)
FAMP 5' TCA AGC CTT GAG GGT CAA GCA AAC TCT TTC ACA ATC AAC 3'
RAMP 5' GTT GAT TGT GAA AGA GTT TGC TTG ACC CTC AAG GCT TGA 3'

12. D11A (GAC to GCC)
FAMP 5' TTC ACA ATC ACC AGT GTT GCC ATG AAG AGC CTG CCG GAC 3'
RAMP 5' GTC CGG CAG GCT CTT CAT GGC AAC ACT GGT GAT TGT GAA 5'

13. D17A (GAC to GCC)
FAMP 5' GAC ATG AAG AGC CTG CCG GCC TGG ACG GTG CAA AAT GGG 3'
RAMP 5' CCC ATT TTG CAC CGT CCA GGC CGG CAG GCT CTT CAT GTC 3'

14. D30A (GAT to GCT)
FAMP 5' ACC CTG CAG TGC TTC GCG GCT GTC AGC ACC ACC TCT CAC 3'
RAMP 5' GTG AGA GGT GGT GCT GAC AGC CGC GAA GCA CTG CAG GGT 5'

15. D51R (GAT to CGT)
FAMP 5' CAG ATG CTG TTC TAT AAG CGT GAC GTG CTG TTT TAC AAC 3'
RAMP 5' GTT GTA AAA CAG CAC GTC ACG CTT ATA GAA CAG CAT CTG 3'

16. D52A (GAC to GCC)
FAMP 5' ATG CTG TTC TAT AAG GAT GCC GTG CTG TTT TAC AAC ATC 3'
RAMP5' GAT GTT GTA AAA CAG CAC GGC ATC CTT ATA GAA CAG CAT 3'

17. D76A (GAC to GCC)
FAMP 5' CCT GAA GTC CGG ATC TAT GCC TCA GGG ACA TAT AAA TGT 5'
RAMP 5' ACA TTT ATA TGT CCC TGA GGC ATA GAT CCG GAC TTC AGG 5'

D. Glutamates

18. E65A (GAG to GCG)
FAMP 5' TCC TCC ATG AAG AGC ACA GCG AGT TAT TTT ATT CTT GAA 3'
RAMP 5' TTC AAG AAT AAA ATA ACT CGC TGT GCT CTT CAT GGA GGA 3'

19. E71A (GAA to GCA)
FAMP 5' GAG AGT TAT TTT ATT CCT GCA GTC CGG ATC TAT GAC TCA 3'
RAMP 5' TGA GTC ATA GAT CCG GAC TGC AGG AAT AAA ATA ACT CTC 3'

20. E90A (GAG to GCG)
FAMP 5' GTG AAT GTG AAC AAC AAA GCG AAA ACC ACT GCA GAG TAC 3'
RAMP 5' GTA CTC TGC AGT GGT TTT CGC TTT GTT GTT CAC ATT CAC 3'

21. E95A (GAG to GCG)
FAMP 5' AAA GAG AAA ACC ACT GCA GCG TAC CAG CTG TTG GTG GAA 3'
RAMP 5' TTC CAC CAA CAG CTG GTA CGC TGC AGT GGT TTT CTC TTT 3'

22.E101A (GAA to GCA)
FAMP 5' GAG TAC CAG CTG TTG GTG GCA GGA GTG CCC AGT CCC GTG 3'
RAMP 5' CAC GGG ACT GGG CAC TCC TGC CAC CAA CAG CTG GTA CTC 3'

Mutations in Domain 2 - Acidic residues

23. E139A (GAA to GCA)
FAMP 5' CCA ATA CAC TTC ACA ATT GCA AAA CTT GAA CTA AAT GAA 3'
RAMP 5' TTC ATT TAG TTC AAG TTT TGC AAT TGT GAA GTG TAT TGG 3'

24. E142A (GAA to GCA)
FAMP 5' TTC ACA ATT GAA AAA CTT GCA CTA AAT GAA AAA ATG GTC 3'
RAMP 5' GAC CAT TTT TTC ATT TAG TGC AAG TTT TTC AAT TGT GAA 3'

25. E145A (GAA to GCA)
FAMP 5' GAA AAA CTT GAA CTA AAT GCA AAA ATG GTC AAG CTG AAA 3'
RAMP 5' TTT CAG CTT GAC CAT TTT TGC ATT TAG TTC AAG TTT TTC 3'

26. E153A (GAG to GCG)
FAMP 5' ATG GTC AAG CTG AAA AGA GCG AAG AAT TCT CGA GAC CAG 3'
RAMP 5' CTG GTC TCG AGA ATT CTT CGC TCT TTT CAG CTT GAC CAT 3'

Residues in domain 3:

27. E239A (GAG to GCG)
FAMP 5' GTG ACT CAC CTG GCC CAG GCG TTT CCA GAA ATC ATA ATT 3'
RAMP 5' AAT TAT GAT TTC TGG AAA CGC CTG GGC CAG GTG AGT CAC 3'

28. E242A (GAA to GCA)
FAMP 5' CTG GCC CAG GAG TTT CCA GCA ATC ATA ATT CAG AAG GAC 3'
RAMP 5' GTC CTT CTG AAT TAT GAT TGC TGG AAA CTC CTG GGC CAG 3'

29. D248A (GAC to GCC)
FAMP 5' GAA ATC ATA ATT CAG AAG GCC AAG GCG ATT GTG GCC CAC 3'
RAMP 5' GTG GGC CAC AAT CGC CTT GGC CTT CTG AAT TAT GAT TTC 3'

APPENDIX B

The enclosed copies are of papers arising out of the work in this thesis.

1. Buckley, C.D., Doyonnas, R., **Newton, J.P.**, Blystone, S.D., Brown, E.J.,Watt, S.M., Simmons, D.L. (1996) Identification of alpha(v)beta(3) as a heterotypic ligand for CD31/PECAM-1. *Journal of Cell Science* 109 437-445.

2. **Newton, J.P.**, Buckley, C.D., Jones, E.Y., Simmons, D.L. (1997) Residues on both faces of the first immunoglobulin fold contribute to homophilic binding sites of PECAM-1/CD31. *Journal of Biological Chemistry* 272 20555-20563.

Journal of Cell Science 109, 437-445 (1996)
Printed in Great Britain © The Company of Biologists Limited 1996
JCS4057

Identification of $\alpha_v\beta_3$ as a heterotypic ligand for CD31/PECAM-1

C. D. Buckley[1,2,*], R. Doyonnas[3,*], J. P. Newton[1], S. D. Blystone[4], E. J. Brown[4], S. M. Watt[3,†] and D. L. Simmons[1,†,‡]

[1]Cell Adhesion Laboratory, Imperial Cancer Research Fund, [2]Nuffield Department of Medicine, and [3]MRC Molecular Haematology Unit, Institute of Molecular Medicine, John Radcliffe Hospital, Headington, Oxford, OX3 9DU, UK
[4]Department of Medicine, Infectious Diseases Division, Washington University School of Medicine, St Louis, Missouri 63110, USA

*C.D.B. and R.D. are joint first authors
†S.M.W. and D.L.S. are joint senior authors
‡Author for correspondence (e-mail: d_simmons@icrf.icnet.uk)

SUMMARY

CD31 (PECAM-1) is a member of the immunoglobulin gene superfamily (IgSF) and has an important role in a number of endothelial cell functions including angiogenesis, inflammation, integrin activation and cell-cell adhesion. CD31 has both homotypic and heterotypic adhesive properties and in common with other IgSF members contains multiple functional domains. Using chimaeric fusion proteins of CD31 and a panel of haematopoietic cell lines we show that CD31 can bind cells in a predominantly homotypic or heterotypic manner depending on the cell line used. Heterotypic binding was found to be cation and temperature dependent and enhanced by Mn^{2+}: all features of integrin mediated binding. Using a panel of anti-CD31 and anti-integrin antibodies we show that $\alpha_v\beta_3$ is a ligand for CD31 on the monocytic cell line U937. The specificity of the interaction between $\alpha_v\beta_3$ and CD31 was further confirmed by solid phase binding assays and the use of $\alpha_v\beta_3$ transfected cells which bound CD31 specifically. Furthermore, we have mapped the binding site for $\alpha_v\beta_3$ to domains 1 and 2 of CD31. The interaction of CD31 with $\alpha_v\beta_3$ may be important in many aspects of endothelial function including leukocyte-endothelial transmigration and angiogenesis.

Key words: Cell adhesion molecule, Integrin, Endothelium, Monocyte

INTRODUCTION

CD31 (PECAM-1) is a cell adhesion molecule (CAM) the extracellular domain of which consists of six Ig C2-related domains (Simmons et al., 1990; Newman et al., 1990; Stockinger et al., 1990). It is highly expressed on endothelium, platelets, about 50% of lymphocytes and cells of myeloid lineage (De Lisser et al., 1994b). It is also expressed on $CD34^+$ haematopoietic progenitor cells in human bone marrow (Watt et al., 1993, 1995a,b). In both endothelial and monocytic cells the turnover of CD31 at the cell surface is rapid; the $t_{1/2}$ being approximately 24 hours (Goldberger et al., 1994).

CD31 has been implicated in a number of biological events, primarily involving inter-endothelial adhesion (Muller et al., 1989; Schimmenti et al., 1992) and leukocyte-endothelial adhesion and transmigration (Muller et al., 1993). A number of animal model studies, using CD31 antibodies, have shown that CD31 is involved in monocyte and neutrophil recruitment during inflammation (Vaporciyan et al., 1993; Bogen et al., 1994). However, CD31 expression on leukocytes is not a prerequisite for transendothelial migration (Bird et al., 1993).

CD31 is also involved in adhesion amplification via β_1 and β_2 integrins (Tanaka et al., 1992; Piali et al., 1993; Berman and Muller, 1995). The molecular basis of this cross talk between CD31 and integrins is undefined. However, it is not restricted to haematopoietic cells as it can also occur in heterologous primate cells (Fawcett et al., 1995). Moreover, co-ligation of CD31 with FcRγII in monocytes leads to the production of pro-adhesive cytokines (Chen et al., 1994). CD31 has also been implicated in T cell and platelet activation with both de novo phosphorylation on serine and threonine residues and cell surface redistribution of CD31 being observed as cells are activated (Newman et al., 1992; Zehnder et al., 1992; Romer et al., 1995). Together these results suggest that CD31 may act as a signalling molecule.

CD31 mediated adhesion is complex involving both homotypic and heterotypic interactions. Homotypic binding involves extensive interdigitation of CD31 on apposing cells and requires all six domains. Key binding sites reside in domains 2-3 and 5-6 (Fawcett et al., 1995). A heterotypic binding site is located within domain 2 which contains a consensus sequence for glycosaminoglycan (GAG) binding (Muller et al., 1992; DeLisser et al., 1993). However, domain 6 also appears to be involved in heterotypic binding as the epitopes for two monoclonal antibodies that block heterotypic but not homotypic binding map to this domain (DeLisser et al., 1994; Yan et al., 1995). CD31 therefore appears to contain multiple functional domains capable of mediating quite different ligand-receptor interactions. How these adhesive options are regulated is not fully understood but a direct role for the cytoplasmic tail has been demonstrated (Baldwin et al., 1994; DeLisser et al., 1994a).

The CD31 gene has a relatively complex structure encompassing more than 65 kb of DNA organized into 16 exons (Kirschbaum et al., 1994). At least three alternatively spliced forms have been identified, one of which encodes a soluble form lacking the transmembrane domain (Goldberger et al., 1994) and in the mouse several splice variants of the cytoplasmic tail have been defined. In view of the recent report that soluble forms of E-selectin and VCAM-1 can act as potent angiogenic stimuli (Koch et al., 1995), soluble and secreted variants of CD31may have a role in angiogenesis.

Studies on the role of CD31 have mainly concentrated on its function on endothelium and leukocytes. However, the role of CD31 in haematopoietic development is poorly understood. Haematopoietic progenitor cells as well as macrophages in the stroma of long term bone marrow cultures both express CD31 (Watt et al., 1993, 1995a,b). Moreover, ligation of CD31 on $CD34^+$ haematopoietic cells seems to result in the activation of VLA-4 but not LFA-1 providing further evidence for the role of CD31 as an adhesion amplifier (Leavesley et al., 1994).

In order to explore the repertoire of binding modes of CD31 on haematopoietic cells we screened a panel of cell lines representing various stages of myeloid and lymphoid lineage development for adhesion to recombinant chimeric forms of human CD31. We found that some cell lines (KG1B, MIK ALL) bound to CD31 in a predominantly homotypic manner whereas others (U937) bound in a predominantly heterotypic manner. Recently, another laboratory examining the adhesion of murine lymphokine-activated killer (LAK) cells and pro-T-cells to recombinant forms of truncated murine CD31 reported that the integrin $\alpha_v\beta_3$ is an additional receptor for CD31 (Piali et al., 1995). In agreement with these findings, we confirm that in the human, CD31 can mediate heterotypic adhesion to $\alpha_v\beta_3$. Furthermore, by using a series of truncated soluble recombinant forms of CD31 in combination with blocking monoclonal antibodies we map the integrin heterotypic binding site to domains 1 and 2 of CD31.

MATERIALS AND METHODS

Cells and reagents

All the cell lines used in this study except MIK-ALL were provided by the Imperial Cancer Research Fund (ICRF) Cell Production Service and were maintained in RPMI/10% FCS. MIK-ALL was cultured as previously described (Watt et al., 1993). The production of K562 cells stably transfected with $\alpha_v\beta_3$ (Kavb3) or vector alone (KRc/RSV) has been described (Blystone et al., 1995). These cells were maintained in either RPMI or IMDM/10%FCS containing 1.2 mg/ml G418 (Genticin, Gibco). All reagents used were from Sigma Chemical Co., unless otherwise specified.

Antibodies

The following monoclonal antibodies (mAbs) were used. Anti-CD31 mAbs were: 9G11 (Simmons et al., 1990); L133.1 (Becton Dickinson, Oxford, UK); hec 7.2 (Endogen, TCS Biologicals Ltd, Bucks, UK); 5.6E (Immunotech, Marseille, France); 10B8 (British Bio-technology, Oxford, UK); CLB/CD31 (Monosan, Bucks, UK); HC1/6 (Serotec, Kidlington, UK); JC70A (provided by Dr J.Cordell, John Radcliffe Hospital, Oxford, UK); CAL31.1 IgG1 (which maps to domain 6 of CD31) was generated in mice after immunisation with a CD31(D1-D6)-Fc chimeric fusion protein. Anti-integrin antibodies were: anti-α_2 integrin clone HAS-6 (ICRF Biotherapeutics and Hybridoma Development Unit, South Mimms, UK); anti-α_3 integrin clone P1B5 (Becton Dickinson, Oxford, UK); anti-α_4 integrin clone HP2/1 (Immunotech, Marseille, France); anti-α_5 integrin clone IIA1 (PharMingen, Cambridge Bioscience, Cambridge, UK); anti-α_6 integrin clone GoH3 (Serotec, Kidlington, UK) anti-α_v integrin clone L230 (provided by Dr J. Marshall, Richard Dimbleby Department of Cancer Research, ICRF Laboratory, Guy's and St Thomas's Hospital, London UK); anti-β_1 integrin clone 13 (Becton Dickinson, Oxford, UK); anti-β_2 integrin MHM23 (Dako, Bucks, UK); anti-β_3 integrin clone RUU-PL 7F12 (Becton Dickinson, Oxford, UK); anti-$\alpha_v\beta_3$ integrin clone LM609 (Chemicon International, Harrow, UK) and clone 23C6 (ICRF Biotherapeutics and Hybridoma Development Unit, South Mimms, UK). Control antibody was anti-VCAM clone BBIG-V1 (R&D systems, Abingdon, Oxford). Polyclonal goat anti-human-Fc Ig was obtained from Sigma Chemical Co.

Chimeric fusion proteins

The CD31 chimeric fusion proteins used in this study consisted of the appropriate NH_2 terminal IgC2 domains of CD31 fused to the Fc region of human IgG1, and have been previously described (Simmons, 1993; Fawcett et al., 1995). A negative control chimeric IgSF-Fc fusion protein (MUC18-Fc) was generated as described previously (Fawcett et al., 1992). All Fc chimeric proteins were purified from COS-1 cell supernatants as previously described (Simmons, 1993), and checked by SDS-PAGE.

Cell adhesion assays

Cell adhesion to soluble chimeric fusion proteins was carried out as previously described (Fawcett et al., 1995) with the following modifications. 96-well adhesion assay plates (Immulon-3; Dynatech Research Laboratories, Chantilly, Virginia, USA) were precoated with 1 μg/well goat anti-human IgGFc and nonspecific sites blocked with 0.4% BSA (Fraction V). Recombinant Fc proteins in PBS were added at 0.5 μg/well. This concentration of Fc protein was shown to be saturating by both ELISA and adhesion assays. Cells were labelled by incubation with the fluorescent dye BCECF-AM (Molecular Probes, Oregon, USA) for 30 minutes and washed twice in assay buffer (RPMI-20 mM Hepes, 0.2% BSA). The labelled cells were added at 1×10^5 cells/well and incubated for 30-35 minutes at 37°C. Plates were washed with prewarmed assay buffer until the cells in the control wells were sufficiently removed as monitored by visual inspection. Typically this was 2-3 times. The attached cells were quantitated using a fluorescence plate reader Cytofluor II (Millipore, Watford, UK) and the percentage of input cells bound calculated after measuring the total fluorescence prior to washing. For some assays, cells were labelled for 24-48 hours with [^{3}H]thymidine (Amersham, Bucks, UK) adherent cells lysed in 1% SDS and incorporated radioactivity counted using a Beckman LS 5000 CE counter.

In experiments where mAbs were added, cells were preincubated with antibodies at a final concentration of 10 μg/ml for 10 minutes at room temperature prior to plating and included throughout the assay. In experiments to analyse the effects of Mn^{2+} on cell binding, $MnCl_2$ was diluted in assay buffer at a final concentration of 0.5 mM and added to the plated cells in each well.

All adhesion assays were performed on at least two independent occasions. Each data point represents the mean of three replicates and the data are expressed as the % of input cells bound ± 1 s.d.

Purification of $\alpha_v\beta_3$ and solid-phase binding assay

$\alpha_v\beta_3$ was purified from the human melanoma cell line DX3. Cells were lifted with 2 mM EDTA in PBS, washed in PBS and lysed in 50 ml of 150 mM NaCl, 2 mM $CaCl_2$, 0.02% NaN_3, 1% NP40, 20 mM Tris-HCl, pH 7.5, 1 mM PMSF, 5 μg/ml leupeptin, 5 μg/ml aprotinin, on ice for 1 hour. The cell lysates were centrifuged at 26,000 rpm and then passed over a 23C6 affinity column (prepared by coupling 23C6 to CNBr-activated Sepharose (Pharmacia) according to the manufacturer's instructions). The column was washed in 150 mM NaCl, 2 mM $CaCl_2$, 0.02% NaN_3, 0.1% NP40,

20 mM Tris-HCl, pH 7.5, and bound material eluted with 150 mM NaCl 1% octyl-glucopyranoside, 10 mM sodium acetate, pH 3.1, and 0.5 ml fractions collected and neutralised with 0.1 ml 1 M Tris-HCl, pH 8.0. Pooled fractions were concentrated using a centricon concentrator (Amicon), and aliquots stored at –70°C. The integrin preparation was pure as judged SDS-PAGE (Fig. 6A) and ELISA using anti-$\alpha_v\beta_3$ mAbs.

Solid-phase binding was performed using a modification of the method of Charo et al. (1990). Purified $\alpha_v\beta_3$ (0.2 mg/ml) was diluted 1:50 in TBS 0.02% NaN_3 containing 1 mM $CaCl_2$ (Buffer A) and 100 μl aliquots added to a 96-well Nunc-Maxisorp ELISA plate (Gibco, Life Technologies). Plates were incubated overnight at 4°C and blocked with 200 μl 5% BSA in buffer A for 1-3 hours at room temperature. Wells were then washed 3 times in TBS, 1 mM $CaCl_2$, 1 mM $MnCl_2$, 1 mg/ml BSA (Buffer B). Aliquots (100 μl) of the Fc protein ligands (at 5 μg/ml) were added with or without mAbs and the plate incubated at 30°C for 3 hours. Wells were washed 3 times in buffer B and bound Fc ligand detected by the addition of peroxidase-conjugated anti-huuman Fc antibody (1:2,000) in buffer B for 30 minutes at room temperature. Wells were then washed 4 times in buffer B and colour developed using OPD substrate (Sigma). The level of non specific binding was determind by the level of ligand binding to wells coated with BSA alone; these values were subtracted from all samples.

Immunofluorescence

Cells were incubated in PBS 0.2% BSA, 5 mM azide at 4°C for 20 minutes with the appropriate antibody at 10 μg/ml followed by FITC labelled goat anti-mouse Ig (or in some cases anti-rat Ig). The median fluorescence intensity was measured on a FACScan (Becton Dickinson, Oxford, UK) and at least 2,000 cells per sample were analysed.

Synthetic peptides

Synthetic peptides LKREKN, NKERKL and REKNLK, used in this study, were synthesised on a Zinsser SMPS 350 multiple peptide synthesiser using standard Fmoc solid phase chemistry and were purchased from Zinsser Analytic, Maidenhead, Berks, UK. These peptides have been used in a previous study (DeLisser et al., 1993) and correspond to residues 150-155 of CD31 (LKREKN), the reverse sequence (NKERKL) and a peptide with the same residue in a scrambled order (REKNLK). Both the 150-155 peptide and its reverse sequence have been shown to block glycosaminoglycan (GAG) mediated heterotypic binding (DeLisser et al., 1993). The peptides were purified by high performance liquid chromatography (HPLC) prior to use and sequence confirmed by mass spectrometry. All three peptides were water soluble and stored in PBS at –20°C prior to use.

RESULTS

Cell-chimeric protein adhesion screen for CD31 binding modes

In order to further explore the binding modes of CD31, we screened a panel of 11 haematopoietic cell lines representing different lineages and stages of development: KG1, KG1A and KG1B (myeloblastic progenitors); Raji, Namalwa and Daudi (B cell), MIKALL (pre-B cell); Molt 4 and HSB2 (T cell); U937 (pro-monocyte), and K562 (erythroleukaemic), for their ability to bind to soluble recombinant CD31(D1-D6)Fc chimeric protein immobilized on plastic via anti-Fc polyclonal antibodies (Fig. 1). The Fc fusion proteins were used at 0.5 μg/well. This system eliminates the possibility of accessory cell-cell interactions which may contribute to background binding in a two-cell system, and is quantitative and reproducible. Moreover, it allows for normalisation of the amount of chimeric protein presented to input cells. We have previously used this approach to define and dissect the homotypic binding mode of CD31 (Fawcett et al., 1995). Of the 11 cell lines screened, three (KG1B, MIK-ALL and U937) bound constitutively and specifically to CD31(D1-D6)Fc and not to a control IgSF-Fc fusion protein MUC-18Fc. (Fig. 1). All three of these cell lines express CD31 on their surface. However, there was no correlation between the level of CD31 expressed by these cells and their ability to bind to CD31(D1-D6)Fc. The binding of the pro-monocytic cell line U937 to CD31(D1-D6)Fc was much stronger than any homotypic adhesion previously measured on haematopoietic cells e.g. MIK-ALL (Fawcett et al., 1995) and suggested that additional mechanisms of CD31 adhesion were operating in this cell line. This was confirmed by the following analysis.

Pattern of cell binding to CD31(D1-D6)Fc deletion series

To further define the nature of CD31 mediated adhesion to U937, KG1B and MIK-ALL, we examined the ability of a nested series of chimeric truncation mutants of CD31-Fc to support binding of these three cell lines. This series of truncated forms of CD31 consists of NH_2 terminal 1, 1-2, 1-3, 1-4, 1-5 and 1-6 IgC2 domains of CD31 fused to the Fc region of human IgG1 which are designated CD31(D1)Fc, CD31(D1-D2)Fc, CD31(D1-D3)Fc, CD31(D1-D4)Fc, CD31(D1-D5)Fc and CD31(D1-D6)Fc. Fig. 2B,C, shows that for both KG1B

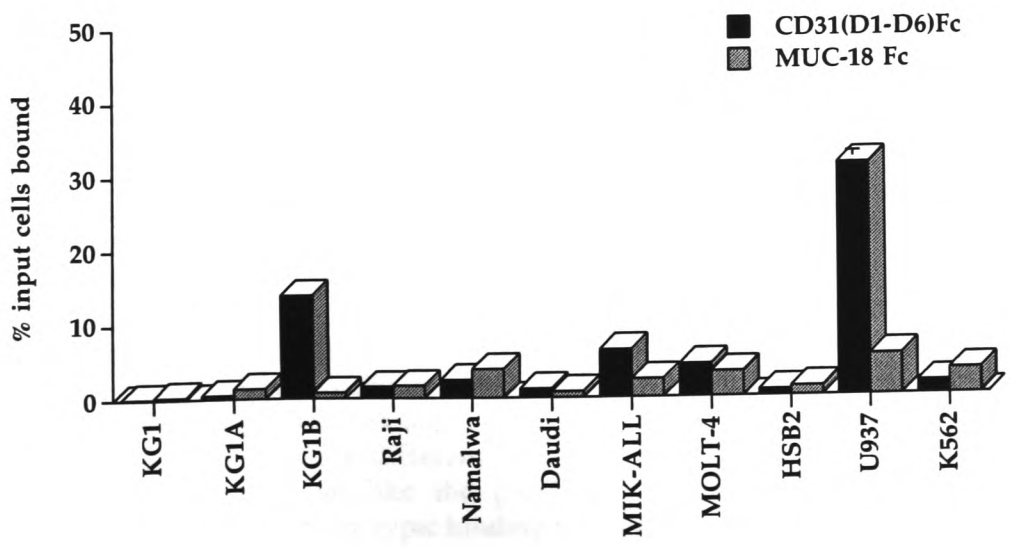


Fig. 1. Cell-chimeric protein adhesion screen of haematopoietic cell lines. Adhesion of 11 haematopoietic cell lines (KG1, KG1A, KG1B, Raji, Namalwa, Daudi, MIK-ALL, MOLT-4, HSB2, U937 and K562) to CD31(D1-D6)Fc or a control IgSF-Fc fusion protein. MUC-18Fc is included as a negative control for each cell line and represents the background level of adhesion in the assay. Results are expressed as the percentage of total input cells bound ± 1 s.d. (n=3).

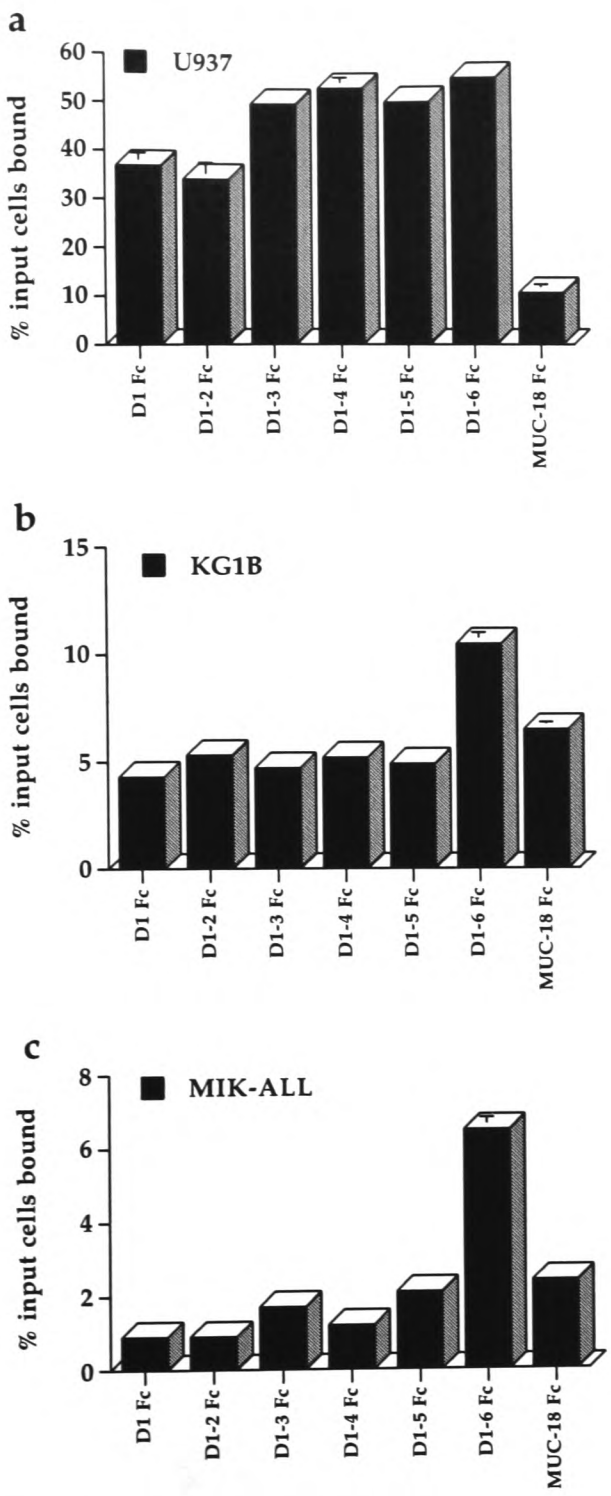


Fig. 2. Pattern of cell binding to CD31Fc chimeric deletion series. Adhesion of (a) U937, (b) KG1B, (c) MIK-ALL to CD31 deletion chimeras. The series used was CD31(D1)Fc, CD31(D1-D2)Fc, CD31(D1-D3)Fc, CD31(D1-D4)Fc, CD31(D1-D5)Fc and CD31(D1-D6)Fc. Background adhesion is to a control protein, MUC18-Fc. Results are expressed as percentage of total input cells bound ± 1 s.d. (n=3).

and MIK-ALL the presence of domain 6 of CD31 was necessary to support significant binding. However, for U937, all the truncation mutants, including the minimal unit CD31(D1)Fc, were able to support significant binding, although for maximal binding the minimal unit was CD31(D1-3)Fc. Domains 4, 5 and 6 did not contribute further to the binding of U937 (Fig. 2A). This suggested that U937 interacted with CD31 in a completely different manner to KG1B and MIK-ALL, and not at all like the previously established homotypic mode. Since homotypic binding has been shown to

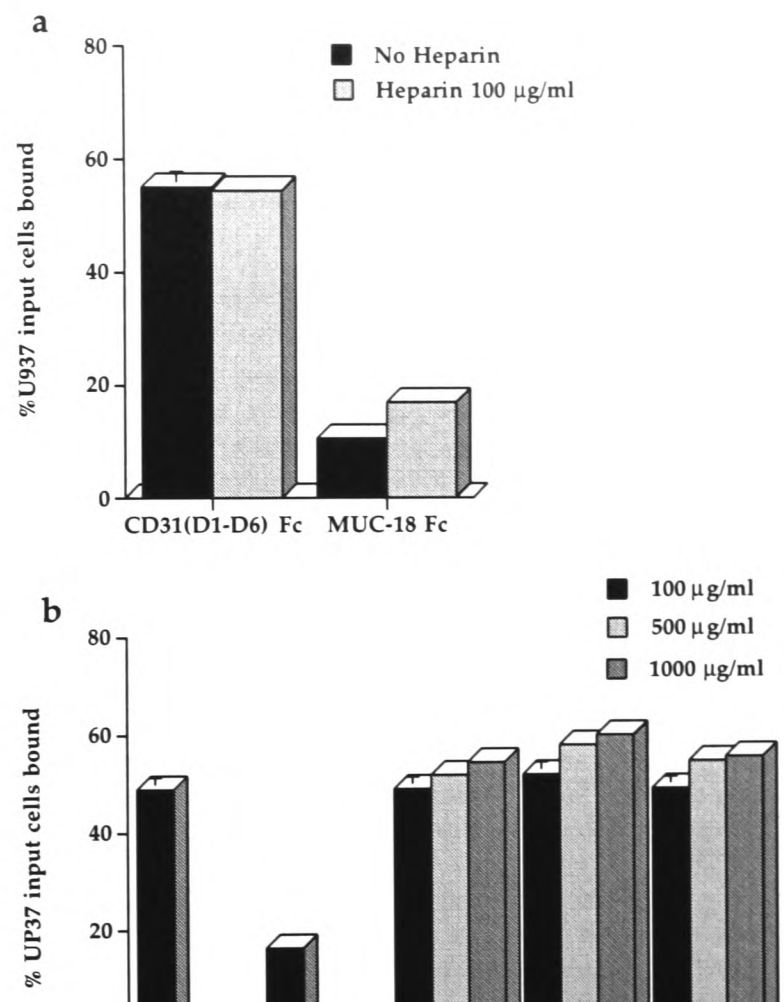


Fig. 3. Lack of involvement of GAGs in adhesion of U937 to CD31(D1-D6)Fc. (a) Effect of heparin. U937 binding to CD31(D1-D6)Fc is not inhibitable by heparin. Cells were allowed to bind in the presence or absence of 100 µg/ml heparin. Background binding is represented by binding to MUC18-Fc. (b) Effect of peptide mimetics. U937 binding to CD31(D1-D6)Fc is not inhibited in the presence of peptide mimetics of the putative GAG recognition sequence in CD31. Cells were incubated in the absence or presence of three concentrations (100 µg/ml, 500 µg/ml and 1,000 µg/ml) of the peptide LKREKN which exactly mimics the sequence of CD31 (residues 150-155); the reverse sequence peptide NKERKL, and a scrambled sequence peptide REKNLK. Background binding is represented by binding to MUC18-Fc. Results are expressed as percentage of total input cells bound ± 1 s.d. (n=3).

require the correct alignment of all six domains of CD31 (Fawcett et al., 1995), this suggested that U937 was binding CD31 in a predominantly heterotypic rather than homotypic manner, and that a novel CD31 counter receptor was expressed by U937.

Heterotypic U937-CD31(D1-D6)Fc interaction does not occur via glycosaminoglycans

A CD31 heterotypic adhesion mode has been reported that involves a site within the second Ig domain of CD31 binding to as yet undefined cell associated glycosaminoglycans (GAGs) (Muller et al., 1992; DeLisser et al., 1993). This binding can be completely blocked by heparin at 100 µg/ml. In addition, short linear peptide sequence recognition motifs have been identified within domain 2 of CD31 (position 150-155 LKREKN, and the reverse NKERKL) that are believed to

engage the GAG structures (DeLisser et al., 1993). We performed adhesion assays in the presence of these reagents. However, none of these reagents blocked the binding of U937 to CD31(D1-D6)Fc (Fig. 3A and B). These data, together with the fact that CD31(D1)Fc, could support significant binding suggested that a novel, non-GAG dependent counter-receptor existed on U937.

Cation, temperature dependence and Mn^{2+} regulation of CD31 mediated adhesion to U937

To further investigate the nature of this new counter-receptor, we examinined whether binding to CD31 was dependent on cations and temperature. As shown in Fig. 4A,B the binding of U937 to CD31(D1-D6)Fc was sensitive to both divalent cations and temperature. The lack of complete inhibition by EDTA and EGTA suggests that a small component of CD31 homotypic, cation independent binding was occurring when U937 bound CD31(D1-D6)Fc. This cation and temperature dependence suggested that the heterotypic counter-receptor on U937 might be an integrin. This was further enforced by the fact that the addition of 0.5 mM Mn^{2+} doubled the binding of U937 to CD31(D1-D6)-Fc. However, the same concentration of Mn^{2+} did not increase the binding of KG1B or MIK-ALL (data not shown). Mn^{2+} regulation is a characteristic feature of integrin mediated binding (Karecla et al., 1995). This stongly suggested that the novel counter-receptor on U937 cells was an integrin.

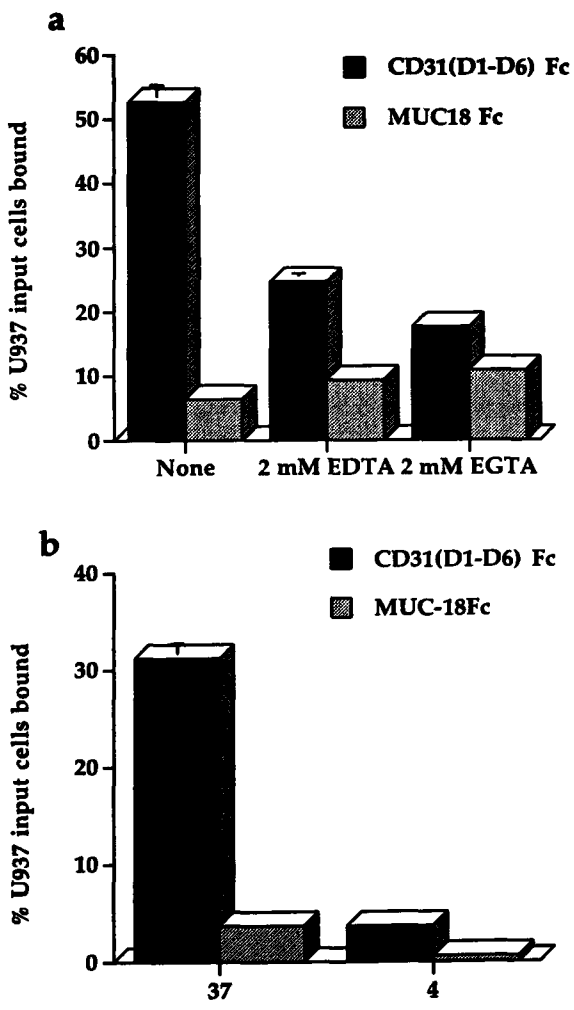


Fig. 4. Cation and temperature dependence of U937 adhesion to CD31(D1-D6)Fc. (a) Cation dependence. Adhesion of U937 cells to plastic coated with CD31(D1-D6)Fc. Cells were incubated in assay buffer alone (0.42 mM Ca^{2+}, 0.4 mM Mg^{2+}) or washed three times in HBSS containing 2 mM EDTA and then assayed in HBSS in the presence of 2 mM EDTA or 2 mM EGTA. (b) Temperature dependence. Adhesion of U937 cells to CD31(D1-D6)Fc either incubated at 37°C or 4°C. For both a and b, the background level of binding is indicated by adhesion to MUC18-Fc. Results are expressed as percentage of total input cells bound ± 1 s.d. n=6 for a; n=3 for b.

Adhesion of U937 to CD31(D1-D6)Fc is inhibited by antibodies to $\alpha_v\beta_3$

To identify the integrin that binds CD31, we established the surface integrin profiles of the three cell lines, U937, KG1B and MIK-ALL, known to bind CD31(D1-D6)Fc. U937 binds CD31 predominantly by the novel integrin heterotypic counter-receptor, compared with KG1B and MIK-ALL, which bind CD31 solely by the homotypic mode. The aim of establishing surface integrin profiles was to determine if there were any integrins that were unique to and/or expressed on U937, that were not on KG1B and MIK-ALL. By using a panel of anti-integrin α and β chain antibodies and flow cytometry we found that the integrin $\alpha_v\beta_3$ was expressed on U937, but not on KG1B or MIK-ALL (Table 1).

We then screened a further panel of anti-integrin adhesion blocking antibodies for their ability to inhibit the binding of U937 to CD31(D1-D6)Fc. Only antibodies to α_v (L230) and $\alpha_v\beta_3$ (LM609) were able to completely inhibit binding to background levels (Fig. 5). In contrast, a non-blocking antibody to $\alpha_v\beta_3$ (mAb 23C6) did not affect binding suggesting that blockade by LM609 was not due to non specific steric effects. Blocking mAbs to other integrins expressed on U937 (α_3, α_5, and β_2) did not affect binding. Although some inhibition did occur with antibodies to α_4, β_1 and β_3 this inhibition was within the limits of plate to plate variation of control cell binding. These results demonstrated that $\alpha_v\beta_3$ was the integrin ligand mediating U937 binding to CD31(D1-D6)Fc.

Specificity of the $\alpha_v\beta_3$ CD31 interaction

To provide additional evidence for a specific interaction between $\alpha_v\beta_3$ and CD31 we examined the binding of CD31(D1-D6)Fc to purified $\alpha_v\beta_3$ using a solid phase assay (Fig. 6A,B). This showed that the interaction between CD31 and $\alpha_v\beta_3$ was specific as a control protein MUC-18Fc did not bind $\alpha_v\beta_3$. Antibodies to both CD31 and $\alpha_v\beta_3$ inhibited

Table 1. Expression of integrin subunits by cell lines

		Median fluorescence intensity		
Antibody	Integrin	U937	KG1B	MIK-ALL
IgG1	Control	5.8	7.7	5.2
HAS-6	α_2	33.9	8.0	n/t
P1B5	α_3	16.5	4.8	6.0
HP2/1	α_4	67.3	45.3	69.7
IIA1	α_5	54.3	31.6	77.7
GoH3	α_6	12.8	10.7	40.6
13	β_1	107.5	69.8	119.7
MHM23	β_2	58.3	74.9	11.9
LM609	$\alpha_v\beta_3$	22.9	8.6	5.8
9G11	CD31	67.3	56.3	46.9

Fluorocytometry was used to determine integrin expression on the three cells lines as described in the materials and methods. Results are expressed as the median fluorescence intensity. Background fluorescence was determined by incubation with a mouse IgG1 control mAb (BBIG-V1). n/t, not tested.

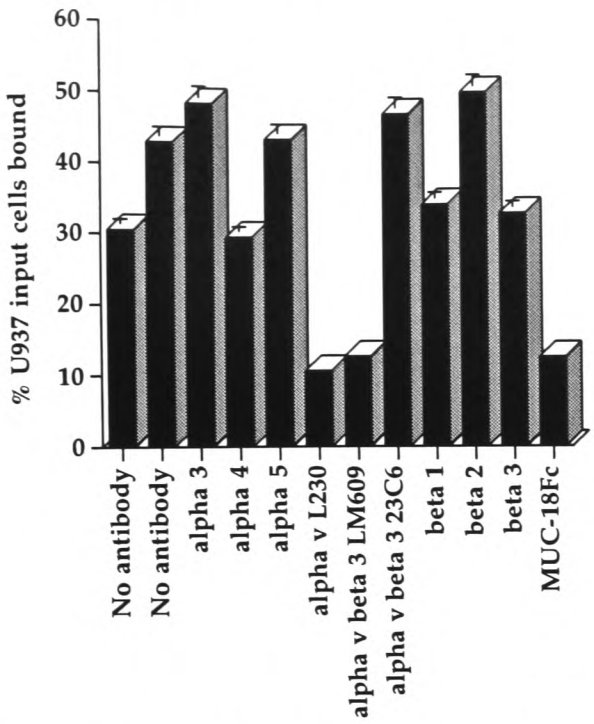


Fig. 5. Antibodies to $\alpha_v\beta_3$ block adhesion of U937 to CD31(D1-D6)Fc. Adhesion of U937 to CD31(D1-6)Fc in the absence or presence of a panel of blocking mAbs to integrins expressed on the surface of U937. Cells were incubated with mAbs at 10 μg/ml for 10 minutes at room temperature before the assay and then the cells were plated in 96-well plates coated with CD31(D1-D6)Fc as described in Materials and Methods. mAbs were present throughout the assay. The mAbs were: anti-α_3 integrin P1B5, anti-α_4 integrin HP2/1, anti-α_5 integrin IIA1, anti-α_v integrin L230, anti-$\alpha_v\beta_3$ integrin LM609, anti-$\alpha_v\beta_3$ integrin 23C6, anti-β_1 integrin 13, anti-β_2 integrin MHM23, anti-β_3 integrin RUU-PL 7F12. Background binding is represented by binding to MUC18-Fc. Two 'no antibody' values from the two separate plates used in this experiment are shown to indicate plate to plate variation of control binding. Results are expressed as percentage of total input cells bound ± 1 s.d. (n=3).

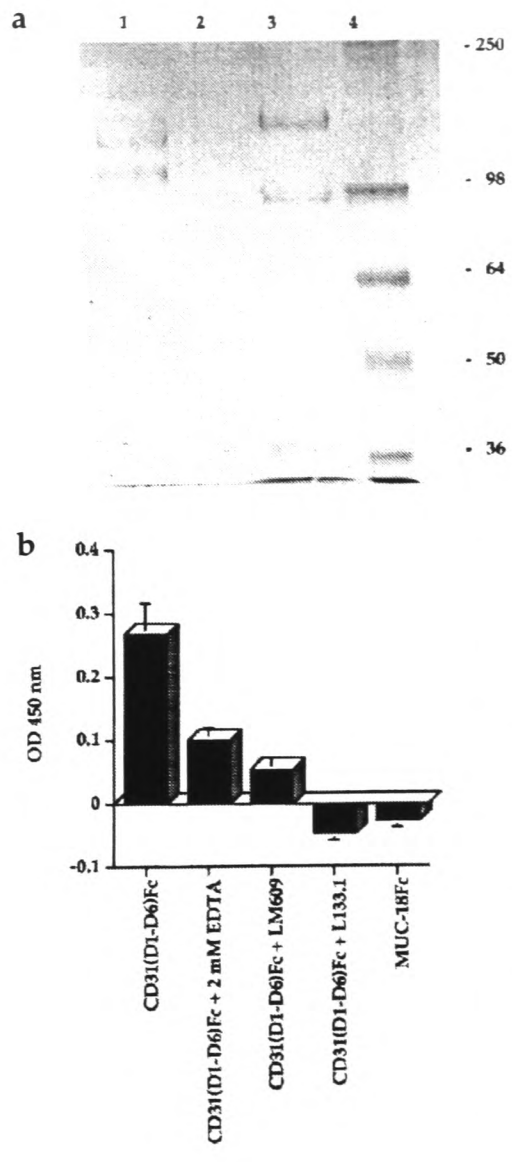


Fig. 6. CD31(D1-D6)Fc binds to purified immobilised $\alpha_v\beta_3$. (a) Characterization of purified $\alpha_v\beta_3$. SDS-PAGE analysis of immunopurified $\alpha_v\beta_3$ under reduced and non reduced conditions. Lane 1, reduced; lane 2, empty; lane 3, non reduced; lane 4, protein markers. Molecular mass markers are indicated (in kDa). The proteins were separared on a 7.5% gel and stained with Coomassie Blue. The α_v and β_3 chains run at 150 and 90 kDa (non reduced), and 125 and 105 kDa (reduced). (b) Binding of CD31 (D1-D6)Fc to immoblilzed $\alpha_v\beta_3$. CD31(D1-D6)Fc or the control protein MUC-18Fc were added to wells coated with $\alpha_v\beta_3$ in the presence or absence of EDTA (2 mM), the $\alpha_v\beta_3$ mAb LM609 (10 μg/ml) or the CD31 mAb L133.1 (10 μg/ml) and incubated for 3 hours at 30°C. A peroxidase-conjugated anti-human Fc antibody was used to detect bound Fc proteins, and background binding of this antibody to BSA subtracted from all samples. Results are expressed as the mean (OD_{450} nm) ± 1 s.d. (n=6).

binding as did 2 mM EDTA confirming the specificity of the CD31/$\alpha_v\beta_3$ interaction.

As further evidence for the specificity of the CD31/$\alpha_v\beta_3$ interaction we examined the binding of K562 cells (which do not express endogenous $\alpha_v\beta_3$) transfected with $\alpha_v\beta_3$ to CD31(D1-D6) Fc. Fig. 7 shows that only cells transfected with $\alpha_v\beta_3$ bound CD31(D1-D6)Fc. Mock transfected cells did not bind CD31(D1-D6)Fc. Furthermore neither transfected nor mock transfected cells bound MUC-18Fc. These K562 transfected cells express $\alpha_v\beta_3$ but no CD31 and therefore can only engage in heterotypic binding.

Mapping the $\alpha_v\beta_3$ binding site on CD31 by adhesion blockade

From the pattern of U937 binding to the CD31-Fc deletion series it was apparent that the binding site for $\alpha_v\beta_3$ on CD31 resided at least in part in domain 1 (Fig. 2A).

To determine whether any other domains of CD31 had additional contribution to CD31-$\alpha_v\beta_3$ mediated adhesion, a panel of 9 anti-CD31 mAbs were screened for their ability to block CD31-$\alpha_v\beta_3$ binding (Fig. 8). This also allowed us to directly compare the blocking abilities of mAbs known to inhibit homotypic binding (Fawcett et al., 1995) with their ability to inhibit $\alpha_v\beta_3$-CD31 adhesion. The anti-CD31 domain 2 mAbs 5.6E and L133.1 inhibited binding to background levels. Both these mAbs have been shown to inhibit CD31 homotypic binding. (Fawcett et al., 1995). The anti-CD31 mAb hec 7.2 which maps to the D1-D2 boundary (Muller et al., 1993), partially inhibited binding. None of the other anti-CD31 mAbs 9G11, JC70A, CLB/CD31, HC1/6, 10B8 and CAL31.1 affected binding. These results suggest that domain 2 of CD31 may contribute to the binding site for $\alpha_v\beta_3$.

DISCUSSION

It has already been established that CD31 exhibits both homotypic and heterotypic adhesive properties. The homotypic mode involves anti-parallel inter-digitation of apposing CD31 molecules. However, the identity of the heterotypic counter-receptor(s) has not been defined, but may involve glycosaminoglycans. By using an adhesion assay that relies on the presentation of a nested series of truncated forms of CD31 made as Fc fusion proteins we have been able to define an alternative CD31 binding mode on the pro-monocytic cell line

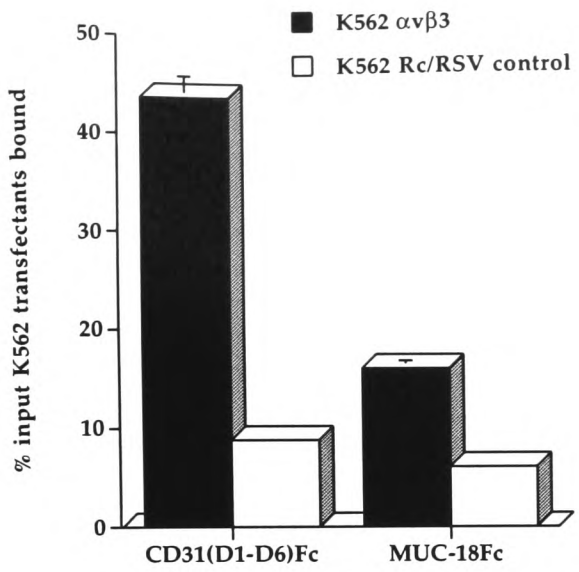


Fig. 7. K562 cells transfected with $\alpha_v\beta_3$ bind CD31(D1-D6)Fc. Adhesion of K562 cells stably transfected with $\alpha_v\beta_3$ or vector alone to wells coated with either CD31(D1-D6)Fc or MUC-18Fc. Cells were washed three times in TBS and incubated in TBS with 0.5 mM Mn^{2+} for 30 minutes at 37°C. Background binding is represented by binding to MUC-18Fc. Results are expressed as percentage of total input cells bound ± 1 s.d. (n=6).

U937. This stategy has allowed us to extend our previous studies on the mapping of the homotypic binding sites in CD31 (Fawcett et al., 1995) to demonstrate that the $CD31^+$ U937 cell line binds to CD31(D1-D6)Fc in a very different manner to other $CD31^+$ leukocytic cell lines. Significant, though not maximal, adhesion occurred with the CD31(D1)Fc fusion protein. This pattern of binding was unlike that observed for homotypic binding where the lack of any one of the six domains of CD31 leads to loss of binding (Fawcett et al., 1995) and suggested that a novel heterotypic counter-receptor for CD31 existed on U937 cells.

Using a combination of biochemical and mAb blocking assays we found that the heterotypic ligand on U937 did not involve cell surface GAGs but instead was the integrin $\alpha_v\beta_3$. Direct evidence for the specificity of the CD31/$\alpha_v\beta_3$ interaction was obtained through a combination of solid phase binding assays and the binding of $\alpha_v\beta_3$ transfectants to CD31. These results confirm for human CD31 a similar observation made by Piali et al. (1995) for murine CD31.

From the work of Piali et al. (1995), and our present study, the concomitant expression of $\alpha_v\beta_3$ and CD31 by a cell may modulate any potential CD31 homotypic binding, with heterotypic binding dominating over homotypic binding.

We have shown that CD31 can bind cells in a predominantly homotypic or heterotypic manner depending on the cell line used. We found that U937 bound CD31 in a predominantly heterotypic manner but that homotypic adhesion could also occur at a low level, since U937 binding to CD31 was not completely inhibited by EDTA or EGTA (Fig. 4A). This suggests that both homotypic and heterotypic modes of binding can operate in parallel. The preferential usage of one adhesion pathway over another to regulate overall cell adhesion has been demonstrated for other integrin/IgSF interactions. For example, there appears to be a hierarchy of binding pathways for the integrins LFA-1 and VLA-4 which are co-expressed on leukocytes (Van Kooyk et al., 1993). Moreover, recent observations in both humans and the mouse have shown that E-cadherin can mediate both homotypic (between epithelial cells) and also heterotypic interactions through adhesion to the mucosal T cell integrin $\alpha_E\beta_7$ (Cepek et al., 1994; Karecla et al., 1995).

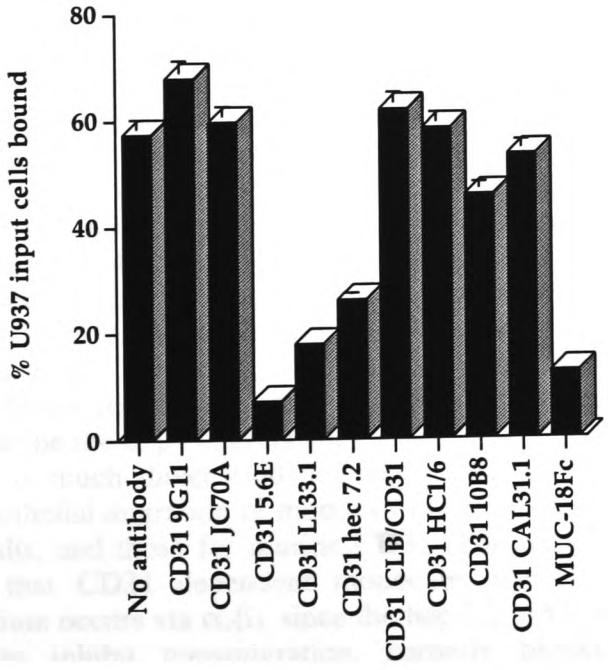


Fig. 8. Antibodies to D1-D2 of CD31 block binding of U937 to CD31(D1-D6)Fc. Adhesion of U937 to CD31(D1-D6)Fc in the absence or presence of a panel of mAbs to various domains of CD31. Assays were performed as in Fig. 5. The mAbs were: anti-CD31(D1) 9G11 and JC70A; anti-CD31(D2) 5.6E, L133.1 and CLB/CD31; anti-CD31(D1-D2) hec 7.2; anti-CD31(D4-D5) HC1/6; anti-CD31(D5) 10B8 and anti-CD31(D6) CAL31.1. Background binding is represented by binding to MUC18-Fc. Results are expressed as percentage of total input cells bound ± 1 s.d. (n=3).

The $\alpha_v\beta_3$ integrin is expressed on U937 but not on KG1B or MIK-ALL both of which bind CD31 solely in a homotypic manner. U937 cells, however, bind CD31 in a predominantly heterotypic manner. Furthermore, because U937 cells bind to CD31(D1-D6)Fc constitutively, this suggests that $\alpha_v\beta_3$ on U937 is expressed in an already activated state which can be further activated by Mn^{2+} ions, a well established external activator of integrin adhesion. The molecular mechanisms that regulate the adhesive phenotype (homotypic versus heterotypic) of CD31 expressing cells remain unknown. Some clues about possible regulatory mechanisms come from the work of DeLisser et al. (1994a) who showed that deletions of the cytoplasmic tail of CD31 can switch CD31 mediated adhesion from predominantly heterotypic (GAG-mediated, not via $\alpha_v\beta_3$) to predominantly homotypic binding. Only the extracellular portions of CD31 are necessary for homotypic binding to occur as measured by direct protein-protein interactions using surface plasmon resonance (our unpublished observations).

The binding site for $\alpha_v\beta_3$ on CD31 resides at least in part in domain 1. Utilising the CD31-Fc chimeric deletion series, we established that CD31(D1)Fc alone could support nearly maximal binding. In addition, three anti-CD31 blocking mAbs (2 of which by ELISA map to domain 2, and one to the domain 1/domain 2 boundary) block the $\alpha_v\beta_3$-CD31 interaction. This implies that domain 2 contributes to the binding site. These mAbs may however exert their blocking activity by sterically

hindering the access of $\alpha_v\beta_3$ to domain 1 of CD31. Maximal binding of $\alpha_v\beta_3$ to CD31 occurs with CD31(D1-D3)Fc. This could implicate a contribution from domain 3 but also could be due to optimal accessiblity and presentation of CD31 to $\alpha_v\beta_3$ away form the anti-Fc coated plastic surface used for the adhesion assays. Domains 4, 5 and 6 do not yield any increase in binding. The issue of accessibility of the IgSF chimeric protein to its counter-receptor also seems to be true of the interaction of ICAM-1 with its receptor on *Plasmodium falciparum* infected erythrocytes (Berendt et al., 1992). The ICAM-1-binding site for malaria infected erythrocytes maps to the first 2 domains yet adhesion to a shortened version of ICAM-1 containing these domains is reduced presumably due to steric hindrance. Therefore from our data we conclude that the binding site for $\alpha_v\beta_3$ on CD31 resides predominantly in domain 1 but that domain 2 may contribue to the binding site.

Both the domain 2 mAbs which are known to block homotypic binding (Fawcett et al., 1995) also blocked heterotypic binding to $\alpha_v\beta_3$. Significantly the hec 7.2 mAb which is known to inhibit monocyte transendothelial migration but does not inhibit homotypic or GAG-mediated heterotypic adhesion, partially inhibited $\alpha_v\beta_3$ mediated heterotypic adhesion. This mAb has been mapped to the D1-D2 boundary (Muller et al., 1993; Yan et al., 1995). Since D2 has been shown to be important on GAG mediated heterotypic binding (De Lisser et al., 1993), these results suggest that D1 and D2 play central roles in mediating homotypic and heterotypic adhesion, and that the binding sites for homotypic and $\alpha_v\beta_3$ mediated heterotypic adhesion must partially overlap, at least as measured by mAb epitope mapping.

From studies which have attempted to map the binding sites of those IgSF members which bind integrins (LFA-1-ICAM 1, 2, 3; VLA-4-VCAM, $\alpha_4\beta_7$-Mad-CAM), a model has emerged which emphasises the dominance of domains 1 and 2 (Holness and Simmons, 1994). Moreover, mutagenesis studies coupled with the crystal structure of vascular cell adhesion molecule-1 (Jones et al., 1995) have suggested that a common structural motif for integrin binding to IgSF members is the presence of an aspartate or glutamate residue in the C-D loop of the Ig like domain to which binding occurs (Bergelson and Hemler, 1995; Loftus et al., 1994). Sequence alignments of CD31 domains 1 and 2 against VCAM-1 domain 1, show that both D1 and D2 of CD31 have aspartate or glutamate residues at exposed regions in their C-D loops (data not shown and Watt et al., 1995a). These residues are key targets for mutagenesis to further define the $\alpha_v\beta_3$ binding site.

There is much direct evidence implicating CD31 in the transendothelial migration of monocytes (Muller et al., 1993). Our results, and those for murine CD31 (Piali et al., 1995), suggest that CD31 dependent monocyte interaction with endothelium occurs via $\alpha_v\beta_3$, since the hec 7.2 mAb, which is known to inhibit transmigration, partially blocks $\alpha_v\beta_3$-mediated heterotypic adhesion to CD31(D1-D6)1Fc. Interestingly, the anti-β_3 mAb RUU-PL 7F12, which is known to block some β_3 mediated cell matrix functions, did not fully block binding to CD31(D1-D6)Fc, suggesting that the binding site for CD31 on $\alpha_v\beta_3$ may be distinct from that for matrix molecules. There are many such examples of selective blocking of ligand binding by mAbs to integrins (Ruiz et al., 1993; Landis et al., 1994; Neugebauer and Reichardt, 1991). The fact that the ligand repertoire of $\alpha_v\beta_3$ includes both CD31 and ECM molecules such as vitronectin, fibronectin and laminin suggests that as transmigration occurs $\alpha_v\beta_3$ may become increasingly activated and able to switch from cell-cell to cell-ECM engagement. In fact it appears to be a general trend for integrins to display a broader range of ligand specificity as they become more activated (Chan and Hemler, 1993).

Finally, the CD31-$\alpha v\beta_3$ receptor-ligand pair has important implications for angiogenesis and endothelial biology since endothelial cells express both $\alpha_v\beta_3$ and CD31. Blocking $\alpha_v\beta_3$ either by mAbs or peptide antagonists has been shown to inhibit angiogenesis and increase apoptosis (Brooks et al., 1994). Furthermore, we have previously shown that CD31(D1-D6) Fc inhibits the growth of endothelial cells and mAbs to CD31 disrupt endothelial monolayer formation (Fawcett et al., 1995). Thus, CD31-CD31 homotypic adhesion and CD31-$\alpha_v\beta_3$ heterotypic adhesion may provide key signals to regulate endothelial proliferation and differentiation.

We thank Dr Ian Bird and Dr Julia Spragg of the Yamanouchi Research Institute, Oxford, for gifts of CD31 peptides and antibodies; Professor Ian Hart and Dr John Marshall, ICRF/Richard Dimbleby Dept. for Cancer Research, Guy's and St Thomas's Hospitals, London, for gifts of anti-αv antibody L230; and Professor John Bell (Nuffield Dept. of Medicine, John Radcliffe Hospital, Oxford) for support and discussions. This work was supported by the Wellcome Tust (Research Training Fellowship awarded to C.D.B.) the Leukaemia Research Fund (R.D. and S.M.W.), European Union Concerted Action on Haematopoietic Stem Cells and the Medical Research Council (S.M.W.), the Yamanouchi Research Institute (PhD studentship awarded to J.P.N.) and the ICRF (D.L.S.).

REFERENCES

Baldwin, H. S., Shen, H. M., Yan, H.-C., DeLisser, H. M., Chong, A., Mickanin, C., Trask, T., Kirschbaum, N. E., Newman, P. J., Albelda, S. M. and Buck, C. A. (1994). Platelet endothelial cell adhesion molecule-1 (PECAM-1/CD31): alternatively spliced, functionally distinct isoforms expressed during mammalian cardiovascular development. *Development* **120**, 2539-2553.

Berendt A. R., McDowall, A., Craig A. G., Bates, P. A., Sternberg, M. J. E., Marsh, K., Newbold, C. I. and Hogg, N. (1992). The binding site on ICAM-1 for Plasmodium falciparum-infected erythrocytes overlaps, but is distinct from, the LFA-1binding site. *Cell* **68**, 71-81.

Bergelson, J. M. and Hemler, M. E. (1995). Do integrins use a 'MIDAS touch' to grasp an Asp? *Curr. Biol.* **5**, 615-617.

Berman, M. E. and Muller, W. A. (1995). Ligation of platelet/endothelial cell adhesion molecule 1 (PECAM/CD31) on monocytes and neutrophils increases the binding capacity of leukocyte CR3 (CD11b/CD18). *J. Immunol.* **154**, 299-307.

Bird, I. N., Spragg, J. H., Ager, A. and Matthews, N. (1993). Studies of lymphocyte transendothelial migration: analysis of migrated cell phenotypes with regard to CD31 (PECAM-1), CD45RA and CD45RO. *Immunology* **80**, 553-560.

Blystone, S. D., Lindberg, F. P., LaFlamme, S. E. and Brown, E. J. (1995). Integrin β3 cytoplasmic tail is necessary and sufficient for regulation of α5β1 phagocytosis by αvβ3 and integrin-associated protein. *J. Cell Biol.* **130**, 745-754.

Bogen, S., Pak, J., Garifallou, M., Deng, X. and Muller, W. A. (1994). Monolclonal antibody to murine PECAM-1 (CD31) blocks acute inflammation in vivo. *J. Exp. Med.* **179**, 1059-1064.

Brooks, P. C., Montgomery, A. M. P., Rosenfeld, M., Reisfeld, R. A., Hu, T., Klier, G. and Cherish, D. A. (1994). Integrin $\alpha_v\beta_3$ antagonists promote tumor regression by inducing apoptosis of angiogenic blood vessels. *Cell* **79**, 1157-1164.

Cepek, K. L., Shaw, S. K., Parker, C. M., Russell, G. J., Morrow, J. S., Rimm, D. L. and Brenner, M. B. (1994). Adhesion between epithelial cells and T lymphocytes mediated by E-cadherin and the αEβ7 integrin. *Nature* **372**, 190-193.

Chan, B. M. C and Hemler, M. E. (1993). Multiple functional forms of the integrin VLA-2 can be derived from a single α2 cDNA clone: Interconversion of forms induced by an anti-β1 antibody. *J. Cell Biol.* **120**, 537-543.

Charo I, F., Nannizzi, L., Smith J. W. and Cherish, D. A. (1990). The vitronectin receptor αvβ3 binds fibronectin and acts in concert with α5β1 in promoting cellular attachment and spreading on fibronectin. *J. Cell Biol.* **111**, 2795-2800.

Chen, W., Knapp, W., Majdic, O., Stockinger, H., Bohmig, G. and Zlabinger, G. J. (1994). Co-ligation of CD31 and FcγRII induces cytokine production in human monocytes. *J. Immunol.* **152**, 3991-3997.

DeLisser, H. M., Yan, H. C., Newman, P. J., Muller, W. A., Buck, C. A. and Albelda, S. M. (1993). Platelet/endothelial cell adhesion molecule-1 (CD31)-mediated cellular aggregation involves cell surface glycosaminoglycans. *J. Biol. Chem.* **268**, 16037-16046.

DeLisser, H. M., Chilkowtowsky, J., Yan, H. C., Daise, M. L., Buck, C. A. and Albelda, S. M. (1994a). Deletions in the cytoplasmic domain of platelet-endothelial cell adhesion molecule-1 (PECAM-1, CD31) result in changes in ligand binding properties. *J. Cell Biol.* **124**, 195-203.

DeLisser, H. M., Newman, P. J. and Albelda, S. M. (1994b). Molecular and functional aspects of PECAM-1/CD31. *Immunol. Today* **15**, 490-495.

Fawcett, J., Holness, C. L. L., Needham, L. A., Turley, H., Gatter, K. C. Mason, D. Y. and Simmons, D. L. (1992). Molecular cloning of ICAM-3, a third ligand for LFA-1, constitutively expressed on resting leukocytes. *Nature* **360**, 481-484.

Fawcett, J., Buckley, C., Holness, C. L, Bird, I. N., Spragg, J. H., Saunders, J., Harris, A. and Simmons, D. L. (1995). Mapping the homotypic binding sites in CD31 and the role of CD31 adhesion in the formation of inter endothelial cell contacts *J. Cell Biol.* **128**, 1229-1241.

Goldberger, A., Middleton, K. A., Oliver, J. A., Paddock, C., Yan, H.-C., DeLisser, H. M., Albelda, S. M and Newman, P. J. (1994). Biosynthesis and processing of the cell adhesion molecule PECAM-1 includes production of a soluble form. *J. Biol. Chem.* **269**, 17183-17191.

Holness, C. L. and Simmons, D. L. (1994). Structural motifs for recognition and adhesion in members of the immunoglobulin superfamily. *J. Cell Sci.* **107**, 2065-2070.

Holness, C. L., Bates P. A., Littler, A. J., Buckley, C. D., McDowall, A., Bossy, D., Hogg, N. and Simmons, D. L. (1995). Analysis of the binding site on intercellular adhesion molecule 3 for the leukocyte integrin lymphocyte function associated antigen 1. *J. Biol. Chem.* **220**, 877-884.

Jones, E. Y., Harlos, K., Bottomley, M. J., Robinson, R. C., Driscoll, P. C., Edwards, R. M., Clements, J. M., Dudgeon, T. J. and Stuart, D. I. (1995). Crystal structure of an integrin-binding fragment of vascular cell adhesion molecule-1 at 1. 8Å resolution. *Nature* **373**, 539-544.

Karecla, P. I., Bowden, S. J., Green, S. J. and Kilshaw, P. J. (1995). Recognition of E-cadherin on epithelial cells by the mucosal T cell integrin $\alpha_{M290}\beta_7$ ($\alpha_E\beta_7$). *Eur. J. Immunol.* **25**, 852-856.

Kirschbaum, N. E., Gumina, R. J. and Newman, P. J. (1994), Organization of the gene for human platelet/endothelial cell adhesion molecule-1 shows alternatively spliced isoforms and a functionally complex cytoplasmic domain. *Blood* **84**, 4028-4037.

Koch, A. E., Halloran, M. M., Haskell, C. J., Shah, M. R. and Polverini, P. J. (1995). Angiogenesis mediated by soluble forms of E-selectin and vascular cell adhesion molecule-1. *Nature* **376**, 517-519.

Landis, R. C., McDowall, A., Holness, C. L. L., Littler, A. J., Simmons, D. L. and Hogg. N. (1994). Involvement of the 'I' domain of LFA-1 in the selective binding to ligands ICAM-1 and ICAM-3. *J. Cell Biol.* **126**, 529-537.

Leavesley, D. I., Oliver, J. M., Swart, B. W., Berndt, M. C., Haylock, D. N. and Simmons, P. J. (1994). Signals from platelet/endothelial cell adhesion molecule enhance the adhesive of the very late antigen-4 integrin of human CD34$^+$ haematopoietic progenitor cells. *J. Immunol.* **153**, 4673-4683.

Loftus, J. C., Smith, J. W. and Ginsberg, M. H. (1994). Integrin-mediated cell adhesion: the extracellular face. *J. Biol. Chem.* **269**, 25235-25238.

Muller, W. A., Ratti, C. M., McDonnell, S. L. and Cohn, Z. A. (1989). A human endothelial cell-restricted externally disposed plasmalemmal protein enriched in intercellular junctions. *J. Exp. Med.* **170**, 399-414.

Muller, W. A., Berman, M. E., Newman, P. J., DeLisser, H. M. and Albelda, S. M. (1992). A heterophilic adhesion mechanism for platelet/endothelial cell adhesion molecule 1 (CD31). *J. Exp. Med.* **175**, 1401-1404.

Muller, W. A., Weigl, S. A., Deng, X. and Phillips, D. M. (1993). PECAM-1 is required for transendothelial migration of leukocytes. *J. Exp. Med.* **178**, 449-460.

Neugebauer, K. M and Reichardt, L. F. (1991). Cell surface regulation of β1-integrin activity on developing retinal neurons. *Nature* **350**, 68-71.

Newman, P. J., Berndt, M. C., Gorski, J., White II, G. C., Lyman, S., Paddock, C. and Muller, W. A. (1990). PECAM-1 (CD31) cloning and relation to adhesion molecules of the immunoglobulin superfamily. *Science* **247**, 1219-1221.

Newman, P. J., Hillery, C. A., Albrecht, R., Parise, L. V., Berndt, M. C., Mazurov, A. V. Dunlop, L. C., Zhang, J and Rittenhouse, S. E. (1992). Activation-dependent changes in human platelet PECAM-1: phosphorylation, cytoskeletal association, and surface membrane redistribution. *J. Cell Biol.* **119**, 239-246.

Piali, L., Albelda, S. M, Baldwin, H. S., Hammel, P., Gisler, R. H. and Imhof B. A. (1993). Murine platelet endothelial cell adhesion molecule (PECAM-1)/CD31 modulates β2 integrins on lymphokine-activated killer cells. *Eur. J. Immunol.* **23**, 2464-2471.

Piali, L., Hemmel, P., Uherek, C., Bachmann, F., Gisler, R. H., Dunon D. and Ihmof, B. A. (1995). CD31/ PECAM-1 is a ligand for $\alpha_v\beta_3$ integrin involved in adhesion of leukocytes to endothelium. *J. Cell Biol.* **130**, 451-460.

Romer, L. H., McLean, N. V., Yan, H.-C., Daise, M., Sun, J. and DeLisser, H. M. (1995). INF-gamma and TNF-alpha induce redistribution of PECAM-1 (CD31) on human endothelial cells. *J. Immunol.* **154**, 6582-6592.

Ruiz, P., Dunon, D., Sonnenberg, A. and Ihmof, B. A. (1993). Suppression of mouse melanoma metastasis by EA-1, a monoclonal antibody specific for α6 integrins. *Cell Adhes. Commun.* **1**, 67-81.

Schimmenti, L. A., Yan, H. C., Madri, J. A. and Albelda S. M. (1992). Platelet endothelial cell adhesion molecule, PECAM-1 modulates cell migration. *J. Cell. Physiol.* **153**, 417-428.

Simmons, D. L., Walker, C., Power, C and Pigott. R. (1990). Molecular cloning of CD31, a putative intercellular adhesion molecule closely related to carcinoembryonic antigen. *J. Exp. Med.* **171**, 2147-2151.

Simmons, D. L. (1993). Cloning cell surface molecules by transient expression in mammalian cells. In *Cellular Interactions In Development* (ed. D. Hartley), pp. 93-128. Oxford University Press, Oxford.

Stockinger, H., Gadd, S. J., Eher, R., Majdic, O., Schreiber, W., Kasinrerk, W. Strass, B., Schnabl, E. and Knapp, W. (1990). Molecular characterisation and functional analysis of the leukocyte surface protein CD31. *J. Immunol.* **145**, 3889-3897.

Tanaka, Y., Albelda, S. M., Horgan, K. J., van Seventer, G. A., Shimizu, Y., Newman, W., Hallam, J., Newman, P. J., Buck, C. A. and Shaw. S. (1992). CD31 expressed on distinctive T cell subsets is a preferential amplifier of β1 integrin-mediated adhesion. *J. Exp. Med.* **176**, 245-253.

Van Kooyk, Y., Van de Wiel van Kemenade, E., Weder, P., Huijbens, J. F. and Figdor, C. G. (1993). Lymphocyte function-associated antigen 1 dominates very late antigen 4 in binding of activated T cells to endothelium. *J. Exp. Med.* **177**, 185-190.

Vaporciyan, A. A., DeLisser, H. M., Yan, H. C., Mendiguren, I. I., Thorn, S. R., Jones, M. L., Ward, P. A. and Albelda S. M. (1993). Involvement of platelet-endothelial cell adhesion molecule-1 in neutrophil recruitment in vivo. *Science* **262**, 1580-1582.

Watt, S. M., Williamson, J., Genevier, H., Fawcett, J., Simmons, D. L, Hatzfeld, A., Nesbitt, S. A. and Coombe, D. R. (1993). The heparin binding PECAM-1 adhesion molecule is expressed by CD34$^+$ hematopoietic precursor cells with early myeloid and B-lymphoid cell phenotypes. *Blood* **82**, 2649-2663.

Watt, S. M., Gschmeissner S. E. and Bates, P. A. (1995a). PECAM-1: Its expression and function as a cell adhesion molecule on hemopoietic and endothelial cells. *Leuk. Lymph.* 17, 229-244.

Watt, S. M., Cardoso, A., Lee-Prudhoe, J., Benton, M. A., Doyonnas, R., Hatzfeld, A., Genevier, H., Porter, C and Hatzfeld, J. (1995b). The adhesion molecules PECAM-1, ICAM-3, and CD33 on CD34$^+$ haematopoietic progenitor cells: a European Concerted Action Approach. In *NATO ASI Series on Cell Biology* (ed. A. Zander), Springer-Verlag, Amsterdam (in press).

Yan, H.-C., Pilewski, J. M., DeLisser, H. M., Romer, L and Albelda S. M. (1995). Localization of multiple functional domains on human PECAM-1 (CD31) by monoclonal antibody epitope mapping. *Cell Adhes. Commun.* **3**, 45-66.

Zehnder, J. L., Hirai, K., Shatsky, M., McGregor, J. L., Levitt, L. J. and Leung, L. L. K. (1992). The cell adhesion molecule CD31 is phosphorylated after cell activation. *J. Biol. Chem.* **267**, 5243-5249.

(Received 16 August 1995 - Accepted 31 October 1995)